Institute of Oceanology
Polish Academy of Sciences

International Environmental Doctoral School
associated with the Centre for Polar Studies
University of Silesia

The influence of environmental factors on the variability of meroplankton in the European Arctic

M.Sc. Weronika Magdalena Patuła

PhD Thesis

written under the supervision of

Dr hab. Marta Ronowicz, Prof. IO PAN

Dr hab. Agata Weydmann-Zwolicka, Prof. UG

Sopot, 2026

Instytut Oceanologii
Polska Akademia Nauk

Międzynarodowa Środowiskowa Szkoła Doktorska
przy Centrum Studiów Polarnych
Uniwersytet Śląski

Wpływ czynników środowiska na zmienność meroplanktonu w Arktyce Europejskiej

mgr Weronika Magdalena Patuła

Rozprawa doktorska
napisana pod kierunkiem
dr hab. Marty Ronowicz, prof. IO PAN
dr hab. Agaty Weydmann-Zwolickiej, prof. UG

Sopot, 2026

Acknowledgements

This doctoral dissertation would not have been possible without the support, wisdom, and encouragement of many exceptional people.

I extend my gratitude to my supervisors, Dr hab. Marta Ronowicz, Prof. IO PAN, and Dr hab. Agata Weydmann-Zwolicka, Prof. UG, for granting me the opportunity to pursue this PhD, for their support, and for thoughtfully guiding me through every stage of this journey.

A special word of thanks goes to Dr Sławomir Kwaśniewski, who truly sparked my passion for Arctic zooplankton research. I am incredibly lucky to have learned from you – thank you for the invaluable knowledge you shared, and your endless patience and understanding throughout our collaboration.

I am sincerely grateful to Dr Agnieszka Beszczyńska-Möller for her generous guidance in helping me navigate and interpret the complexities of hydrographic regimes of Fram Strait and Western Spitsbergen Shelf.

My appreciation also goes to all the co-authors of the research findings included in this work for sharing their expertise, constructive feedback, and the countless hours spent in consultations.

I would like to thank all my colleagues at the Marine Ecology Department for providing a welcoming environment to carry out my doctoral research. I am particularly grateful to Marta Głuchowska for her empathy and understanding, Mateusz Ormańczyk for the great discussions and companionship during long hours spent in the lab, as well as Lech Kotwicki, Zosia Legeżyńska, Kaja Bałazy, and Kasia Grzelak for their uplifting words and encouraging conversations whenever self-doubt set in.

My heartfelt thanks go to the crew and science team of s/y Oceania (2021-2022) – especially Romuald Obuchowski, Gosia Kitowska, Hesia Niedźwiecka, and Przemek Makuch – without whom collecting the field material would have been impossible. Thank you for your hands-on help, moral support during tough moments, the fantastic atmosphere on board, and all those enjoyable hours spent catching up over coffee, both on board and off.

I want to express my sincere gratitude to the leadership and administrative team of the International Environmental Doctoral School, especially Prof. Ksenia Pazdro, Dr hab. Mariusz Grabiec, Prof UŚ, Dr Michał Ciepły, and Ms Regina Terlecka. Without your assistance, navigating the academic milestones and completing this dissertation would not have been feasible. Thank you for your support – both professional and personal.

I am just as lucky to have shared this path with my fellow PhD candidates, especially Tanmay Keluskar, Emily Chen, Kasia Stachniak, and Dagmara Litwicka. Thank you for your sound advice, great company during classes and conferences, shared travels, and all the laughter along the way!

Warm thanks go to my colleagues at work – above all Marta Szczepanek, Patrycja Nowakowska, Bernabé Moreno, Ania Sowa, and Marek Lubośny, for the endless chats (scientific and otherwise), the time spent together outside the Institute, and the constant encouragement over the years. I couldn't have crossed the finish line without you.

I also wish to express my sincere appreciation to my Mentors, Beata Szymczycha and Ania Pouch, for their time during our Mentoring Program sessions, their wise career guidance, and for gently bringing me back to earth whenever I overthought things.

My thanks go also to Oliwia Waszyńska, manager of my HIMERO project, for her ongoing assistance, friendly talks, and patience in answering my endless project-management queries.

I am also indebted to the administrative and financial departments at IO PAN for deftly guiding me through the maze of institutional procedures with extraordinary patience and helpfulness.

To my Friends: thank you for your rock-solid patience, for listening to my venting during critical moments, and for bearing with me – in particular over the intense final months of writing. Knowing I can always count on you means the world to me.

To anyone else who supported me along the way, whether through a kind word or a helping hand – thank you.

Na koniec dziękuję mojej Rodzinie. Dziękuję za wychowanie, wsparcie mojej edukacji i za to, że zawsze jesteście moim oparciem i motywacją w dążeniu do celów – zarówno naukowych, jak i osobistych.

Funding

The work presented in this thesis was co-funded by the project HIMERO ("Spatial and temporal variability of the hidden Arctic meroplankton diversity as a key for understanding rapidly progressing environmental changes"; No. 2021/41/N/NZ8/02735; National Science Centre, Preludium 20; PI - Weronika Patuła).

The long-term Arctic monitoring program AREX, as well as general logistics, were supported by the statutory funds of the Institute of Oceanology of the Polish Academy of Sciences (IO PAN). I am grateful to the crew of the s/y Oceania and the scientific team from IO PAN for their invaluable help and assistance during fieldwork and sampling.

Contribution to sample collection, reagents for laboratory analysis, manuscript preparation, and Open Access publication was supported by the following projects:

1. *HIDEA ("Hidden diversity of plankton in the European Arctic"; NCN OPUS 2017/27/B/NZ8/01056);*
2. *ASCOMEA ("Influence of Atlantification on succession and biotic components in the shallow hard-bottom ecosystem in the Arctic"; NCN OPUS 2019/33/B/NZ8/02154);*
3. *ANALOG ("Influence of rapidly progressing climate change on polar marine organisms - investigations along naturally occurring environmental analogues of future climate changes"; NCN OPUS 2020/37/B/ST10/02905);*
4. *HYDMEA ("Hydroid meadows as habitat formers in polar regions"; No. 2023/51/B/NZ8/02512);*
5. *The open-access publication was co-funded by the project "JUST TRANSITION – POTENCJAŁ UNIWERSYTETU ŚLĄSKIEGO PODSTAWĄ SPRAWIEDLIWEJ TRANSFORMACJI REGIONU" (FESL.10.25-IZ.01.0369/23-003), implemented under the European Funds for Silesia 2021–2027 and co-financed by the Just Transition Fund.*

Additionally, I was supported by a scientific scholarship from the project TWINS; When co-existence means separation – ecological niche partitioning between sibling zooplankton species in warming Arctic; No. 2021/41/B/NZ8/02735).

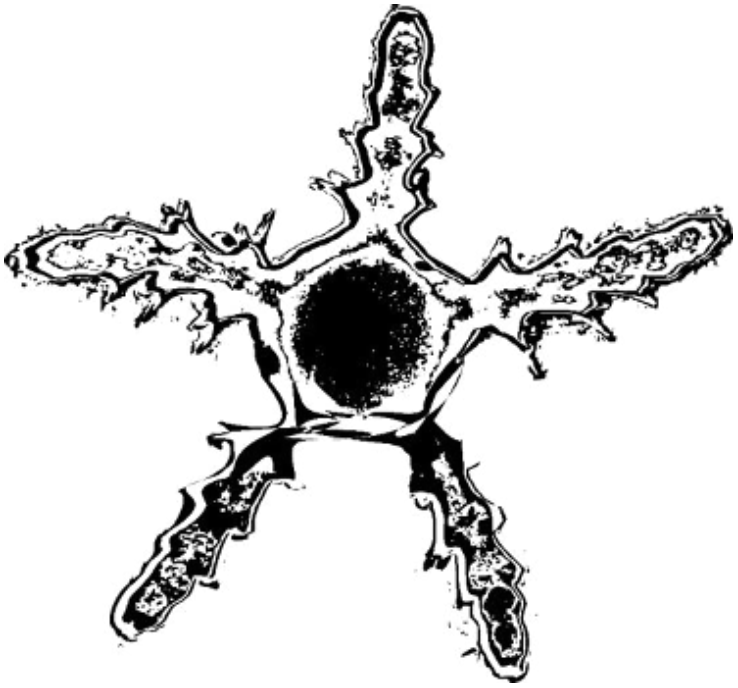

"Never give up on a dream just because of the time it will take to accomplish it. The time will pass anyway."

Earl Nightingale

List of abbreviations

Abbreviation/Skrót	Explanation	Objaśnienie
18S	V1-V2 region of the 18S rRNA gene	Region genu V1-V2 18S rRNA
AH	Above halocline	Powyżej halokliny
ANOSIM	Analysis of similarities	Analiza podobieństwa
ArW	Arctic Water	Woda Arktyczna
AW	Atlantic Water	Woda Atlantycka
BH	Below halocline	Poniżej halokliny
chl *a*	Chlorophyll *a*	Chlorofil *a*
CLUSTER	Hierarchical agglomerative clustering	Hierarchiczna aglomeracyjna analiza skupień
cox1	Cytochrome c oxidase subunit I gene fragment	Fragment genu podjednostki I oksydazy cytochromu c
CTD	Conductivity, Temperature, Depth	Sonda CTD
dbRDA	Distance – based Redundancy analysis	Analiza redundancji oparta na macierzach odległości
DistLM	Distance – based Linear Models	Liniowe modele oparte na macierzach odległości
DNA	Deoxyribonucleic Acid	Kwas deoksyrybonukleinowy
DVM	Diel Vertical Migration	Dobowa migracja pionowa
eDNA	Environmental DNA	DNA środowiskowe
H′	Shannon-Wiener diversity index	Wskaźnik różnorodności Shannona-Wienera
HTS	High-throughput sequencing	Sekwencjonowanie wysokoprzepustowe
IPCC	Intergovernmental Panel on Climate Change	Międzyrządowy Zespół ds. Zmian Klimatu
J′	Pielou's evenness index	Wskaźnik równomierności Pielou
KT	Kongsfjorden Transect	Transekt Kongsfjorden

nMDS	Non-metric multidimensional scaling	Niemetryczne skalowanie wielowymiarowe
NwAFC	Norwegian Atlantic Frontal Current	Norweski Frontalny Prąd Atlantycki
NwASC	Norwegian Atlantic Slope Current	Norweski Atlantycki Prąd Stokowy
PCR	Polymerase chain reaction	Reakcja łańcuchowa polimerazy
PERMANOVA	Permutational Multivariate Analysis of Variance	Permutacyjna wielowymiarowa analiza wariancji
PERMDISP	Permutational Multivariate Analysis of Dispersion	Permutacyjna wielowymiarowa analiza dyspersji
S	Taxonomic richness	Bogactwo taksonomiczne
SIMPROF	Permutation based similarity profile test	Permutacyjny test profili podobieństwa
SPC	Spitsbergen Polar Current	Spitsbergeński Prąd Polarny
SW	Surface Water	Woda Powierzchniowa
WSC	West Spitsbergen Current	Prąd Zachodniospitsbergenski
WSS	West Spitsbergen Shelf	Szelf Zachodniospistbergeński

Table of contents

Abstract **18**

Streszczenie po polsku **23**

Chapter I Introduction **29**

1.1 Arctic environment 29

1.2 Meroplankton definition 30

1.3 The role of meroplankton in marine ecosystems 33

1.3.1 Meroplankton dispersal and hydrographic connectivity 35

1.4 Pelagic-benthic coupling and life-history strategies in the Arctic 36

1.5 Environmental drivers of larval distribution across spatial and temporal scales 37

1.5.1 Temporal and interannual variability of zooplankton communities 38

1.5.2 Vertical stratification and physical barriers in the water column 38

1.5.3 Environmental differences between open waters, shelf, and fjord habitats 39

1.6 Methodological advances in meroplankton research: from morphology to metabarcoding 40

1.6.1 Traditional morphology-based taxonomy and its challenges 40

1.6.2 Application of High-Throughput Sequencing (HTS) and DNA metabarcoding in marine ecology 41

1.6.3 Integration of morphological and molecular approaches for assessing larval diversity 42

1.7 Aims, objectives, and outline of the thesis 42

Chapter II Abridged Atlas of Meroplankton – European Arctic and West Norwegian Coast **46**

2.1 Rationale and objectives of the larval atlas 46

2.2 Note on data reuse and publication status 46

2.3 Introduction and methodological background 47

2.4 Sample processing and image acquisition 47

Chapter III Long-term spatiotemporal shifts in meroplankton community composition as a signature of Arctic Atlantification 59

3.1 Introduction 59

3.2 Materials & Methods 61

3.2.1 Study area 61

3.2.2 Meroplankton sampling and analysis 62

3.2.3 Data processing 63

3.2.3.1 Hydrography 63

3.2.3.2 Data classification and environmental setting 64

3.2.3.3 Statistical analysis 65

3.3 Results 67

3.3.1 Environmental conditions 67

3.3.1.1 Spatiotemporal variability of temperature and salinity 67

3.3.1.2 Temperature and salinity anomalies over the 2001-2016 period 70

3.3.2 Meroplankton community 74

3.3.2.1 Environmental drivers of meroplankton community structure 74

3.3.2.2 Meroplankton spatiotemporal composition 79

3.3.2.2.1 Temporal changes in the meroplankton community 79

3.3.2.2.2 Spatial and temporal changes with distance from the shelf to open waters…… 80

3.3.2.2.3 Spatial and temporal changes with latitude 84

3.4 Discussion 88

3.4.1 Environmental control over the meroplankton community 88

3.4.2 Shelf-offshore gradient vs latitude 89

3.4.3 Temporal changes and diversity shift 90

3.4.4 Meroplankton as early warning signals 90

3.4.5 Methodology limitations and future perspectives 91

3.5 Conclusions 92

Chapter IV Halocline as an environmental barrier for the larvae of Arctic marine benthic invertebrates 93

4.1 Introduction 93

4.2 Materials & Methods 95

4.2.1 Study area 95

4.2.2 Measurements and sampling 97

4.2.3 Laboratory analysis 99

4.2.4 Data processing 100

4.3 Results 101

4.3.1 Environmental conditions 101

4.3.2 Meroplankton community 103

4.3.3 Meroplankton community variation across environmental conditions 104

4.3.4 The meroplankton assemblage structure above vs below halocline 107

4.3.4.1 *Meroplankton Taxa* 107

4.3.4.2 *Polychaeta larvae* 108

4.3.4.3 *Echinodermata larvae* 108

4.3.4.4 *Other larvae* 109

4.4 Discussion 111

4.4.1 The role of halocline in shaping the meroplankton community 111

4.4.2 Distribution of marine benthic invertebrates larvae above and below the halocline. 112

4.4.3 Meroplankton distribution and benthic-pelagic coupling along the Kongsfjorden Transect. 114

4.5 Conclusions 116

Chapter V Integrating morphological and multi-marker metabarcoding (18S rRNA & *cox1*) to map meroplankton diversity along the NE Atlantic shelf 118

5.1 Introduction 118

5.2 Materials & Methods 121

5.2.1 Study Area 121
5.2.2 Fieldwork 122
5.2.2.1 Environmental parameters and chlorophyll *a* sampling 122
5.2.2.2 Meroplankton collection 123
5.2.3 Laboratory analysis 123
5.2.3.1 Chlorophyll *a* 123
5.2.3.2 Meroplankton morphological identification workflow 124
5.2.3.3 Meroplankton metabarcoding laboratory workflow 126
5.2.3.3.1 DNA extraction 126
5.2.3.3.2 Gene markers and primers 128
5.2.3.3.3 DNA amplification and library preparation 129
5.2.4 Data processing 130
5.2.4.1 Hydrography 130
5.2.4.2 Bioinformatic pipeline 130
5.2.4.3 Statistical analysis 132
5.3 Results 133
5.3.1 Environmental conditions 133
5.3.2 Methodological comparison of meroplankton taxa richness 136
5.3.3 Taxonomic composition and inter-methodological match 138
5.3.4 Meroplankton community structure and spatial patterns 149
5.3.5 Environmental drivers of meroplankton community 154
5.4 Discussion 157
5.4.1 From morphology to metabarcoding 158
5.4.2 Traditional morphology-based meroplankton taxonomy: challenges and limitations 158
5.4.3 Integrating two markers to capture larval diversity 159
5.4.4 Integration of the two approaches, morphological and molecular 161

5.5 Conclusion 164

Chapter VI Summary and Conclusions 165

6.1 Summary 165

6.2 Conclusions and future perspectives 167

References 169

List of Tables 186

List of Figures 188

Supplementary materials 193

Authors' contribution table 210

Abstract

In recent decades, the European Arctic has experienced warming at a rate much faster than the rest of the globe, a phenomenon known as polar (or Arctic) amplification, driven largely by the loss of sea ice and the resulting reduction in surface albedo. According to IPCC reports from 2021 and 2022, this progressive degradation of the cryosphere drives profound structural and functional changes in ecosystems. Both rising air temperatures and the intensified influx of relatively warm, saline Atlantic waters (a process known as "Atlantification") shape Arctic marine ecosystems by modifying water mass transport, mixing processes, and the formation of frontal zones. This, in turn, leads to local, regional, and large-scale changes across open ocean waters, shelf areas, and fjords. Furthermore, the significant loss of sea ice and the shortening of its seasonal duration directly affect primary production and water-column stratification. These changes disrupt the synchronization between biotic and abiotic ecosystem components, affecting primary production and pelagic-benthic coupling, and, later, the structure of entire trophic food webs.

This study focuses on meroplankton, which consists mainly of the larvae of benthic marine invertebrates. Meroplankton represents a temporary component of the zooplankton community, inhabiting the water column exclusively during their early life cycle. The duration of a this pelagic phase ranges from a few hours to several months. During this time, larvae encounter a range of adverse environmental conditions, such as physico-chemical fluctuations, variable water currents, predatory pressure, and changes in food availability, which strongly determine their survival, proper development, settlement success on the seabed, and ability to colonize new areas.

Meroplankton plays a key role in the marine environment by pelagic and benthic ecosystems (a process known as pelagic-benthic coupling). It serves as a crucial component of the food web, acting as as prey for predatory zooplankton and juvenile fish – and actively contributes to carbon and organic matter cycling through phytoplankton consuming and participating in the microbial loop. Due to their short life cycles and high sensitivity to environmental shifts (including variations in temperature, salinity, or primary production dynamics), larval survival and supply directly shape the recruitment success and future structure of adult benthic populations. Consequently, meroplankton functions as a sensitive indicator for detecting both sudden disturbances and long-term ecosystem shifts, providing valuable insights into Arctic marine trajectories amid ongoing global warming.

However, to fully assess the potential of using meroplankton as an indicator of changes in Arctic ecosystems, it is necessary to revisit the fundamentals of their identification and of their diversity assessment. So far, identification methods based on traditional microscopic analysis have largely been limited to categorization at higher taxonomic levels (classes, orders, and, less frequently, families). Many zooplankton studies treat meroplankton as a single aggregate or focus only on the most abundant groups (e.g., Bivalvia veligers, or Echinodermata and Cirripedia larvae), while grouping other less abundant taxa with rare holoplankton in an "other" category. Such an approach results in the loss of key information regarding taxonomic composition and, consequently, the potential environmental impact on meroplankton or its role in carbon cycling. These limitations can be overcome by developing molecular methods such as DNA barcoding (analysis of individual specimens) and DNA metabarcoding (analysis of entire communities), which enable the determination of the true taxonomic composition of meroplankton. Nevertheless, each of these methods has its limitations: the traditional morphological approach delivers precise data on environmental abundance, population structure, and developmental stages (e.g., nauplius, cypris, veliger, zoea, megalopa) but lacks taxonomic resolution. On the other hand, molecular methods provide detailed taxonomic information, often to the species level, but do not allow for identification of developmental stages or estimation of exact individual abundance.

Therefore, the aim of this doctoral dissertation was to assess the variability, spatial distribution, and community structure of meroplankton in the European Arctic. The study targeted a key marine gradient, spanning the West Spitsbergen Current (WSC) and Kongsfjorden (Svalbard). Through a dual approach combining classical morphological identification and DNA metabarcoding, the work evaluates how integrating methodological frameworks improves analytical resolution and inference The study comprises four main research chapters in which the complementary use of different methodological tools was demonstrated, enabling more precise hypothesis verification and inference, as well as the full utilization of meroplankton as an indicator of environmental changes.

In **Chapter II**, an original atlas of pelagic larvae, complete with photographic documentation, was developed to serve as a reference for the consistent identification of material in **Chapters IV** and **V**. Serving as the primary methodological basis of the entire thesis, this atlas guarantees taxonomic continuity across all analytical steps in which morphological examination provides the common baseline.

To gain insight into the general structure of meroplankton and its spatial and temporal changes in the European Arctic, in **Chapter III** a large-scale, multi-year analysis of

meroplankton communities in the area influenced by the West Spitsbergen Current was conducted. This current transports relatively warm, saline Atlantic waters, driving the process of "Atlantification", which can carry boreal larvae to high latitudes. Using a 16-year time series (2001-2016), the spatial and temporal variability of meroplankton assemblages within the pelagic layer (mostly 200-0 m) was investigated. By categorizing sampling stations into shelf, main Atlantic water stream (core), and open water (offshore) zones, it was demonstrated that the structure of meroplankton communities in the West Spitsbergen Current region was shaped primarily by the properties of the inflowing Atlantic waters and the spatial zonation extending from the shelf toward the open ocean, rather than by a latitudinal gradient from south to north. The transition zone between the shelf and open waters constituted a more significant ecological barrier than geographic distance alone, whereas the main flow of the West Spitsbergen Current acted as a transit zone facilitating larval dispersal. It is worth noting that, in general, thermal phases (warm vs cold years) did not influence meroplankton variability. However, the meroplankton showed a strong response to specific hydrographic extremes. Cooler years (e.g., 2010) favoured higher taxonomic diversity and abundance peaks for certain groups (e.g., Cirripedia cyprids), whereas warm years (e.g., 2006) showed a significant decline in taxonomic richness over the 16-year study period. These patterns indicated that progressive warming led to a reduction in the number of taxa within the larval pool, as higher temperatures and the influx of Atlantic waters favoured only a few dominant groups, with Bivalvia veligers, for instance, accounting for up to 70% of the community in open waters and the main current during warm years, therefore displacing more diverse meroplankton assemblages. The results suggested that meroplankton can serve as a sensitive early-warning indicator of ecosystem changes, responding with a decline in diversity much more rapidly than long-lived adult benthic populations. Consequently, further warming may weaken pelagic-benthic coupling by shifting larval assemblages toward thermally tolerant, less diverse communities, thereby altering energy transfer between the pelagial and the benthos.

In the subsequent part of the study (**Chapter IV**), the influence of a selected environmental variable on the formation of meroplankton communities within the water column was investigated, assessing the role of a halocline as a physical environmental barrier to larval migration. A significant outcome of this work was the examination of halocline's impact on the vertical distribution of meroplankton in relation to environmental variables in the European Arctic (using the Kongsfjorden Transect as a study area). The hypothesis that a strong vertical salinity gradient (halocline) acts as a physical barrier shaping benthic larval communities was confirmed, as evidenced by significant differences in taxonomic composition and assemblage

structure above and below this layer. Specific taxa and larval morphotypes exhibited preferences for particular water layers, likely driven by differences in their salinity tolerances and responses to mixing dynamics. In the fjord environment, the presence of a halocline restricted vertical migration, promoting the retention of some larvae within the fjord. Conversely, on the shelf, where stratification was weaker and conditions were more dynamic, larval dispersal and exchange with adjacent waters were more evident. Furthermore, differences in the dominance of major groups were observed along the transect: the warmer, less dynamic conditions of the fjord favoured greater diversity among Polychaeta larvae (which preferred stable, deeper waters below the halocline), whereas the more dynamic conditions on the West Spitsbergen shelf promoted the dominance of Echinodermata larvae (concentrated above the halocline). The observed differences in the vertical distribution of major taxonomic groups above and below the halocline indicated that salinity-driven stratification (explaining around 30% of total meroplankton variation) was an important factor shaping meroplankton communities. Certain taxa occurred within specific layers, indicating differing tolerances or adaptive strategies to salinity and turbulence. In addition to Echinodermata larvae, Cirripedia cyprids were physically retained above the halocline. In contrast, Bivalvia veligers occurred throughout the entire water column, though they were also retained in high concentrations at the glacier-influenced inner-fjord station. Additionally, spatial sorting was noticed across the gradient, as Bryozoa occurred exclusively near the glacier, Gastropoda and Decapoda were found strictly inside the fjord, and Ascidiacea were present on the open shelf, indicating clear differences in ecological tolerances and retention strategies regarding salinity gradients and turbulence. Summing up, in fjordic systems, the presence of a halocline can lead to the retention of certain larvae within the fjord, whereas the more dynamic shelf environment, characterized by weaker stratification, enhances their dispersal and exchange with adjacent water masses.

In **Chapter V**, a multidisciplinary approach was used to characterize the structure of meroplankton in the Northeast Atlantic shelf region. The complementarity of the traditional morphological approach and modern molecular methods (DNA metabarcoding using two markers: V1-V2 region of 18S rRNA gene (18S) and cytochrome c oxidase subunit I gene fragment (*cox1*)) was used in assessing meroplankton structure and diversity on the Northeast Atlantic shelf. It was shown that traditional microscopic analysis is crucial for identifying larval developmental stages (e.g., zoea, megalopa, cypris, veliger) and analyzing population age structure, whereas DNA metabarcoding reveals hidden taxonomic diversity (enabling identification down to the genus and/or species levels), a capability particularly crucial for Bivalvia and Gastropoda larvae that are difficult to identify morphologically. Furthermore, the

application of two different genetic markers highlighted their distinct yet complementary analytical properties: the nuclear V1-V2 18S rRNA region effectively reflected large-scale shifts in the meroplankton community structure associated with different water masses, while the mitochondrial *cox1* marker provided higher taxonomic resolution and was more sensitive to micro-scale, station-specific shifts in larval composition. Combining these methods enabled detailed mapping of meroplankton diversity. It revealed that the Norwegian Coast (NC) and Barents Sea (BS) regions are the primary "hotspots" of taxonomic richness on the Northeast Atlantic shelf, although diversity drops markedly in the Atlantic Water (AW) zone and on the West Spitsbergen shelf (WS). Water salinity and temperature were the key environmental factors shaping these spatial patterns.

In summary, the comprehensive analysis of the spatial and temporal variability of the Arctic meroplankton diversity conducted in this study confirms that benthic invertebrate larvae are highly sensitive indicators of changes occurring in the marine environment. The demonstrated complementarity of classical morphological methods and modern molecular tools constitutes a highly recommended methodological approach. In addition, an atlas of larvae, accompanied by comprehensive photographic documentation, was developed as a reference for consistent identification throughout this thesis and as a lasting taxonomic resource for future studies. The use of DNA metabarcoding reveals previously hidden taxonomic diversity within the meroplankton, which, when combined with traditional developmental-stage analysis, elevates taxonomic resolution achieved. This approach not only facilitates a better understanding of pelagic-benthic coupling but, above all, establishes a solid foundation for formulating more precise research hypotheses and ensuring more accurate interpretation and inference in future meroplankton studies. Furthermore, it may enable the creation of a complementary standard for meroplankton analysis to support the long-term monitoring of changes in Arctic and sub-Arctic ecosystems driven by the observed global warming.

Streszczenie po polsku

W ostatnich dekadach rejon Arktyki Europejskiej doświadczał zjawiska znacznie szybszego ocieplenia w porównaniu z resztą globu, znanego pod pojęciem amplifikacji polarnej (arktycznej), napędzanej w dużej mierze przez zanik lodu morskiego i wynikające z tego zmniejszenie albedo powierzchni. Według raportów IPCC z 2021 i 2022 roku postępująca degradacja kriosfery prowadzi do istotnych zmian strukturalnych i funkcjonalnych w ekosystemach. Zarówno wzrost temperatury powietrza, jak i intensyfikacja napływu relatywnie ciepłych i słonych wód atlantyckich (tzw. proces atlantyfikacji) kształtują morskie ekosystemy Arktyki, wpływając na transport mas wodnych, procesy mieszania oraz tworzenie się stref frontalnych. To z kolei przekłada się na zmiany lokalne, regionalne i wielkoskalowe w strefie otwartych wód oceanicznych, szelfów oraz fiordów. Ponadto postępujący zanik lodu morskiego i skrócenie okresu jego występowania wpływają bezpośrednio na produkcję pierwotną oraz stratyfikację wód. Zaburza to synchronizację funkcjonowania organizmów pomiędzy strefą biotyczną a abiotyczną – od produkcji pierwotnej, przez sprzężenie pelagiczno-bentosowe, aż po struktury całych sieci troficznych.

Przedmiotem niniejszej pracy jest meroplankton, tworzony w dużej mierze przez pelagiczne larwy morskich bezkręgowców bentosowych. Stanowią one tymczasowy element zooplanktonu, przebywający w toni wodnej wyłącznie podczas wczesnego etapu swojego cyklu życiowego. Czas trwania tej fazy pelagicznej waha się od kilku godzin do nawet kilku miesięcy. W tym czasie larwy napotykają szereg niekorzystnych warunków środowiskowych (m.in. wahania fizykochemiczne, zmienność prądów wodnych, są narażone na presję drapieżniczą czy zmienną dostępność pokarmu), które wpływają na ich przeżywalność, prawidłowy rozwój, sukces osiedlania się na dnie oraz zdolność do kolonizacji nowych rejonów.

Meroplankton odgrywa kluczową rolę w środowisku morskim łącząc ekosystemy pelagiczne i bentosowe (proces ten znany jest jako sprzężenie pelagiczno-bentosowe). Jest ważnym elementem sieci troficznej, gdzie stanowi pokarm dla drapieżnego zooplanktonu czy młodocianych stadiów ryb, a także aktywnie uczestniczy w obiegu węgla i materii organicznej poprzez konsumpcję fitoplanktonu oraz udział w pętli mikrobiologicznej. Ze względu na krótki cykl życiowy oraz wysoką wrażliwość na zmiany środowiskowe (w tym wahania temperatury, zasolenia czy dynamikę produkcji pierwotnej), przeżywalność larw i ich dopływ bezpośrednio kształtują sukces rekrutacji i przyszłą strukturę dorosłych populacji bentosowych. W konsekwencji meroplankton pełni funkcję czułego wskaźnika pozwalającego na

wykrywanie zarówno gwałtownych zaburzeń, jak i długoterminowych przekształceń ekosystemu, dostarczając cennych informacji o kierunkach zmian w arktycznym środowisku morskim w dobie postępującego globalnego ocieplenia.

Jednak aby ocenić pełny potencjał wykorzystania meroplanktonu jako indykatora zmian w ekosystemach arktycznych, należy powrócić do podstaw jego identyfikacji oraz zrozumienia zasad oceny jego różnorodności. Dotychczasowe metody oznaczania oparte na tradycyjnej analizie mikroskopowej ograniczały się w większości do kategoryzacji na wyższych poziomach taksonomicznych (klasy, rzędy, rzadziej rodziny). Wiele prac zooplanktonowych traktuje meroplankton zbiorczo lub analizuje wyłącznie najliczniej występujące taksony (np. weligery Bivalvia, larwy Echinodermata czy Cirripedia), podczas gdy pozostałe taksony zalicza się wraz z rzadszymi przedstawicielami holoplanktonu do kategorii "inne". Przy takim podejściu traci się kluczowe informacje o składzie taksonomicznym, a tym samym o potencjalnym wpływie meroplanktonu na środowisko, czy jego udziale w obiegu węgla. Rozwiązaniem tych ograniczeń jest rozwój metod molekularnych, takich jak barkodowanie DNA (analiza pojedynczych osobników) oraz metabarkodowanie DNA (analiza całych zbiorowisk), które pozwalają poznać rzeczywisty skład taksonomiczny meroplanktonu. Niemniej jednak każda z tych metod posiada swoje limity: tradycyjne podejście morfologiczne pozwala uzyskać precyzyjne dane o liczebności w środowisku oraz strukturze populacyjnej i stadiach rozwojowych (np. pływik, cypris, weliger, żywik, megalopa), lecz brakuje mu rozdzielczości taksonomicznej. Z kolei metody molekularne dostarczają szczegółowych informacji taksonomicznych, często pozwalające na identyfikację nawet do poziomu gatunku, lecz nie pozwalają na rozróżnienie stadiów rozwojowych ani oszacowanie dokładnej liczebności osobników.

Celem niniejszej rozprawy doktorskiej była zatem ocena zmienności, rozmieszczenia przestrzennego oraz struktury zbiorowisk meroplanktonu w Arktyce Europejskiej. Badania koncentrowały się na kluczowym gradiencie środowiskowym, obejmującym obszar Prądu Zachodniospitsbergeńskiego po fiord Kongsfjorden (Svalbard). Dzięki zastosowaniu podejścia łączącego klasyczną identyfikacje morfologiczną z metabarkodingiem DNA, w pracy oceniono, w jaki sposób integracja różnych metod badawczych wpływa na poprawę rozdzielczości analiz oraz jakości wnioskowania. Praca składa się z czterech głównych rozdziałów badawczych, w których wykazano, że komplementarne zastosowanie obu tych narzędzi metodologicznych pozwala na precyzyjniejsze weryfikowanie hipotez, wnioskowanie oraz pełne wykorzystanie meroplanktonu jako wskaźnika zmian środowiskowych.

W **Rozdziale II** na potrzeby badań opracowano autorski atlas pelagicznych larw wraz z dokumentacją fotograficzną, który stanowił podstawę referencyjną dla konsekwentnego oznaczania materiału w **Rozdziałach IV** i **V**. Atlas ten, będący główną podstawą metodologiczną całej pracy, zapewnia ciągłość taksonomiczną na wszystkich etapach analizy, w których wspólnym punktem wyjścia są badania morfologiczne.

Aby zgłębić ogólną strukturę meroplanktonu oraz jej zmienność przestrzenno-czasową w Arktyce Europejskiej, w **Rozdziale III** przeprowadzono wielkoskalową i wieloletnią analizę zbiorowisk meroplanktonu w rejonie oddziaływania Prądu Zachodniospitsbergeńskiego, transportującego relatywnie ciepłe i bardziej słone wody atlantyckie (proces atlantyfikacji), które mogą nanosić larwy pochodzenia borealnego w wysokie szerokości geograficzne. Wykorzystując 16-letni szereg czasowy (2001-2016), zbadano zmienność przestrzenną i czasową zespołów meroplanktonu w warstwie pelagicznej (głównie 200-0 m). Uwzględniając podział stacji badawczych na rejon szelfu, głównego strumienia wody atlantyckiej oraz wód otwartych, potwierdzono, że struktura zbiorowisk meroplanktonu w rejonie Prądu Zachodniospitsbergeńskiego była kształtowana przede wszystkim przez właściwości napływających wód atlantyckich oraz strefy przestrzenne od szelfu w stronę otwartych wód oceanicznych, a nie przez gradient szerokości geograficznej z południa na północ. Strefa przejścia między szelfem a wodami otwartymi stanowiła przy tym istotniejszą barierę ekologiczną niż sam dystans geograficzny, podczas gdy główny strumień Prądu Zachodniospitsbergeńskiego pełnił funkcję strefy tranzytowej sprzyjającej rozprzestrzenianiu się larw. Warto podkreślić, że ogólne fazy termiczne (lata ciepłe vs zimne) nie wyjaśniały zmienności badanych zbiorowisk, jednak meroplankton wykazywał silną reakcję na specyficzne ekstrema hydrograficzne. Lata chłodniejsze (np. 2010) sprzyjały wyższej różnorodności taksonomicznej oraz szczytom liczebności niektórych grup (np. cypridy Cirripedia), podczas gdy w latach ciepłych (np. 2006) odnotowano znaczny spadek bogactwa taksonomicznego w całym 16-letnim okresie badań. Wskazuje to, że postępujące ocieplenie prowadzi do spadku liczby taksonów w puli larwalnej, gdzie wyższa temperatura i napływ wód atlantyckich spowodują faworyzację zaledwie kilka dominujących grup (w latach ciepłych weligery Bivalvia osiągały do 70% udziału w wodach otwartych i głównym strumieniu prądu), wypierając bardziej zróżnicowane zbiorowiska meroplanktonu. Uzyskane wyniki wskazują, że meroplankton może służyć jako wrażliwy wskaźnik wczesnego ostrzegania przed zmianami w ekosystemie, reagując spadkiem różnorodności znacznie szybciej niż długowieczne populacje dorosłego bentosu. W konsekwencji dalsze ocieplenie może osłabić sprzężenie pelagiczno-bentosowe poprzez przesunięcie składu zespołów larwalnych w kierunku

zbiorowisk bardziej odpornych na zmiany temperatury i mniej zróżnicowanych, co doprowadzi do zmiany przepływu energii między pelagialem a bentosem.

W dalszej części pracy, w **Rozdziale IV** przeprowadzono badania nad wpływem wybranej zmiennej środowiskowej na kształtowanie się zbiorowisk meroplanktonu w kolumnie wody, oceniając rolę halokliny jako fizycznej bariery środowiskowej dla migracji larw. Istotnym wynikiem tej pracy było zbadanie wpływu halokliny na pionowe rozmieszczenie meroplanktonu w odniesieniu do zmiennych środowiskowych w Arktyce Europejskiej (na przykładzie Transektu Kongsfjorden). Potwierdzono hipotezę, że silny pionowy gradient zasolenia (haloklina) stanowi barierę fizyczną kształtującą zespoły larwalne organizmów bentosowych, o czym świadczyły istotne różnice w składzie taksonomicznym i strukturze zespołów powyżej i poniżej tej warstwy. Poszczególne taksony i morfotypy larw wykazywały preferencje do konkretnych warstw wody, co prawdopodobnie wynika z ich odmiennej tolerancji na zasolenie oraz dynamikę mieszania mas wodnych. W środowisku fiordowym obecność halokliny ograniczała pionową migrację, sprzyjając zatrzymywaniu (retencji) części larw wewnątrz fiordu. Z kolei na szelfie, gdzie stratyfikacja była słabsza, a warunki bardziej dynamiczne, ułatwione było rozprzestrzenianie się larw i ich wymiana z wodami sąsiednimi. Ponadto wzdłuż transektu zaobserwowano różnice w dominacji głównych grup organizmów, gdzie cieplejsze i mniej dynamiczne warunki w fiordzie sprzyjały większej różnorodności larw Polychaeta (które preferowały stabilne głębsze wody poniżej halokliny), podczas gdy bardziej dynamiczne warunki na szelfie Zachodniego Spitsbergenu sprzyjały dominacji larw Echinodermata (powyżej halokliny). Zaobserwowane różnice w pionowym rozmieszczeniu głównych grup taksonomicznych względem halokliny wskazywały, że stratyfikacja wód wywołana różnicami zasolenia (odpowiadające za około 30% całkowitej zmienności meroplanktonu), była istotnym czynnikiem kształtującym zbiorowiska meroplanktonu. Niektóre taksony występowały w określonych warstwach, co świadczyło o ich zróżnicowanej tolerancji lub odmiennych strategiach adaptacyjnych w zakresie zasolenia i turbulencji. Oprócz larw Echinodermata, powyżej halokliny obecne były larwy Cirripedia, podczas gdy larwy Bivalvia, gromadziły się głównie poniżej halokliny na stacji wewnątrz fiordu, będącej pod wpływem lodowca. Odnotowano również przestrzenne zróżnicowanie wzdłuż badanego gradientu: Bryozoa występowały wyłącznie w pobliżu lodowca, Gastropoda i Decapoda obserwowano wyłącznie wewnątrz fiordu, a Ascidiacea obecne były na otwartym szelfie, co wskazuje na wyraźne różnice w tolerancji ekologicznej oraz strategiach retencji w kontekście gradientów zasolenia i turbulencji. Podsumowując, systemach fiordowych obecność halokliny może prowadzić do zatrzymywania niektórych larw w obrębie fiordu,

z kolei bardziej dynamiczne środowisko szelfowe (o słabszej stratyfikacji wód) ułatwia ich rozprzestrzenianie i wymianę z sąsiednimi masami wód.

W **Rozdziale V,** zastosowano podejście multidyscyplinarne w celu zobrazowania struktury meroplanktonu w rejonie północno-wschodniego szelfu atlantyckiego. Wykazano, że komplementarność tradycyjnego podejścia morfologicznego oraz nowoczesnych metod molekularnych (metabarkodowania DNA z użyciem dwóch fragmentów markerowych: regionu V1-V2 genu 18S rRNA "18S" i genu podjednostki I oksydazy cytochromu c "*cox1*") jest kluczowa w ocenie struktury i różnorodności meroplanktonu na szelfie północno-wschodniego Atlantyku. Potwierdzono, że tradycyjna analiza mikroskopowa jest niezastąpiona do określania stadiów rozwojowych larw (np. żywik, megalopa, cypris, weliger) i analizy struktury wiekowej populacji, podczas gdy metabarkodowanie DNA ujawnia ukrytą różnorodność taksonomiczną (pozwalając na identyfikację aż do poziomu rodzaju i gatunku), co jest szczególnie istotne dla trudnych do oznaczania morfologicznie larw Bivalvia czy Gastropoda. Ponadto zastosowanie dwóch markerów pokazało ich odmienne i uzupełniające się właściwości analityczne w uchwyceniu zmienności meroplanktonu: jądrowy fragment regionu V1-V2 genu 18S rRNA skutecznie odzwierciedlał wielkoskalowe zmiany w strukturze zespołów meroplanktonu powiązane z różnymi masami wodnymi, podczas gdy mitochondrialny marker *cox1* zapewniał wyższą rozdzielczość taksonomiczną, będąc bardziej wrażliwym na mikroskalowe, specyficzne dla poszczególnych stacji przesunięcia w składzie larw. Połączenie tych metod pozwoliło precyzyjnie zmapować różnorodność meroplanktonu i wykazać, że rejon Wybrzeża Norweskiego (NC) oraz Morza Barentsa (BS) stanowią główne "hotspoty" bogactwa taksonomicznego na szelfie północno-wschodniego Atlantyku, podczas gdy w strefie wód atlantyckich (AW) oraz u zachodnich wybrzeży Spitsbergenu (WS) różnorodność ta wyraźnie spada. Wykazano także, że to zasolenie i temperatura są głównymi czynnikami środowiskowymi kształtującymi te wzorce przestrzenne.

Podsumowując, spójna analiza przestrzennej i czasowej zmienności różnorodności meroplanktonu Arktyki przeprowadzona w niniejszej pracy potwierdza, że larwy bentosowych bezkręgowców są niezwykle wrażliwym indykatorem zmian zachodzących w środowisku morskim. Wykazana komplementarność klasycznych metod morfologicznych i nowoczesnych narzędzi molekularnych stanowi z kolei solidne podejście metodologiczne. Ponadto opracowano atlas larw, wzbogacony o dokumentację fotograficzną, który posłużył jako kluczowe źródło odniesienia przy spójnej identyfikacji materiału w ramach niniejszej pracy, a jednocześnie stanowi trwały punkt odniesienia dla przyszłych badań taksonomicznych. Wykorzystanie metabarkodowania DNA pozwala na ujawnienie dotychczas ukrytej

różnorodności taksonomicznej meroplanktonu, co w połączeniu z tradycyjną analizą stadiów rozwojowych podnosi rozdzielczość taksonomiczną na wysoki poziom. Takie podejście nie tylko umożliwia lepsze zrozumienie relacji pelagiczno-bentosowych, ale przede wszystkim stwarza solidny fundament pod precyzyjniejsze stawianie hipotez badawczych oraz bardziej trafną interpretację wyników i wnioskowanie w przyszłych pracach nad meroplanktonem. Ponadto pozwoli to na utworzenie komplementarnego standardu analiz meroplanktonu do długoterminowego monitorowania zmian w ekosystemach arktycznych i subarktycznych pod wpływem obserwowanego globalnego ocieplenia.

Chapter I Introduction

1.1 Arctic environment

Arctic marine ecosystems are among the ecosystems experiencing the most rapid impacts of global warming. These encompass both structural and functional transformations in marine and terrestrial environments (Screen & Simmonds, 2010, Yadav et al., 2020). According to assessments by the Intergovernmental Panel on Climate Change (IPCC), such shifts affect polar regions at scales exceeding the global average, leading to cryospheric degradation (IPCC, 2021; 2022). Polar regions are now transforming into warmer, more dynamic environments, while historically they were characterized by extremely cold environments with extensive seasonal ice cover (Wassmann et al., 2015). This transition is driven by interactions between a warming atmosphere and multi-scale oceanographic processes shaping the Arctic climate (Polyakov et al., 2020), with altered physicochemical conditions driving adaptation and structuring ecological interaction dynamics within the European Arctic (Renaud et al., 2015).

The most visible consequence of recent climate change in the European Arctic is a strong reduction in sea ice coverage, extent, and thickness. Shorter ice seasons further impact ocean temperatures and energy dynamics (Shu et al., 2022; Wang et al., 2020), shifting the ice-albedo to accelerate heat transfer from the ocean to the atmosphere during ice-free months (Screen & Simmonds, 2010; Timmermans & Marshall, 2020). At the same time, physical and chemical properties of the water are changing, manifesting in rising water temperatures, altered stratification patterns, and extended periods of light availability for marine organisms (Hop et al., 2002; Tverberg et al., 2019). These hydrographic changes, well-documented in regional studies across Svalbard fjords, influence climate and cause cascade effects throughout the marine food web (Głuchowska et al., 2016; Szeligowska et al., 2020; Weydmann-Zwolicka et al., 2021b), affecting primary production, pelagic-benthic coupling, and marine trophic networks in the European Arctic (Ambrose & Renaud, 1995; Griffith et al., 2017; Ronowicz et al., 2024).

One of the key factors driving environmental changes in the European Arctic is the so-called Atlantification, which involves an increased influx of relatively warmer and more saline Atlantic waters into higher latitudes and deeper into the Arctic Ocean (Orvik & Niiler, 2002; Polyakov et al., 2017; Schauer et al., 2004). Research conducted over nearly 30 years in the European Arctic sector, specifically around western Spitsbergen and Fram Strait (Beszczyńska-Möller et al., 2012; McPherson et al., 2026; Walczowski et al., 2012), reveals distinct warming driven by the inflow of these water masses. This phenomenon not only

contributes to the loss of sea ice and a reduction in its seasonal duration, but also alters water-column mixing processes, directly impacting the ecological dynamics of marine organisms (Ingvaldsen et al., 2021; Polyakov et al., 2020). These changes can manifest as accelerated physiological processes in animals, including zooplankton, a key component of the pelagic zone (Weydmann et al., 2018), thereby modifying their abundance, biomass, and community structure in the regions where these waters flow into higher latitudes (Głuchowska et al., 2017; Kwaśniewski et al., 2012; Stempniewicz et al., 2021; Strzelewicz et al., 2022). Furthermore, the expansion of boreal water masses, facilitates the influx and colonization of boreal organisms further north – a process commonly referred to as borealization (Hop et al., 2019; Renaud et al., 2015; Weydmann et al., 2014). This shift may significantly alter biodiversity in the pelagic zone, including meroplankton, and, consequently, the interactions between pelagic and benthic communities, particularly in the Arctic shelf and fjord regions (Descôteaux et al., 2021; Ershova et al., 2019). It might lead to intense competition for habitat and food resources while also intensifying predation pressure. Consequently, increased competition for habitat and food, alongside altered predation pressure, is driving a long-term reorganization of marine biodiversity that affects biological processes from pelagic food webs to benthic assemblages (Mańko et al., 2020; Ramondenc et al., 2025; Ronowicz et al., 2024; Sowa et al., 2023; Wassmann et al., 2015).

Zooplankton is widely recognized as a key biological indicator due to its specific correlations with distinct water masses. Analyzing zooplankton taxonomic structure and its shifts in the environment allows scientists to track the influx of Atlantic waters and assess borealization in sub-Arctic and Arctic regions (Głuchowska et al., 2017; Weydmann et al., 2014; Weydmann et al., 2018). Thus, changes in zooplankton communities can serve as an effective tool for assessing responses to global warming, Atlantification, and regional or local environmental changes (Kwaśniewski et al., 2012; Schrage et al., 2025; Weydmann-Zwolicka et al., 2021a).

1.2 Meroplankton definition

Meroplankton is a temporary part of zooplankton and consists mainly of organisms that spend part of their life cycle in the pelagic environment, typically ranging from hours to months (Mileikovsky, 1971). It includes the larval stages of both benthic and some nektonic organisms (Figure I. 1) (Thorson, 1950). For this study, the term "meroplankton" refers to the larvae of marine benthic invertebrates (e.g., polychaetes, echinoderms, crustaceans, and mollusks) (Young et al., 2002). These organisms spend their larval phase in the water column before

metamorphosing into juveniles or adults and settling on the seafloor (Scheltema, 1986). While in the water column, they constitute a large portion of the zooplankton, alongside holoplankton – organisms that, in contrast to meroplankton, spend their entire life cycle in the water column (Larink & Westheide, 2011).

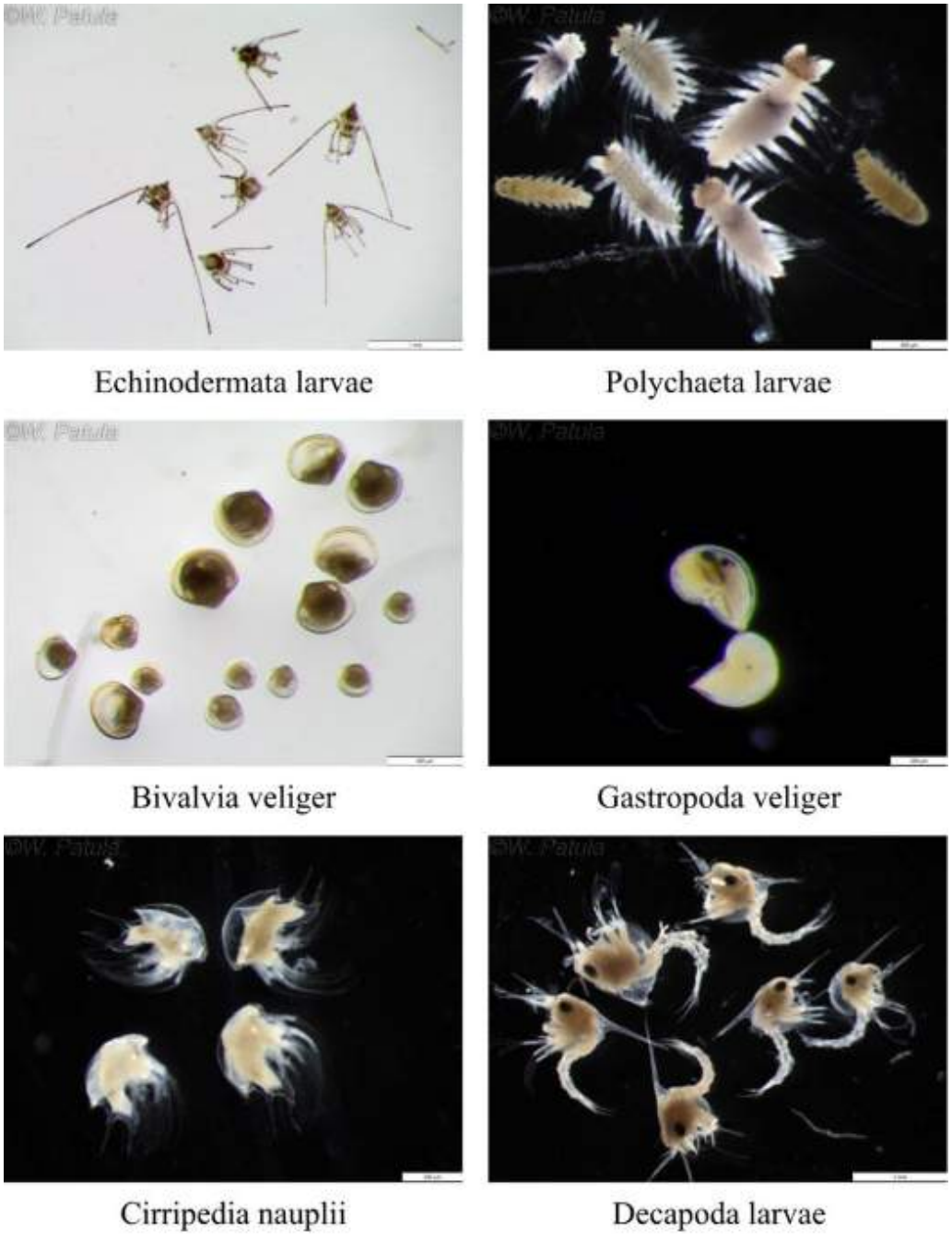

Figure I. 1 Examples of marine benthic invertebrate larvae of major meroplankton groups. Photo credit: W. Patuła.

Larvae of marine benthic invertebrates are characterized by a brief presence in the water column and high sensitivity to environmental changes affecting their physiological and

morphological development. Their pelagic phases are closely linked to the physicochemical properties of seawater (including fluctuations in temperature, salinity, and primary production), demonstrating a rapid response to disturbances in the water column, far quicker than the adult form on the seafloor (Figure I. 2) (Metaxas, 2001; Scheltema, 1986; Thorson, 1950). Furthermore, the complex life cycles of these organisms render key developmental processes – including reproductive success, dispersal, and the colonization of new habitats – highly vulnerable to climate-induced environmental shifts. Therefore, such warming-driven changes can potentially alter recruitment patterns long before associated stress manifests within the benthic environment itself (Ambrose & Renaud, 1995; Griffiths et al., 2017; Metaxas, 2001; Ronowicz et al., 2024; Schrage et al., 2025; Sowa et al., 2023; Thorson, 1950). Consequently, detailed monitoring of the dynamics and structure of meroplankton assemblages provides invaluable data at a high temporal and spatial resolution, capturing the ongoing reorganization of Arctic marine ecosystems, and provides a dynamic framework to assess resilience and the mechanisms driving future trajectories under ongoing warming (Ershova et al., 2019; 2021; Hop et al., 2019; Ramondenc et al., 2025; Weydmann-Zwolicka et al., 2021b).

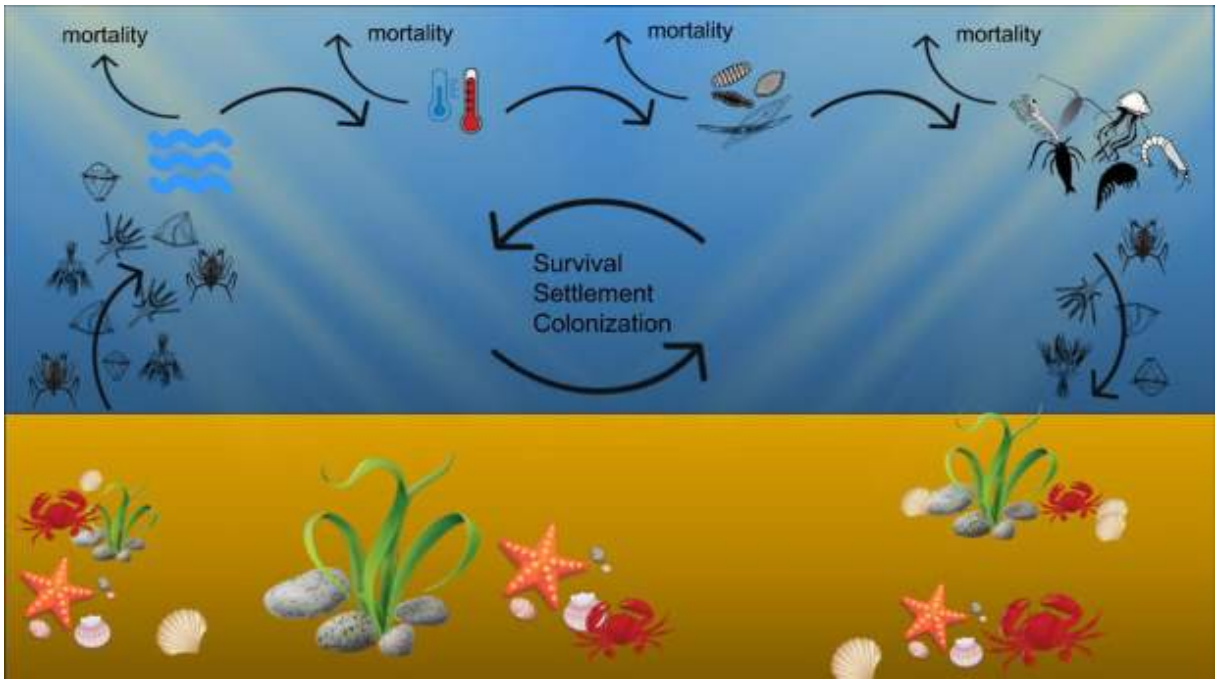

Figure I. 2 Diagram of a generalized life cycle of a benthic invertebrates with a meroplanktonic larval stage (modified based on Maldonado & Young, 2009).

The degree of larval sensitivity depends directly on their life-history strategies. Benthic invertebrates have evolved various developmental strategies that determine how larvae released into the water column utilize food resources (Milekovsky, 1971):

- Planktotrophic larvae – suspended in the water column, these larvae feed primarily on phytoplankton (relying on bloom periods) or microzooplankton. Benthic organisms are highly productive, releasing high numbers of eggs into the water column during the time of reproduction. These eggs can survive in the pelagic zone for a long time. Their survival success strongly depends on their timing relative to phytoplankton blooms. Therefore, if there is no match, larvae face a high risk of mortality (Cushing, 1990; Thorson, 1950).
- Lecithotrophic larvae – this type of larva does not actively feed in the water column, instead, it relies on yolk reserves, rich in lipids and proteins inherited from a parental organism. Although often larger, they are usually produced in smaller numbers due to the associated reproductive effort and spend much less time in the water column than planktotrophic larvae. This strategy may be the dominant type in polar and deep-sea environments, where food availability is rare or absent (Marshall & Keough, 2007; Pearse et al., 1991).
- Demersal larvae – this developmental mode is linked to the benthos and is non-pelagic. Some benthic species skip the pelagic phase in their reproductive strategies through direct development, parental care (brooding), or the production of demersal larvae that remain in the immediate vicinity of parent individuals (the near-bottom zone). In such cases, although dispersal and colonization of new areas are hindered, local recruitment success and development under favourable environmental conditions are enhanced, as seen, for example, in the certain families of Bryozoa (Kukliński et al., 2013).

1.3 The role of meroplankton in marine ecosystems

Meroplankton plays a fundamental role in marine ecosystems as a dual-directional bridge within pelagic-benthic coupling (Graf, 1992; Rowe et al., 1975). It facilitates an upward flux of energy and biomass from the benthos to the pelagic zone when adult benthic organisms release larvae into the water column in synchronization with environmental cues and sea-ice dynamics (Daase et al., 2021). On the other hand, it drives a downward flux from the pelagic zone back to the benthos when surviving larvae complete their development, undergo metamorphosis, and settle onto the seafloor, thereby replenishing benthic populations and transferring significant organic biomass to the benthic environment (Griffiths et al., 2017). Through this dual role, meroplankton serves as a central engine in the transfer of organic matter and the flow of energy. In the water column, larvae provide a rich source of high-quality food for other pelagic organisms, including zooplankton, fish, and filter feeders (Dalpadado et al., 2016). Organisms feeding on meroplankton transform this organic matter

into energy accessible to higher trophic levels, while also contributing to the microbial loop and primary production cycles (Wassmann et al., 2015). However, these early developmental stages are highly sensitive to climate change, including rapidly shifting conditions such as variations in water temperature, salinity, and food availability. Such environmental changes can significantly impact larval development and settlement success (Griffiths et al., 2017; Hays et al., 2005), directly disturbing communities within the water column as well as underlying benthic populations (Renaud et al., 2015).

In polar regions, maintaining a pelagic larval stage involves functional and ecological risks for benthic organisms due to extreme seasonality, fluctuating water temperatures, and narrow time windows of food availability during short phytoplankton blooms (Thorson, 1950). Nevertheless, pelagic larval development remains a common strategy in high-latitude environments because of the ecological advantages it provides. Releasing larvae into the water column reduces local benthic competition for space and food resources on the seafloor (Mileikovsky, 1971). Furthermore, it facilitates long-distance larval dispersal, supporting the colonization of new habitats, particularly during periods of high primary production (Ershova et al., 2019; Scheltema, 1986). Because primary production in polar regions is heavily constrained by sea ice cover, low temperatures, and the duration of the polar night (Hop et al., 2002), the main influx of organic matter into the pelagic zone is restricted to a short period of spring blooms (Ambrose & Renaud, 1995). To maximize reproductive success during this narrow window, benthic organisms have evolved reproductive cycles closely synchronized with the seasonal pulses of pelagic production events (Søreide et al., 2022). Environmental events such as rapid increases in water temperature and shifts in light availability trigger larval release, ensuring that offspring enter the water column when food resources (such as diatoms and microzooplankton) are most abundant. This synchronization enhances metabolic rates, allowing larvae to accelerate early developmental stages, shorten their pelagic duration, and minimize the impact of predation (Allen, 2008; Assmy et al., 2023; Griffiths et al., 2017).

However, climate-driven warming may impact this evolutionary timing through the mechanism described by Cushing's (1990) "match-mismatch" hypothesis. While rising ocean temperatures can cause phytoplankton blooms to occur earlier in the season, many benthic organisms still rely on fixed photoperiods or slower temperature shifts to time their reproduction (Edwards & Richardson, 2004; Fernandes et al., 2012). This decoupling can result in larvae entering the water column during the late phase or after the peak of a bloom when food supplies are already depleted. With reduced access to food, larvae experience prolonged development, increased mortality, higher predation risk, and lower metamorphosis success

(Pechenik, 1998; Rumrill, 1990), thereby reducing recruitment rates and reshaping the overall structure of benthic communities (Carroll & Ambrose, 2012).

1.3.1 Meroplankton dispersal and hydrographic connectivity

Many benthic organisms have limited ability to move; therefore, the success of colonizing other regions or habitats depends on hydrodynamic processes within the water column, linked to ocean currents, which can transport larvae over large distances (Pineda et al., 2007; Scheltema, 1986). Here, two main mechanisms can be distinguished: (i) advection and population connectivity, where long-distance larval transport links distant subpopulations and facilitates gene flow between regions (Cowen & Sponaugle, 2009; Descôteaux et al., 2022); and (ii) retention, where local bathymetry, keep larvae close to the parent organisms, such as in fjords or bays, which ensure self-recruitment and population stability (Cottier et al., 2010; Ronowicz et al., 2024).

Larval dispersal via transport within water masses is the primary mechanism for colonizing new areas (Scheltema, 1986). Such transport is particularly significant in polar regions influenced by drastic environmental changes such as retreating glaciers exposing new habitats, or shifts in hydrological conditions (e.g., rising seawater temperatures and salinity linked to the influx of Atlantic waters into the Arctic Ocean, a process known as "Atlantification") (Ingvaldsen et al., 2021; Polyakov et al., 2020). Recruitment success is strongly correlated with the duration of the larval stage in the water column, and a longer period allows for a wider geographic expansion (Shanks, 2009). Furthermore, the response to climate change plays a crucial role because, driven by Atlantification, larvae may reach previously inaccessible or unfavourable areas, altering local biodiversity and driving the borealization of the Arctic benthic communities (Renaud et al., 2015; Weydmann et al., 2014).

Population genetics provides essential tools for measuring the consequences of larval dispersal and population connectivity. Extensive dispersal ranges suggest a high potential for gene flow, which can result in low genetic differentiation across broad geographic scales in many benthic organisms (Hellberg, 2009). Opposite, topographic barriers, local retention systems, or the organisms' behavioural adaptations (e.g., in fjords or glacial bays) can create cryptic population structures (Cowen & Sponaugle, 2009); therefore, founder effects and genetic bottlenecks during the colonization of new areas may lead to the establishment of only a subset of the source population's gene pool (Wares & Cunningham, 2001). Furthermore, post-settlement selection occurs, where genetic studies reveal differences between the larval pool

and surviving adults, potentially indicating strong environmental pressure or natural selection in harsh polar regions (Toonen & Grosberg, 2011).

1.4 Pelagic-benthic coupling and life-history strategies in the Arctic

Marine ecosystems can be divided into pelagic (water column) and benthic (seafloor) environments, differing not only in the organisms that inhabit them but also in the processes that occur there and the factors that influence them. While historically studied separately, these realms are linked by continuous interaction through the exchange of carbon, nutrients, and organisms, a process known as "pelagic-benthic coupling" (Graf, 1992; Griffiths et al., 2017; Rowe et al., 1975). As generally defined by Hargrave (1973), this coupling is a functional relationship connecting pelagic processes, such as the microbial loop, temporal mismatches in production, seasonality, and water temperature changes (Eilertsen et al., 1989; Graf, 1992; Piepenburg et al., 1997; Wassmann et al., 2003), with benthic parameters including community structure, biomass, feeding behaviour, reproductive cycles, and geochemical processes (Ambrose & Renaud, 1995, 1997; Graf, 1989; Grebmeier & McRoy, 1989; Hobson et al., 1995). Looking at the whole ecosystem, this exchange of energy, mass, and nutrients plays an important role in the functioning of food webs and biogeochemical cycles (Griffiths et al., 2017). These processes interact with pelagic factors like primary production, nutrient concentrations, sea-ice cover, and sedimentation rates. As shown in the western Barents Sea (Renaud et al., 2008) and Fram Strait (Ramondenc et al., 2025), the efficiency and timing of coupling depend on local oceanographic conditions and sea-ice dynamics driving the biological carbon pump.

Several main mechanisms drive pelagic-benthic coupling. Vertical carbon flux is driven by sinking organic particles, which are often regulated by planktonic community structure (Ramondenc et al., 2025). During rapid spring blooms, phytoplankton and ice algae deliver large quantities of fresh, high-quality organic matter to the seafloor with limited water-column degradation, directly stimulating benthic biomass (Grebmeier & Barry, 1991; Hobson et al., 1995). Biological activities such as bioturbation, bioirrigation, benthic suspension feeding, diel vertical migration (DVM), and pelagic larval stages further modify material fluxes, while the discharge of inorganic nutrients from bottom sediments resupplies the water column, stimulating primary production (Griffiths et al., 2017). However, these processes depend on light availability, temperature, and depth (Ronowicz et al., 2024) and are vulnerable to climate and anthropogenic pressures, including sea-ice loss, warming, eutrophication, and fishing (Grebmeier & Barry, 1991; Griffiths et al., 2017).

An important feature of pelagic-benthic coupling is the relationship between pelagic phenology and benthic reproductive strategies. In polar ecosystems, primary production is limited to a short seasonal window, linking the life-history strategies of holoplankton and meroplankton to sea-ice dynamics (Daase et al., 2021). Meroplanktonic organisms rely on an ecological match in which adult benthic organisms must time larval release to coincide with ice-algae blooms and high food availability. Successful larval survival, transport, and settlement directly link pelagic food webs to the support and structure of benthic populations (Pearse et al., 1991; Thorson, 1950).

While pelagic larvae must adapt to this short window of food availability, adult benthic organisms face distinct ecological pressures, such as extreme seasonality, cold temperatures, and a pulsed food supply (Gray & Elliott, 2009). Benthic species have evolved specific adaptations: many Arctic organisms (such as long-lived bivalves, brachiopods, and cold-water corals) exhibit slow growth, delayed maturity, and extended lifespans (Brey, 1999). Many polar species synchronize gametogenesis with the annual organic flux and store large lipid reserves during summer to fuel reproduction through the polar winter (Clough et al., 1997). Furthermore, while some species produce planktotrophic larvae feeding in the water column, many utilize lecithotrophic development, producing yolk-rich eggs that allow larvae to develop independently when food is scarce (Marshall & Keough, 2007; Thorson, 1950). Ultimately, the success of these strategies depends on the efficiency of pelagic-benthic coupling, as changes in organic matter flux directly drive benthic recruitment and population dynamics (Grebmeier & Barry, 1991; Griffiths et al., 2017).

1.5 Environmental drivers of larval distribution across spatial and temporal scales

The distribution patterns, dispersal, recruitment, and colonization success of meroplanktonic larvae are governed by complex interactions among physical, chemical, and biological forces operating across diverse environments at both spatial and temporal scales (Metaxas, 2001; Thorson, 1950). Due to the varying duration a given larva spends in the water column before settling on the seabed, it is highly sensitive and exposed to fluctuating environmental conditions (Pineda et al., 2007; Scheltema, 1986). Consequently, determining how environmental variability shapes meroplankton communities requires long-term studies, the selection of distinct habitats, and an understanding of their vertical distribution within the water column (Hop et al., 2002; Węsławski et al., 2010).

1.5.1 Temporal and interannual variability of zooplankton communities

To understand the mechanisms and long-term dynamics of marine ecosystems, particularly temporal and interannual variability, robust temporal research designs are required; these must account for multi-year variability that either masks or interacts with climate-change signals (Stübner et al., 2016; Weydmann-Zwolicka et al., 2021b). Long-term time-series data are invaluable in ecological research, enabling the identification of baseline characteristics of marine communities, their variability, and their responses to various environmental conditions and changes (Søreide et al., 2022). In the high Arctic latitudes, a region subject to the pressures of Atlantification and constant water mass variability, interannual studies encompass both the constant and temporary components of the pelagic food web.

The primary component of zooplankton, holoplankton, rapidly reflects hydrographic conditions, temperature anomalies, and peaks in primary production in the marine environment (Assmy et al., 2023; Kwaśniewski et al., 2012). On the other hand, meroplankton, the temporary zooplankton component, is sensitive to changes in environmental factors such as temperature and food availability, as well as to the reproductive cycles of their benthic parent organisms (Stübner et al., 2016; Weydmann-Zwolicka et al., 2021a). Detecting such signals in both holoplankton and meroplankton is crucial for capturing and distinguishing short-term fluctuations from long-term ecological changes and shifts in trophic relationships (Głuchowska et al., 2017; Schrage et al., 2025).

1.5.2 Vertical stratification and physical barriers in the water column

The vertical dimension of the water column plays a crucial role in the distribution and transport of pelagic larvae, whose dispersal depends heavily on ocean currents (Metaxas, 2001; Pineda et al., 2007). Vertical gradients, defined by pycnoclines, thermoclines, and haloclines, act as natural barriers for planktonic organisms or zones of accumulation. These gradients can restrict vertical migration, cause the aggregation of suspended particles, and decouple surface transport from processes occurring in deeper layers of water (Arellano et al., 2012; Metaxas & Young, 1998b). Since meroplankton larvae often exhibit specific behaviours, such as ontogenetic or diel vertical migrations, in response to changes in density and temperature, physical stratification directly determines whether larvae remain in favourable nursery areas or are transported to the open sea (Cronin & Forward, 1986; Mazurkiewicz et al., 2024; Queiroga & Blanton, 2005). Moreover, some vertical boundaries can create specific microenvironments in which extreme temperatures and salinity levels approach the limits of organisms' physiological tolerance, directly influencing their metabolic

and developmental rates. Therefore, that interrelationship determines settlement success, spatial distribution patterns, and post-metamorphosis survival in dynamic marine ecosystems (Metaxas, 2001; Pechenik et al., 1998).

1.5.3 Environmental differences between open waters, shelf, and fjord habitats

The spatial diversity of habitats occupied by the larvae of marine benthic invertebrates, ranging from open-ocean pelagic zones and dynamic shelf zones (influenced by both land and open waters) to distinct fjordic systems characterized by unique hydrological conditions and anthropogenic pressures, significantly determines the physicochemical properties of the environment in which a given larva develops and completes its life cycle (Hop et al. 2002; Ormańczyk et al. 2017). Each of these habitats affects meroplankton and imposes specific environmental pressures:

- Open ocean waters (pelagic zone) – here, large-scale oceanic circulation exerts a strong influence, involving the advection of deep-water masses and the associated high flow energy (Nilsen et al. 2016; Orvik & Niiler 2002). In such an environment, larvae are exposed to constant temperature fluctuations, dynamic long-distance transport, and the influence of oceanic frontal zones, processes heavily driven by regional advective pathways (Głuchowska et al., 2017; Weydmann et al., 2014). These factors can, on the one hand, facilitate connectivity between populations while, on the other, isolate them from suitable benthic settlement sites (Banse 1986; Cowen & Sponaugle 2009).
- Shelf regions – characterized by complex interactions between coastal currents, sea-ice dynamics (including cover duration), and pelagic-benthic coupling (Carroll & Ambrose, 2012; Pawłowska et al., 2011; Renaud et al., 2008) – serve as dynamic transition zones for larvae; here, mixing-induced nutrient enrichment fosters high primary production, and thus food availability for meroplankton development, enhancing multidimensional trophic interactions (Trudnowska et al., 2012). Thereby enhancing their chances of survival. On the other hand, however, such dynamic changes at the interface of hydrographic boundaries can push organisms toward open waters, thereby increasing their mortality (Ambrose & Renaud, 1995; Descôteaux et al., 2022; Grebmeier & McRoy, 1989).
- Fjord systems – function partly as enclosed basins subject to intense freshwater runoff from melting glaciers or terrestrial rivers. Furthermore, they are influenced by local upwelling and by the intense sedimentation of organic and inorganic glacial material (Cottier et al., 2010; Szeligowska et al., 2022; Włodarska-Kowalczuk et al., 2016). While

restricted water circulation favours larval retention and the maintenance of stable local populations (Hop et al., 2006, 2019; Stübner et al., 2016; Walkusz et al., 2009), the influx and sedimentation of glacial material severely limit feeding efficiency by clogging filtration apparatuses, thereby inducing osmotic and physiological stress in developing meroplanktonic larvae (Hop et al., 2023; Włodarska-Kowalczuk et al., 2007). Gradients specific to this environment directly shape the potential for larval retention or dispersal, the level of metabolic stress, and the recruitment success of local benthic invertebrate populations (Metaxas, 2001; Kuklinski et al., 2013; Thorson, 1950).

1.6 Methodological advances in meroplankton research: from morphology to metabarcoding

Not long ago, classical methods for studying zooplankton (including meroplankton) relied on labour-intensive microscopic identification. However, recent technological advances have shifted how scientists study and monitor changes in marine environments (spanning both pelagic and benthic realms and their relationships) (Descôteaux et al., 2021, 2022; Ershova et al., 2019). Rapid climate change, progressive Atlantification, and the resulting pressures on Arctic and other ecosystems drive the need for new tools capable of providing higher temporal and taxonomic resolution in the study areas (Hop et al., 2019; Weydmann-Zwolicka et al., 2021b). In this context, combining classical morphological taxonomic analysis with rapidly evolving molecular methods could improve the monitoring of these sensitive marine ecosystems, enabling the discovery of hidden biological and functional diversity and allowing for the testing of hypotheses with greater accuracy (Ershova et al., 2019, 2021; Hop et al., 2019; Schrage et al., 2025; Walczyńska et al., 2019; Weydmann-Zwolicka et al., 2021a).

1.6.1 Traditional morphology-based taxonomy and its challenges

The traditional taxonomic approach to analyzing zooplankton, and meroplankton in particular, has long relied on the microscopic identification of specific morphological traits. This method undoubtedly forms the foundation of ecological research worldwide, including in polar regions, enabling studies on both the baseline structure and long-term dynamics of these communities (Głuchowska et al., 2016; Kwaśniewski et al., 2012; Scheltema, 1986; Thorson, 1950). However, the morphological analysis of meroplankton is often fraught with inaccuracies due to identification difficulties, as many marine invertebrate larvae exhibit high morphological plasticity, displaying cryptic variation across developmental stages or resembling even closely related taxa. Accordingly, taxonomic identification becomes extremely

challenging, and often impossible, when trying to classify specimens to the genus or species level (Ershova et al., 2019; Metaxas, 2001; Weydmann et al., 2018). Furthermore, in an era of new technological and methodological developments, the classical taxonomic approach faces significant difficulties: a lack of taxonomic experts, funding challenges for morphology-based research, and doubts among journal editors about publishing studies that rely on such methodologies (Dupérré, 2020; Kotov & Gololobova, 2016). These limitations mean that large-scale, frequent ecological monitoring is time-consuming, costly, and increasingly prone to errors arising from subjective assessment (Głuchowska et al., 2017; Hop et al., 2019; Walczyńska et al., 2019).

1.6.2 Application of High-Throughput Sequencing (HTS) and DNA metabarcoding in marine ecology

To overcome the limitations of traditional methods for analyzing organismal communities, modern science is increasingly turning to molecular techniques such as high-throughput sequencing (HTS), including DNA barcoding of individual specimens (Descôteaux et al., 2021) and DNA metabarcoding of environmental samples. By relying on standardized, specific genetic markers, such as the fragment of universal cytochrome c oxidase subunit I (*cox1*) gene for invertebrates (Leray et al., 2013) or the V1-V2 region of 18S rRNA gene (18S) (Leduc et al., 2019; Qihang et al., 2022; Wangensteen et al., 2018). These methods enable the rapid assessment and monitoring of complex eukaryotic assemblages in marine environments across broad spatial and temporal scales (Ríos-Castro et al., 2021). This approach reduces analysis time and facilitates the detection of rare taxa or those difficult to identify using standard morphology-based methods; it also enables the detection of organisms that might otherwise be destroyed during sampling or sample preservation.

However, like any other technique, this molecular approach has its limitations. A primary drawback is the inability to determine the community's numerical structure, as the number of sequence reads does not directly correlate with actual biomass, organism density, or abundance within a sample. Genetic analysis is influenced by numerous variables, such as DNA extraction efficiency, variations in gene copy numbers across individuals and taxa, and errors inherent in the PCR process itself (Ershova et al., 2019; 2021). A second key issue is that such analyses sequence everything present in the sample, including dead organisms and detritus, which distorts the assessment of the living component of the community. A third challenge lies in incomplete reference databases against which sequences found in a sample must be matched;

if a certain sequence is missing from a database, it remains either unassigned or, worse, misidentified, depending on the quality of the database's curation.

1.6.3 Integration of morphological and molecular approaches for assessing larval diversity

Despite the respective advantages and disadvantages of each of the described methods, they are frequently presented globally as competing analytical approaches. However, none of them is entirely sufficient on its own; naturally, the choice depends on the research questions posed and the specific information sought from the analysis. The most appropriate approach, and one that is gradually being adopted (despite some lingering opposition) is to combine these two methods as complementary tools, which offers a promising way to uncover biodiversity, including cryptic species forms, and to track the dynamics of change in marine ecosystems more precisely (Pires & Marinoni, 2010; Salis et al., 2024). Such complementarity is already being applied in polar and Arctic regions, for instance, in studies by Coguiec et al. (2021), Descôteaux et al. (2021), and Mazurkiewicz et al. (2024), representing a highly promising direction for both biodiversity research and the monitoring of large-scale changes in marine ecosystems. This approach enables cross-validation of method effectiveness and rigorous data verification. Above all, it provides a comprehensive picture of environmental processes, thereby undoubtedly enhancing the quality of inferences drawn from research questions and hypotheses (Pires & Marinoni, 2010; Salis et al., 2024; Schrage et al., 2025; Walczyńska et al., 2019).

1.7 Aims, objectives, and outline of the thesis

This study aimed to assess the variability and spatial distribution of meroplankton in the European Arctic, especially within the West Spitsbergen Current and a West Spitsbergen fjord (Kongsfjorden, Svalbard Archipelago) – a model system characterized by distinct hydrological conditions and exposed to ongoing environmental changes. In addition to routine qualitative and quantitative morphological analyses based on microscopy, metabarcoding (high-throughput DNA sequencing) was employed as a rapid, precise method to assess the biodiversity of marine meroplankton assemblages for the planned doctoral dissertation. To ensure consistent and accurate morphological identification across all samples, a comprehensive taxonomic reference atlas of meroplankton morphotypes was specially developed for this study. By combining traditional identification techniques with modern genetic methods, it was possible to obtain data regarding meroplankton abundance, larval types, and previously unrecognized taxonomic diversity within the studied community.

This thesis is divided into 6 parts. Foremost, **Chapter I** presents an extended general introduction that provides the background and context for the study and subsequently outlines the research aims, specific objectives, and hypotheses. **Chapter II** describes the development of an atlas of marine benthic invertebrate larvae as part of the study's methodological framework. The main part of the thesis comprises **Chapters III**, **IV**, and **V**, which are structured as a set of manuscripts for publication and address the main aims, objectives, and hypotheses. Here, it is worth noting that the methodology in these chapters is not presented as a separate paragraph at the beginning, since it differs across chapters. Hence, it is easier to follow when kept within each chapter. The summary chapter (**Chapter VI**) contains a summary discussion of the thesis findings, conclusions, and future directions for meroplankton studies. Finally, the entire cited scientific literature is listed, after which the lists of tables, figures, and supplementary data for the main chapters are provided.

While each chapter addresses specific study aims within its scope, they collectively address broader research questions and hypotheses that unify the entire body of work. To bridge the gap between methodological development, broad spatial-temporal trends, and fine-scale physical dynamics, this thesis addresses four primary research questions:

1. What is the true taxonomic diversity of Arctic meroplankton, and can molecular tools reveal hidden diversity undetected by traditional morphology?

2. How do climate change and the ongoing Atlantification over the past two decades influence the abundance and taxonomic composition of meroplankton in the European Arctic?

3. How do environmental and hydrographic gradients along the West Spitsbergen Current shape the spatial variability and diversity of larval assemblages?

4. Does the presence of physical water-column barriers, specifically the halocline, determine the vertical distribution and taxonomic separation of meroplankton?

To address these questions, four main hypotheses were formulated:

H.1: Temporal and spatial variability in the abundance and taxonomic composition of benthic invertebrate larvae is driven by temperature and salinity gradients (from south to north) resulting from the progressive inflow of warm Atlantic water over the last two decades (addressed in **Chapter III**);

H.2: Shifts in hydrographic conditions (temperature, salinity, chlorophyll *a*) differentiate the spatial distribution and community structure of meroplankton across regional scales (addressed in **Chapters III** & **V**);

H.3: The presence of a halocline acts as an environmental barrier that significantly differentiates meroplankton taxonomic composition within the water column (addressed in **Chapter IV**);

H.4: Metabarcoding, as an advanced molecular tool, reveals hidden meroplankton diversity that remains undetected through traditional morphological approaches (addressed in **Chapter V**).

To address these overarching hypotheses, specific objectives and sub-hypotheses were established within individual chapters:

Chapter II

Objective:

Obj. II. 1: To develop a comprehensive photographic atlas of meroplankton morphotypes from the European Arctic and the West Norwegian Coast, providing a standardized visual reference needed for accurate meroplankton identification in the rapidly changing Arctic and sub-Arctic regions.

Chapter III

Objectives:

Obj. III. 1: to quantify interannual variability in meroplankton taxonomic composition across a 16-year time series;

Obj. III. 2: to identify environmental drivers shaping larval assemblages;

Obj. III. 3: to assess how spatial gradients influence meroplankton community structure and diversity;

Obj. III. 4: to determine if major larval taxonomic groups exhibit any shifts in abundance and spatial distribution in response to environmental variability.

Hypotheses:

H.III. 1: Spatial differences, particularly across the shelf to open waters transition, combined with hydrographic conditions, exert a stronger control on the meroplankton communities than the latitudinal variation (from south to north);

H.III. 2: Intensified Atlantic water inflow leads to community reorganization, favouring ubiquitous taxa and reducing overall taxonomic diversity compared to colder periods;

H.III. 3: Meroplankton community composition may serve as an early biological indicator of Atlantification, due to its possible rapid response to environmental changes.

Chapter IV

Objective:

Obj. IV. 1: to assess the influence of a halocline on the vertical distribution of meroplankton in relation to environmental conditions in the European Arctic.

Hypothesis:

H.IV. 1: Halocline plays a crucial role in structuring meroplankton communities by acting as a barrier for larvae of benthic invertebrates, resulting in differences in their taxonomic composition above and below this pronounced vertical salinity gradient.

Chapter V

Objectives:

Obj. V. 1: to assess the effectiveness of integrated taxonomic approaches: to what extent is the detection of meroplankton diversity improved by the integration of morphological and multi-marker genetic approaches compared to classical morphological identification alone?

Obj. V. 2: to analyze community with environment interactions: how do the taxonomic composition and distribution patterns of meroplankton reflect the diverse hydrographic regimes present along the NE Atlantic shelf?

Hypothesis:

H.V. 1: Integrating morphological, 18S rRNA, and *cox1* multi-marker data provides higher taxonomic resolution and more accurate mapping of meroplankton diversity hotspots than traditional morphological analysis alone, thereby revealing unique community responses to distinct hydrographic conditions.

Chapter II Abridged Atlas of Meroplankton – European Arctic and West Norwegian Coast

2.1 Rationale and objectives of the larval atlas

The morphological identification of marine invertebrate larvae causes a significant challenge in marine ecology. Many larval stages are cryptic and highly similar in appearance, which often leads to misidentification or inconsistent taxonomic resolution among researchers. Traditional identification keys may be outdated or lack the locally relevant reference material needed for accurate identification in the rapidly changing Arctic and sub-Arctic regions.

To address these limitations, the Atlas of Meroplankton was developed as a standardized photographic resource to support sample processing and morphotype classification. By providing comprehensive, high-resolution images of meroplankton morphotypes from the European Arctic and West Norwegian Coast, the atlas facilitates identification and promotes consistency and reproducibility in sample analysis. Importantly, this atlas served as the foundational reference for identifying larval specimens analyzed in the subsequent sections of this study.

Furthermore, this atlas is designed to serve as a practical tool for the broader scientific community. It will assist taxonomists and ecologists in identifying Arctic meroplankton, thereby improving data comparability across different monitoring programs and accelerating our understanding of how sensitive larval communities respond to ongoing climate-driven shifts in polar marine ecosystems.

2.2 Note on data reuse and publication status

The illustrated guide presented in this work is an abridged compilation of selected photographs of meroplankton morphotypes. It has been adapted from the officially published and publicly accessible online database developed within the HIMERO project (granted by the Polish National Science Center and led by Weronika Patuła). The original dataset and full web repository can be accessed at:

Patuła, W., 2025. Atlas of Meroplankton – European Arctic and West Norwegian Coast

https://www.iopan.pl/projects/HIMERO/index.php;

https://doi.org/10.48457/himero

2.3 Introduction and methodological background

This illustrative section presents documentation of meroplankton morphotypes collected during the summer seasons of 2021 and 2022 onboard R/V Oceania. Sampling was carried out across the European Arctic, encompassing the Northeast Atlantic Shelf, the West Spitsbergen Shelf, and the West Spitsbergen fjords (Hornsund, Isfjorden, and Kongsfjorden), as well as along the West Norwegian coast. This geographic range represents a unique model system characterized by varying water regimes, where warm Atlantic Water (AW) and cold Arctic Water (ArW) interface, heavily influencing sensitive larval communities.

The primary objective of this illustrated guide is to support the morphological identification of marine invertebrate larvae by presenting a high-resolution visual reference. The original data were gathered as part of the HIMERO project, which aims to uncover meroplankton diversity and monitor its shifts in it driven by different environmental conditions in the Arctic undergoing global warming.

2.4 Sample processing and image acquisition

Field Collection: Meroplankton samples were collected using a Juday plankton net with a 56 μm mesh size and immediately preserved in 95% ethyl alcohol to maintain specimen integrity for further molecular analysis.

Morphotype Classification: Larvae were examined under an Olympus SZX16 stereomicroscope and classified into subjectively defined morphotypes based on distinct diagnostic morphological characteristics.

Image Documentation: High-resolution photographic documentation was performed using Olympus cellSens Standard 2.1 software to ensure consistent analysis and scale calibration across all samples.

The following photographic plates (Table II. 1) constitute the illustrative atlas of major meroplankton groups and morphotypes identified within the study area.

Table II. 1 Photographic documentation of meroplankton morphotypes collected in the European Arctic and along the West Norwegian coast. Photo credit: W. Patuła.

ECHINODERMATA



Pluteus



Ophiopluteus1



Ophiopluteus2



Ophiuroidea Juvenile1

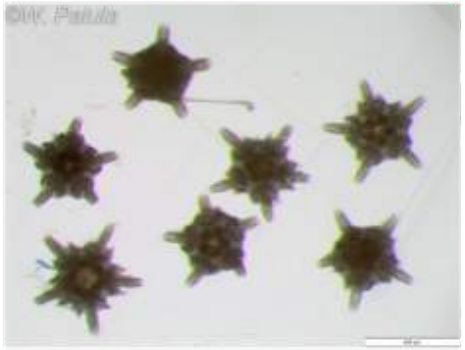

Ophiuroidea Juvenile2

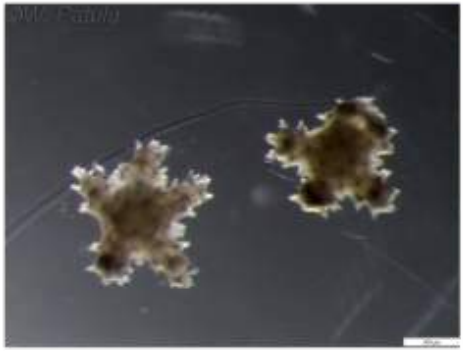

cf. Ophiuroidea Juvenile3

ECHINODERMATA cont.

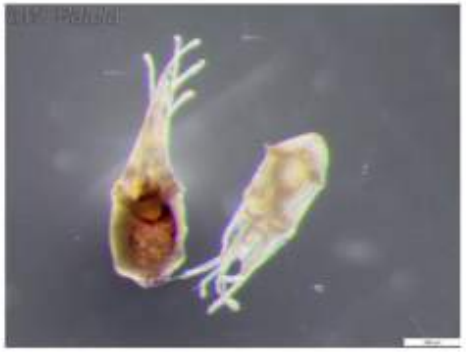

Echinopluteus1



Echinopluteus2



Echinopluteus3

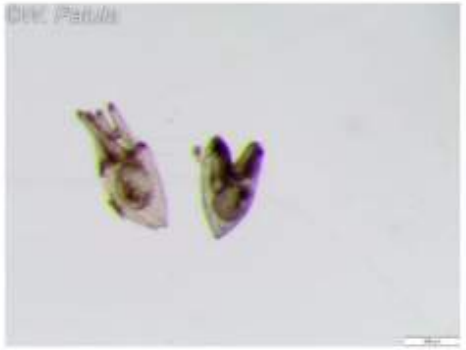

Echinopluteus4



Echinoidea Juvenile1



Auricularia

ECHINODERMATA cont.



Doliolaria/Pentactula



Brachiolaria1

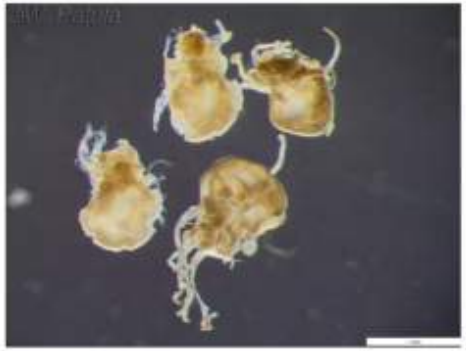

Brachiolaria2

ECHINODERMATA

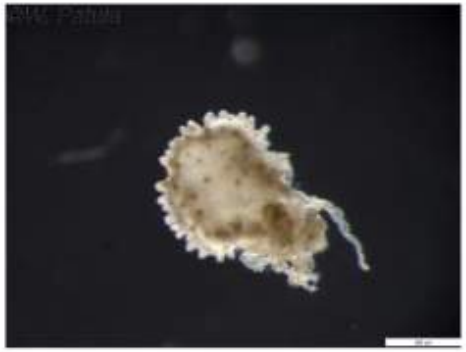

Asteroidea Juvenile1

POLYCHAETA



cf. Apmphinomidae



cf. Pectinariidae

POLYCHAETA cont.



cf. Phyllodocidae



cf. Polynoidae



cf. *Prionospio*



cf. Spionidae

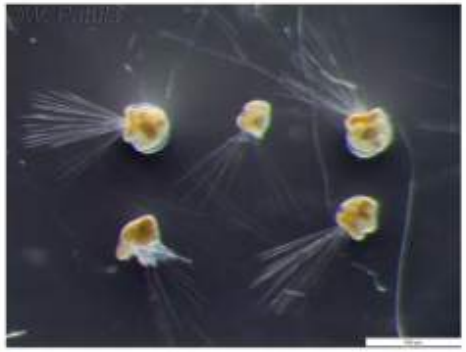

cf. Oweniidae

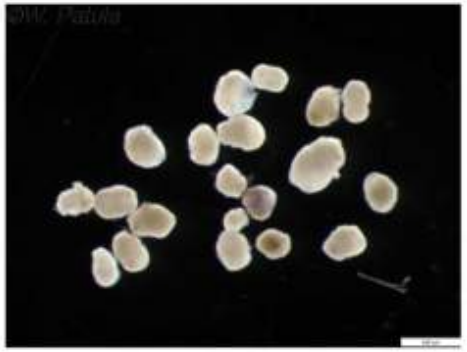

trochophorae

POLYCHAETA cont.

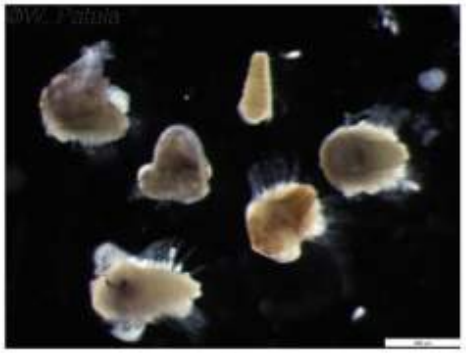

metatrochophorae

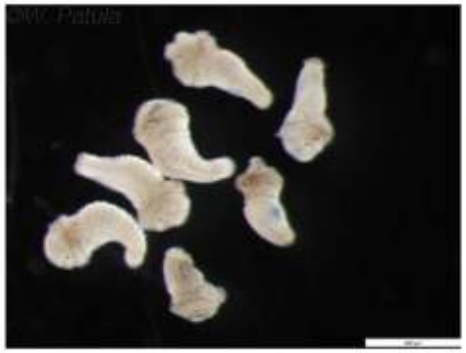

metatrochophorae



unidentified



unidentified



unidentified



unidentified

CIRRIPEDIA

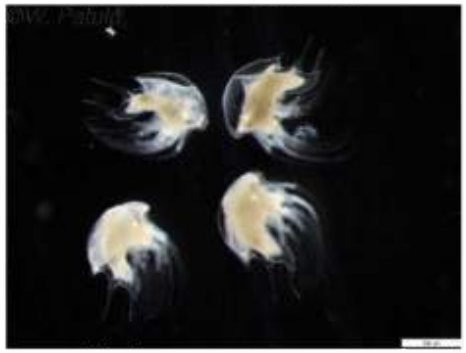

nauplii1



nauplii1



nauplii2



nauplii2



nauplii3

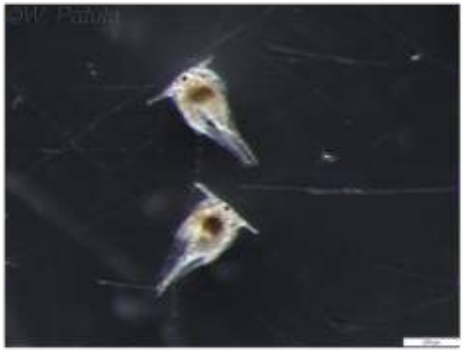

nauplii3

CIRRIPEDIA cont.



cypris1



cypris2

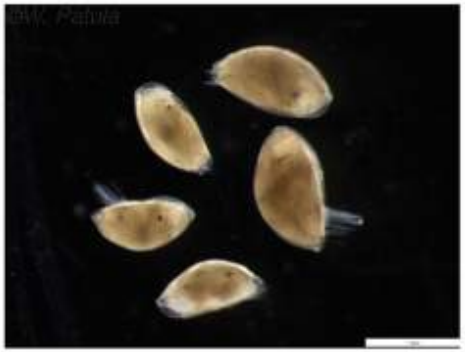

cypris3

CIRRIPEDIA

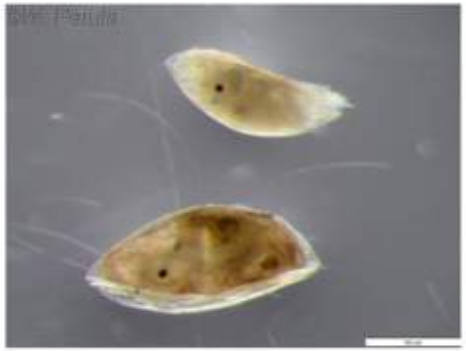

cypris1 & 3

DECAPODA



Pagurus zoea



Pagurus megalopa

DECAPODA cont.



Hyas zoea



Hyas megalopa



unidentified zoea



unidentified zoea



unidentified megalopa



unidentified megalopa

BRYOZOA

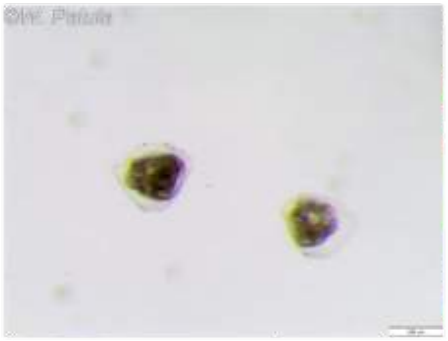

Cyphonautes1



Cyphonautes2



Cyphonautes1 & 2

BRYOZOA



Cyphonautes1 & 2

BIVALVIA

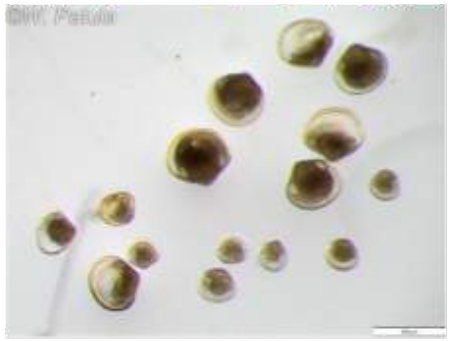

veliger

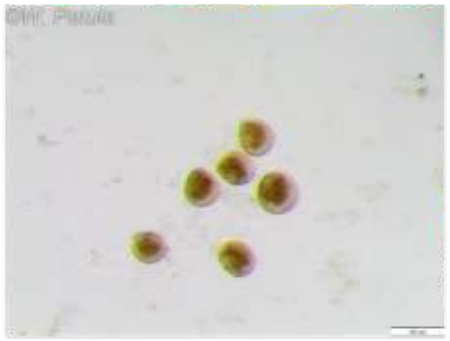

veliger

GASTROPODA



veliger

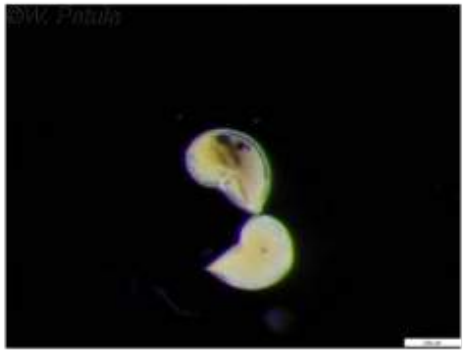

veliger



veliger

PHORONIDAE



actinotroch

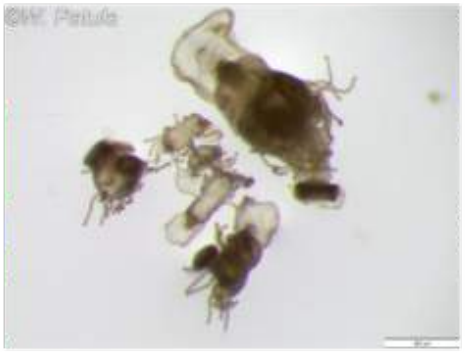

actinotroch

ASCIDIACEA



tadpole

NEMERTEA

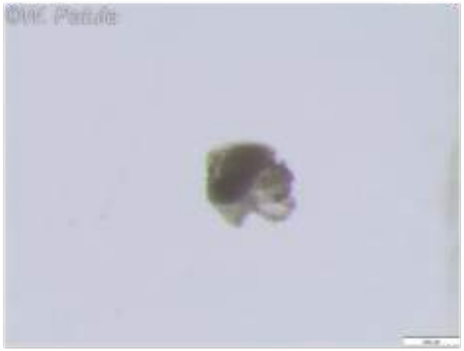

pilidium

ENTEROPNEUSTA



tornaria

ANTHOZOA

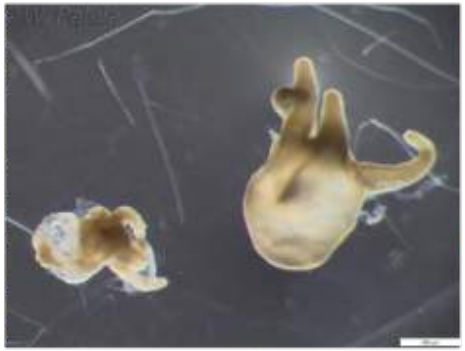

cerinula

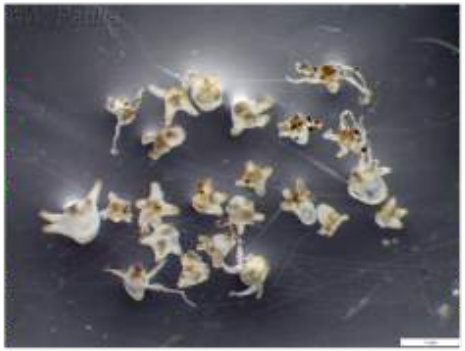

cerinula

Chapter III Long-term spatiotemporal shifts in meroplankton community composition as a signature of Arctic Atlantification

3.1 Introduction

Over the past few decades, the Arctic has been profoundly affected by global warming. Arctic temperatures are increasing much faster than in other parts of the world (IPCC, 2021), and the Arctic Ocean is warming at more than twice the global mean rate (Shu et al., 2022). The changes are mainly related to increased oceanic heat transport (Cheng et al., 2025; Tsubouchi et al., 2021), the decline in Arctic sea ice (Screen & Simmonds, 2010; Wang et al., 2020), and the shifts in ocean circulation (Timmermans & Marshall, 2020). The increasing influence of Atlantic water (AW) in the Arctic Ocean, referred to as Atlantification (Årthun et al., 2012; Polyakov et al., 2017), is associated with a warmer Atlantic inflow, salinity increase, weakened stratification, and a progressive transition of Atlantic water masses in the Arctic Ocean (e.g., Ingvaldsen et al., 2021; Polyakov et al., 2020). The West Spitsbergen Current (WSC) is the primary pathway by which Atlantic water enters the Arctic Ocean through Fram Strait (Rudels et al., 2005; Walczowski et al., 2012), and several studies highlight its significant role in conveying temperature and salinity anomalies poleward (Beszczynska-Möller et al., 2012; Głuchowska et al., 2017). Atlantification of the Arctic Ocean also affects primary producers and pelagic consumer communities, including zooplankton (Ingvaldsen et al., 2021; Mańko et al., 2020; Mańko et al., 2022a; Wassmann et al., 2015; Weydmann et al., 2018). Alongside changes in water-mass characteristics, a noticeable shift of boreal species northwards is observed in the European Arctic (Polyakov et al., 2020; Weydmann et al., 2014). The properties and strength of the Atlantic inflow through Fram Strait into the Arctic Ocean exhibit strong variability on seasonal, interannual, and decadal time scales (Beszczynska-Möller et al., 2012; McPherson et al., 2026; Stempniewicz et al., 2021), although the present contribution of AW to the Arctic Basin based on observational data is not yet adequately defined. Moreover, concurrent biological observations are scarce, limiting understanding of how changes in physical properties affect the Arctic marine ecosystem. Therefore, the biological responses of planktonic communities to intensified Atlantic Water advection, the primary driver of Arctic Atlantification, remain poorly understood and difficult to project.

Climate change significantly impacts marine ecosystems, sometimes irreversibly (Carstensen & Weydmann, 2012). Long-term observational series are the only means of obtaining information on the complex processes underlying change in marine areas, especially

in sensitive polar regions. Such datasets provide the necessary temporal resolution to reveal changes in population structure, abundance, and biodiversity, which are essential for understanding broader ecosystem functioning. Finally, sustained observations allow for the determination of trend directions and a more comprehensive understanding of ecological responses to warming, and constitute a vital basis for further research on the long-term impact of environmental shifts.

In recent years, long-term observations have shown that the zooplankton community has changed throughout the North Atlantic in response to climate change (Carstensen et al., 2019; Kwaśniewski et al., 2012; Mańko et al., 2022b; Weydmann et al., 2014; Weydmann et al., 2018). These changes are primarily driven by increased advection of warm Atlantic waters, leading to greater dominance of Atlantic-boreal over Arctic-polar assemblages. Such structural reorganizations have implications for the energy flow to higher trophic levels. Nonetheless, most studies have focused mainly on holoplankton (the majority of zooplankton), and thus little is known about the relationship between environmental conditions and meroplankton in the Arctic.

Meroplankton consist mainly of benthic invertebrate larvae that can spend from hours to months in the pelagic zone, often constituting a major portion of the zooplankton community (Głuchowska et al., 2016). These organisms play a crucial role in Arctic food webs as grazers of primary production (Michelsen et al., 2017) and as prey for planktonic predators (Allen, 2008; Short et al., 2013). Transported by ocean currents, they also facilitate the dispersal of benthic organisms, enabling the colonization of new areas (Shanks, 2009). However, during the larval phase in the pelagic environment, larvae are highly influenced by changes in, e.g., temperature, salinity, and food availability (Weydmann-Zwolicka et al., 2021), which affect their survival and settlement success (Ronowicz et al., 2024). Therefore, as meroplankton communities are sensitive to physical changes in the water, shifts in their diversity and abundance may serve as early indicators of ecosystem change. These shifts may reflect the poleward advection of boreal and sub-Arctic species (Renaud et al., 2015; Schrage et al., 2025; Weydman-Zwolicka et al., 2014) and/or the effects of Atlantification more rapidly than those observed in seafloor adult communities (Kirby et al., 2008; Lindley & Kirby, 2008; Schrage et al., 2025).

This study aimed to characterize, for the first time, changes in meroplankton composition across the broad area of WSC influence, which transports Atlantic waters into the warming Arctic Ocean. This study was designed to analyze a long-term dataset (2001-2016) in order to: (1) quantify interannual variability in meroplankton taxonomic composition across a

16-year time series; (2) identify environmental drivers shaping larval assemblages; (3) assess how spatial gradients influence meroplankton community structure and diversity; and (4) determine if major larval taxonomic groups exhibit any shifts in abundance and spatial distribution in response to environmental variability.

It was hypothesized that spatial differences, particularly across the shelf-to-open-waters transition, combined with hydrographic conditions, exert stronger control on meroplankton communities than latitudinal variation (from south to north). Furthermore, I expected that intensified Atlantic water inflow leads to community reorganization, favouring ubiquitous taxa and reducing overall taxonomic diversity compared to colder periods. Finally, it was assumed that meroplankton community composition may serve as an early biological indicator of Atlantification, given its potential for rapid responses to environmental changes.

3.2 Materials & Methods

3.2.1 Study area

The study area was located in the northeastern part of the Norwegian Sea west of Bear Island and in the northeastern part of the Greenland Sea in Fram Strait (Figure III. 1). The research region covers a broad area influenced by the Atlantic water carried northward by the Norwegian Atlantic Slope Current (NwASC) along the western open boundary of the Barents Sea, and by the West Spitsbergen Current (WSC) in Fram Strait. In Fram Strait, it comprises the West Spitsbergen Shelf (WSS; coastal area with depths <200 m) and two WSC branches, representing the WSC core and offshore branch (Beszczynska-Möller et al., 2012). The West Spitsbergen Current carries the warm and salty waters of Atlantic origin along the shelf break and upper continental slope in the eastern Fram Strait (Aagaard et al., 1987; Schauer et al., 2004) and constitutes the main source of oceanic heat and salt to the Arctic Ocean (Boyd & D'Asaro, 1994). The WSC core is represented by the narrow and strong flow of Atlantic water, originating from the Norwegian Atlantic Slope Current (Skagseth et al., 2004), while the WSC offshore branch is formed by merging AW flow from the upstream Norwegian Atlantic Frontal Current (NwAFC, Orvik & Niiler, 2002) as it reaches Fram Strait. The West Spitsbergen Shelf is dominated by cold and freshened Arctic water (ArW) carried by the Spitsbergen Polar Current (SPC; Nilsen et al., 2016), which flows around the southern tip of Svalbard, bringing Arctic-origin waters formed in the Barents Sea (Strzelewicz et al., 2022; Tverberg et al., 2019). Mixing and exchange between AW and ArW occur along the West Spitsbergen Polar Front (Strzelewicz et al., 2022), separating the WSC core from the WSS water masses.

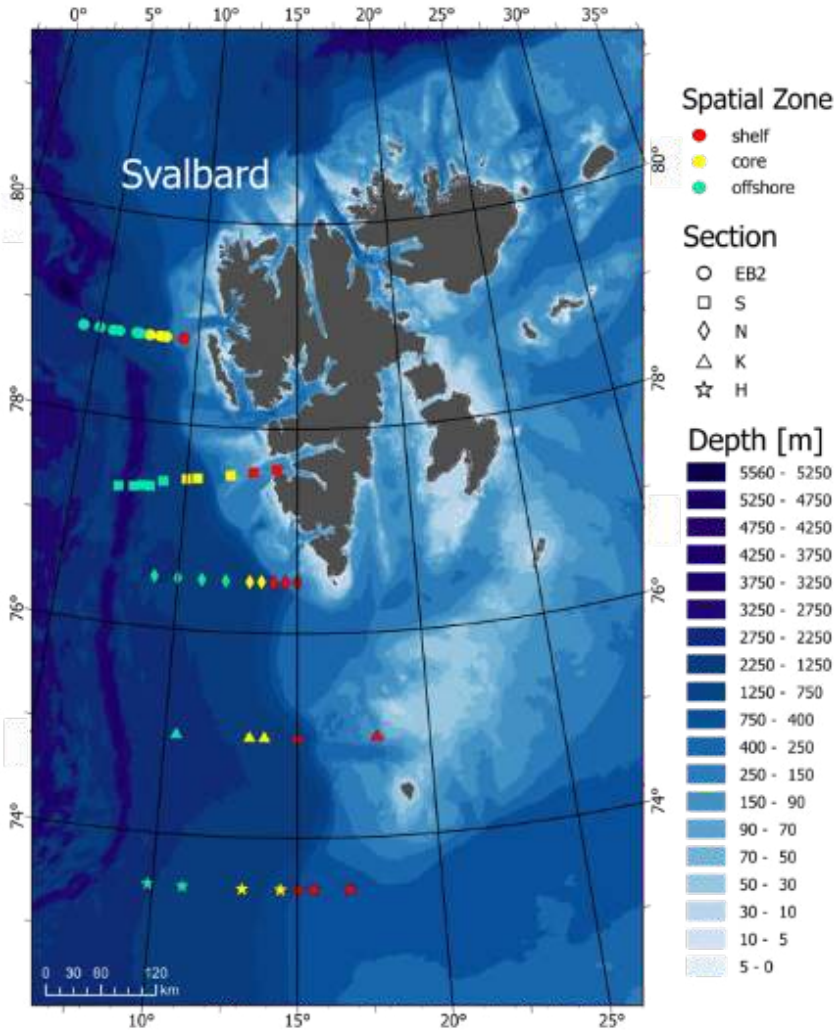

Figure III. 1 Study area and sampling locations (2001-2016) shown along the sections arranged from south to north. Stations are differentiated by spatial zones – shelf, core, offshore – represented by distinct colours, while marker shapes distinguish sections.

3.2.2 Meroplankton sampling and analysis

Data on the taxonomic composition and abundance of meroplankton were obtained from zooplankton samples collected at stations located from shelf to the sea, on five latitudinal sections (H; K; N; S; EB2) distributed from the south to the north along the flow of the West Spitsbergen Current (WSC) (Figure III. 1), in the area defined by the coordinates from 73.48° to 78.84° N and 4.16° to 19.42° E.

Prior to zooplankton sampling, the full-depth temperature and salinity profile was measured at each station to distinguish the optimal depth for plankton sampling. The CTD (conductivity, temperature, depth) measurements were carried out using the SBE 9/11+ system (Sea-Bird Electronics, Inc.), equipped with double-T and S sensors. Temperature and conductivity sensors were pre-cruise-calibrated, and salinity measurements were post-cruise

corrected against water samples. The mean salinity and temperature for the stratified sampling were calculated by averaging the CTD profiles at each station across the depth layers used for zooplankton collection.

Each year, from 2001 to 2016, stratified zooplankton sampling was conducted from mid-June to mid-July on board the RV Oceania (Institute of Oceanology, Polish Academy of Sciences) from the epipelagic zone (0-200 m). Zooplankton sampling was performed by vertically stratified net tows with the use of the WP-2 type net with a mechanical closing system (UNESCO, 1968) (180 μm mesh and 0.25 m^{-2} square opening). The towing speed was around 1 m s^{-1}. Immediately after collection, the zooplankton samples were preserved in a 4% borax-buffered formaldehyde solution in seawater.

Over the years, the time shifting of collected material was limited to no more than 10 calendar days. Due to logistical constraints, weather, and sea-ice conditions, the exact coordinates of the sampling stations may vary slightly over the years, and sampling at all stations was not possible every year. A total of 41 stations were sampled. While 589 stratified hauls were taken (from different depth layers, usually three per station, up to 200 m), the data were integrated into a single layer (usually 200-0 m per station) to match the hydrographic depth layer and then used for meroplankton analysis.

The collected zooplankton samples were analyzed in the laboratory, and meroplankton were identified to the lowest possible taxonomic level (Olympus SZX 7; objective: SZX-ACH 1X; ocular lens: WHSZ10X/10X-H) according to the protocol of Postel et al. (2000). Due to similarities in the morphological structure of larvae, it is very often difficult to identify specimens to the species or genus level. Therefore, in this study, meroplankton was described and mainly assigned to groups such as Phylum or Class. In the case of decapod larvae, it was possible to ascribe some of them to the genus level. The abundance of meroplankton was calculated as the number of individuals per cubic meter of seawater (ind m^{-3}).

3.2.3 Data processing

3.2.3.1 Hydrography

CTD data were processed using the standard SBE Data Processing Software and additional dedicated tools developed in MATLAB. Pressure, temperature, and practical salinity data are accurate to 0.5 dbar, 0.002°C, and 0.003, respectively. All vertical profiles were averaged at 1 m intervals before averaging in the sampling layers.

To provide environmental background for the analyses of biological samples, temperature and salinity profiles were vertically averaged over the upper ocean layer from

0 to 200 m. The 200-0 m layer was chosen because it covers the surface layer and the upper part of the Atlantic water in the WSC (Walczowski et al., 2012) and corresponds to the depth range where most meroplankton samples were collected.

For the time series of mean water massess properties in the upper 200-0 m layer at individual sections, temperature and salinity profiles were first interpolated onto regular grids with vertical and horizontal resolutions of 1 km and 10 m, respectively. To calculate normalized anomalies of mean temperature and salinity for each section, the mean values of each parameter were calculated for the 200-0 m layer and over the part of the section, covering the shelf, the AW core over the shelf break, and its offshore extension. To visualize spatiotemporal changes using Hovmöller diagrams, the gridded data at the entire length of each section were averaged vertically over 200-0 m and plotted against longitude and time. Normalized anomalies were calculated by subtracting the long-term mean (2001-2016) of each parameter and dividing by its standard deviation.

Horizontal distributions of temperature and salinity were constructed from vertical averages of individual profiles over 200-0 m, remapped from geographical to Cartesian coordinates, and interpolated onto regular grids. All calculations and visualizations were performed in MATLAB, except the spatial maps, which were plotted using Surfer (Golden Software).

3.2.3.2 Data classification and environmental setting

Sampling stations were grouped into: i) spatial zones (shelf, core, offshore), ii) sections (H; K; N; S; EB2), and iii) thermal phase (cold, intermediate, warm sampling years), which were based on temperature anomalies (Figure III. 2a; Figure III. 3; Figure III. 4). Years were classified as warm or cold based on an anomaly threshold of approximately ± 0.5 standard deviations or larger (with negative values indicating cold years), though the generalized classification (Table III. 1) accounts for discrepancies between visual anomalies and observed conditions. To address this, we present thermal phases for each section and spatial zone individually, with a final "generalized" classification based on the prevailing anomaly across all sections (Table III. 1). Furthermore, it must be noted that the 200-0 m layer integrates both Atlantic Water (AW) and Surface Water (SW); therefore, the classified thermal phases for specific sections may reflect broader upper-ocean variability rather than changes in the AW core alone.

In the southernmost sections H and K, the influence of two upstream branches of Atlantic water inflow (NwASC and NwAFC) can be seen, with varying zonal extent over the

observation period. The core stations at both sections are representative of the main flow of Atlantic water (NwASC), hugging the shelf break of the eastern Greenland Sea. The stations depicted as offshore reflect the impact of Atlantic water carried in the deep basin along the Knipovich Ridge (NwAFC), which, due to its longer transit, cools more than the AW core but retains its salinity signature. Atlantic water flows originating from two upstream branches merge in the southern Fram Strait and become less distinguishable in the northern sections.

The sampling sites were visualized with ArcGIS Pro software (Esri, 2025). For the following statistical analyses, all environmental parameters and meroplankton abundance were averaged over the depth range of the corresponding meroplankton sampling layer (typically 200-0 m).

Table III. 1 Classification of years (2001–2016) into thermal phase based on temperature anomalies, Hovmöller diagram analysis, and horizontal distributions of temperature (Figure III. 2a; Figure III. 3, Figure III. 4).

Year	2001	2002	2003	2004	2005	2006	2007	2008	2009	2010	2011	2012	2013	2014	2015	2016
	Classification for individual sections															
Section H																
Section K																
Section N																
Section S																
Section EB2																
	Classification for individual spatial zones															
Shelf																
Core																
Offshore																
	General classification for the entire study region															

Classification: cold – blue; intermediate – grey; warm – red; no data - white

3.2.3.3 Statistical analysis

To evaluate differences in meroplankton community structure across spatial and temporal scales, several multivariate analyses were performed using PRIMER v7 with the PERMANOVA+ add-on (Anderson, 2014; Anderson et al., 2008; Clarke & Gorley, 2015; Clarke & Warwick, 2001). All analyses were based on a Bray-Curtis similarity matrix calculated from fourth-root transformed abundance data to balance the contributions of dominant and rare taxa. The relative influence of four main factors – Spatial Zone (fixed: shelf, core, offshore), Section (fixed: H, K, N, S, EB2), Thermal Phase (fixed: years classification),

and Year (random nested in Thermal Phase) – was tested using a Permutational Multivariate Analysis of Variance (PERMANOVA) with 9999 permutations of residuals under a reduced model and using Type I (sequential) sums of squares (Anderson, 2008).

To assess whether the observed patterns were driven by shifts in community composition (location) or by differences in community stability (dispersion), a distance-based test for homogeneity of multivariate dispersions (PERMDISP; Anderson, 2006) was applied for each factor (9999 permutations). This test allowed us to determine the degree of temporal and spatial heterogeneity within the defined groups.

Finally, to visualize the stability of group centroids and represent the confidence in the mean community composition, Bootstrap Averages (Anderson, 2008) were calculated for all four factors (Spatial Zone, Section, Thermal Phase, Year). For each group, 25 bootstraps were performed with a minimum Spearman correlation Rho = 0.99. The resulting 50% bootstrap regions were plotted in a non-metric multidimensional scaling (nMDS) space to assess the degree of separation or overlap between years of sampling, thermal regimes and geographical areas.

The relationship between meroplankton abundance and environmental parameters (temperature, salinity, maximum station depth) was evaluated using distance-based linear models (DistLM) and redundancy analysis (dbRDA). This approach enabled the identification of environmental drivers that explain variation in meroplankton taxonomic composition. Model fitting used a best selection procedure followed by forward selection, evaluated with adjusted R^2 values (Anderson et al., 2008).

Taxonomic Richness (S), Shannon-Wiener diversity (H'), and Pielou's evenness (J') were calculated to assess diversity. Taxonomic richness (S) was determined as the total number of identified taxa per sample, uncorrected for sample size. The Shannon-Wiener index (H') was used to assess overall diversity based on both richness and abundances, while Pielou's evenness (J') evaluated whether the community was dominated by a few taxa or more evenly distributed. These indices reflect community complexity across spatial and temporal gradients. Differences between groups (spatial zones, sections, years) were tested using Kruskal-Wallis tests followed by pairwise Dunn tests with multiple-testing corrections.

The sampling sites were visualized in ArcGIS Pro (Esri, 2025). Subsequent statistical tests and visualizations were performed in R 4.4.1/4.4.2 (main packages: *base* (version 4.0.0), *dplyr* (version 1.1.4), *ggplot2* (version 3.5.1), *readxl* (version 1.4.3), *svglite* (version 2.1.3), *vegan* (version 2.7.3), *tidyr* (version 1.3.2), *tidyverse* (version 2.0.0)) (Oksanen et al., 2001;

R Core Team, 2025; Wickham, 2016; Wickham & Bryan, 2023; Wickham et al., 2019, 2023, 2024a 2024b). Significance for all tests was set at $p \leq 0.05$.

3.3 Results

3.3.1 Environmental conditions

3.3.1.1 Spatiotemporal variability of temperature and salinity

The study area was influenced by the interplay between warm and salty Atlantic Water (AW) transported northward by the Norwegian Atlantic Current and the West Spitsbergen Current and colder and fresher Arctic Water (ArW) originating from the Barents Sea and flowing northwards over the West Spitsbergen shelf as the Polar Spitsbergen Current (Figure III. 2; Figure III. 3)). The northern part of the study region was also impacted by the surface Arctic water where the uppermost part of inflowing AW water was mixed with the cold and freshened water from sea ice melt. Spatial distribution of summer temperatures averaged in the upper 200 m layer exhibited significant interannual changes (Figure III. 2). Periods such as 2001-2003 and 2008-2010 and 2012 represented so-called "cold phases", when the inflowing AW was less warm and the influence of ArW along the coast was more pronounced. In contrast, 2006 and 2015-2016 showed a state of "warm years" characterized by elevated temperatures in the upper layer and a larger eastward expansion of warm AW towards the shelf (Figure III. 2).

In the 2000s, the salinity patterns followed temperature distributions with the bands of higher salinity (>35.1) indicating a warm AW core. The highest salinity along the Atlantic inflow was observed in 2011, accompanied by relatively high AW temperature (albeit lower than during the 2006 peak). The strongest signature of the less saline waters along the West Spitsbergen shelf was found in the early years of the observing period, collocated with the cold shelf waters (Figure III. 3).

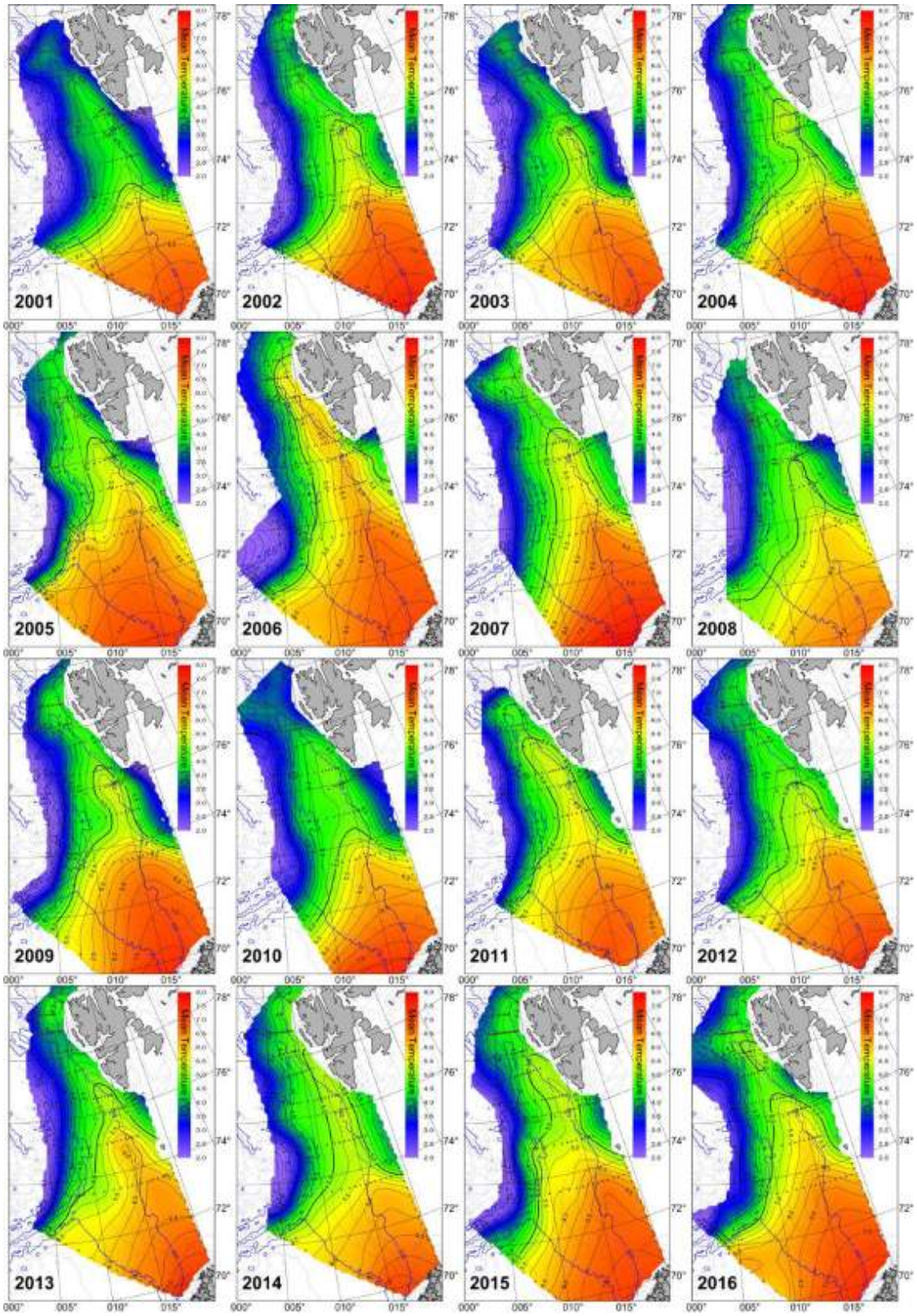

Figure III. 2 Horizontal distributions of temperature averaged in the upper 200 m layer for the period 2001-2016 in the Atlantic water inflow region in the eastern Nordic Seas

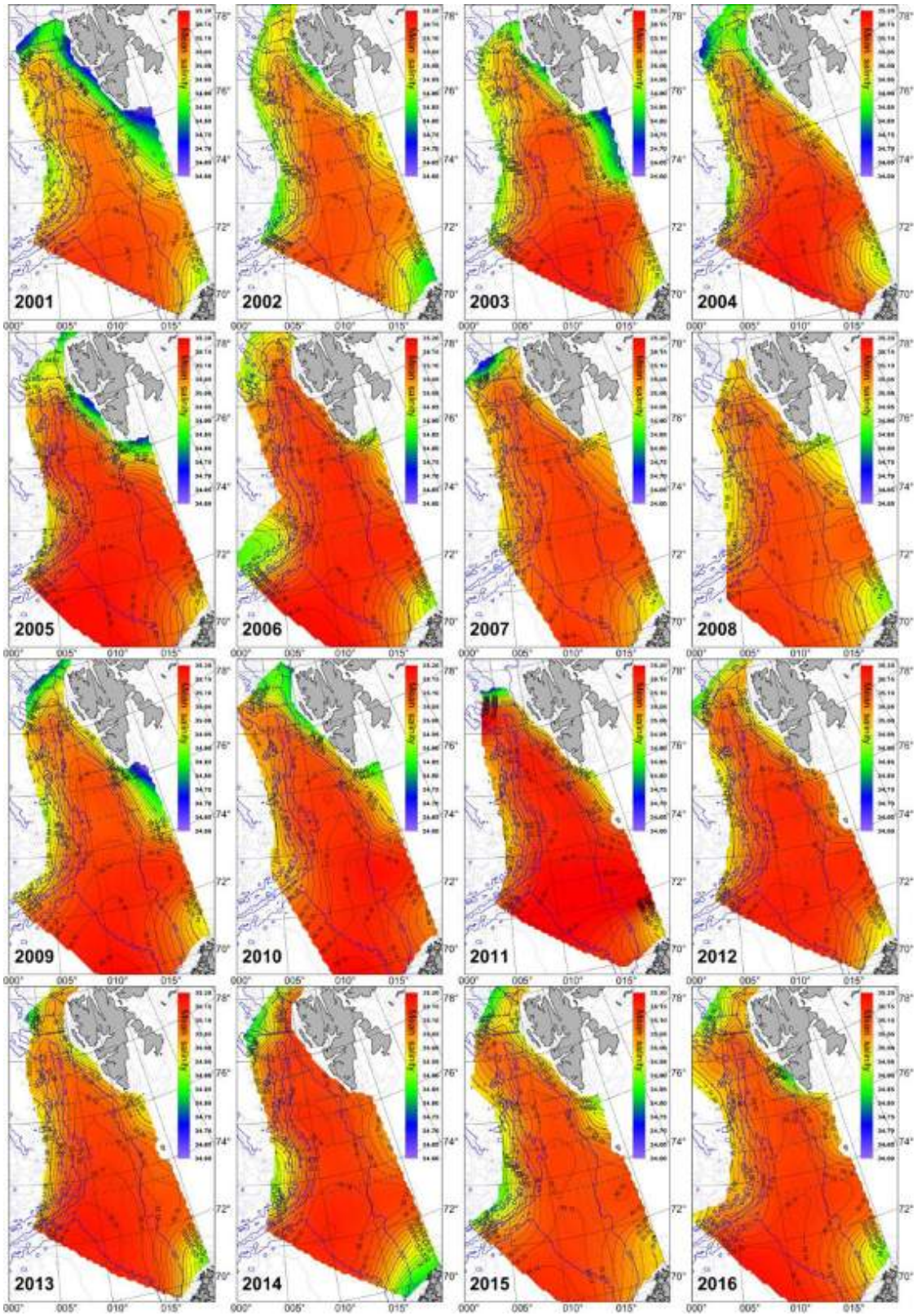

Figure III. 3 Horizontal distributions of salinity averaged in the upper 200 m layer for the period 2001-2016 in the Atlantic water inflow region in the eastern Nordic Seas.

3.3.1.2 Temperature and salinity anomalies over the 2001-2016 period

The anomaly plots provide a crucial high-resolution view of shifting marine climate across the five sections (H, K, N, S, EB2) over the study period (Figure III. 4). Most sections exhibit strong negative anomalies in both temperature (red) and salinity (blue) in the period 2001-2005, which preceded the period of a strong warm anomaly. The strongly negative temperature anomaly was found in 2001, in particular on H, K, and EB2 sections (Figure III. 4). Overall, during the first period of the 2000s, both temperature and salinity recovered from strongly negative anomalies at the beginning of this period towards the warm and salty conditions which peaked in 2006. In 2006, a strongly positive temperature anomaly was observed at all sections, marking the inflow of exceptionally warm Atlantic water to the eastern Nordic Seas and Fram Strait. The positive temperature anomalies were also clearly pronounced in 2015-2016 on nearly all sections (except section S in 2015, marking the second warming period in the AW inflow). Positive salinity anomalies were found at all sections in 2010-2012 (at the section S in 2011-2012). Nevertheless, each section had its unique characteristics. Temperature and salinity anomalies seem to be better pronounced with more consistent year-to-year variability at the southern sections H and K (Figure III. 4). They cross the AW flow along the eastern rim of the Greenland Sea, where dominant variability is set by the properties of advected Atlantic water and regional air-sea interactions. At the northern sections in Fram Strait (S, EB2), variability in the upper 200-0 m layer results not only from changes in the AW inflow coming from the south but also reflects changes in the surface layer which is a mixture of cooled Atlantic water, the fresher/colder water originating from the Spitsbergen Polar Current or the Polar Surface Water coming from the north, and the underlaying Atlantic water layer. Therefore, stronger year-to-year variability in the upper 200 m layer can be expected at the northern sections.

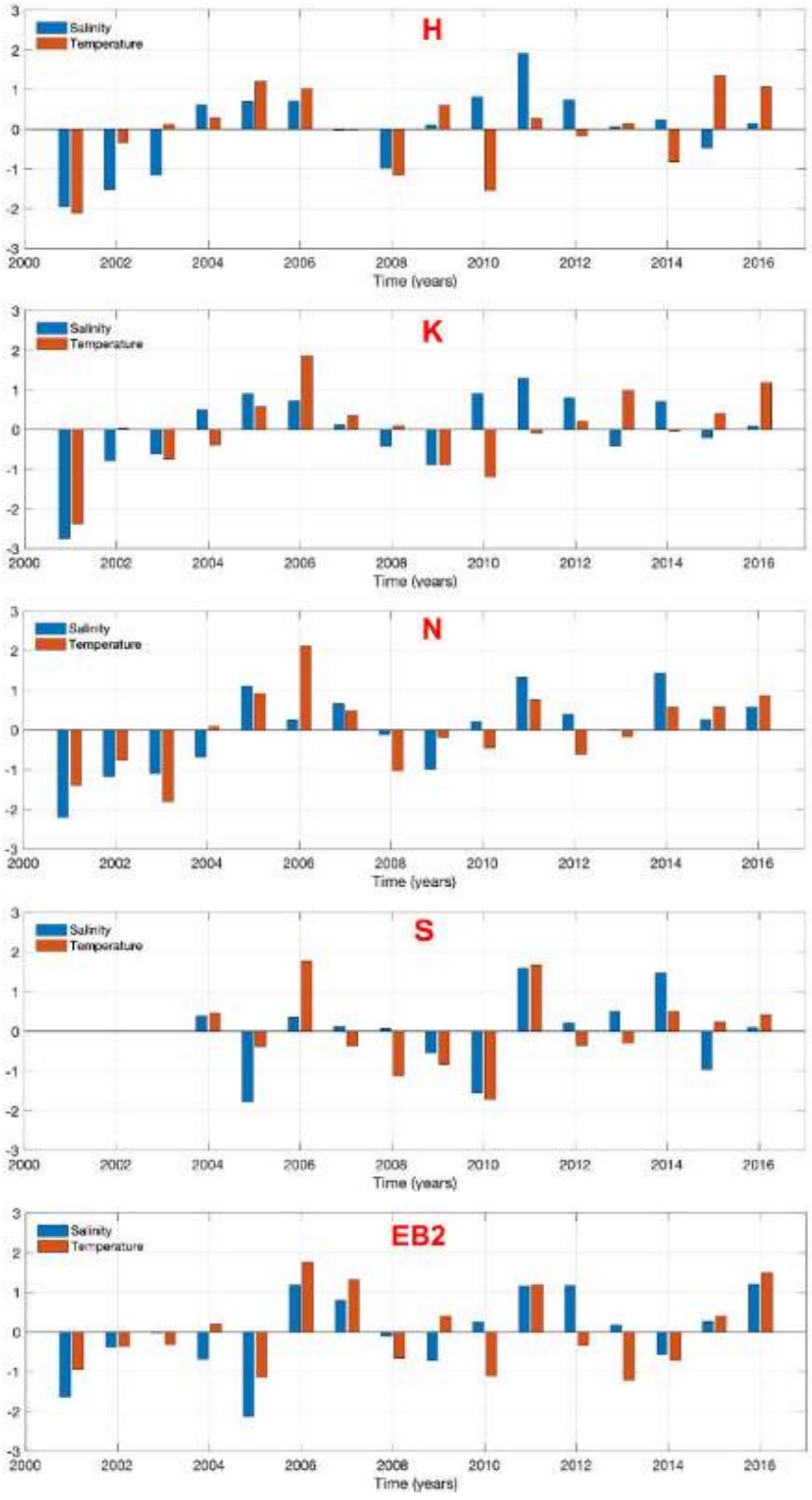

Figure III. 4 Normalized anomalies of temperature and salinity in the 200-0 m layer (y axis) at five sections (H; K; N; S; EB2) in 2001-2016. Anomalies are calculated relative to the long-term mean for each section (2001-2016).

Hovmöller plots show the longitudinal (west-to-east) distribution of temperature anomalies over time relative to the 2001-2016 baseline (Figure III. 5). At all sections, the strongest positive anomalies were concentrated in the core of the West Spitsbergen Current. In Fram Strait, the positive anomalies found on the shelf result from intermittent intrusions of warm Atlantic water from the WSC core onto the shallower shelf and into the fjords. In 2006, a significant temperature rise found at all sections marked a massive warming event related to the exceptionally warm and saline Atlantic water inflow. At the southern section's H and K, the 2006 warming was not only strongest in the AW core but also extended significantly further east onto the shelf (beyond 15°E) than in previous years (Figure III. 5). In Fram Strait (sections N and EB2), the warm anomaly observed in 2006 (relative to the long-term mean) was particularly strong and widespread (across the entire section in the southern and central Fram Strait but limited to the AW inflow in northern Fram Strait). In the years 2013-2016, a shift from patchy anomalies to more consistent warming was observed, spreading westward in the offshore AW branch. The EB2 section remains colder throughout the years (Figure III. 5), reflecting the effective dumping of warm anomalies during their northward progression and the larger impact of cold Arctic waters in the surface layer.

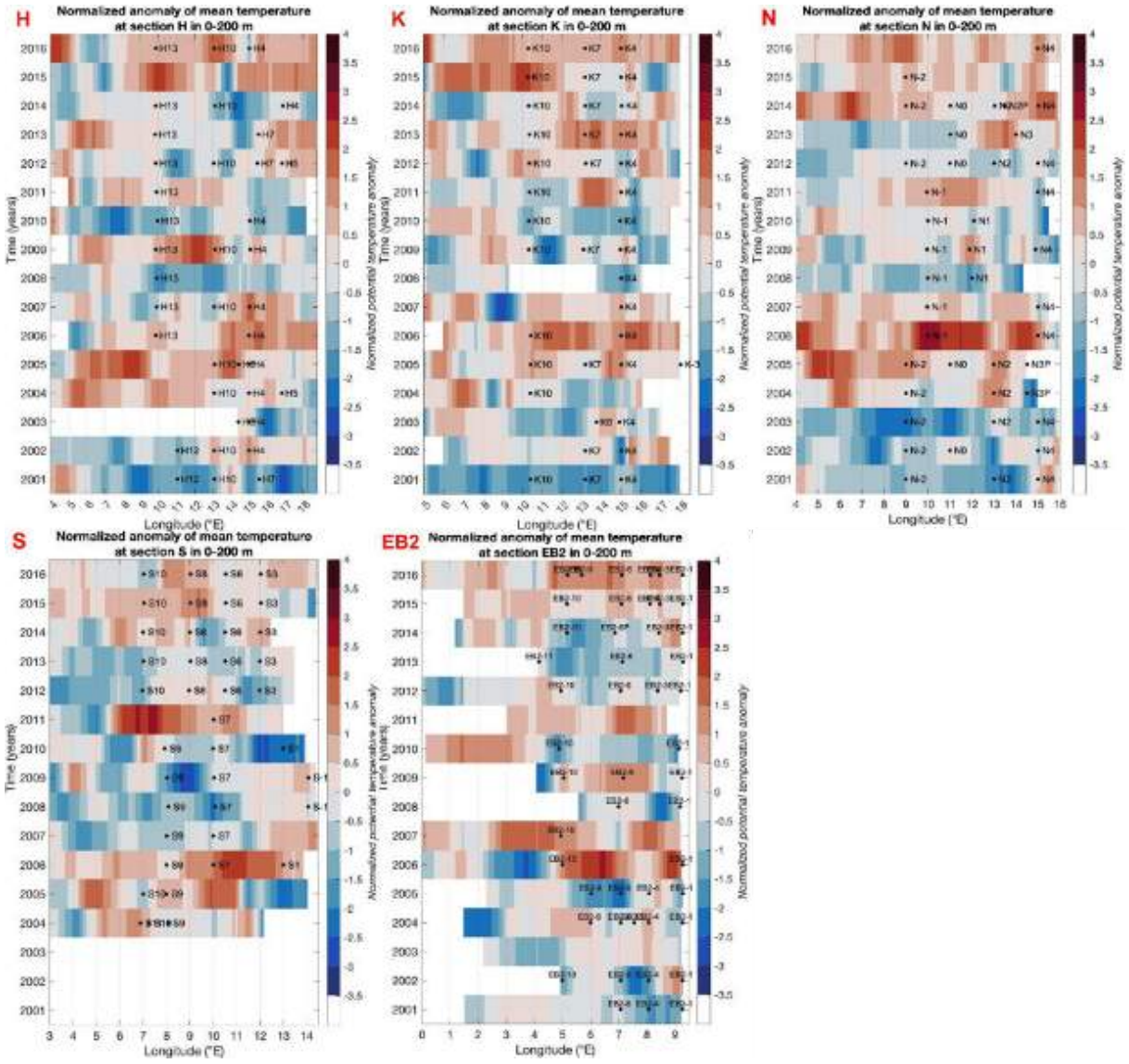

Figure III. 5 Hovmöller diagrams of normalized temperature anomalies at five sections from the West Spitsbergen shelf towards the deep basin. Anomalies were calculated relative to the long-term mean (2001-2016) for each respective section (except S with the mean of 2004-2016 over the measurement period). Black dots indicate zooplankton sampling stations. The x-axis represents longitude, while the y-axis shows the temporal evolution from 2001 to 2016. Note the different zonal extent of each section.

3.3.2 Meroplankton community

Across the study area, a total of 18 meroplanktonic taxa were identified, representing a broad taxonomic range including the larvae of Cirripedia, Decapoda, Nemertea, Gastropoda, Bivalvia, Polychaeta, Echinodermata, Bryozoa, and Hemichordata. Over the 16-year period, the taxonomic richness remained relatively stable, fluctuating between 7 (in 2008) and 12 taxa (in 2006). In contrast, total meroplankton abundance exhibited high interannual variability, ranging from a minimum of 21 ind m^{-3} in 2011 to a maximum of 1184 ind m^{-3} in 2015. The community was characterized by the consistent dominance of Echinodermata larvae (dominant in 11 out of 16 years) and Bivalvia veligers (dominant in 5 years). A notable shift occurred in 2010, when Cirripedia cypris larvae became the most abundant group in the meroplankton community (Figure III. 8).

Spatially, both the WSC core and shelf zones supported the highest taxonomic richness (16 taxa), with peak meroplankton abundances reaching 2325 and 1907 ind m^{-3}, respectively. Echinodermata larvae were predominantly characteristic for these zones. In contrast, the offshore zone exhibited lower taxonomic richness (12 taxa) and was dominated by Bivalvia veligers. Latitudinal patterns showed that while taxonomic richness was relatively uniform across the south-north gradient (ranging from 12 taxa at section S to 14 at EB2; H), abundances were significantly higher at the northernmost sections (S: 2061 ind m^{-3}; EB2: 1816 ind m^{-3}). The lowest meroplankton abundance was noted at section K (179 ind m^{-3}). Bivalvia veligers constituted the dominant meroplankton group at most northern sections (EB2), whereas Echinodermata larvae prevailed at the rest of the section (H; K; N; S) (Figure III. 8).

3.3.2.1 Environmental drivers of meroplankton community structure

The DistLM analysis (Table III. 2) and the dbRDA plot (Figure III. 6) illustrated relationships between the meroplankton community structure and environmental conditions. Maximum bottom depth was identified as the most important environmental factor, explaining 16.59% of the variation, followed by temperature and salinity, which together accounted for an additional 7.6% of the variation (Table III. 2).

Table III. 2 Results of Distance-based linear model analysis (DistLM) for meroplankton taxonomic community and abundance with environmental factors; significant results are marked in red.

Marginal Tests							
Variable	**SS(trace)**		**Pseudo-F**		**P**		**Prop.**
Bottom Depth	49714		41,397		0,0001		0,16599
Salinity	14329		10,451		0,0001		0,047842
Temperature	8531,1		6,0983		0,0005		0,028484
Sequential Tests							
Variable	**Adj. R^2**	**SS(trace)**	**Pseudo-F**	**P**	**Prop.**	**Cumul.**	**res.df**
Bottom Depth	0,16198	49714	41,397	0,0001	0,16599	0,16599	208
Salinity	0,19226	4724,9	4,0818	0,0021	0,015775	0,20385	206
Temperature	0,18023	6615,7	5,6315	0,0001	0,022089	0,18808	207

The dbRDA analysis showed that the first two axes explained 19.9% of the total variation in the meroplankton community. A clear zonation and division along the first axis (dbRDA1) revealed distinct meroplankton assemblages between the spatial zones (Figure III. 6). The main environmental variables shaping the meroplankton community were the depth gradient and salinity. The offshore meroplankton assemblage was separated from the shelf one. Maximum bottom depth and salinity were strongly correlated with the composition of the offshore meroplankton assemblage. Temperature, on the other hand, appeared to have a greater influence on the variation within the shelf and core meroplankton assemblages (Figure III. 6).

Latitudinal differentiation of meroplankton assemblages did not show a clear structure, whereas distance from the shelf to open waters had a greater influence on meroplankton assemblages. However, individual sections showed specific trends in meroplankton assemblages within spatial zones (Figure III. 6). The meroplankton assemblages from sections H (located southernmost) and S (above 75°N) showed extremes in distribution along the vertical axis (dbRDA2) and were separated from each other on the shelf. Southernmost (H) meroplankton assemblage was almost exclusively concentrated in the lower part of the graph (negative dbRDA2 values) and clearly separated from the rest of the meroplankton assemblages further north within the shelf zone, suggesting a more substantial temperature effect on the meroplankton taxonomic composition (Figure III. 6). While meroplankton assemblage from section S was much more dispersed along the vertical axis, reaching high positive values on the dbRDA2 axis, resulting from weak explanation of community structure by environmental variables. The meroplankton assemblage from the northernmost section (EB2) seemed to be the

most ubiquitous. It was found both in the north in the shelf zone and deep in the offshore zone (Figure III. 6).

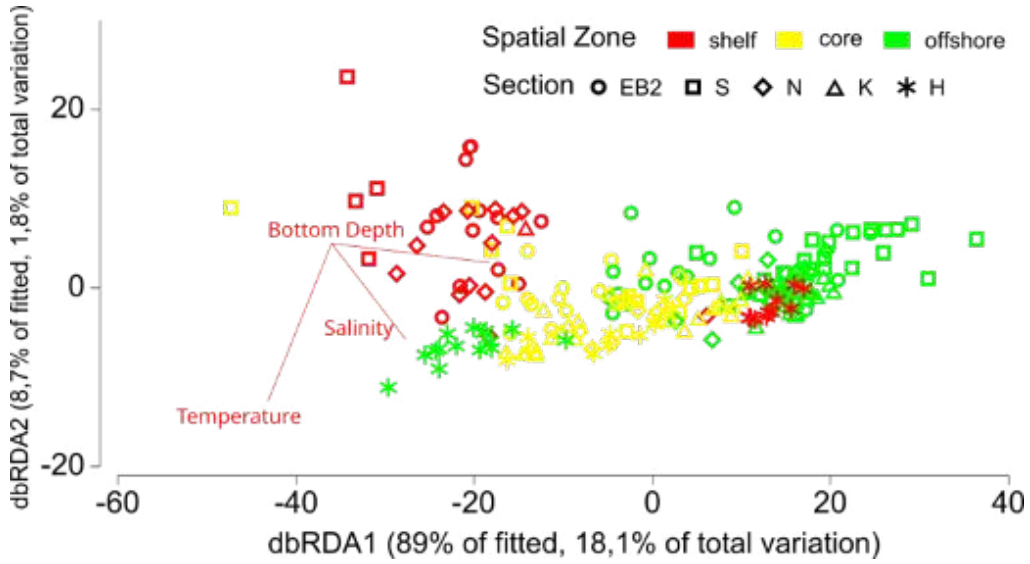

Figure III. 6 The dbRDA ordination plot based on meroplankton community composition and abundance with environmental variables (red vectors). Colours indicate spatial zones, and symbols indicate sections. Data were fourth-root transformed, and resemblance was calculated using Bray-Curtis similarity.

The PERMANOVA results showed that meroplankton community structure was mainly shaped by Spatial Zone, Section and Year (nested in Thermal phase), rather than within the thermal phase itself (Table III. 3). Among the spatial factors, the spatial zone was the most important driver (Pseudo−F=14.88, p=0.0001), explaining 16.03% of the total community variation. Latitudinal differences (section) were also significant (Pseudo−F=2.80, p=0.0005), but they accounted for a smaller part of the variance (4.32%).

Looking at temporal dynamics, the specific year (nested in thermal phase) had a strong effect on the meroplankton assemblages (Pseudo−F=2.36, p=0.0002, ECV=6.81%), which shows high year-to-year changes. However, the year classification into thermal phase was not statistically significant (Pseudo−F=0.92, p=0.5200). This lack of significance, even though the Bootstrap Averages (Figure III. 7) showed some visual separation between centroids, is likely due to high variation within each group. The PERMDISP test for the thermal phase was close to the significance level (p=0.0854), suggesting that high variability within years may mask the overall differences between warm and cold periods. In contrast, PERMDISP was significant for spatial zone ($p<0.05$) and section ($p<0.05$), meaning that community heterogeneity (dispersion) changes across different areas.

The Bootstrap Averages (Figure III. 7) confirmed these patterns. Although the 50% bootstrap probability regions for warm, cold, and intermediate years did not overlap, the high dispersion of individual annual points within these regions indicates significant inter-annual variability (Figure III. 7c). This suggests that while thermal phases distinguish the community structure, the response to warming is modified by year-specific environmental conditions.

Significant interactions were found between spatial zone and section (Pseudo−F=1.90, p=0.0003, ECV=5.59%), whereas no significant interactions occurred between spatial factors and the thermal phase ($p > 0.05$; Table III. 3). This suggests that the spatial pattern of meroplankton communities (from shelf to offshore) remains consistent regardless of the thermal regime. Furthermore, the high residual variation (64.30%) suggests that a substantial part of the community structure is driven by local events or factors not captured in the model, rather than by predictable spatiotemporal interactions.

Table III. 3 Results of a four-factor multivariate PERMANOVA for meroplankton descriptor sets with 9999 permutations; significant results are marked in red.

Factor	df	SS	√ECV	ECV%	MS	Pseudo-F	P(perm)	Unique perms
	Meroplankton community composition							
Spatial Zone	2	38691	16.495	**16.034**	19345	14.88	0.0001	9937
Section	4	16610	8.5578	**4.316**	4152.6	2.8043	0.0005	9937
Thermal phase	2	4807.2	0	0.000	2403.6	0.92164	0.52	9934
Year (Thermal phase)	13	33538	10.751	**6.810**	2579.9	2.3645	0.0002	9872
Spatial Zone*Section	8	15826	9.7362	**5.586**	1978.2	1.8979	0.0003	9856
Spatial Zone* Thermal phase	4	5892.9	4.7594	1.335	1473.2	1.4016	0.14	9910
Section*Thermal phase	8	8719.9	0	0.000	1090	0.94516	0.5547	9883
Spatial Zone* Year (Thermal phase)	26	26771	0	0.000	1029.6	0.94368	0.5969	9889
Section* Year (Thermal phase)**	48	55363	5.2497	1.624	1153.4	1.0571	0.3741	9845
Spatial Zone*Section* Thermal phase **	14	12014	0	0.000	858.12	0.94322	0.5801	9884
Spatial Zone*Section* Year (Thermal phase) **	31	27812	0	0.000	897.16	0.82226	0.8213	9881
Residuals	49	53463	33.032	64.296	1091.1			
Total	209	3.00E+05		100				

Significant level was p=0.05,
Statistically significant results are marked in red values, p<0.05,
Meroplankton data = similarity resemblance matrix on fourth root transformed data,
df – degrees of freedom,
SS – sum of squares
√ECV – the square root of the estimated components of variation (ECV), indicating the relative magnitude of the effect for each factor,
ECV% - Percentage of the Estimated Components of Variation (ECV) to the total variation; represents the relative contribution of each term to the overall multivariate variance,
MS – means of squares,
** – The analysis was conducted on an unbalanced design containing empty cells in the factor combinations, primarily due to unavoidable missing samples at specific stations or years. Type I sequential sums of squares were applied to account for the hierarchical and unbalanced structure of the data.

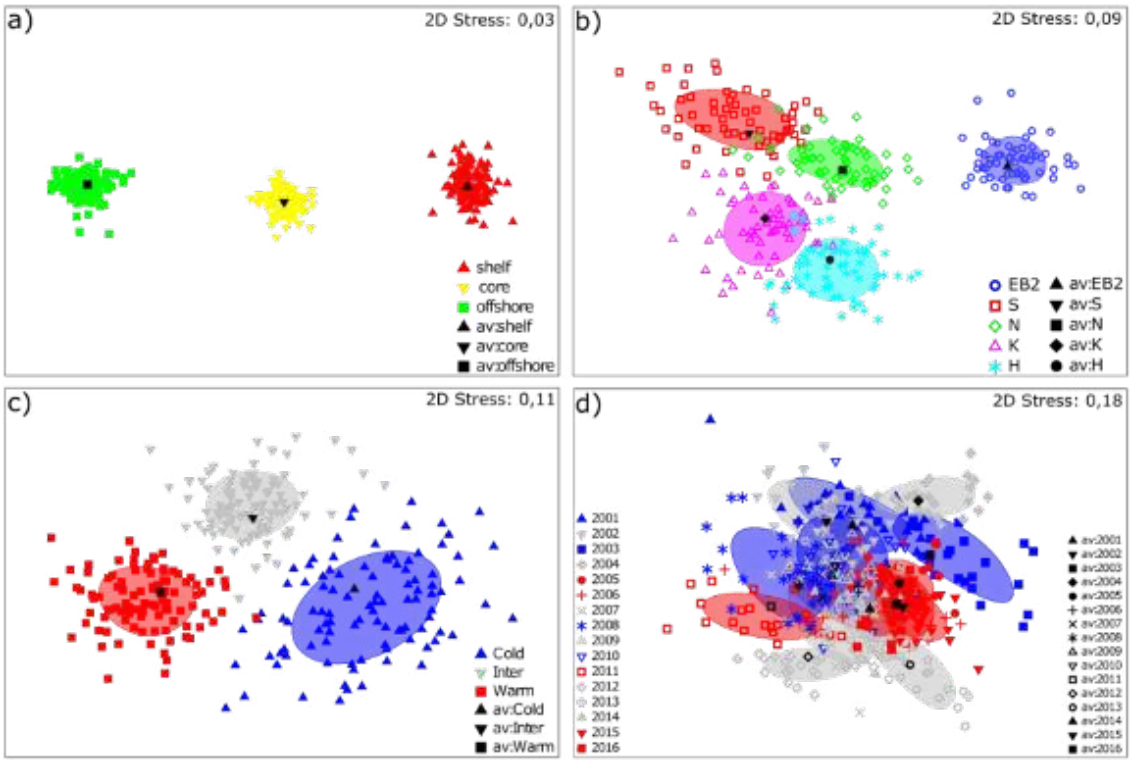

Figure III. 7 Non-metric multidimensional scaling (nMDS) ordination plots based on bootstrap averages for meroplankton community composition. Plots were constructed from a Bray-Curtis similarity matrix of fourth-root transformed abundance data. Groupings are visualized across four main factors: (a) Spatial Zone, (b) Section, (c) Thermal phase, and (d) Year of sampling. Each point represents the group centroid, surrounded by 50% bootstrap probability regions (based on n=25 bootstraps per group). 2D stress for each ordination is indicated within the individual panels.

3.3.2.2 Meroplankton spatiotemporal composition

3.3.2.2.1 Temporal changes in the meroplankton community

The highest taxonomic diversity of meroplankton was recorded in 2002, 2007, and 2010 (Figure III. 8). A consistent dominance of Echinodermata larvae was observed in the study area. Bivalvia veligers also accounted for a significant share, though their contribution decreased in 2004–2005, 2010, and 2015. Lower proportions of Echinodermata were observed in 2011 and 2012, years in which Bivalvia veligers dominated the meroplankton community, reaching or exceeding 70% of the total composition (Figure III. 8). Bryozoa larvae occurred sporadically over several years, reaching their relative maximum in 2003 and 2007. However, a clear downward trend was observed from 2007 onward, leading to their near disappearance from the studied environment. The highest share of Cirripedia cypris was recorded in 2010 (nearly a quarter of the community), coinciding with a marked cooling of the water masses, although

Echinodermata larvae still represented the largest fraction that year. Finally, Gastropoda veligers and Polychaeta larvae were consistently present throughout the study period, although they accounted for a small percentage of the overall meroplankton community (Figure III. 8).

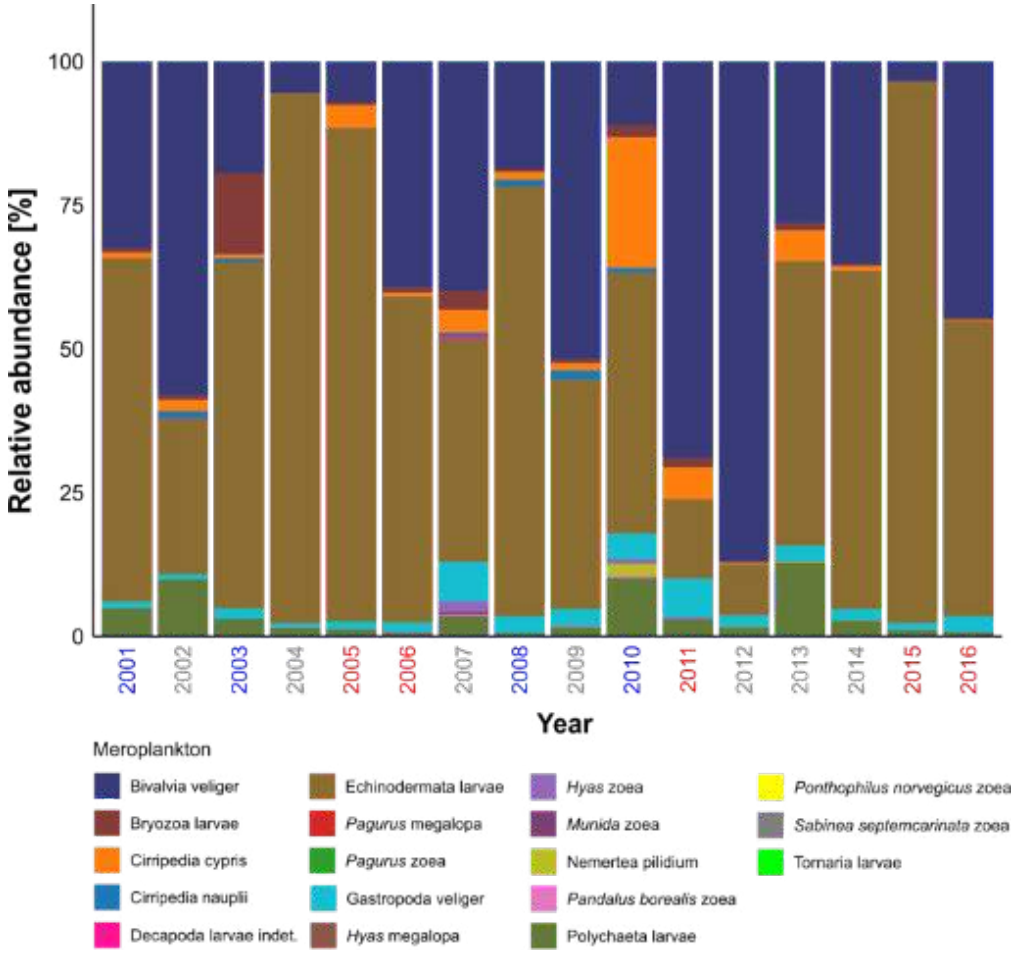

Figure III. 8 Relative abundance and taxonomic composition of meroplankton community (2001-2016). Stacked bar charts show the annual relative abundance of individual taxa, illustrating long-term shifts in the meroplankton community structure across the study area. Years are marked with thermal phase (warm in red, intermediate in grey, cold in blue).

3.3.2.2.2 Spatial and temporal changes with distance from the shelf to open waters

The integrated dataset demonstrates a consistent pattern in meroplankton distribution, indicating that Bivalvia veligers showed an increase in dominance over Echinodermata larvae moving towards the open sea, whereas the dominance of the Echinodermata larvae occurred closer to the shelf (Figure III. 9 "All Years"). The distribution of the remaining meroplankton taxa followed a spatial gradient: Bryozoa larvae were present mainly in the shelf and core spatial zones, while Cirripedia cypris were characteristic of the offshore zone. The relative share of Gastropoda veligers and Polychaeta larvae remained consistent across all spatial zones

(Figure III. 9, "All Years"). Exceptions occurred in the core zone in 2007, and 2010, and the offshore zone in 2006, 2011, and 2012, where Bivalvia became dominant while the share of Echinodermata was less prominent. In 2010, a peak in Cirripedia cypris contribution was recorded in the offshore zone (exceeding 50% of total composition), while Gastropoda veligers and Bryozoa larvae showed high shares in the core zone. Bryozoa larvae reached their highest contribution in 2003 within the shelf and core zones, while in 2006, 2007, 2008, and 2010, they were primarily limited to the core zone (Figure III. 9). Similarly, Gastropoda veligers showed higher shares in the core and offshore zones compared to the shelf, peaking in 2008 and 2010 in the core zone. Polychaeta larvae contributed the most in 2002 and 2013, with a nearly uniform distribution across all zones, and Hyas zoea larvae were recorded in the core zone in 2007 (Figure III. 9).

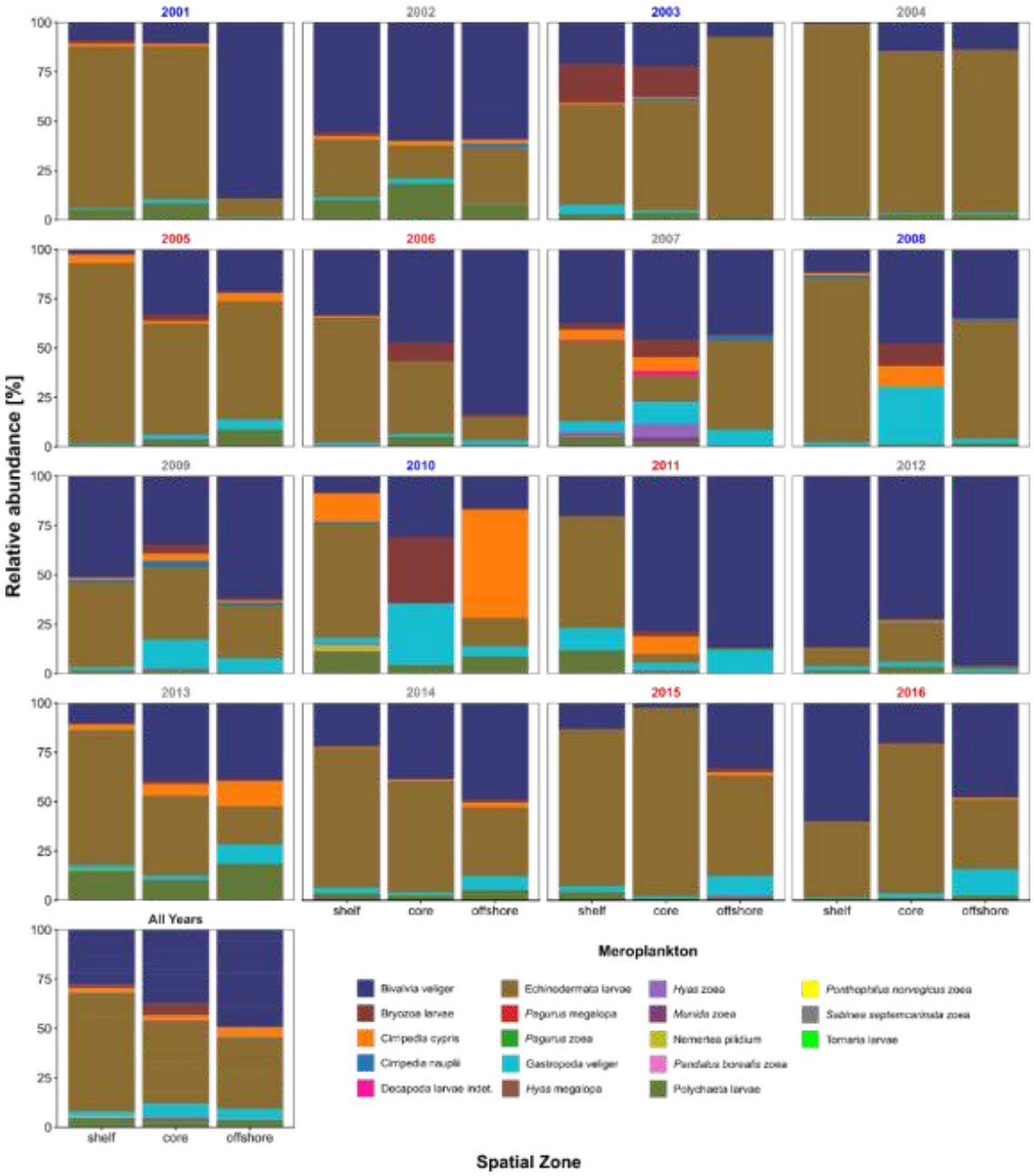

Figure III. 9 Interannual and spatial variability of meroplankton taxonomic composition across the West Spitsbergen shelf-to-basin gradient (Spatial Zones; 2001-2016). Panels show the relative abundance [%] of taxa within three distinct zones: shelf, core (Atlantic Water core), and offshore. The "All Years" panel provides a multi-year synthesis of the community structure for each spatial zone. Years are marked with thermal phase (warm in red, intermediate in grey, and cold in blue).

Taxonomic richness (S) followed a depth gradient, with the highest values observed on the shelf and the lowest in the offshore zone (Figure III. 10). In the core zone, taxonomic richness was usually similar to or lower than that on the shelf, with S being higher in the core than on the shelf only in 2003 and 2011. Notably, 2016 was the year with the lowest S across

all zones, which in the previous years were similar (Figure III. 10). Despite interannual fluctuations, statistically significant differences in meroplankton taxonomic richness between zones within the sampled years were detected only in 2001, 2005, 2009, 2010, and 2013 (Table SIII. 1). However, the post-hoc Dunn test showed that the significant differences in meroplankton taxonomic richness were only between the shelf and offshore zones in 2005 and 2009 (Table SIII. 2). Within the integrated dataset, no statistically significant interannual differences in taxonomic richness were observed within any of the spatial zones (Table SIII. 3).

In contrast to taxonomic richness, the Shannon-Wiener diversity index (H′) was usually the highest in the core zone and lowest on the shelf (Figure III. 10). This pattern was consistent during the years 2001-2006; however, in 2007, 2010, and 2011, H′ was higher on the shelf than in the remaining zones. The Pielou evenness index (J′) followed a similar pattern, with the highest values typically observed in the core and, in some years, in the offshore zone. A decline in both H′ and J′ was observed across all zones in 2004, marking the period of lowest biodiversity in the study. Overall, the core zone exhibited the highest H′ (Figure III. 10 "All Years"), though no consistent long-term increasing or decreasing trend was observed across the study period.

Significant spatial differences in meroplankton taxonomic diversity (H′) were observed in 2001 (between core and offshore), 2005 (between shelf and core), and 2007 (Tables SIII. 4 & SIII. 5). In 2007, however, the Kruskal-Wallis test indicated spatial variation, subsequent Dunn's post-hoc comparisons did not identify any significant pairwise differences (Table SIII. 5). Pielou's evenness (J′) recorded a significant spatial effect in 2005, with significant contrasts between the shelf vs core and shelf vs offshore zones (Tables SIII. 6 & SIII. 7). Within the integrated dataset, statistically significant interannual differences in both H′ and J′ were observed specifically within the offshore zone. However, Dunn's post hoc comparisons were unable to identify any significant differences between years (Tables SIII.8, SIII.9, SIII.10 & SIII.11).

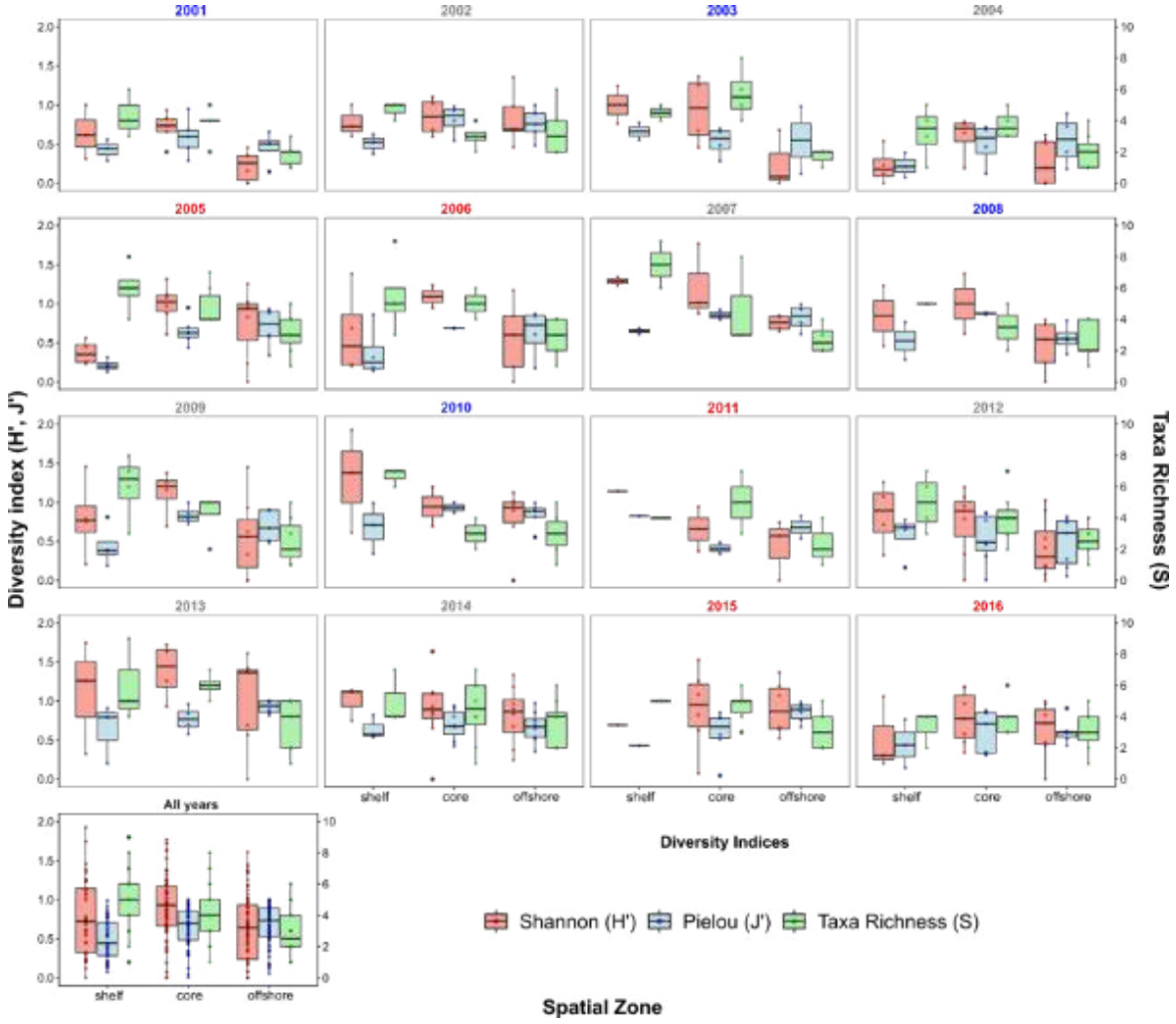

Figure III. 10 Interannual variability of meroplankton diversity indices (H′, J′) and taxonomic richness (S) across the West Spitsbergen shelf-to-basin gradient (Spatial Zones; 2001-2016). Boxplots represent the median and interquartile range; whiskers indicate the minimum and maximum values. Individual points represent all sampled data, providing a visualization of data distribution and sample size. Taxonomic richness (S) is displayed on the secondary y-axis. The "All Years" panel provides a multi-year synthesis for the entire study period. Years are marked with thermal phase (warm in red, intermediate in grey, cold in blue).

3.3.2.2.3 Spatial and temporal changes with latitude

Echinodermata larvae consistently contributed a higher share than Bivalvia veligers across all sections, although both groups remained the dominant constituents of the meroplankton community (Figure III. 11 "All Years"). Bryozoa larvae were predominantly associated with southern sections (H & K), while Cirripedia cypris were distributed across sections H, K, and N. Gastropoda veligers exhibited a clear latitudinal decline, with decreasing

share towards the north. Polychaeta larvae were present in low shares but occurred consistently across all sections (Figure III. 11 "All Years").

An interannual trend was observed in the dominance of Echinodermata and Bivalvia larvae (Figure III. 11). At southern sections (H, K) and occasionally in S, Bivalvia veligers frequently showed higher proportions than Echinodermata. In contrast, further north (sections S & EB2), the community composition shifted towards the dominance of Echinodermata larvae. Notable deviations from this pattern occurred in some intermediate and warm years, like at section K in 2004 and section S in 2005, where Bivalvia (and Gastropoda in the latter case) became the dominant groups. In 2007, section K showed high taxonomic diversity, with noticeable shares of Bryozoa larvae, Gastropoda veligers, and Decapoda larvae (both *Hyas* zoea and Decapoda indet.) Bryozoa larvae reached their highest relative shares in 2003 and 2010 on southern sections (H, K), with an additional peak occurring in 2015 on section N (Figure III. 11). A high peak in Cirripedia cypris was noticed in 2010 at section N, in opposite to section S, which showed very even community composition with not a single dominant (Echinodermata larvae, Cirripedia cypris and nauplii, Gastropoda veligers, Nemertea pilidium, Polychaeta and Bivalvia veligers (Figure III. 11). Between 2001 and 2005, Gastropoda veligers were rare from southern sections, appearing regularly only after 2006. A similar trend was noted for Cirripedia cypris, while Cirripedia nauplii showed increased abundance in 2008, 2009, and 2012, mainly on section H. Polychaeta larvae peaked in 2002 and 2013, with higher abundances on southern sections (H, K, N) than on northern ones, and *Hyas* zoea was recorded on section K in 2007 (Figure III. 11).

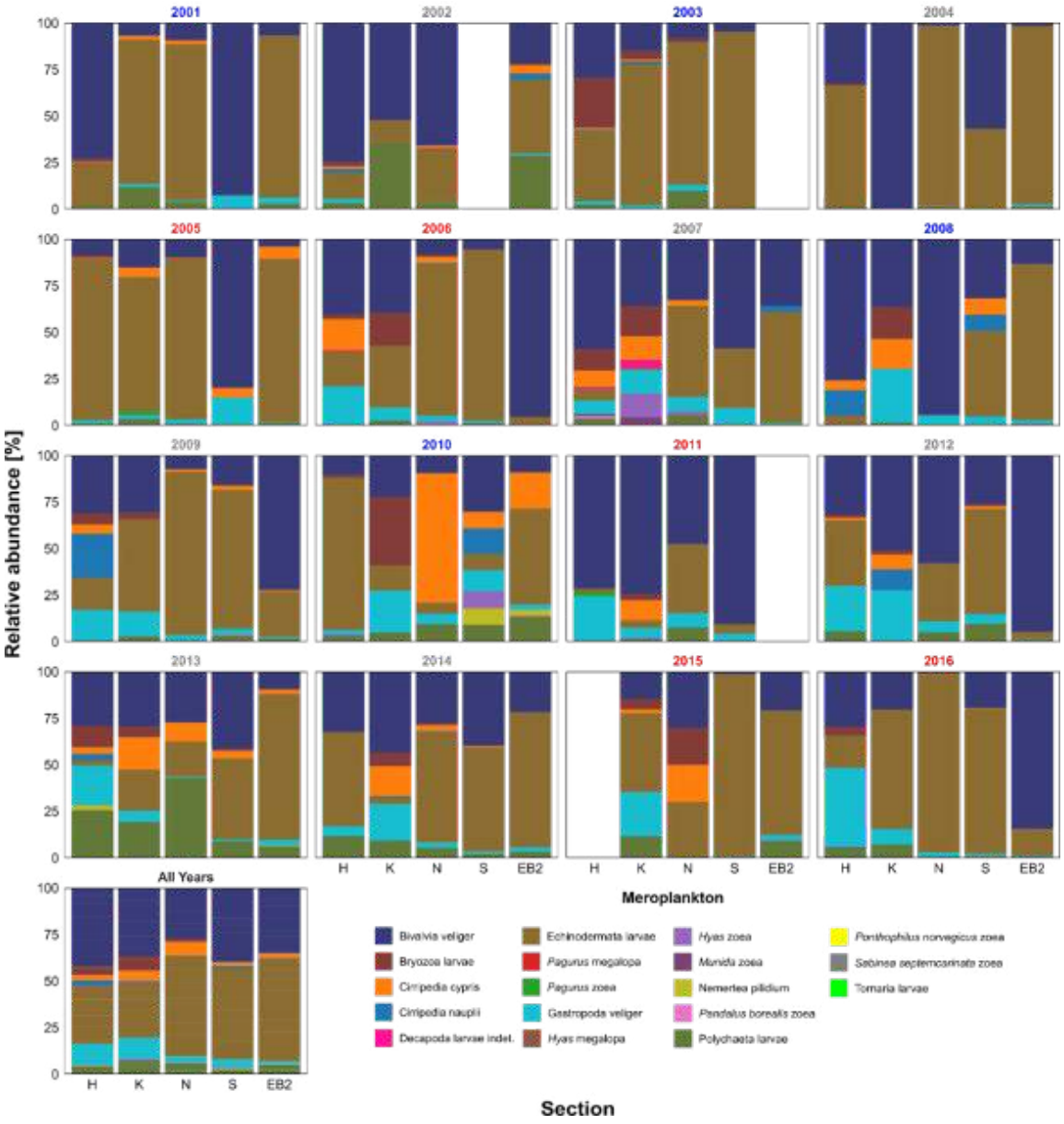

Figure III. 11 Interannual and spatial variability of meroplankton taxonomic composition across five sampling sections (2001-2016). Panels show the annual relative abundance [%] of individual taxa within five distinct sections: H, K, N, S, and EB2. The "All Years" panel provides a multi-year synthesis of the community structure for each section. Years are marked with thermal phase (warm in red, intermediate in grey, cold in blue).

Taxonomic richness (S) across the latitudinal gradient from south to north revealed high interannual variability (Figure III. 12), and no consistent pattern emerged from the long-term comparison (Figure III. 12 "All years"). The southernmost section (H) showed relatively high S in 2002-2003 and a peak around 2013. Section S showed the greatest fluctuations, starting with very low richness (2002-2005), followed by sharp increases in 2009 and 2013. The highest recorded peak in S among all sections was noted at section K. Almost all sections (especially

K and S) showed a simultaneous drop in richness in 2004 (Figure III. 12). Despite interannual fluctuations, there were no statistically significant differences in meroplankton taxonomic richness between sections within the sampled years (Table SIII. 12), and analysis of the integrated dataset confirmed that S showed no significant interannual variations within any of the sections (Table SIII. 13).

In the long-term, the highest H′ and J′ were observed in the south (sections H & K; Figure III. 12), while northern sections (S & EB2) usually showed the lowest taxonomic diversity and evenness. Section K showed peaks in H′ (e.g., 2007, 2013), often correlating with high J′. The northern section S showed the most extreme fluctuations in J′, with values falling to near-zero in 2003 and 2005. High variability also occurred in the middle section (N), with low values in 2008-2009 and 2016. Overall, the diversity and evenness of the meroplankton community showed a slight decline towards the north (Figure III. 12, "All Years"), though no consistent long-term trend was observed.

Significant spatial differences in meroplankton taxonomic diversity (H′) were revealed only in 2015, specifically between the K and S sections (Tables SIII. 14 & SIII. 15). For Pielou's evenness (J′), a significant spatial effect was detected only in 2014 (Table SIII. 16), although subsequent post-hoc comparisons did not show specific significant differences between sections (Table SIII. 17). Furthermore, within the integrated dataset, no statistically significant interannual differences in either H′ or J′ were observed within any of the individual sections (Tables SIII. 18 & SIII. 19).

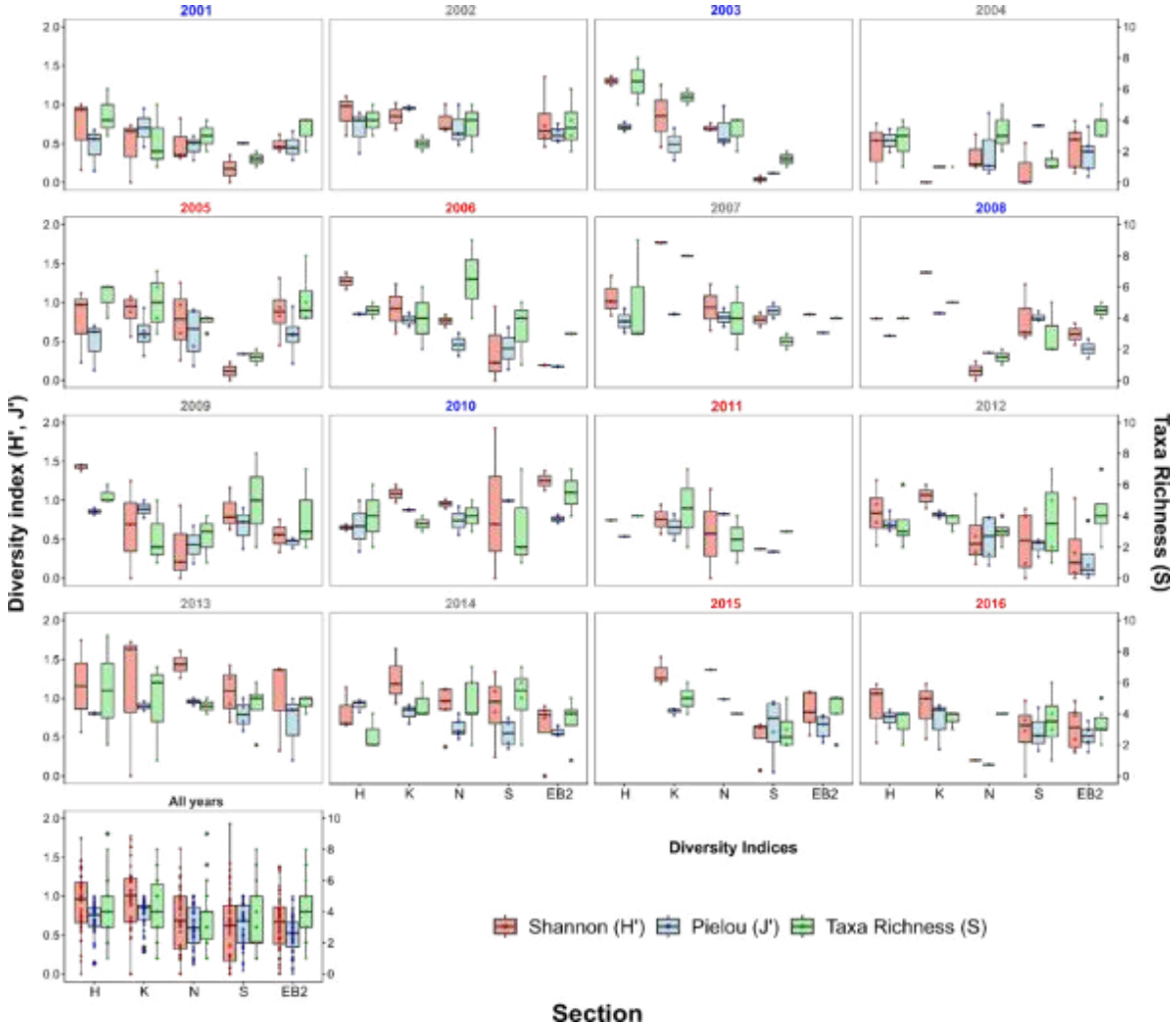

Figure III. 12 Interannual variability of meroplankton diversity indices (H′, J′) and taxonomic richness (S) across five sampling sections (2001-2016). Boxplots represent the median and interquartile range; whiskers indicate the minimum and maximum values. Individual points represent all sampled data, providing a visualization of data distribution within each section. Taxonomic richness (S) is displayed on the secondary y-axis. The "All Years" panel provides a multi-year synthesis for each section over the entire study period.

3.4 Discussion

3.4.1 Environmental control over the meroplankton community

The 16-year time series analyzed in this study reveals that the meroplankton community structure was primarily governed by hydrographic conditions and spatial zones, with latitudinal position playing a secondary role. We found out that larval distribution patterns across the shelf-to-offshore gradient remained relatively consistent over time, yet they were highly sensitive to interannual fluctuations in Atlantic water properties. These findings support the role of

meroplankton as a sensitive biological indicator of hydrographic shifts in the warming Arctic Ocean.

Multivariate analyses confirmed that bottom station depth and temperature were the strongest predictors of meroplankton taxonomic composition, suggesting that these larval assemblages were closely associated with specific properties and the extent of AW inflow in each year of sampling. This direct response to physical forcing suggests that meroplankton are not just drifting randomly; their presence reflects the strength and properties of upper layer circulation (among other factors not studied here) (Weydmann-Zwolicka et al., 2021a), as the WSC brings more warm and salty AW towards the Arctic Ocean, it has a significant impact on the pelagic system (Hop & Wiencke, 2019). This supports the idea that, in the warming Arctic, changes in water masses' properties (mainly temperature) are the primary driver of biological organization. A strong link between the properties of AW inflow and pelagic–benthic connectivity aligns with the broader pattern of Arctic Atlantification (Polyakov et al., 2020), in which the warming inflow of Atlantic water (AW) serves as a physical forcing rather than a background environmental change.

3.4.2 Shelf-offshore gradient vs latitude

One of our most interesting findings is that the spatial shelf-core-offshore gradient was a much more important factor for meroplankton than latitude. Even though the WSC moves north, the most pronounced differences in community composition occur across the current. The core of the WSC acts as a transitional mixing zone where coastal and oceanic taxa meet. This finding supports earlier observations that frontal zones between regions dominated by different water masses represent strong boundaries for biological fluxes in the Arctic Ocean (Głuchowska et al., 2016; Mańko et al., 2022b). Offshore waters showed stable but low diversity, potentially due to environmental filtering. Greater depths and more uniform water masses likely limit species occurrence to those specifically adapted to these conditions (Trudnowska et al. 2012).

On the other hand, the shelf remains a highly dynamic and heterogeneous environment, and consequently, we saw high variability and episodic peaks in richness there. This high variability is likely due to the shelf being much more complex, with localized currents, distinct habitats, and variable recruitment from the bottom. Therefore, bathymetry and water mass composition act together as a filter controlling larval survival and distribution across the region.

3.4.3 Temporal changes and diversity shift

The long-term observations (2001-2016) showed a strong link between periods of pronounced changes in ocean conditions and changes in meroplankton community composition. Interestingly, years with weaker Atlantic water influence (colder years) revealed higher diversity and more even distribution of taxa. Colder conditions appear to facilitate greater species coexistence (e.g., in 2007 or 2010, when, alongside Bivalvia veligers, Echinodermata larvae or Cirripedia, Bryozoa larvae, Gastropoda veligers, Polychaeta, or Decapoda were present), reducing the likelihood of dominance by a single group. In contrast, during warmer years, the entire system underwent simplification due to elevated temperatures, aligning with the observed restructuring of zooplankton communities in the North Atlantic (Carstensen et al. 2019; Kwaśniewski et al., 2012). While overall taxonomic richness declined, a few dominant, meroplanktonic taxa became increasingly prevalent (Echinodermata larvae; Bivalvia veligers), constituting around 90% of the total (e.g., in 2004, 2005, and 2014). This pattern suggests that warming acts as a selective environmental filter; rather than simply introducing new boreal taxa (Weydmann et al., 2014), it appears to favour the most tolerant taxa to environmental changes while excluding others. Such dynamics are consistent with the hypothesis that rapid environmental forcing promotes taxonomic homogenization and that if Arctic warming continues at its current rate, communities are likely to shift toward less diverse but more thermally tolerant assemblages (Mańko et al., 2020).

3.4.4 Meroplankton as early warning signals

The results showed that the larvae respond quickly to environmental variability, proving that meroplankton communities might detect ecosystem transitions much earlier than adult benthic assemblages, which often show a significant time lag in their response to hydrographic forcing While adult populations on the seafloor might take years to shift, the larval composition in the water column reflects the immediate impact of changing properties of the Atlantic water inflow (Heiskanen et al., 2016; Schrage et al., 2025; Sowa et al., 2023).

The presence of atypical or boreal taxa in areas where conspecific adults are still absent highlights the power of advective transport in the WSC (Renaud et al., 2015). These larvae are essentially the "pioneers" of Atlantification. Their distribution patterns, driven by ocean currents, determine their future recruitment success and colonization of the new areas (Ronowicz et al., 2024; Shanks, 2009). Monitoring pelagic larval stages provides a better understanding of how Arctic benthic communities will look in the future. Before the changes are visible on the seafloor, the changes are already well underway, making meroplankton

a critical early-warning tool for climate-driven biological change. These findings suggest that broadly tolerant groups, particularly Echinodermata larvae and Bivalvia veligers, display the highest resistance to intensified Atlantic water advection. Therefore, their consistent dominance throughout the 16-year time series indicates they are likely to expand their footprint and successfully colonize new benthic habitats as the Arctic continues to warm.

3.4.5 Methodology limitations and future perspectives

The 180 µm mesh size used in this study is standard for mesozooplankton sampling, however it might underestimate smaller larval stages (Makatun & Wedmann-Zwolicka, 2025; Weydmann-Zwolicka et al., 2021). Nevertheless, some earlier studies (Kirby et al., 2008; Michelsen et al., 2017) used the same or a larger mesh size to filter meroplankton. Also, sampling was restricted to the summer months, so we did not capture the full annual cycle or winter dynamics, which remain a black box in Arctic research (Berge et al., 2015; Daase et al., 2021). However, these limitations do not influence the main conclusions of this analysis. The consistency of the patterns observed over 16 consecutive years across different spatial gradients and changing environmental conditions provides strong evidence that the proposed links are valid on interannual to decadal time scales.

Among the limitations of this study is also the level of taxonomic identification, which, due to small individual sizes and morphological similarities among larvae, was mainly possible at the level of Phylum or Class. While our 16-year morphological dataset provides a necessary baseline, DNA barcoding and metabarcoding would help to bridge the remaining taxonomic gaps (Descôteaux et al., 2021; Ershova et al., 2021; Schrage et al., 2025; Walczyńska et al., 2019). Moving from traditional microscopy to high-throughput sequencing (NGS) would enable the identification of "cryptic" larvae that look identical but belong to different climatic regimes, such as boreal vs arctic species. The next step should be combining long-term time series with environmental DNA (eDNA) surveys. This combined approach would allow detection of the arrival of new species even when their abundance is too low to be captured by standard plankton nets. By building more comprehensive reference databases for Arctic taxa, we can turn meroplankton monitoring into a high-resolution early-warning system for the Atlantification of the Arctic Ocean. Integrating molecular methods with oceanographic models will help predict not only present species distributions but also future changes in the benthic-pelagic system under Arctic warming.

3.5 Conclusions

The 16-year study provides a comprehensive baseline for understanding how changes in hydrographic conditions influence meroplankton communities in the Atlantic sector of the Arctic. The meroplankton community in the WSC region is primarily driven by variations in Atlantic water inflow and bathymetry (spatial zones) rather than by latitudinal gradients. The shelf–offshore transition acts as a more significant ecological barrier than geographic distance, with the WSC core functioning as a transitional zone that facilitates larval dispersal.

While broad thermal phases (warm vs cold) did not explain the community variance, the environment showed strong responses to specific hydrographic extremes. Colder years (e.g., 2010) supported higher taxonomic diversity and peaks in some groups, such as Cirripedia cypris, whereas warmer years (e.g., 2016) resulted in the lowest taxonomic richness observed across the entire study period.

It was observed that climate-driven warming leads to a lower number of taxa in the larval pool. Warmer conditions and Atlantic water inflow favour only a few dominant groups, suggesting that the community becomes less diverse under sustained warming. Specifically, Bivalvia veligers reached high dominance (up to 70%) in offshore and core zones during warm or intermediate years, replacing more diverse assemblages.

Such shifts indicate that meroplankton could serve as sensitive early-warning indicators of ecosystem shifts. Their potentially rapid response to interannual changes could enable them to show a decrease in diversity more quickly than long-lived benthic populations, which could serve as a tool for monitoring the borealization of the Arctic Ocean. Our findings suggest that continued warming would likely affect the link between pelagic and benthic ecosystems by favouring thermally tolerant, low-diversity larval assemblages.

The results presented in this chapter have been submitted to Progress in Oceanography:
***Patuła, W.**[*], Kwaśniewski, S., Olszewska, A., Beszczyńska-Möller, A., Kukliński, P., Ronowicz, M., & Weydmann-Zwolicka, A. Long-term spatiotemporal shifts in meroplankton community composition as a signature of Arctic Atlantification (under review; submission date: 04.09.2026)*
[*]*corresponding author*

Chapter IV Halocline as an environmental barrier for the larvae of Arctic marine benthic invertebrates

4.1 Introduction

Many marine benthic invertebrates produce larval stages known as meroplankton, which play a crucial role in determining their spatial distribution. Remaining in the pelagic realm for hours to months, meroplankton disperse, enabling benthic organisms to explore new areas and eventually settle in new habitats (Metaxas & Saunders, 2009). Larvae are typically smaller than 2 mm, with low swimming abilities and speeds ranging from 1 to 15 mm s^{-1} (Metaxas, 2001; Strathmann, 1987; Young, 1995). For many years, scientists believed that meroplankton could not actively control their horizontal movement (Scheltema, 1986) and relied on ocean currents and water masses for dispersal (Chia et al., 1984; Shanks, 1995). However, as knowledge about meroplankton has increased, new studies have shown that they can actively move in the water column to some extent (Epifanio & Garvine, 2001; Luckenbach & Orth, 1992; Metaxas, 2001; Queiroga & Blanton, 2005). Their vertical movements can be achieved via swimming or sinking at velocities greater than those of vertical currents (Chia et al., 1984; Metaxas, 2001), triggered by ciliary propulsion, muscular activity, and changes in buoyancy, enabling shifts over large distances (e.g., in some crustacean or bivalve larvae; (Bonicelli et al., 2016; Cronin & Forward Jr., 1986; dos Santos et al., 2008; Lindley & Williams, 1994; Manuel et al., 1996).

The survival, growth, and settlement of meroplankton are influenced by both biotic (e.g., predators, food availability) and abiotic (e.g., salinity, temperature, light, tides, currents) (Maldonado & Young, 2009; Ronowicz et al., 2024; Rumrill, 1990; Sowa et al., 2023; Young, 1987; Young, 1995) factors. Food quality and availability can influence larval anatomical structure and physiology, affecting their passive dispersal by regulating their swimming abilities and densities in water column discontinuities, which can further influence their distribution in relation to haloclines (Hart & Strathmann, 1994; Metaxas & Young, 1998a; Strathmann, 1987; Thompson & Harrison, 1992). Larvae with greater resistance to environmental fluctuations can be transported over longer distances by ocean currents (Banse, 1986; DeVries et al., 1994; Ebert & Russel, 1988; Tremblay & Sinclair, 1992; Young, 1987). However, since covering all environmental drivers in Arctic field studies is challenging, our knowledge about meroplankton remains incomplete, with many aspects still requiring further research.

Salinity affects various factors and physicochemical properties of seawater, including gas absorption and saturation, viscosity, density, and osmolality (Kinne, 1966). Its gradients create haloclines, which can act as barriers, especially for small taxa. Steep changes in physical parameters of the marine environment, such as thermoclines, pycnoclines, or haloclines, exert physiological stress on invertebrate larvae, which may influence their development, survival, and vertical distribution (Daigle & Metaxas, 2011; Metaxas & Young, 1998b; Raby et al., 1994; Roberts Jr., 1971; Sameoto & Metaxas, 2008; Saranchova & Flyachinskaya, 2001; Tremblay & Sinclair, 1990; Vázquez & Young, 1996). Due to the limited behavioural abilities of meroplankton, larvae attempt to avoid these boundary zones by congregating above, below, or within a halocline layer (Hansen, 1951; Morgan et al., 1997; Raby et al., 1994; Thiébaut et al., 1992; Tremblay & Sinclair, 1990; Williams, 1985). However, most studies on the impact of salinity on meroplankton vertical migration have focused on a single taxonomic group or species (Bell & Brown, 1995; Connor & Epifanio, 1985; Mann et al., 1991; Roberts Jr., 1971), highlighting the need to deepen this knowledge in the rapidly changing European Arctic.

This study was conducted in western Spitsbergen (Svalbard Archipelago) along a well-studied area spanning from Kongsfjorden to the adjacent shelf and slope, hereafter referred to as the Kongsfjorden Transect (KT). This area has been the site of ongoing ecosystem research, including long-term monitoring of physicochemical parameters and biological processes (Hop & Wiencke, 2019). Kongsfjorden experiences significant physical and chemical variability due to the influence of Arctic and Atlantic water masses (Cottier et al., 2005; Svendsen et al., 2002; Tverberg et al., 2019). The ecosystem is shaped by regular intrusions of the of West Spitsbergen Current (WSC) waters of Atlantic origin, changing hydrographic conditions (such as water temperature, salinity, and stratification), melting snow, ice, glaciers, and riverine output, leading to strong seasonal and multi-annual fluctuations in environmental conditions and marine biota (Cottier et al., 2010; Wiencke & Hop, 2016). Therefore, the Kongsfjorden Transect is an ideal model system for studying and predicting interactions between a changing environment and the organisms that inhabit the area. Zooplankton studies along the KT – encompassing dynamics, taxonomic structure, and seasonal and inter-annual community changes (Głuchowska et al., 2016; Hop & Wiencke, 2019; Kwaniewski et al., 2003; Lischka & Hagen, 2016; Ormańczyk et al., 2017; Walkusz et al., 2009) – reveal that the area is rich in zooplankton fauna. Furthermore, notable shifts in taxonomic composition over the past decade show an increasing mixture of native and advected species (Dalpadado et al., 2016; Kwaśniewski et al., 2003; Ormańczyk et al., 2017). However, little is known about

meroplankton diversity, which is grouped into higher taxa or simply categorized as "meroplankton" or "others" in most studies (Głuchowska et al., 2016; Trudnowska et al., 2020; Willis et al., 2006).

The main objective of this study was to assess the influence of the halocline on the vertical distribution of meroplankton in relation to environmental conditions in the European Arctic. It was hypothesized that the halocline plays a crucial role in structuring meroplankton communities by acting as a barrier to benthic invertebrate larvae, resulting in differences in their taxonomic composition above and below this pronounced vertical salinity gradient. This study investigated meroplankton diversity and distribution across the halocline, providing additional insights into larval morphotype variation, taxa associated with distinct water layers, and differences in community structure between shelf and fjord regions.

4.2 Materials & Methods

4.2.1 Study area

Meroplankton sampling was conducted from July 31 to August 3 in 2021, from the shelf (forefront) to the inner part of Kongsfjorden, an open, glacial fjord on the west coast of Spitsbergen (Figure IV. 1), hereafter termed the Kongsfjorden Transect (KT). Sampling in mid-summer reflects the timing of research cruises aboard the R/V Oceania, which are conducted only during the summer months due to annual monitoring expeditions and Arctic operational constraints. Therefore, it was not possible to collect samples during the spring peak of benthic organism reproduction, when meroplankton abundance is expected to be the highest.

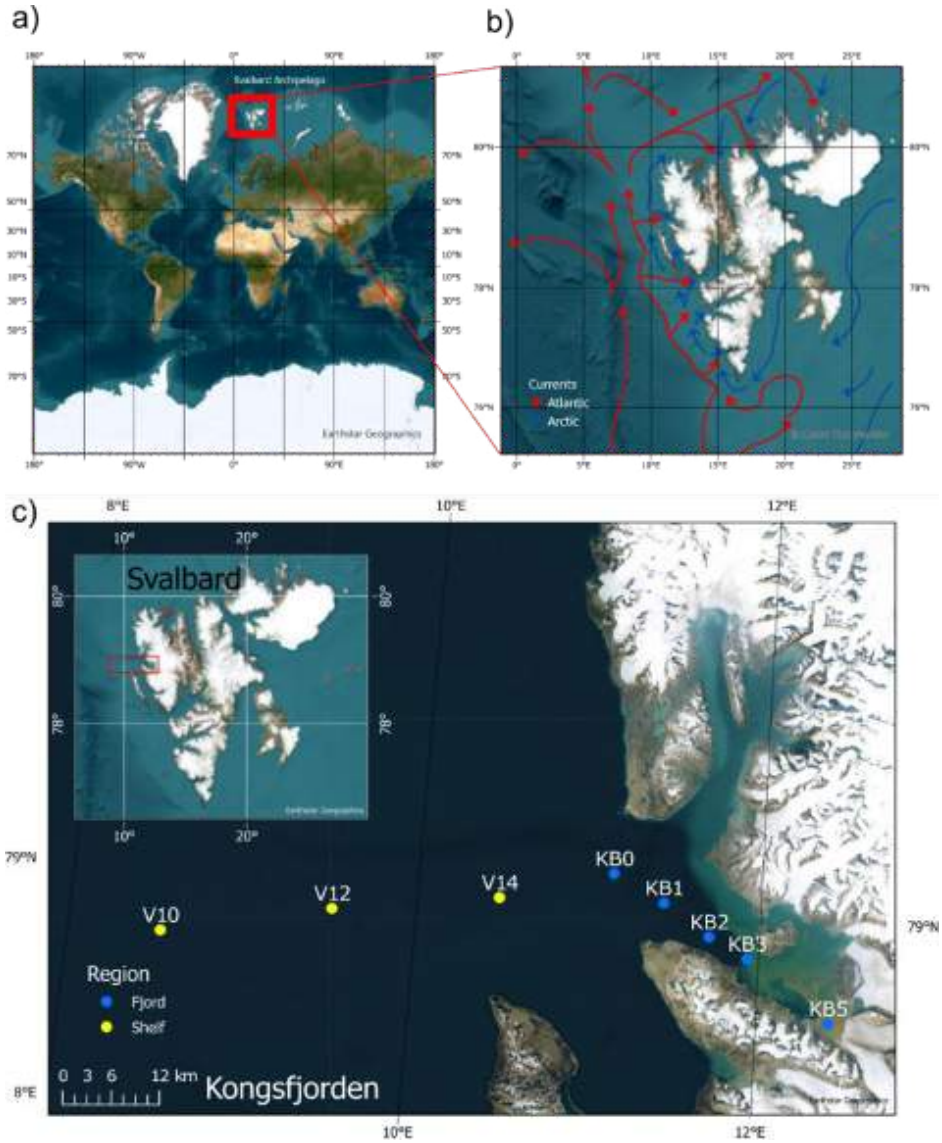

Figure IV. 1 Study area: Svalbard Archipelago on a global map (a), with schematic ocean current circulation including their origin (based on Assmy et al. (2023)) (b), and sampling sites along the Kongsfjorden Transect, with stations divided into fjord and shelf regions based on Hop and Wiencke (2019) (c).

The connection of the fjord to the adjacent shelf and the Fram Strait is facilitated through Kongsfjordrenna, a deep channel without a sill, which causes the area to be strongly influenced by the advection of relatively warm and salty Atlantic Water (AW, >3°C, >34.9) transported by the West Spitsbergen Current (WSC) (Svendsen et al., 2002). These waters mix with the Arctic Water (ArW, -1.5-1.0°C, 34.30-34.80) that inflows from the shelf areas, and together they form the Transformed Atlantic Water (TAW, >1°C, >34.7) (Cottier et al., 2005; Svendsen et al., 2002), which drives the physical and biological conditions of this marine environment (Cottier et al., 2005; Dalpadado et al., 2016; Hop et al., 2006).

Advection, wind-driven circulation, and tidal mixing facilitate water mass exchange and may contribute to both the recruitment of meroplankton into the inner fjord and the export of larvae produced within it. The inner fjord is strongly influenced by freshwater runoff from marine-terminating glaciers (Angelo et al., 2018; Calleja et al., 2017), resulting in enhanced stratification and more Arctic conditions than the outer fjord (Hop et al., 2002; Lydersen et al., 2014). This runoff also contributes to benthic-pelagic coupling by promoting the advection and sinking of organic matter (Hop et al., 2002), which can influence biological processes within the fjord.

The marine ecosystem along the KT is diverse, with strong seasonal and multiannual changes observed. Its location and the surrounding environment, with rapid shifts in hydrographic conditions (Cottier et al., 2005; Svendsen et al., 2002; Wiencke & Hop, 2016), determine the timing of the spring phytoplankton bloom, taxonomic composition of organisms inhabiting the area, and the flow of matter (Hop et al., 2006; Hop & Wiencke, 2019; Lalande et al., 2016; Piwosz et al., 2015). Closer to glaciers, the increasing inflow of inorganic matter released from glacier mass leads to a decrease in the rate of primary production. This change in environmental conditions drives shifts in the composition and structure of phyto- and zooplankton communities, favouring species adapted to lower light availability and increased turbidity (Piwosz et al., 2009; Walkusz et al., 2009). In summer, meltwater, rainfall, and river inflow contribute to a less saline surface layer, which, combined with the intrusion of relatively warm and saline AW, leads to strong stratification in the water column. The summer salinity gradient along the KT reflects this stratification of about a 1-unit difference from the surface to the bottom, thereby influencing the occurrence and depth of the halocline (Cottier et al., 2005; Noufal et al., 2017).

4.2.2 Measurements and sampling

Environment measurements

To determine hydrological conditions along the Kongsfjorden Transect prior to zooplankton sampling, water temperature, salinity, and fluorescence were measured at each station using a CTD profiler (Conductivity Temperature Depth, Sea-Bird Electronics 911), which was lowered through the entire water column. Based on fluorescence peaks measured during the preceding CTD profiles, the depth layers for collecting water samples for the chlorophyll *a* (chl *a*) concentration analysis were selected.

To accurately assess chlorophyll *a* concentration at a given depth layer, either above the halocline (AH) or below the halocline (BH), 2-3 water samples were taken for the AH depth

layer, while 3 – 6 were collected for the BH depth layer (Table IV. 1). The number of water samples for AH and BH depended on the layer's thickness, station depth, and environmental conditions. Each sample contained 1 L of seawater (per depth), from which 250 mL was filtered separately through Whatman GF/F filters (nominal pore size: 0.75 μm). Afterward, the filters were folded, wrapped in aluminum foil, and frozen at -80°C until further analysis. The chl *a* concentration data were treated as a proxy for food availability for meroplankton in the subsequent statistical analyses.

Table IV. 1 Sampling details: water depths used for chlorophyll *a* concentration analysis and depth layers for meroplankton samples (AH – Above the halocline; BH – Below the halocline).

Station	**Area**	**Coordinates**		**Depths for chlorophyll *a* samples [m]**										**Depth layers for meroplankton samples [m]**	
		Latitude	*Longitude*	*AH*			*BH*							*AH*	*BH*
V10	Shelf	78.9351	8.5363	0	21		30	48	10	16	18	28		21-0	288-30
V12	Shelf	78.9786	9.5118	0	20		48	66	85	12	15			20-0	153-48
V14	Shelf	79.0066	10.4766	0	5		60	13	26					5-0	260-60
KB0	Fjord	79.0426	11.1326	0	5		50	15	29					5-0	295-50
KB1	Fjord	79.0131	11.433	0	5	15	50	11	14	25	35			15-0	355-50
KB2	Fjord	78.978	11.706	0	5		25	45	60	70	15	29		5-0	295-25
KB3	Fjord	78.9555	11.932	0	5		25	80	10	17	33			5-0	335-25
KB5	Fjord	78.886	12.4301	0	5		40	50	80					5-0	80-40

Meroplankton sampling

Halocline layers were distinguished based on vertical salinity profiles in the water column, and depth layers for meroplankton sampling were defined accordingly (Table IV. 1). For the effective collection of benthic invertebrate larvae, meroplankton samples were collected from the two depth layers, AH and BH, using a vertically hauled Juday plankton net (mesh size: 56μm, square opening 0.10 m^2, with an attached closing system) (Weydmann-Zwolicka et al., 2021a). The net was hauled at a speed of approximately 1 m s^{-1}. After collection, the samples were preserved in 96% ethyl alcohol. In total, 16 samples were collected. Although replicate sampling at each station was not performed due to logistic constraints, the inclusion of many stations differing in depth and hydrographic characteristics allowed us to assess whether vertical distribution patterns across the halocline followed a consistent trend independent of local variability, thus prioritizing spatial representativeness over replication.

4.2.3 Laboratory analysis

Chlorophyll a

In the laboratory, the filters were defrosted at room temperature, and pigments were extracted overnight (12-18h) in 10 mL of 90% acetone at 4°C in the dark. Subsequently, the samples were centrifuged at 3000 rpm for 2 min. After calibration with pure chlorophyll *a* (Sigma S6144), the supernatant was measured using a Trilogy® fluorometer (Turner Designs Inc.) following the EPA 445.0 method (Arar & Collins, 1997). Measurements were taken before and after acidification with 100 µL 0.1 M HCl (Arar & Collins, 1997). The results were then recalculated to determine chl *a* concentration, expressed in mg m^{-3}. Finally, chl *a* concentrations were averaged for the AH and BH depth layers using a weighted average with weights adjusted to layer thickness (Dąbrowska et al., 2020).

Meroplankton

Meroplankton samples were examined morphologically under a stereomicroscope (Olympus SZX7). During the analyses, the entire community was identified to the lowest possible taxonomic level, following the method proposed by Postel et al. (2000). The macro fraction was identified gradually throughout the analysis, both while examining subsamples (when larger individuals were encountered) and during final inspection of the whole sample. Benthic invertebrate larvae were analyzed and categorized into subjectively defined morphotypes, where distinguishable, based on their morphology within higher taxonomic levels (Table IV. 2). The morphotypes were then photographed using an Olympus SZX16 stereomicroscope with Olympus cellSens Standard 2.1 software, in order to create an atlas of morphological forms identified during the analyses (Table IV. 2; Patuła, 2025, https://doi.org/10.48457/himero). In some cases, morphotypes labeled as "juvenile" (e.g., Ophiuroidea juvenile1 and juvenile2) were designated based on their visual appearance in the plankton (star-shaped body with slender arms separated from the central disc) rather than representing benthic juveniles already settled in the substrate. This approach followed previous studies that used photographic documentation (e.g., Larink & Westheide, 2011; Young et al., 2002). The numbering of morphotypes served to distinguish visually similar forms that may potentially correspond to different genera/species, rather than to indicate the developmental stage or order in which larvae were encountered. Finally, meroplankton abundance was expressed as the number of individuals per cubic meter of seawater (ind m^{-3}), which allowed meaningful comparison between the designated layers. Since a flowmeter was

not used, the water volume sampled by the Juday net was calculated mathematically as the product of the haul depth (h) and the mouth area (A) of the net (V = A x h).

Table IV. 2 Classification of meroplankton: taxonomic assignment and larval morphotypes. Note that different morphotypes within a certain taxa may potentially correspond to different genera/species.

Meroplankton Morphotype Abbreviations			
	Meroplankton Taxa	***Long name of larvae morphotype***	***Short name of larvae morphotype***
1	Echinodermata	Pluteus	Pluteus
2	Echinodermata	Ophiopluteus1	Ophio1
3	Echinodermata	Ophiopluteus2	Ophio2
4	Echinodermata	Ophiuroidea juvenile1	OphiJuv1
5	Echinodermata	Ophiuroidea juvenile2	OphiJuv2
6	Echinodermata	Echinopluteus1	Echinopl1
7	Polychaeta	Poly_trochophorae	Poly_troch
8	Polychaeta	Poly_metatrochophorae	Poly_metatroch
9	Polychaeta	Poly_mitraria cf. Owenidae	Poly_cf. Owenidae
10	Polychaeta	Poly_larvae1 cf. Polynoidae	Poly_cf. Polynoidae
11	Polychaeta	Poly_larvae2 cf. Spionidae	Poly_ cf. Spionidae
12	Polychaeta	Poly_larvae3 cf. Phyllodocidae	Poly_cf. Phyllodocidae
13	Polychaeta	Poly_larvae4 cf. *Prionospio* spp. (Spionidae)	Poly_cf. *Prionospio* spp.
14	Polychaeta	Polychaeta unidentified	Poly_indet.
15	Bivalvia	Bivalvia veliger	Biv_veliger
16	Cirripedia	Cirripedia cypris1	Cirr_cyp_1
17	Cirripedia	Cirripedia cypris2	Cirr_cyp_2
18	Cirripedia	Cirripedia cypris3	Cirr_cyp_3
19	Gastropoda	Gastropoda veliger	Gast_veliger
20	Bryozoa	Bryozoa cyphonautes1	Bryo_cypho1
21	Ascidiacea	Ascidiacea tadpole	Asci_tadpole
22	Nemertea	Nemertea pilidium	Nem_pilid
23	Decapoda	*Pagurus* zoëa	*Pagu*_zoëa
24	Decapoda	*Pagurus* megalopa	*Pagu*_megalopa
25	Decapoda	Decapoda unidentified zoëa	Decap_indet. zoëa

4.2.4 Data processing

Sampling stations were grouped into two regions along the Kongsfjorden Transect (Figure IV. 1): the shelf area (V10; V12; V14) and the fjord (KB0; KB1; KB2; KB3; KB5) (Hop et al., 2023; Hop & Wiencke, 2019). The sampling sites were visualized using ArcGIS Pro (Esri, 2025). CTD datasets from the cruise were processed using the SBE Data Processing Software, with vertical profiles averaged at 1 m intervals. For the purpose of statistical analyses, all environmental parameters were averaged over the depth range corresponding to the respective meroplankton sampling layer (Table IV. 1). Further calculations and visualizations

of physicochemical water properties variability (temperature, salinity, and chlorophyll *a*) as well as meroplankton community structure were performed using Microsoft Excel and R 4.4.1/4.4.2 (R Core Team, 2025).

Multivariate analyses using PRIMER 7 with Permanova+ software (Clarke et al., 2014; Clarke & Gorley, 2015) were performed to analyze the meroplankton community, including the distinguished morphotypes. Log-transformed abundance data were used to downweight the impact of dominant taxa on the results, and the resemblance matrix was based on the Bray-Curtis similarity. We used hierarchical agglomerative clustering (CLUSTER) to present meroplankton taxonomic composition and abundance similarity between the studied stations. As a result, we obtained a tree showing samples grouped into clusters. A permutation-based similarity profile test (SIMPROF) was simultaneously applied to test for statistically significant ($p=0.05$) clusters (Clarke & Gorley, 2015). A one-way analysis of similarities (ANOSIM) was applied to test whether the meroplankton morphotype composition statistically differed between the AH and BH assemblages and between the groups obtained by CLUSTER. The AH/BH division was used only as a categorical factor to illustrate assemblage separation.

Distance-based redundancy analysis (dbRDA) was performed using PRIMER-e with PERMANOVA+ software together with DistLM analysis, to evaluate the contribution of environmental variables (temperature, salinity, chlorophyll *a*) to the abundance of different morphotypes present in the meroplankton community. Although salinity was used to define the above- and below-halocline (AH and BH) layers during sampling, it was treated as a continuous environmental variable in the DistLM analysis to evaluate its contribution to the variation in meroplankton community composition across the entire dataset. The dbRDA analysis combined two approaches that allowed us to: 1) examine the response of the meroplankton community across multiple environmental variables simultaneously and 2) identify factors that best explain variation in the taxonomic composition and abundance. The first model was performed using a best selection procedure to determine which factors explained the most variation. Subsequently, forward selection was applied, with the best-fitting relationship determined based on adjusted R^2 values (Anderson et al., 2008). The significance level for all analyses was set at $p \leq 0.05$.

4.3 Results

4.3.1 Environmental conditions

During sampling in summer 2021, seawater temperature along the Kongsfjorden Transect varied from 1.32°C at the bottom to 4.92°C at the surface inside the fjord and from

1.23°C to 5.73°C on the adjacent shelf. Salinity ranged from 34.70 at the bottom to 31.65 at the surface inside the fjord, and from 34.85 to 33.47 on the shelf (Figure IV. 2). The halocline layer began at depths ranging from 5 to 21 m, with a thickness of 9 to 55 meters on the shelf and from 20 to 35 meters inside the fjord (Figure IV. 2; Table IV. 1).

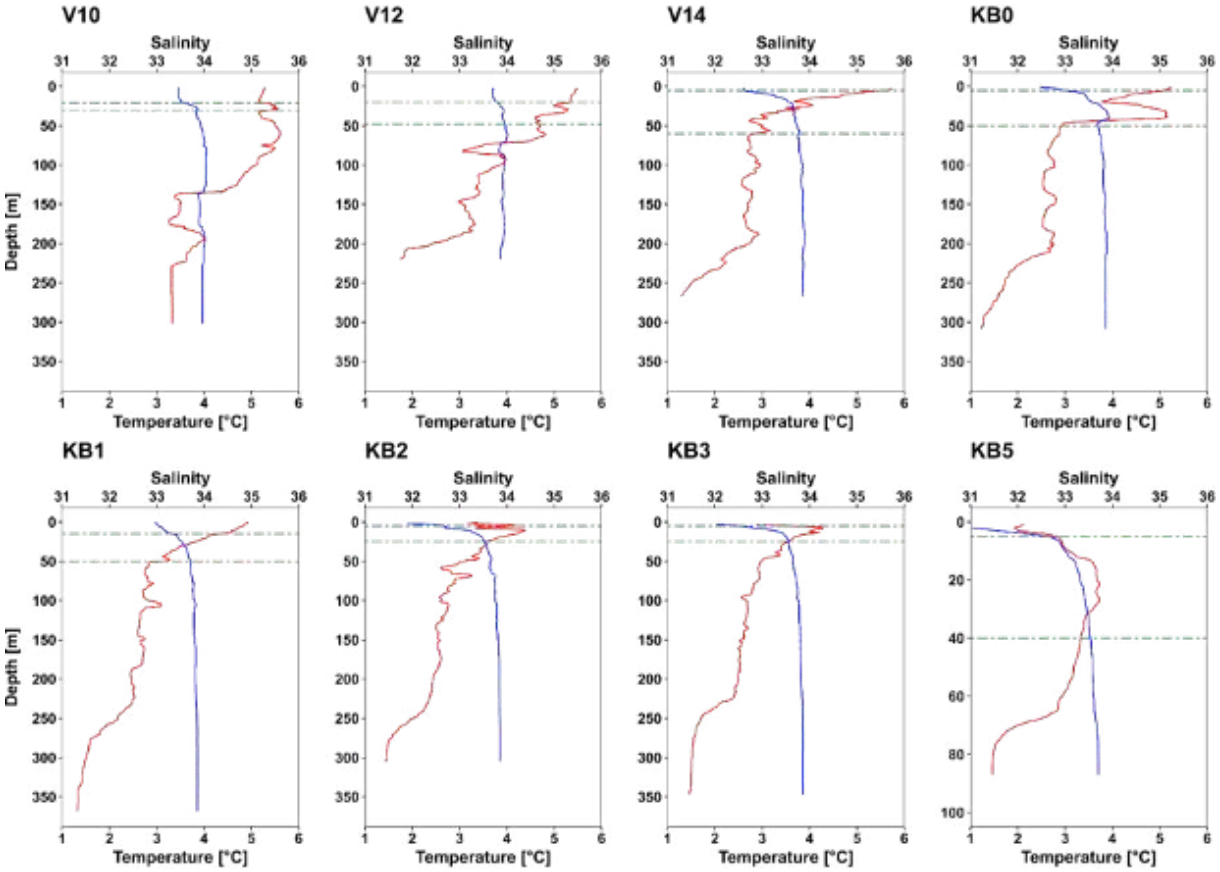

Figure IV. 2 Vertical profiles of temperature (red lines) and salinity (blue lines) with a marked halocline layer (green horizontal dashed lines) at each sampling station along the studied Kongsfjorden Transect. Note the station KB5, located in the innermost part of the fjord, has a different depth scale.

The overall trend in mean temperature and salinity showed an increase from the fjord to the shelf along the KT (Figure SIV. 1a, b). This increase was more pronounced above the halocline (AH), with temperature rising from 2.29°C to 5.22°C and salinity from 32.61 to 34.47 (Figure SIV. 1a and b, respectively). Inside the fjord, temperature and salinity gradually increased from the glacier towards its entrance. On the shelf, hydrological conditions were more stable, except at stations V12 and V10, which had higher salinity (~34.5) than the other KT stations (Figure SIV.1a, b). Below the halocline (BH), environmental conditions remained stable, with temperature around 2.5°C and salinity around 34.8, except at the two outermost shelf stations (V12: T=3.44°C, S=34.93; V10: T=4.17°C, S=34.97) (Figure SIV. 1a, b). Station

KB5, located near the glacier, exhibited much lower salinity in both AH and BH compared to the other sampling stations (Figure SIV. 1b).

Chlorophyll *a* (chl *a*) concentration varied along the KT. Below the halocline (Figure SIV. 1c), chl *a* concentrations were an order of magnitude lower than those at AH (Figure SIV. 1d). Above the halocline, inside the fjord, chl *a* concentration increased toward the mouth of the fjord (from 0.001 to 0.043 mg m^{-3}). Along the shelf, a general trend toward the open ocean was similar but more variable (Figure SIV. 1c). Below the halocline, chl *a* concentration increased at the shelf stations toward the open ocean (from 0.001 to 0.009 mg m^{-3}), while more fluctuations were observed in the fjord's inner part (Figure SIV. 1d).

4.3.2 Meroplankton community

Of the 16 samples collected along the Kongsfjorden Transect, the following nine main meroplankton taxa, spanning from order to phylum level, were observed: Bivalvia, Echinodermata, Polychaeta, Cirripedia, Bryozoa, Gastropoda, Decapoda, Ascidiacea, and Nemertea (Figure IV. 3). A total of 25 larval morphotypes were distinguished based on their characteristic morphological features, including six Echinodermata, eight Polychaeta, three Cirripedia, three Decapoda, as well as one morphotype for each of the remaining groups (Table IV. 2). Bivalvia veligers were the most abundant in all samples, dominating the entire meroplankton community (Figure IV. 3). Although their abundance was generally higher above the halocline, they were also relatively numerous below it.

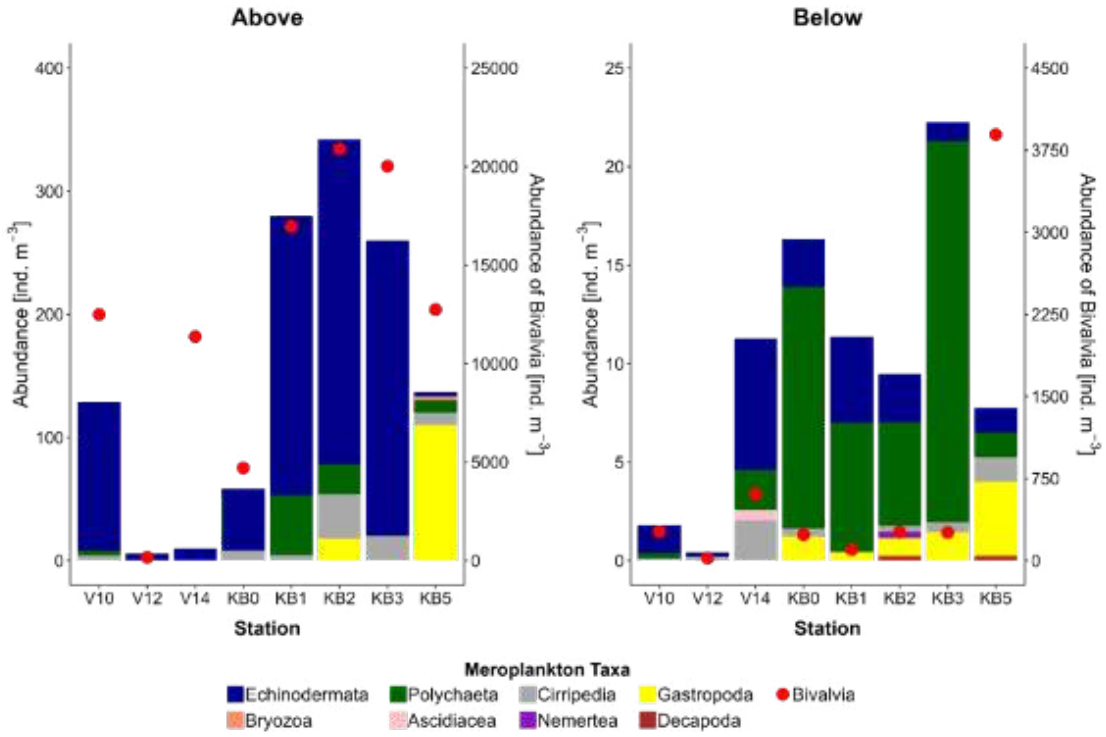

Figure IV. 3 The abundance of main meroplankton taxa at the sampling sites above (left) and below (right) the halocline along the Kongsfjorden Transect: from the shelf to the inner fjord. The right axis indicates the abundance of Bivalvia veligers (red dots). Note the different scales for abundance in both plots.

4.3.3 Meroplankton community variation across environmental conditions

A statistically significant and clear separation between AH and BH was observed in the morphotype meroplankton composition and abundance (ANOSIM test: $p<0.006$; $R=0.603$). The conducted cluster analysis revealed two distinct meroplankton assemblages between AH (Group A) and BH (Groups B;C;D;E). Additionally, inside the assemblage BH there were two significant groups for the inside the fjord (Group E) and the shelf meroplankton assemblage (Group C) (Figure IV. 4). The differences were significant between cluster Groups "A" and "C" and "A" and "E" (Global Test: $p=0.0001$, $R=0.779$; ANOSIM $p=0.0006$; $R=0.745$ and $p=0.0006$; $R=0.909$; respectively) (Figure IV. 4). Bivalvia veligers dominated in all separated groups, but in Group A they were counted in the thousands (from 3892 to 20 898 ind m^{-3}), while in the remaining groups in the hundreds (100 to 607 ind m^{-3}) (Figure IV. 3). That put the station KB5 from BH (Bivalvia veligers = 3892 ind m^{-3}) together with the AH stations (Group A), and V12 from AH (Bivalvia veligers = 166 ind m^{-3}) together with the BH stations (Group C). In addition to Bivalvia veligers in Group E, Poly_larvae4 cf. *Prionospio* spp. (Spionidae) were

also noticed in higher abundances (from 4 to 17 ind m^{-3}). The low abundance of Bivalvia veligers (22 ind m^{-3}), the absence of Polychaeta larvae, the occurrence of Cirripedia cypris3 (station V12 in BH (Group B)), and the strong domination of Gastropoda veligers (station KB1 in BH (Group D)) made these assemblages the outliers (Figure IV. 3; Figure IV. 4).

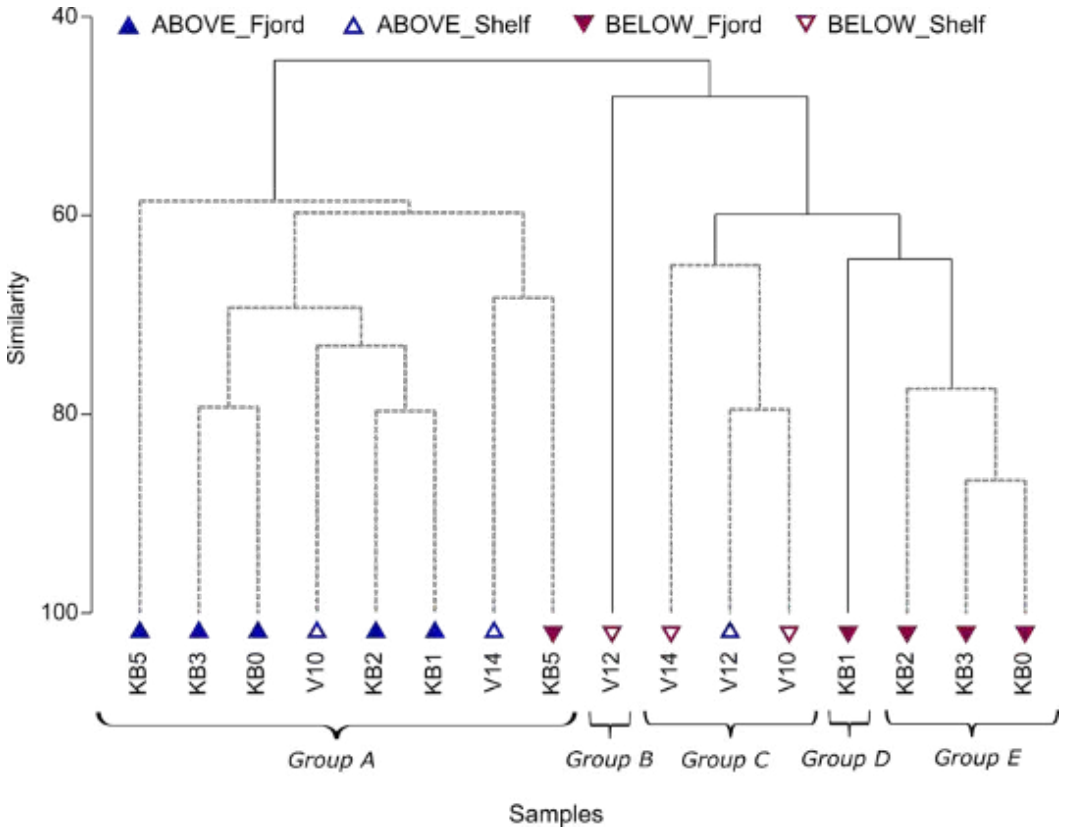

Figure IV. 4 A dendrogram based on CLUSTER analysis, on meroplankton morphotype structure and abundance at the sampling sites above and below the halocline along the studied transect. The solid lines represent significant splits according to the SIMPROF tests (type 1: analyse: samples – permute within: variables; no. of permutations: 9999; sig. level: 5%, resemblance measure: S17 Bray-Curtis similarity).

The DistLM analysis, illustrated by the dbRDA plot (Figure IV. 5), which represented relationships between the meroplankton community structure and environmental conditions, also indicated differences in the meroplankton community between AH and BH. Consequently, salinity was the most important environmental factor, explaining 30.78% of meroplankton variation. The second-most influential variable was chlorophyll *a*, accounting for 17.78% of variation (Table IV. 3).

Table IV. 3 Results of Distance-based linear model analysis (DistLM) for meroplankton morphotype structure and abundance with environmental factors; Significant results are marked in red.

Marginal Tests							
Variable	**SS(trace)**		**Pseudo-F**	**P**		**Prop.**	
Salinity	5580.7		6.2263	0.0005		0.30783	
Chlorophyll a	3269.2		3.0801	0.0256		0.18033	
Temperature	3128.6		2.9200	0.0293		0.17257	
Sequential Tests							
Variable	**Adj. R^2**	**SS(trace)**	**Pseudo-F**	**P**	**Prop.**	**Cumul.**	**res.df**
Salinity	0.25839	5580.7	6.2263	0.0001	0.30783	0.30783	14
Chlorophyll a	0.40654	3224	4.4950	0.0003	0.17784	0.48567	13
Temperature	0.43356	1109	1.6199	0.1504	0.061173	0.54684	12

The dbRDA plot revealed distinct meroplankton assemblages in AH and BH, as well as shelf and fjord regions, in which the first two axes explained 49.8% of the total variation (Figure IV. 5). Above the halocline, the fjord and shelf meroplankton assemblages were more widely separated in the ordination plot. Larvae observed inside the fjord were correlated with lower salinity (from 32.61 to 34.71). In contrast, the shelf meroplankton assemblage was correlated with higher food availability (chl *a*). Below the halocline, the fjord assemblage was correlated with higher salinity (from 34.61 to 34.97) and characterized mainly by the increasing abundances of Polychaeta and Decapoda larvae, which were negatively correlated with temperature and chlorophyll *a* (Figure IV. 5).

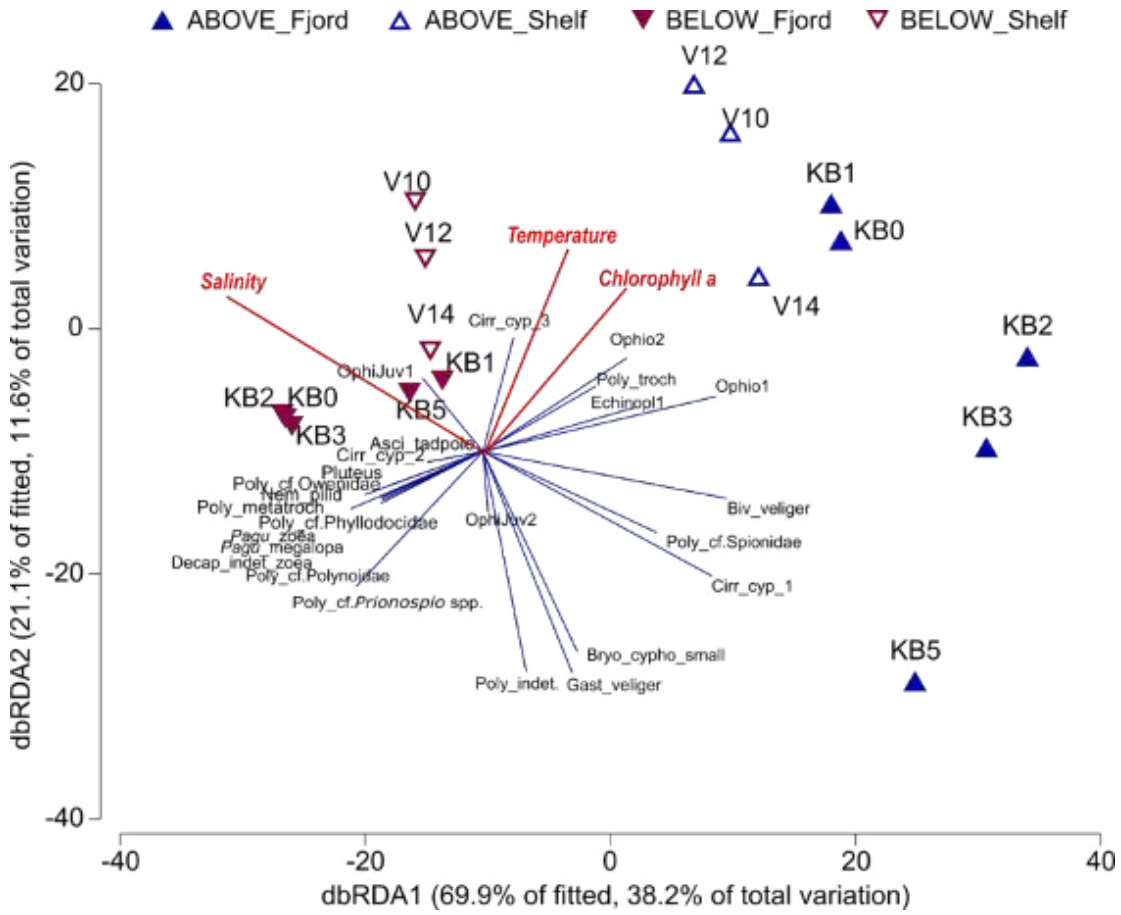

Figure IV. 5 The dbRDA ordination plot of all meroplankton morphotypes (blue arrows), environmental variables (red arrows), and samples.

4.3.4 The meroplankton assemblage structure above vs below halocline

4.3.4.1 *Meroplankton Taxa*

The meroplankton assemblage above the halocline (AH) showed considerably higher abundances along the KT compared to the below-halocline (BH) assemblage (Figure IV. 3). In both layers, Bivalvia veligers were dominant, with greater abundance in AH (Figure IV. 3). In the AH assemblage, Echinodermata larvae were relatively abundant throughout the KT (~0.2-264 ind m^{-3}), whereas in the BH assemblage Polychaeta larvae were numerous (~0-19 ind m^{-3}) (Figure IV. 3). Cirripedia larvae were observed across the KT in both AH and BH (from 0 to 36 ind m^{-3} and from 0 to 2 ind m^{-3}, respectively), while Gastropoda veligers were mainly found in BH but less numerous compared to AH (from 0 to 3 ind m^{-3} and from 0 to 110 ind m^{-3}, respectively). The larvae of Ascidiacea, Nemertea, and Decapoda were present exclusively in BH, whereas Bryozoa larvae were observed only in AH (Figure IV. 3).

4.3.4.2 *Polychaeta larvae*

The most diverse group was Polychaeta, represented by eight larval morphotypes (Figure IV. 6A, B). In the AH assemblage, abundances were generally higher than in BH, and they were also higher inside the fjord than on the shelf (Figure IV. 6A). Poly_trochophorae and Poly_larvae4 cf. *Prionospio* spp. (Spionidae) were the most abundant morphotypes overall and occurred in both the AH and BH layers. Above the halocline, Polychaeta larvae were found only at shelf station V10, where Poly_trochophorae dominated (~4 ind m^{-3}) (Figure IV. 6A). In contrast, in the fjord, four morphotypes were numerous in AH: Poly_trochophorae, Poly_larvae4 cf. *Prionospio* spp. (Spionidae), Poly_larvae2 cf. Spionidae, and Polychaeta unidentified.

Below the halocline, the diversity was lower on the shelf than in the fjord (Figure IV. 6B). While Poly_larvae4 cf. *Prionospio* spp. (Spionidae) were highly abundant in both regions (0-17 ind m^{-3}), Poly_mitraria cf. Owenidae was notable at shelf station V14. Poly_trochophorae was more frequent inside the fjord and dominated the assemblage at BH station KB5 near the glacier (Figure IV. 6B). Additionally, Polychaeta_metatrochophorae, Poly_mitraria cf. Owenidae, Poly_larvae1 cf. Polynoidae, and Poly_larvae3 cf. Phyllodocidae were observed exclusively in BH (Figure IV. 6A, B).

4.3.4.3 *Echinodermata larvae*

Echinodermata was the second most diverse group, with six larval morphotypes. No clear pattern was observed between the shelf and fjord assemblages within either AH or BH (Figure IV. 6C, D). Nevertheless, larval abundance in AH was much higher in the fjord than on the shelf (Figure IV. 6C). Above the halocline, the entire KT was dominated by Ophiopluteus1 (3-252 ind m^{-3}), except at shelf station V14, where Ophiopluteus2 was dominant. Echinopluteus1 was observed only in AH, both on the shelf and inside the fjord (Figure IV. 6C, D).

In the BH assemblage, larval abundance was comparable between the shelf and fjord areas (Figure IV. 6D). Pluteus and Ophiuroidea juvenile1 were present only in BH (Figure IV. 6C, D). On the shelf, Ophiuroidea juvenile1 was recorded only at station V10, while Ophiuroidea juvenile2 dominated station KB0 at the fjord entrance. Pluteus larvae were observed both on the shelf (V14) and inside the fjord (stations KB1 and KB2) (Figure IV. 6C, D). Ophiopluteus1 was less numerous in BH than in AH (0-3 ind m^{-3}), but its relative abundance among BH morphotypes remained noticeable.

4.3.4.4 *Other larvae*

Other identified larval groups included Cirripedia, Bryozoa, Gastropoda, Decapoda, Ascidiacea, and Nemertea. Although their overall abundances were lower, they contributed to the taxonomic diversity of both the AH and BH assemblages. Their distribution patterns varied between assemblages and locations, with some morphotypes restricted to specific stations or water layers (Figure IV. 6E, F).

Among the three Cirripedia larval morphotypes, Cirripedia cypris1 was the most abundant, ranging from 0 to 36 ind m^{-3} in AH and from 0 to 1 ind m^{-3} in BH. In the AH assemblage, Cirripedia larvae dominated, particularly on the shelf, with Cirripedia cypris1 being the most abundant at station V10 (Figure IV. 6E). In contrast, in the fjord, Cirripedia cypris3 and Gastropoda veligers were more numerous. Bryozoa cyphonautes1 was observed exclusively in AH, near the glacier at station KB5. Overall, larval abundance in AH was higher inside the fjord than on the shelf (Figure IV. 6E).

In the BH assemblage, Cirripedia larvae continued to dominate on the shelf, with single observation of Ascidiacea larvae at station V14 (Figure IV. 6F). However, in the fjord Gastropoda veligers were dominant, while Cirripedia cypris1 occurred less frequently. Decapoda larvae, which were observed only in BH, were present at station KB5 near the glacier (Decapoda unidentified zoëa) and at station KB2, where all three Decapoda larvae (*Pagurus* zoëa, megalopa, and Decapoda unidentified zoëa) were recorded. A single occurrence of Nemertea pilidium was also noted at station KB2. Similar to AH, larval abundance in BH was higher in the fjord compared to the shelf (Figure IV. 6F).

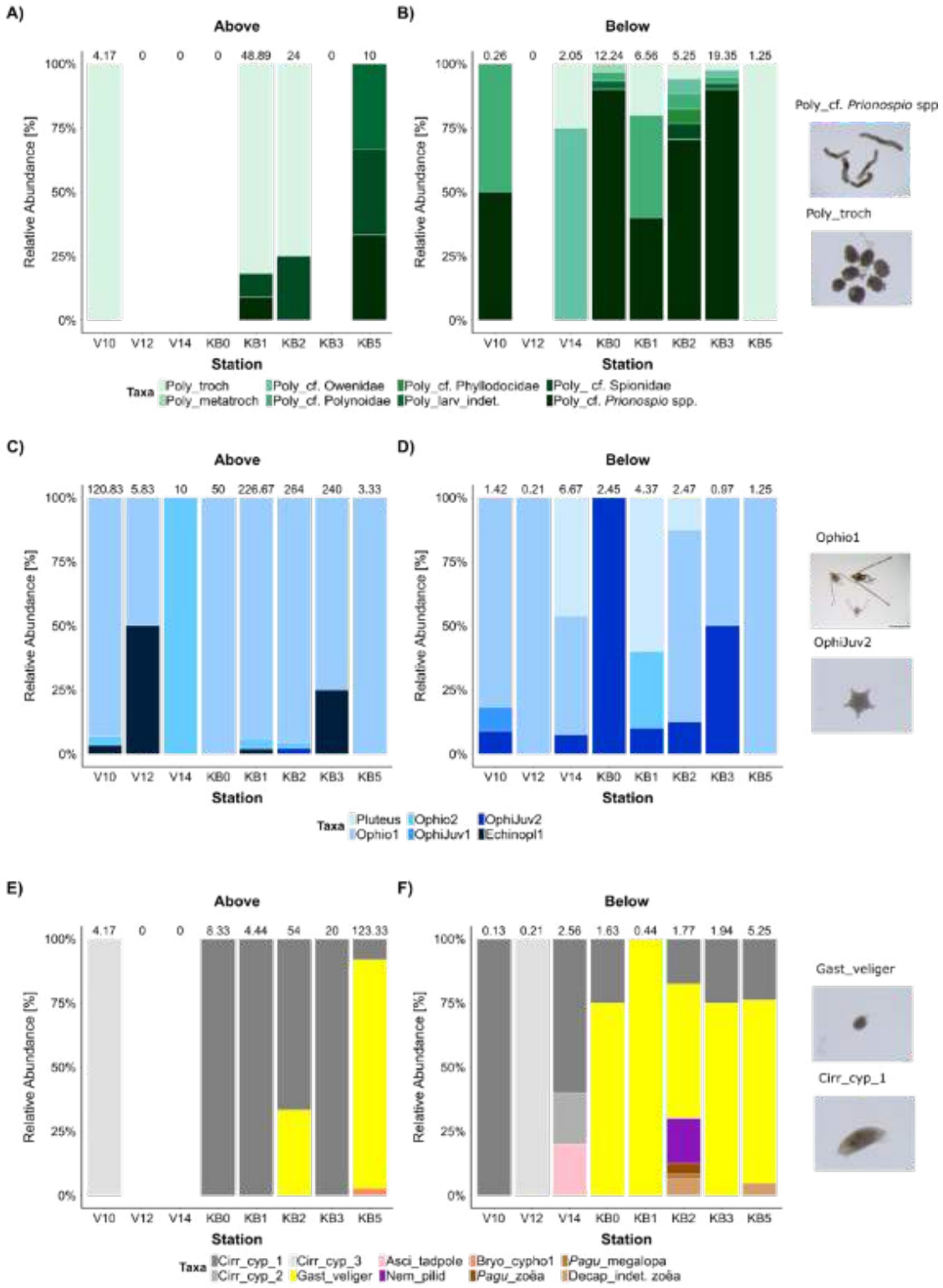

Figure IV. 6 Meroplankton morphotype distribution at the sampling sites above and below the halocline for Echinodermata (A; B), Polychaeta (C; D), and the remaining taxa (E; F) along the Kongsfjorden Transect. Note that Figure IV. 6 (E; F) does not include Bivalvia veligers, which are presented in Figure IV. 3. Values above each bar represents the total abundance [ind m^{-3}] of larvae at the given station within the represented groups.

4.4 Discussion

4.4.1 The role of halocline in shaping the meroplankton community

This study provided a detailed, morphotype-level analysis of Arctic marine benthic invertebrates larvae, confirming our hypothesis that the halocline functions as a physical barrier influencing the vertical structure and composition of meroplankton assemblages observed above and below the halocline. The observed separation of meroplankton assemblages between the AH and BH layers along the Kongsfjorden Transect was additionally supported by the DistLM results, which identified salinity – treated as a continuous gradient – as the main factor explaining 30.78% of variability in the meroplankton, confirming its role beyond the categorical halocline division. Although salinity was used to define the halocline during sampling, its inclusion as a continuous variable in DistLM did not represent circular reasoning, but rather allowed the assessment of how gradual changes in salinity across the fjord influence meroplankton community structure.

Food availability (represented by chlorophyll *a* concentration) was identified as the second most important environmental variable influencing meroplankton, and explained 17.78% of its variation. These findings are consistent with previous research emphasizing that both physical and biological factors – such as salinity stratification and food availability – play crucial roles in shaping larval distribution and survival (Cowen & Sponaugle, 2009). In the Arctic fjords, the halocline can often acts as a retention zone – an ecological barrier formed by a physical structure influencing larval behaviour by limiting dispersal and exposure to advection, predation, and environmental stress (Hidalgo et al., 2014; James, 2021; Szeligowska et al., 2020, 2022). As highlighted by Metaxas (2001), larval distribution in the water column frequently reflects behavioural responses to these environmental gradients, promoting retention in favourable habitats, where hydrodynamic structure and larval behaviour jointly reduce dispersal and enhance recruitment success.

The remaining ~50% of variation in the meroplankton community composition, unexplained by the tested environmental variables, may have resulted from a combination of factors not captured in this study. These include local variability in temperature, chlorophyll *a* concentration, and other food-related parameters, as well as biological interactions such as predation, competition, and behavioural responses of larvae to micro-scale turbulence (Cowen & Sponaugle, 2009; Metaxas, 2001; Pineda et al., 2007). Mortality during larval dispersal, advection by currents and glacier runoff, and short-term patchiness in plankton distributions may also contribute to this unexplained variation (Hop et al., 2002;

Qian & Chia, 1991). Therefore, while salinity and food availability clearly structure the vertical distribution of meroplankton, a complex interplay of additional physical, chemical, and biological processes likely drives the majority of community dynamics (Scheltema, 1986).

4.4.2 Distribution of marine benthic invertebrates larvae above and below the halocline

Marked differences in different meroplankton taxa distribution and abundance were observed between layers above (AH) and below the halocline (BH). Polychaeta larvae were more numerous and diverse below the halocline (BH), where salinity and temperature conditions were more stable but food availability was lower, indicating potential differences in life strategies such as feeding mode or developmental timing (Almeda et al., 2009; Metaxas, 2001; Qian & Chia, 1991). Abe et al. (2014) found that planktonic Polychaeta larvae in Onagawa Bay preferred greater depths, particularly below the pycnocline, where environmental conditions were more stable, likely to avoid surface turbulence and predation while optimizing developmental conditions. Similar patterns may also occur in Arctic and sub-Arctic regions, where the water column is often stratified and hydrological conditions can either favour or hinder larval survival.

In contrast to Polychaeta, Echinodermata larvae were more abundant above the halocline (AH), probably benefiting from higher food availability despite greater salinity fluctuations, suggesting their broader tolerance to environmental variability (Fabricius et al., 2010; Fenaux et al., 1994). This pattern supports the idea that different taxa may respond differently to halocline-related stressors and that haloclines can act as retention zones, influencing larval distribution and potentially enhancing local recruitment (Arellano et al., 2012; Metaxas & Young, 1998b). Moreover, the lower abundance of Echinodermata larvae observed in our study (264 and 240 ind m^{-3} in the AH layer at stations KB2 and KB3, respectively) compared to previous reports (10 560 and 11 670 ind m^{-3} in surface waters at stations K2 and K3; Walkusz et al., 2009) may reflect reduced food availability, which could negatively affect larval growth, development, and survival. This difference in abundance may also partly result from the limited sampling in our study, as only a single sample was collected at each site and time, nearly 20 years after the previous survey, which may not fully capture temporal variability. Additionally, it could be influenced by the unequal thickness of the AH and BH layers, particularly for rarer larval forms.

Bivalvia veligers were abundant in both the AH and BH layers, and remained the dominant meroplankton group along the Kongsfjorden Transect. Similar observations were recorded in Kongsfjorden (Głuchowska et al., 2016 (22nd-27th of July); Ormańczyk et al., 2017

(5th-8th of August); Weydmann-Zwolicka et al., 2021b (August 9th)) as well as in other Spitsbergen fjords like Hornsund (Ormańczyk et al., 2017 (27th-29th of July); Trudnowska et al., 2020 (August 7th)) or Isfjorden (Stübner et al., 2016 (August); Weydmann-Zwolicka et al., 2021a (30th-31st of July, 1st, 2nd and 5th of August)). However, their abundances were substantially higher in our study (counts in the thousands), which is similar only to studies from Billefjorden (Søreide et al., 2022 (23rd of July)). Although the increase may be related to the advection of Bivalvia larvae from Atlantic Water masses – as Spitsbergen's fjords host both Arctic and boreal bivalve species (Carroll & Ambrose, 2012; Pawłowska et al., 2011; Różycki, 1992) – the higher concentrations in the fjords compared to the shelf (unlike in earlier studies: Hop et al., 2023, 2019; Walkusz et al., 2009), suggest that local retention and accumulation also play an important role. This pattern may be driven by enhanced food availability in surface waters, lower turbulence, and the proximity to adult bivalve populations in the inner fjord. Notably, at the glacier-influenced station KB5, an aggregation of veligers was observed below the halocline (BH), further indicating that stratification and reduced mixing can form effective zones of larval accumulation.

Cirripedia larvae were relatively scarce, likely due to the timing of sampling campaign. Their naupliar stages peak in spring, synchronized with algal blooms, and require several weeks to develop into cyprid stages (Søreide et al., 2022; Walczyńska et al., 2019). This study, was conducted at the beginning of August, a period when cyprid stages are most prominent and nauplii are likely no longer abundant in the water column (Høeg et al., 2015). Interestingly, cyprids were more abundant in the surface layer (AH), similar to patterns observed in Billefjorden (Søreide et al., 2022), suggesting that the larvae may be temporarily retained in surface waters, unable to cross the salinity gradient and descend for settlement (dos Santos et al., 2007; Søreide et al., 2022). Higher Cirripedia larvae abundance throughout the water column in both the fjord and shelf areas was observed compared to previous findings (Hop et al., 2023), which may result from differences in sampling methods (i.e., smaller net mesh size in this sampling). Alternatively, it may indicate that cyprid dispersal over extensive shelf areas is influenced by ocean currents and upwelling/downwelling events (Broitman et al., 2005; Noda, 2004). These processes, combined with water column stratification – driven by salinity gradients and halocline presence – likely affect the horizontal and vertical distribution of larvae. This distribution pattern aligns with findings from an upwelling system off the Portuguese coast, where Cirripedia larval distribution were shaped by salinity and current dynamics (dos Santos et al., 2007). The retention of cirripede cypris larvae above the halocline can enhance local recruitment because the halocline acts as a physical and

physiological barrier limiting vertical mixing and larval dispersal into deeper layers. By remaining in surface waters, larvae benefit from higher food availability, which supports their energy needs during the search for suitable settlement substrates (Crisp, 1974; Pineda et al., 2007). This localized retention increases the chances of successful settlement and contributes to maintaining dense cirripede populations in specific coastal areas. Thus, the halocline functions both as a selective barrier and a retention layer for Cirripedia larvae, shaping their vertical distribution.

Overall, the observed pattern of larval distribution along the Kongsfjorden Transect highlighted the importance of environmental gradients – particularly the halocline – and its interaction with the thermocline – in shaping meroplankton diversity and vertical structure. The depth of the chlorophyll *a* maximum relative to these gradients may influence larval distribution through food availability, affecting not only meroplankton, but also holoplankton throughout the year. Differences in the vertical distribution of Bivalvia, Echinodermata, and Polychaeta larvae between the AH and BH layers may arise not only from species-specific tolerances to environmental conditions and feeding preferences but also result from higher mortality in other layers or greater dilution within the larger BH water volume. Thus, the absence of a certain larval type in a given layer does not necessarily indicate a true absence, but could also reflect mortality or temporal displacement. It should be noted that our study was conducted over a relatively short, four-day summer sampling period, limiting replication and temporal generalization. These larval groups may serve as biological proxies of salinity stratification and halocline dynamics, as suggested by the distinct meroplankton taxonomic composition observed above and below the halocline. Their differential vertical distribution indicates both preferences and specific retention strategies in the Arctic fjords.

4.4.3 Meroplankton distribution and benthic-pelagic coupling along the Kongsfjorden Transect

To understand the origin and distribution of marine larvae in Kongsfjorden and on the adjacent shelf, it is essential to consider the adult benthic community composition and hydrographic conditions. Stations along the Kongsfjorden Transect exhibit different benthic habitats, including both soft and hard substrates. The proportions of dominant meroplanktonic taxa may reflect local benthic communities, with currents and circulation of water masses playing a significant role in structuring benthic-pelagic coupling (Cowen & Sponaugle, 2009; Pineda et al., 2007; White et al., 2019). An exception is station KB5, in the innermost fjord's basin, which is under the influence of a melting glacier and therefore subject to very dynamic

conditions and a high load of suspended inorganic matter, potentially affecting the survival of benthic larvae. For example, Bryozoa larvae were found only at KB5 while Ascidiacea larvae were present exclusively on the shelf at V14, demonstrating that these taxa may have specific habitat preferences. Gastropoda and Decapoda larvae were observed only in the fjord (KB0-KB5), while Cirripedia, Polychaeta, Echinodermata, and Bivalvia larvae were present along the entire transect, showing broader distribution across various habitats. These results support the view, previously suggested by other studies (White et al., 2019; Włodarska-Kowalczuk et al., 2016), that local habitat conditions play a key role in larval settlement, affecting species distributions and developmental stages. However, it should be noted, that in our study, only a single sample was collected at each station, which means that temporal variability and rarer larval occurrences may not be fully captured. Therefore, the observed patterns of meroplankton distribution should be interpreted as a short-term depiction of the system rather than a definitive representation of larval dynamics across the fjord or season.

In fjord ecosystems, larval retention is particularly significant for species adapted to settle in sheltered environments, which may offer more stable conditions than the dynamic, open shelf waters. Studies have shown that the enclosed nature and complex circulation patterns of fjords can lead to higher accumulation of benthic larvae, enhancing recruitment success. For instance, Meyer et al. (2017) found that recruitment of benthic invertebrates in Svalbard fjords varied significantly among locations, with factors like temperature and depth influencing settlement patterns. Similarly, Kukliński et al. (2013) observed that the seasonality of larval occurrence and recruitment in the Arctic fjords is closely linked to environmental variables such as temperature and salinity, with lower salinity potentially leading to reduced larval presence in the water column – either due to increased mortality or dispersal from unfavourable conditions. Together, these results emphasize how fjord-specific environmental gradients – particularly salinity – shape both larval distribution and benthic community composition, while distinct settlement and recruitment patterns across fjord and shelf habitats in Kongsfjorden reflect the sensitivity of different taxa to local physical conditions.

Future studies should consider applying molecular tools, such as barcoding and metabarcoding to complement traditional morphological analysis, especially in Arctic meroplankton studies (Descôteaux et al., 2021; Ershova et al., 2019; Walczyńska et al., 2019). High-throughput sequencing enhances taxonomic resolution by uncovering cryptic diversity, enabling the tracking of species-specific responses to environmental shifts. By applying these methods, future studies may identify meroplankton taxa to the genus or even species level,

explore larval development strategies and feeding adaptations, and utilize meroplankton diversity as biological indicators of environmental change.

4.5 Conclusions

This study expanded the understanding of meroplankton structure and dynamics in European Arctic fjords, using Kongsfjorden as a model, by integrating detailed morphotype analysis with hydrographic data. It highlighted how variations in hydrographic conditions – particularly salinity gradients, food availability, long-term AW inflows, tidal mixing, and wind-induced surface currents – may indicate potential ecological shifts in the Arctic fjords. These changes could influence the distribution, species composition, and survival strategies of meroplankton communities. These mechanisms may facilitate larval recruitment from the shelf to the inner fjord as well as the export of larvae produced within the fjord, while freshwater input and enhances stratification in the inner basin can promote local larval retention. In particular, warmer and less dynamic conditions in Kongsfjorden may allow for a more diverse range of Polychaeta larvae, while more turbulent conditions on the shelf of the western Spitsbergen may promote the dominance of Echinodermata larvae.

The differing vertical distributions of major taxonomic groups across the AH and BH layers suggest that salinity-driven stratification act as a key structuring factor for meroplankton communities. Certain taxa appeared to be associated with specific layers, indicating different tolerances or adaptive strategies to salinity and turbulence. In the context of the Artic fjordic systems, the presence of a halocline may lead to the retention of certain meroplanktonic taxa within the fjord, while a more dynamic shelf environment, characterized by weaker stratification, may facilitate larval dispersal and exchange with adjacent waters. These observations underscore the importance of local hydrographic conditions, particularly salinity gradients and halocline strength, in shaping meroplankton community composition in the Arctic fjord systems.

However, this study was based on a single summer sampling event, which limits the ability to generalize our findings across seasons or years. Temporal variability in hydrography, primary production, and benthic reproductive cycles could substantially affect meroplankton composition and abundance. Additionally, differences in layer thickness (AH vs BH) and the lack of replicate samples may have introduced a sampling bias, particularly for rarer larval forms. Therefore, while our observations provide valuable insight into summer meroplankton dynamics in the Kongsfjorden Transect, long-term and seasonal studies

are required to fully understand the processes driving recruitment, retention, and dispersal of meroplankton in Arctic fjord systems.

The results presented in this chapter have been published in:
***Patuła, W**.[*], Ronowicz, M., Kukliński, P., & Weydmann-Zwolicka, A. (2026). Halocline as an environmental barrier for the larvae of Arctic marine benthic invertebrates. Progress in Oceanography, 242, 103649. https://doi.org/10.1016/j.pocean.2025.103649*

[*]*corresponding author*

This study is an open access article distributed under the terms of the Creative Commons Attribution License (CC BY)

Chapter V Integrating morphological and multi-marker metabarcoding (18S rRNA & *cox1*) to map meroplankton diversity along the NE Atlantic shelf

5.1 Introduction

The Arctic is currently undergoing a transformation driven by intensifying climate warming and the influx of warmer, more saline Atlantic waters, a process known as Atlantification (Ingvaldsen et al., 2021; Polyakov et al., 2020). Among ongoing sea ice loss and rising temperatures, the region faces potentially irreversible changes to both its terrestrial and marine ecosystems (Descamps et al., 2017; Screen & Simmonds, 2010; Yadav et al., 2020). The primary passage for transporting warm Atlantic water northward is the West Spitsbergen Current (WSC), an extension of the Norwegian Coastal Current (NCC) (Aagaard et al., 1987; Orvik & Niiler, 2002). Together, they transport vast volumes of warm Atlantic water not only toward western Spitsbergen but also into the southern Barents Sea and the western Svalbard shelf (Årthun et al., 2012; Beszczyńska-Möller et al., 2012; Walczowski et al., 2012). On the other hand, from the direction of the Barents Sea, the influence of the East Spitsbergen Current (ESC) and the Sørkapp Current brings cooler Arctic waters toward Bear Island and western Spitsbergen (Rudels et al., 2005). Therefore, the subsequent mixing of Atlantic and Arctic waters creates a unique environment (Cottier et al., 2005; Hop et al., 2006; Tverberg et al., 2019). Furthermore, Atlantification drives the northward influx of boreal taxa, which could, in the future, force native species into deeper waters, displace them, and shift their ranges northward, or even lead to their extinction (Polyakov et al., 2017; Renaud et al., 2015; Weydmann et al., 2014). Consequently, gaining insight into the physicochemical processes occurring in the Arctic is essential for effectively monitoring ecosystem changes, particularly in the marine environment of the European Arctic, in response to global warming (Heiskanen et al., 2016; Hop et al., 2023; Weydmann-Zwolicka et al., 2021b).

Meroplankton, comprising the larval stages of many marine organisms, including benthic invertebrates, plays a pivotal role in marine ecosystems (Cowen & Sponaugle, 2009; Pineda et al., 2007). In contrast to holoplankton, which spend their entire life cycle in the water column, meroplankton are temporarily associated with the water column only during the larval phase (Kukliński et al., 2013; Stübner et al., 2016). Studying meroplankton is crucial because they are highly sensitive to environmental changes or stressors such as changes in temperature, salinity, ocean currents, food availability, and predation pressure, all of which affect their survival, development, and success in colonizing new areas (Metaxas, 2001; Metaxas & Saunders, 2009; Patuła et al., 2026; Young, 1987, 1995). As the Arctic warms,

investigating how these factors influence meroplankton structure is important, especially given that recruitment potential and the taxonomic and functional composition of these organisms determine the structure of future benthic communities (Meyer et al., 2017; Ronowicz et al., 2024; Schrage et al., 2025). Moreover, because meroplankton respond rapidly to environmental changes, they can serve as early indicators of shifts within marine ecosystems (Kirby et al., 2008; Lindley & Kirby, 2007). For example, changes in larval taxonomic composition may impact the food web, nutrient cycling, and carbon sequestration on the Northeast Atlantic Shelf (Ershova et al., 2019; Szeligowska et al., 2020). Therefore, unrevealing meroplankton ecology and taxonomic composition is necessary for predicting the future stability and diversity of Arctic ecosystems in the context of pelagic-benthic coupling (Renaud et al., 2015; Weydmann-Zwolicka et al., 2021a).

Despite the importance of traditional microscopy for identifying benthic larvae, this approach has clear limitations that hinder accurate assessments of Arctic meroplankton biodiversity and ecosystem functions (Descôteaux et al., 2021; Weydmann-Zwolicka et al., 2021a). Morphological analysis *via* microscopy rarely gives definitive answers. Many larvae look similar, or even identical, and lack the characteristic features needed to distinguish them during early developmental stages. Therefore, traditional morphological analysis often underestimates true species diversity because many organisms are morphologically indistinguishable (Lindeque et al., 2013). Relying solely on morphological analysis leads to underestimation of diversity, taxonomic uncertainty, and errors, as species richness is typically aggregated at higher taxonomic levels (such as orders, classes, or families) rather than at the genus or species level. Furthermore, morphological analysis is extremely laborious and time-consuming. It requires a high level of taxonomic expertise, a skill set that is becoming increasingly rare in an era of rapidly evolving technologies and new analytical methods for zooplankton and meroplankton (Bucklin et al., 2016).

This taxonomic barrier prevents us from obtaining the high-resolution data required to track the influx of boreal species associated with the Atlantification of the Arctic or to quantify true meroplankton diversity (Ershova et al., 2019; Patuła et al., 2026). Accordingly, we cannot accurately determine the roles of meroplankton in ecosystems, their physiological tolerances, or distribution patterns, nor can we determine whether local or global factors drive the observed changes. Consequently, morphological analysis alone is currently insufficient to address increasingly complex research questions in oceanography, particularly in the Arctic, where the impacts of global warming are clearly visible. Therefore, there is a need for robust, scalable, and accurate identification techniques to support traditional morphological approaches and

address their present limitations in meroplankton analysis. Recent studies increasingly highlight that integrating DNA metabarcoding with traditional methods significantly improves marine biodiversity assessments and enables rapid monitoring of community dynamics (Kim et al., 2025; Peng et al., 2026; Weydmann-Zwolicka et al., 2024).

To mitigate the limitations of morphological analysis, this study integrates morphological and molecular approaches for meroplankton analysis. In addition to traditional morphology, metabarcoding was employed to analyze the entire meroplankton community structure. For this purpose, two complementary genetic markers were used: 18S rRNA gene (18S) and the cytochrome c oxidase subunit I gene (*cox1*) (Bucklin et al., 2016). The nuclear 18S rRNA marker is highly conserved, serving as a reliable foundation for the broad classification of major groups and providing a comprehensive overview of community structure (Pawłowski et al., 2012). In contrast, the *cox1* gene is more variable, providing the resolution needed to distinguish between closely related, often cryptic species (Lindeque et al., 2013). By utilizing both markers, taxonomic diversity is effectively characterized, often down to the species level. This dual-marker strategy enabled the overcoming of the barriers of morphological analysis, generating a robust molecular dataset that reveals hidden diversity within the Arctic meroplankton community (Descôteaux et al., 2021; Walczyńska et al., 2019; Weydmann-Zwolicka et al., 2021a). Ultimately, combining these methods enables a deeper understanding of meroplankton assemblages and the specific responses of individual taxa or species to environmental changes in the study area.

To resolve the identified knowledge gaps, traditional morphological analysis was integrated with high-throughput multi-marker metabarcoding (18S rRNA and *cox1*) to investigate meroplankton assemblages collected across the NE Atlantic shelf during the summer of 2021. This research aims to provide a high-resolution map of diversity hotspots and to establish a protocol for future monitoring. The following objectives and research questions were addressed: i) to assess the effectiveness of integrated taxonomic approaches by determining which multi-marker genetic approaches enhance meroplankton diversity detection relative to classical morphology alone, and ii) to characterize community-environment interactions by examining how meroplankton taxonomic composition and distribution patterns reflect the diverse hydrographic regimes present along the NE Atlantic shelf?

It was hypothesized that integrating morphological, 18S, and c*ox1* multi-marker data provides higher taxonomic resolution and more accurate mapping of meroplankton diversity hotspots than traditional morphological analysis alone, thereby revealing unique community responses to distinct hydrographic conditions.

5.2 Materials & Methods

5.2.1 Study Area

The study area encompasses a comprehensive latitudinal gradient extending from the Norwegian coast to the high-Arctic waters of Svalbard (Figure V. 1). This region is primarily defined by the poleward transport of warm, saline Atlantic Water (AW) carried by the Norwegian Atlantic Slope Current (NwASC) and the West Spitsbergen Current (WSC) into the Fram Strait (Beszczynska-Möller et al., 2012). The stations PhM1-PhM5 provide a southern baseline, capturing the influence of the Norwegian Coastal Current, while the central transect encompassing H3, V22, V26, V29, V31, V34, and K-3 serves as a transition zone where Atlantic-influenced waters interact with the Barents Sea shelf edge.

As the current progresses northward, the shelf break stations (Z2, S3, EX3, EB2-1, N4) are directly impacted by the WSC, which acts as the main source of heat and salt for the Arctic Ocean (Aagaard et al., 1987; Boyd & D'Asaro, 1994; Schauer et al., 2004). Additionally, the West Spitsbergen Shelf is impacted by cold, freshened Arctic Water (ArW) transported by the Spitsbergen Polar Current (Nilsen et al., 2016). This current, constituting an extension of the East Spitsbergen Current, transports Arctic-origin water masses formed in the Barents Sea around the southern tip of Svalbard, contributing to the distinct cooling and freshening of the shelf environment (Strzelewicz et al., 2022; Tverberg et al., 2019). Mixing and exchange between AW and ArW occur along the West Spitsbergen Polar Front (Strzelewicz et al., 2022). Finally, the northernmost reaches of the study area, represented by stations Y5 and WB3, are situated near Fram Strait, where the interplay between the WSC and these cold Arctic water masses creates a complex hydrographic regime that modulates the larval development and distribution patterns discussed in this study.

Sampling stations were classified into four distinct zones based on their prevailing hydrographic conditions and the influence of major ocean currents (Figure V. 1): the Norwegian Coast zone (NC), characterized by the influence of the Norwegian Coastal Current (NCC); the Atlantic Water influenced zone (AW); the Barents Sea zone (BS), under the influence of cold Barents Sea water, East Spitsbergen Current (ESC) and the Sørkapp Current (SC); and the West Spitsbergen shelf zone (WS), governed by shelf conditions and the West Spitsbergen Current (WSC). The sampling sites were visualized using ArcGIS Pro software (Esri, 2025).

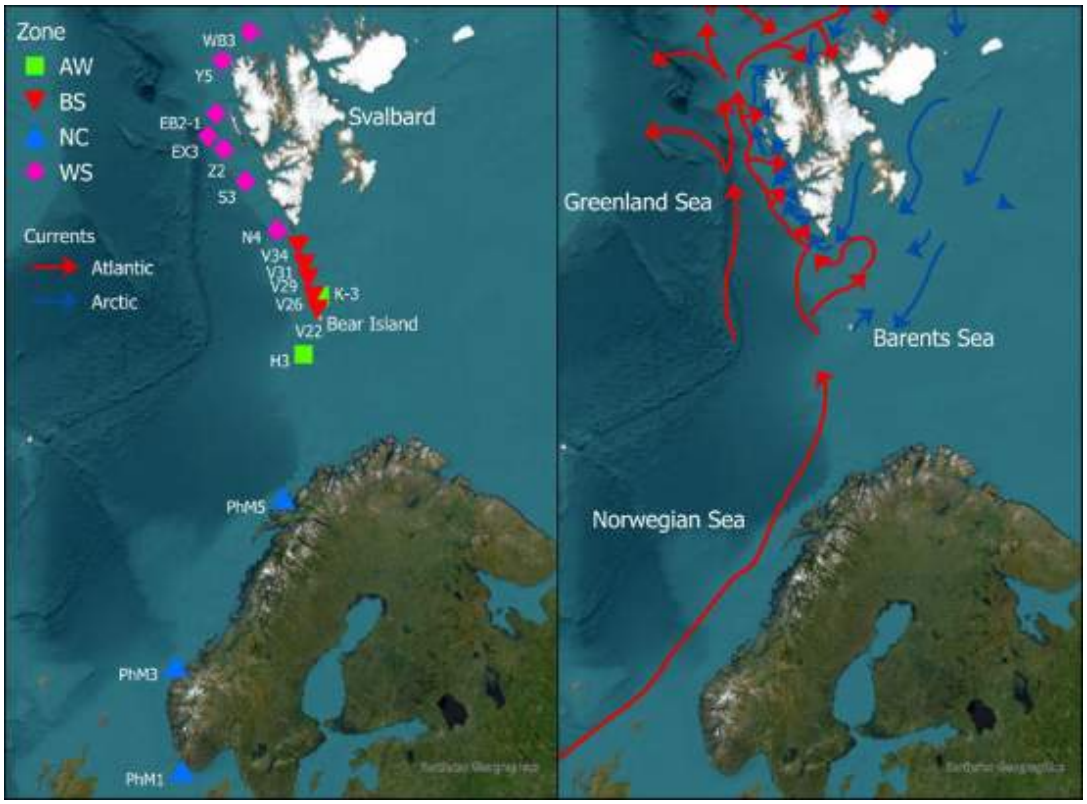

Figure V. 1 Study area: meroplankton sampling sites along the North-east Atlantic Shelf with stations divided into four study zones (NC – Norwegian Coast; BS – Barents Sea; AW – Atlantic Water, and WS – West Spitsbergen shelf), with schematic ocean current circulation including their origin (based on Assmy et al. (2023)).

5.2.2 Fieldwork

5.2.2.1 Environmental parameters and chlorophyll *a* sampling

To characterize the hydrological environment across the 17 stations located along the NE Atlantic shelf, vertical profiles of temperature, salinity, and fluorescence were recorded. These measurements were conducted from mid-June to late July 2021, using a Sea-Bird Electronics 911 CTD profiler deployed through the entire water column (Table V. 1). This sampling transect specifically targeted the area influenced by the West Spitsbergen Current, extending from the Norwegian coast to the High Arctic and the Barents Sea region from the east part.

Chlorophyll *a* (chl *a*) concentrations were used as an indicator of food resources for the meroplankton communities. Water samples were obtained using Niskin bottles, with sampling depths ranging from 5 to 7 discrete strata per station (Table V. 1), to ensure representative coverage of the water column's thickness and local conditions (from the seafloor to the surface), which were determined by real-time fluorescence peaks observed during the CTD downcasts.

From each 1 L seawater sample, a 250 mL subsample was filtered through Whatman GF/F filters (0.70 µm pore size). The resulting filters were immediately secured in aluminium foil and stored at -80°C for subsequent laboratory quantification.

Table V. 1 Sampling details: water depths used for chlorophyll *a* concentration analysis and depth layers for meroplankton samples.

Station	Coordinates		Depth layers for meroplankton samples [m]	Depths for chlorophyll *a* samples [m]
	Latitude	*Longitude*		
PhM1	58.0886	6.078817	330-0	0-30-65-85-200-300
PhM3	62.9245	5.448917	85-0	0-15-35-65-85
PhM5	69.2601	15.560483	50-0	0-10-17-32-50
H3	73.4995	17.479317	400-0	0-10-40-85-400
V22	74.6171	18.7511	65-0	0-17-25-45-65
V26	74.9488	18.4105	68-0	0-7-15-25-68
K-3	75.0002	18.9995	150-0	0-10-55-100-150
V29	75.3814	17.9114	100-0	0-10-50-75-100
V31	75.6999	17.548933	200-0	0-7-25-55-100-200
V34	76.1251	17.0006	275-0	0-15-35-150-275
N4	76.5001	15.00135	150-0	0-10-40-80-155
S3	77.5331	12.000617	155-0	0-25-50-100-155
Z2	78.16673	9.999683	250-0	0-40-75-115-250
EB2-1	78.8333	9.265883	195-0	0-15-60-85-175
EX3	78.41627	8.502267	175-0	0-10-50-75-195
Y5	79.75443	9.8416	360-0	0-30-60-140-360
WB3	80.2201	12.483367	175-0	0-20-50-70-175

5.2.2.2 Meroplankton collection

At each of the 17 stations, larvae were collected from the entire water column (from the bottom to the surface) to capture the full community coverage. Sampling was performed using a Juday plankton net (opening: 0.10 m^2; mesh size: 56 µm). The net was hauled at a constant velocity of ~1 m s^{-1}. Immediately after collection, the concentrated plankton samples were fixed in 96% ethanol to ensure suitability for both morphological and subsequent molecular analyses. Following 24 h of fixation, the ethanol was replaced to ensure optimal preservation.

5.2.3 Laboratory analysis

5.2.3.1 Chlorophyll *a*

To quantify chlorophyll *a* concentration, pigments were extracted from the frozen GF/F filters. After thawing at room temperature, each filter was submerged in 10 mL of 90% acetone and incubated in darkness at 4°C for 12-18 hours. To separate the supernatant, samples were

centrifuged for 2 minutes at 3000 rpm. Chlorophyll *a* concentrations were determined using the non-acidification and acidification technique (EPA Method 445.0) with a Trilogy® fluorometer (Turner Designs Inc.) (Arar & Collins, 1997), which was pre-calibrated using a pure chl *a* standard (Sigma S6144). Following acidification with 100 µL of 0.1 M HCl, the final concentrations were calculated and expressed in mg m^{-3} (Arar & Collins, 1997). To obtain a representative value for each sampling stratum, we calculated weighted averages of chl *a* based on the vertical thickness of each specific depth layer (Dąbrowska et al., 2020).

5.2.3.2 Meroplankton morphological identification workflow

The taxonomic composition and abundance of meroplankton were first assessed *via* traditional microscopy. First, each whole sample was analyzed using an Olympus SZX7 stereomicroscope, with individuals identified to the highest possible taxonomic resolution following Postel et al. (2000). The macro fraction was identified gradually throughout the analysis, both while examining subsamples (when larger individuals were encountered) and during inspection of the entire sample. Total abundance was standardized to individuals per cubic meter (ind m^{-3}). Following morphological analysis, each sample was split in half using a Motoda plankton sub-sampler, with one half designated for subsequent molecular metabarcoding.

Within broader taxonomic groups, larvae were further classified into distinct morphotypes based on observable morphological features (Table V. 2). Representative individuals from each category were documented and photographed using an Olympus SZX16 stereomicroscope equipped with cellSens Standard 2.1 software. This systematic documentation served as the basis for a morphological atlas (Patuła, 2025), ensuring consistency in identification across the latitudinal gradient from the Norwegian shelf to Svalbard.

Table V. 2 Classification of meroplankton: Taxonomic assignment and morphotypes. Note that different morphotypes within a certain taxa may potentially correspond to different genera/species.

	Meroplankton Morphotype Abbreviations		
	Meroplankton Taxa	***Long name of larvae morphotype***	***Short name of larvae morphotype***
1	Echinodermata	Pluteus	Pluteus
2	Echinodermata	Ophiopluteus1	Ophio1
3	Echinodermata	Ophiopluteus2	Ophio2
4	Echinodermata	Ophiuroidea juvenile1	OphiJuv1
5	Echinodermata	Ophiuroidea juvenile2	OphiJuv2
6	Echinodermata	Ophiuroidea juvenile3	OphiJuv3
7	Echinodermata	Echinopluteus1	Echinopl1
8	Echinodermata	Echinopluteus2	Echinopl2
9	Echinodermata	Echinopluteus3	Echinopl3
10	Echinodermata	Echinoidea juvenile1	EchiJuv1
11	Echinodermata	Holothuroidea doliolaria/pentactula	Holo_dolio/pent
12	Echinodermata	Holothuroidea auricularia	Holo_auri
13	Echinodermata	Brachiolaria1	Brach1
14	Echinodermata	Brachiolaria2	Brach2
15	Echinodermata	Asteroidea juvenile1	AsterJuv1
16	Polychaeta	Poly_trochophorae	Poly_troch
17	Polychaeta	Poly_metatrochophorae	Poly_metatroch
18	Polychaeta	Poly_mitraria cf. Owenidae	Poly_cf. Owenidae
19	Polychaeta	Poly_larvae1 cf. Polynoidae	Poly_cf. Polynoidae
20	Polychaeta	Poly_larvae2 cf. Spionidae	Poly_ cf. Spionidae
21	Polychaeta	Poly_larvae3 cf. Phyllodocidae	Poly_cf. Phyllodocidae
22	Polychaeta	Poly_larvae4 cf. *Prionospio* spp.	Poly_cf. *Prionospio* spp.
23	Polychaeta	Poly_larvae5 cf. Amphinomidae	Poly_cf. Amphinomidae
24	Polychaeta	Poly_larvae6_cf. Pectinariidae	Poly_cf. Pectinariidae
25	Polychaeta	Polychaeta unidentified	Poly_indet.
26	Bivalvia	Bivalvia veliger	Biv_veliger
27	Cirripedia	Cirripedia nauplii1	Cirr_naup_1
28	Cirripedia	Cirripedia nauplii2	Cirr_naup_2
29	Cirripedia	Cirripedia nauplii3	Cirr_naup_3
30	Cirripedia	Cirripedia cypris1	Cirr_cyp_1
31	Cirripedia	Cirripedia cypris3	Cirr_cyp_3
32	Gastropoda	Gastropoda veliger	Gast_veliger
33	Bryozoa	Bryozoa cyphonautes1	Bryo_cypho1
34	Bryozoa	Bryozoa cyphonautes2	Bryo_cypho2
35	Decapoda	*Pagurus* zoëa	*Pagu*_zoëa
36	Decapoda	*Hyas* zoëa zoëa	*Hyas*_ zoëa
37	Decapoda	Decapoda unidentified zoëa	Decap_indet. zoëa
38	Decapoda	Decapoda unidentified megalopa	Decap_indet. megalopa
39	Anthozoa	Anthozoa cerinula	Anth_cerinu
40	Enteropneusta	Enteropneusta tornaria larvae	Enter_torna
41	Phoronidae	Phoronidae larvae	Phoro_larv

5.2.3.3 Meroplankton metabarcoding laboratory workflow

5.2.3.3.1 DNA extraction

DNA extraction

The total genomic DNA was isolated from samples collected in 2021. For the isolation, one-half of each sample was used following an initial splitting procedure. Extractions were performed using the Genomic Midi AX kit (A&A Biotechnology, Gdynia, Poland) according to the manufacturer's general framework, with significant modifications optimized for varying sample density and heterogeneity. Due to substantial differences in the physical properties of the biological material, processing parameters such as the number of falcon tubes used to homogenize each sample, centrifugation cycles, and lysis conditions were dynamically adjusted for individual samples (as described in the following steps) to ensure efficient cell disruption and maximum DNA yield.

Sample preparation and mechanical homogenization

To remove trace ethanol from storage, each sample was rinsed thoroughly with ultrapure water (MiliQ) using a laboratory mesh strainer (56 µm mesh size) and then drained. Depending on the total sample density, the material was processed either intact or subdivided into balanced, even-numbered parts to prevent equipment overloading and ensure balance during downstream centrifugation. Mechanical cell disruption was performed using a bead-beating homogenizer (Benchmark Scientific, USA). Samples were transferred into 5 mL tubes preloaded with Ø2.8 mm stainless steel beads and subjected to a homogenization cycle at 4100 rpm for 90 s. For denser or highly resilient samples, a secondary homogenization pulse at 4100 rpm for 20 s was applied.

Chemical lysis

To optimize homogenization and lysis efficacy in high-density samples, after mechanical homogenization, the standard TE buffer and lysis buffer L1.4 were added directly to the tubes containing stainless steel beads and the homogenized sample. For samples with high density (approximately 1.5-2.0 mL of material), a mixture of 1.5 mL TE buffer and 1.5 mL L1.4 buffer was introduced directly into the bead-beating tubes. For smaller samples (approximately 1.0 mL of material), the volumes were adjusted to 500 µL of TE and 500 µL of L1.4, maintaining a strict 1:1 buffer ratio. Following homogenization, the resulting lysates were evenly distributed into 1.5-2.0 mL microcentrifuge tubes. Proteinase K (100-150 µL, adjusted relative to sample density) was added to each tube. The mixtures were thoroughly homogenized

by vortexing and inversion, then incubated in a thermomixer at 50-51°C overnight with continuous agitation at 400 rpm.

DNA purification and elution

Prior to column loading, the overnight lysates were vortexed. To prevent membrane clogging by undigested particulate matter from dense samples, a pre-clearing centrifugation step was introduced: lysates were centrifuged at 4500 rpm for 10 min, and the clear supernatant was collected. The supernatants (combining up to three microcentrifuge tube volumes per individual sample) were loaded into the AX column units nested within 15 mL conical tubes (from the set of Genomic Midi AX kit). The samples were centrifuged in a swinging-out rotor (Eppendorf Centrifuge 5810 R) to drive them through the silica membrane. Due to the high viscosity and variable filtration rates of specific sample matrices, standard centrifugation (2 min at 3000 rpm, followed by 3 min at 3200 rpm) was insufficient for certain samples. For highly viscous extracts, repeated centrifugation cycles (ranging from 4 to 9 consecutive runs at stepwise increasing speeds up to 3500 rpm) were performed, accompanied by gentle mechanical disruption of retained surface debris with a sterile pipette tip to restore flow dynamics.

The Spin 100AX columns were transferred into fresh 15 mL tubes, and 2.5 mL of washing buffer K2 was applied to the membrane. The columns were centrifuged at 3000-3200 rpm for 2 min. This washing step was repeated under identical conditions to ensure the complete removal of cellular contaminants and residual proteins, with short supplementary spins (1 min at 3100 rpm) applied as necessary to ensure complete pass-through of the wash solution. To elute the bound genomic DNA, the columns were transferred to clean 15 mL collection tubes. A volume of 550 µL of elution buffer K3 was added directly to each column membrane, followed by a 2 min incubation at room temperature. The eluate was collected via centrifugation at 3000 rpm for 1 min. To maximize total DNA recovery, this elution step was repeated with an additional 550 µL of buffer K3 under identical incubation and spin parameters, giving a final pooled eluate of approximately 1.1 mL.

DNA precipitation and purification

The pooled eluate was transferred into nuclease-free 2.0 mL microcentrifuge tubes. Isopropanol (880 µL) was added to each tube to precipitate the nucleic acids. To precipitate the DNA, the samples were centrifuged at 14 000 rpm for 15 min at room temperature. The supernatant was carefully decanted, and the DNA was washed by adding 500 µL of 70%

ethanol, followed by centrifugation at 14 000 rpm for 5 min. The ethanol supernatant was carefully removed *via* pipetting, avoiding disturbance to the DNA. The samples were air-dried at room temperature for 10 to 60 min to eliminate any residual ethanol. Finally, the purified DNA was resuspended in 100 µL of TE buffer. The concentration of the DNA isolates was measured using a NanoDrop One spectrophotometer (Thermo Fisher Scientific, Waltham, MA, USA), and the samples were stored at -20°C for further molecular analyses.

5.2.3.3.2 Gene markers and primers

To analyze the meroplankton community structure, a multi-marker metabarcoding approach combining nuclear and mitochondrial gene regions was used. In pilot tests, four regions of the nuclear 18S rRNA gene (18S; regions: V1-V2, V4, V7, and V9) were evaluated. Among these, the 18S rRNA region V1-V2 showed the highest amplification success and provided the best results for taxonomic diversity. This region is characterized by highly conserved primer-binding sites, which reduce amplification bias while providing good resolution across a wide range of marine organisms (Ershova et al., 2021; Wangensteen et al., 2018). As a complementary marker, the fragment of mitochondrial cytochrome c oxidase subunit I (*cox1*) gene was selected. Because *cox1* evolves faster in animals than the nuclear 18S rRNA, higher nucleotide variability is expected, and better taxonomic resolution is provided at the species level (Leray & Knowlton, 2015; Tagliabue et al., 2026).

The combination of these two markers is particularly effective for meroplankton studies, as these communities consist of morphologically identical larvae from highly divergent taxonomic groups (Descôteaux et al., 2021, 2022). While the conserved 18S rRNA ensures that broad phyla (such as Mollusca, Annelida, or Arthropoda) are not missed due to primer mismatch, the highly variable *cox1* marker allows these larvae to be linked to their specific adult benthic species.

Primers for *cox1* were chosen based on modified protocols by Descôteaux et al. (2021), Ershova et al. (2021), and Wangensteen et al. (2018), (based on proposed markers by Leray et al., 2013), by whom primers were optimized for marine metazoans and meroplanktonic groups. The *cox1* fragments were targeted using the degenerate primers mlCOIintF-XT (5′–GGWACWRGWTGRACWITITAYCCYCC–3′) and jgHCO2198 (5′–TAIACYTCIGGRTGICCRAARAAYCA–3′). While the 18S rRNA: region V1-V2 was amplified using the forward primer F04 (5′–GCTTGTCTCAAAGATTAAGCC–3′; Fonseca et al., 2010) and the modified reverse

primer R22-mod (5′–CTGCTGCCTTCCTTRGA–3′; Sinniger et al., 2016). Amplicon lengths were approximately 313 bp for *cox1* and 375 bp for V1-V2 18S rRNA, each including 8 bp of forward and reverse primer tags.

All oligonucleotides were synthesized by Eurofins Genomics (Germany) with unique 8-nucleotide tags appended at the 5' end, allowing for sample multiplexing within unique libraries (Esling, 2015). Samples were multiplexed using this tagging strategy, and unique libraries were created for sequencing in a single run.

5.2.3.3.3 DNA amplification and library preparation

Polymerase chain reaction (PCR) amplifications were performed in a final reaction volume of 20 µL. Each reaction mixture contained 10 µL of AmpliTaq Gold DNA Polymerase Master Mix (Thermo Fisher Scientific, USA), 0.64 µL of non-acetylated bovine serum albumin (BSA; concentration 5µg /µL), 1 µL of each forward and reverse primer (at a final concentration of 2 µM), 5.36 µL of ultrapure water, and 2 µL of DNA template. During the method validation phase, severe PCR inhibition was observed due to the high concentration of inhibitory substances present in the fully homogenized DNA sample matrices. To obtain PCR products, all DNA templates were diluted 20-fold prior to amplification, and non-acetylated BSA was added to the master mix to bind and neutralize any remaining co-extracted inhibitors. Identical thermal cycling profiles were utilized for both the 18S rRNA and *cox1* markers. The amplification program consisted of an initial denaturation step at 95°C for 10 min, followed by 40 cycles of denaturation at 94°C for 1 min, annealing at 45°C for 1 min, and extension at 72°C for 1 min. A final elongation step was performed at 72°C for 5 min (modified from Wangensteen et al., 2018).

The success of the amplifications was verified *via* agarose gel electrophoresis. Amplicons were loaded onto a 1% agarose gel and separated at 110 V for 40 min. Following verification, the PCR products were purified using the Clean-Up Concentrator kit (A&A Biotechnology, Poland) according to the manufacturer's protocol. The concentration and quality of the purified DNA were subsequently quantified using a spectrophotometer (BioTek Epoch Microplate Spectrophotometer). For samples that exhibited insufficient DNA concentration or poor purity parameters after the initial purification, supplementary PCR amplifications were performed. These additional products were purified and subsequently pooled with the initial replicates of the respective sample to ensure adequate material for downstream sequencing. To monitor for potential contamination, four negative controls (each consisting of molecular-grade water and reagents without a DNA template) were included: two

were processed during the initial PCR assays, and two were included in the supplementary amplification runs. Finally, all individualized sample libraries (separate for 18S and *cox1*) were combined in proportional equimolar ratios to create a single pooled library for final sequencing, with a target sequencing depth of 300,000 reads per sample. High-throughput sequencing was performed by Novogene on the Illumina NovaSeq 6000 platform using a 2×250 bp paired-end (PE250) strategy.

5.2.4 Data processing

5.2.4.1 Hydrography

CTD datasets were processed using the SBE Data Processing Software, with vertical profiles averaged at 1 m intervals. Potential temperature was calculated as a function of depth using the *oce* package in R (version 1.8-4; Kelley et al., 2022). For statistical analyses, all environmental parameters were averaged over the entire water column from the bottom to the surface. Vertical profiles of temperature, salinity, and fluorescence were plotted against depth. Fluorescence profiles were visualized alongside chlorophyll *a* data to provide a comprehensive environmental context. However, for statistical purposes, integrated (weighted) chl *a* values calculated for the entire water column were prioritized. This methodology was adopted as fluorescence signals may include detrital material (dead phytoplankton), and thus may not serve as a fully reliable proxy for food availability for meroplankton. Further calculations and visualizations were performed using Microsoft Excel and R 4.4.1/4.4.2, mainly with the: *base* (version 4.0.0), *dplyr* (version 1.1.4), *ggplot2* (version 3.5.1), *oce* (version 1.8.4), *readxl* (version 1.4.3), *tidyr* (version 1.3.2), *tidyverse* (version 2.0.0), and *svglite* (version 2.1.3) packages (Kelley et al., 2022; Oksanen et al., 2001; R Core Team, 2025; Wickham, 2016; Wickham & Bryan, 2023; Wickham et al., 2019, 2024a; 2024b).

5.2.4.2 Bioinformatic pipeline

Dataset and sampling origin

For genetic analyses, one-half of the total zooplankton sample collected at each of the 17 study stations during the 2021 cruise was utilized. One additional station initially designated for this region was excluded before downstream analysis due to sequence quality filtering.

Sequence processing and denoising

The bioinformatic workflow was implemented within the SLIM pipeline (Dufresne et al., 2019) hosted on IO PAN servers. Initial demultiplexing was performed using

unique tag sequences added to both forward and reverse primers, as described in the demultiplexing algorithm. Subsequently, the DADA2 algorithm (Callahan et al., 2016) integrated within the SLIM framework was employed for quality trimming, sequence filtering, denoising (inference of Amplicon Sequence Variants – ASVs), merging of forward and reverse reads, and chimera removal.

Taxonomic assignment

Taxonomic assignment was marker-specific. For the 18S dataset, sequences were annotated using the *vsearch* algorithm with the PR2 database (Guillou et al., 2013) *via* the SLIM web interface, using the reference database (pr2_version_5.1.0_SSu_UTAX.fasta; accessed on July 25, 2025). Although primarily designed for protists, PR2 was selected for its high curation quality and suitability for metazoan identification in this study. For the *cox1* dataset, sequences were compared against the BOLD database (Animal Secondary Markers (Public); Ratnasingham & Hebert, 2007) using the BOLDigger3 software (operating mode 2: Genus and Species Search; Buchner & Leese, 2020), accessed on November 21, 2025; https://github.com) running in a Linux environment.

To maximize detection of total meroplankton diversity, no ASVs were filtered by read abundance. Therefore, low-abundance sequences (e.g., singletons or <10 reads) were retained. ASVs that remained unclassified or unclear after initial assignment were further checked using a stand-alone BLASTn search (accessed in May, 2026) against the NCBI non-redundant nucleotide database. Taxonomic assignment thresholds based on sequence percent identity were defined as follows: species (≥99%), with lower thresholds assigned to genus (≥97%), family (≥95%), order (≥93%), or class (≥90%); these criteria were applied only to alignments with a query coverage of >80%. Sequences failing these criteria were labelled as "unassigned".

Contamination removal and data filtering

Data structuring and integration were performed using the *phyloseq* package (version 1.48.0; McMurdie & Holmes, 2013), while potential contamination and sequencing noise were assessed and filtered using the *decontam* package (version 1.24.0; Davis et al., 2018) in R. The background noise was identified by analyzing the negative control samples alongside the field samples by "*prevalence*" methods with a threshold = 0.3). A conservative threshold of 0.3 was applied to identify and remove contaminants. The high abundance of specific sequences detected in the negative controls was primarily attributed to a concurrent phytoplankton bloom, likely *Phaeocystis* sp., that introduced environmental DNA noise during sample collection.

Following decontamination, the dataset was filtered to isolate meroplanktonic taxa. The workflow, applied consistently to both 18S rRNA and *cox1* datasets, followed these steps:

1. Decontamination: removal of contaminant ASVs identified through negative controls, followed by the removal of negative control samples.
2. Taxonomic filtering: removal of sequences classified as unassigned (including non-target bacteria/eukaryotic/phytoplankton reads) to isolate the target Metazoa community;
3. Spatial subset: subsetting the final database to include only the 17 stations selected for this study;
4. Data normalization: application of Cumulative Sum Scaling (CSS) using the *metagenomSeq* package in R (version 1.46.0; Paulson et al., 2013) to ensure data comparability. Normalization was performed on the full Metazoa community of the 17 stations to account for sample-specific library sizes and scaling factors;
5. Meroplankton subset: Filtering out non-meroplanktonic taxa (e.g., holoplankton) from the normalized 17-station dataset to retain only the final meroplanktonic ASVs for downstream multivariate analyses.

Details of the read counts tracked throughout this filtering and normalization pipeline are summarized in Table SV. 1 presented in the Supplementary Materials section.

5.2.4.3 Statistical analysis

Multivariate analyses were performed using PRIMER 7 with the PERMANOVA+ add-on (Clarke & Gorley, 2015; Clarke et al., 2014). A significance level of $p \leq 0.05$ was applied to all statistical tests throughout this study. To ensure robust ecological analysis, the data were prepared as follows: morphological abundance/molecular data were transformed prior to analysis to balance the influence of dominant and rare taxa. A fourth-root transformation was applied to the morphological data, whereas genetic data (18S rRNA and *cox1)* underwent specific normalization procedures (CSS). For multivariate community analyses, specifically non-metric Multidimensional Scaling (nMDS), distance-based Linear Models (distLM), dbRDA (distance-based Redundancy Analysis), and PERMANOVA (Permutational Multivariate Analysis of Variance), the read counts were normalized using the Cumulative Sum Scaling (CSS) method implemented in the *metagenomeSeq* package (version 1.46.0; Paulson et al., 2013). In this process, the optimal quantile for scaling was determined using the *cumNormStat* function, and data were subsequently transformed *via cumNorm* and *MRcounts* (with log=TRUE to stabilize variance). Resemblance matrices for all datasets were based on the Bray-Curtis similarity. Additionally, barplots of relative taxonomic abundance were

generated from these normalized datasets to illustrate community composition across the sampled stations.

nMDS was used to visualize community structure in ordination space and to assess the consistency of a priori-defined groupings (NC – Norwegian Coast, BS – Barents Sea, AW – Atlantic Water, WS – West Spitsbergen Shelf). Differences in meroplankton community structure between zones were tested using a one-way PERMANOVA with Zone as a fixed factor. Due to the limited number of samples within subsets, analyses were performed using sequential (Type I) sums of squares, with 9999 unrestricted permutations of the raw data (Anderson et al., 2008). Monte Carlo tests were used to obtain valid p-values despite the limited number of unique permutations. Pairwise tests were subsequently conducted to identify significant differences between specific zone groupings.

The influence of environmental variables (temperature, salinity, and chlorophyll *a*) on the meroplankton community was evaluated using dbRDA combined with DistLM. This approach allowed for the simultaneous assessment of community responses to multiple environmental factors and the identification of drivers that best explain community variation. The "Best" selection procedure was applied, and the best-fitting models were selected based on Adj. R^2 values, with significance assessed using 9999 permutations (Anderson et al., 2008).

In addition, the absolute taxonomic richness (S) per station and per zone was calculated for each methodological approach (morphology, 18S rRNA, and *cox1*) and visualized using descriptive plots to compare method-specific taxonomic coverage across zone selections.

5.3 Results

5.3.1 Environmental conditions

The hydrographic structure of the study area, analyzed using vertical temperature and salinity profiles from 17 stations, revealed distinct regional patterns in water-column stratification (Figure V. 2). Red curves represented temperature [°C], while blue curves indicated salinity, both plotted against depth [m].

Stations such as PhM1, PhM3, PhM5, and WB3 showed sharp, highly defined pycnoclines/haloclines and thermoclines within the upper water layer (up to 50 m), where surface freshening and warming created strong vertical stratification (Figure V. 2). In contrast, stations such as V22, V26, K-3 and H3 demonstrated remarkable halocline stability with near-isohaline conditions throughout the water column, together with pronounced thermal stratification at station K-3 and V26, or gradual cooling of the waters down to 400 m at station H3. More complex, non-linear patterns at stations S3, EB2-1, EX3, and Y5 suggested the

presence of complex mixing processes, water mass intrusions, or the influence of local hydrographic factors (Figure V. 2).

For instance, station V22 revealed low temperatures (~1°C) throughout the entire water column, in contrast to WB3, PhM1, and N4, which remained warm in the surface and subsurface layers (3–12°C). The clustering of data points across most deep stations (e.g., PhM1, H3, V34, Y5) showed a move toward homogenous, cold, and saline values in the deep layers, while high variability in the surface (50-0 m) layer highlighted the strong sensitivity to atmospheric forcing, ice melt, and seasonal heating variability (Figure V. 2).

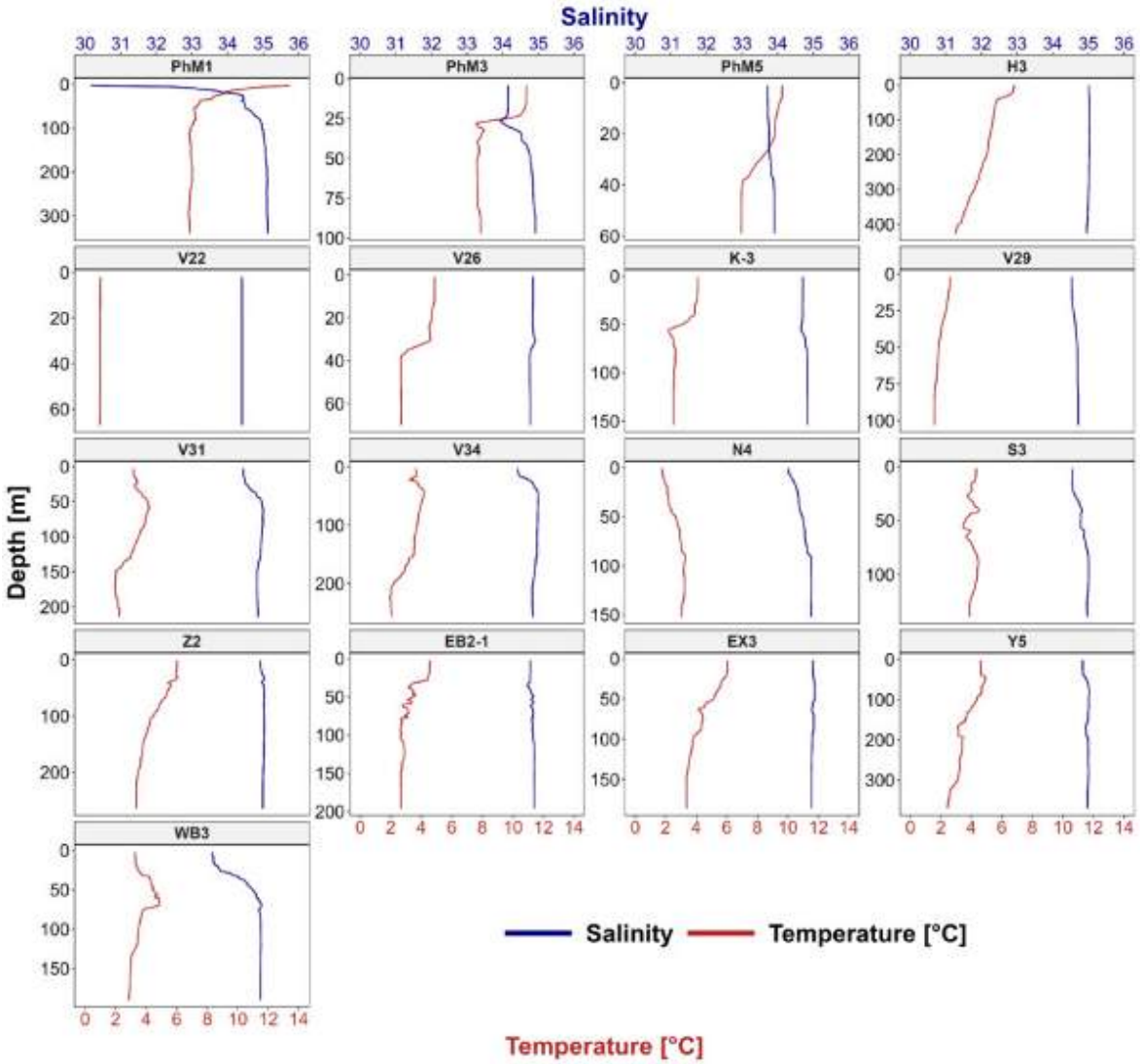

Figure V. 2 Vertical hydrographic profiles of temperature and salinity across the 17 sampling stations. Red lines represent temperature ([°C], lower axis) and blue lines represent salinity (upper axis) plotted against depth [m] on the reversed y-axis. Note that the depth scale (y-axis) varies between stations to match local maximum sampling depths.

Vertically continuous fluorescence profiles and discrete in situ chlorophyll *a* concentrations showed spatial, bathymetric, and regional variability across the study area. Highest concentrations and strong subsurface chlorophyll maxima were consistently confined to the upper euphotic layer (50-0 m) (Figure V. 3).

Regional differences aligned with water mass distribution and coastal topography. Along the Norwegian coast (PhM1, PhM3, PhM5), chlorophyll *a* values were relatively low and strictly confined to the upper 20-30 m. In contrast, stations around and north of Bear Island (V-section: V22 to V34) exhibited highly variable, dynamic vertical profiles with multiple peaks extending deeper into the water column. Along the West Spitsbergen shelf (N4 and northward: S3, Z2, EB2-1, EX3, Y5, WB3), strong fluorescence peaks were concentrated in the upper 50 m. By contrast, open-ocean stations potentially influenced by Atlantic Water masses (K-3 and H3) displayed distinct vertical structures, with K-3 showing an exceptionally pronounced chlorophyll a maximum near 50 m depth (Figure V. 3).

Continuous CTD fluorescence profiles generally aligned with discrete bottle samples, although below 100 m depth, values sharply declined toward zero across all deep stations.

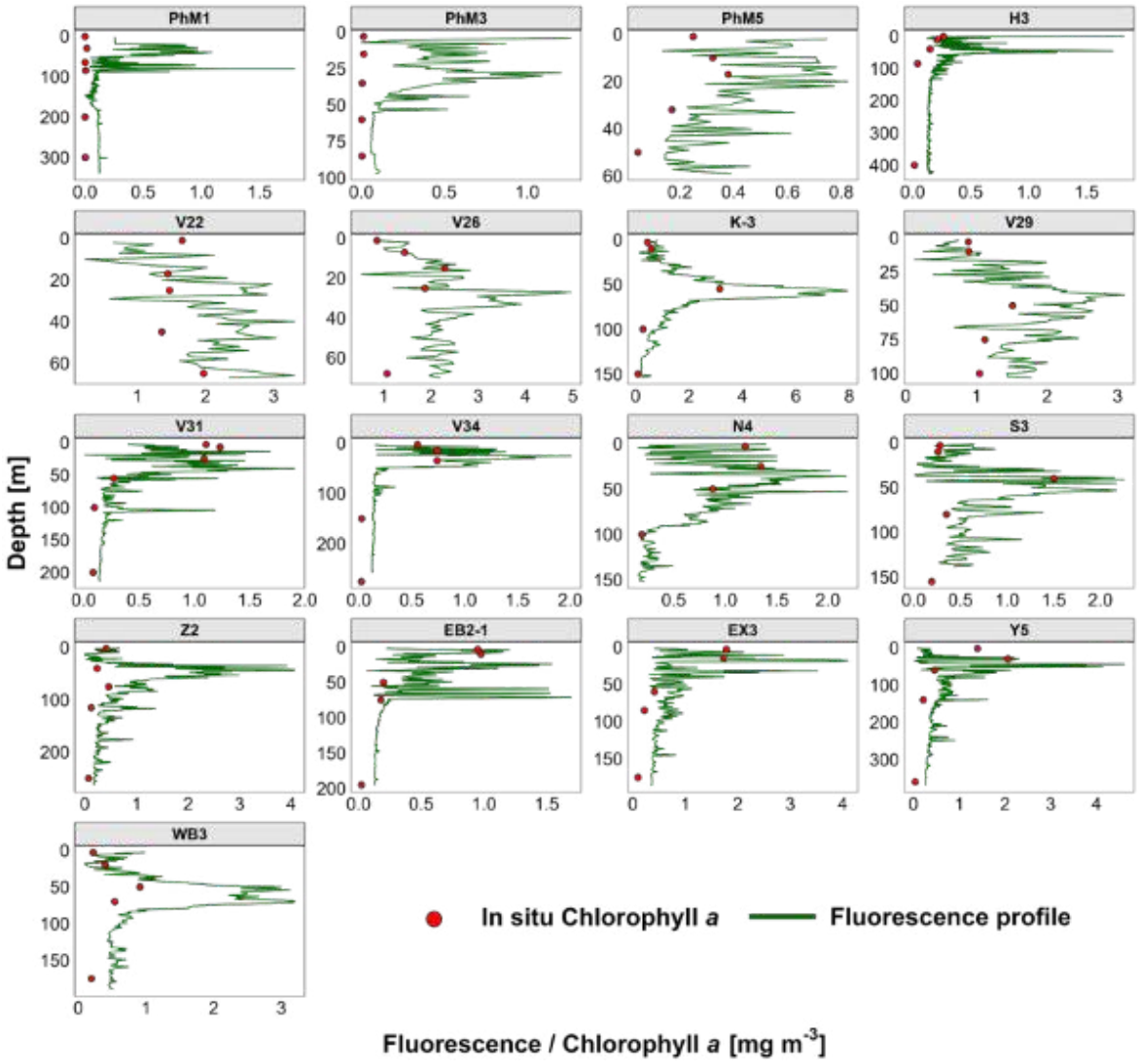

Figure V. 3 Vertical depth profiles of CTD fluorescence ([mg m^{-3}], dark green line] and discrete in situ chlorophyll *a* concentrations ([mg m^{-3}], red points) across 17 sampling stations plotted against depth [m] on the reversed y-axis. Note that the depth scale (y-axis) varies between stations to match local maximum sampling depths.

5.3.2 Methodological comparison of meroplankton taxa richness

The quality filtering and decontamination procedures significantly reduced the raw read depth, primarily due to the exclusion of non-target microeukaryotic sequences classified as unassigned (Table SV. 1). After removing contaminants and unassigned taxa (which accounted for 95.41% of reads in 18S and 82.25% in *cox1*), the dataset was filtered to 17 study stations. From the Metazoa community, a final datasets of 19 388 reads (18S) and 54 694 reads (*cox1*) were retained for meroplanktonic ASVs before CSS normalization (Table SV. 1).

The study indicated a total taxonomic richness of 52 taxa identified via the *cox1* marker, 46 via the 18S rRNA marker, and 41 through morphological examination across the entire study area. Significant variability in taxa richness was observed both between stations and across the three methodologies. Stations in the south (PhM1; PhM3) demonstrated the highest overall taxonomic diversity, while others, such as WB3 and N4, further north, showed lower richness. Furthermore, the two analytical methods and 2 different molecular markers differed in their capability to detect taxonomic richness. For example, at stations (PhM1; H3; V34), morphological identification indicated a higher count, whereas at others (PhM5; Z2; EX3), molecular markers (*cox1*; 18S) revealed a greater number of taxa (Table SV. 2).

By aggregating data at the zone level rather than the station level, taxa richness was generally comparable across all three datasets within each distinctive zone, providing a robust assessment of the overall biodiversity within each area (Figure V. 4). The NC zone consistently showed the highest biodiversity across all methods (33 – 37 taxa), suggesting it is a highly productive or species-rich environment compared to the others. In contrast, the BS, AW, and WS zones showed lower overall richness. Moreover, although the 18S sequencing showed the highest taxa detection in the NC and BS zone, the *cox1* method appears to be more effective in capturing taxonomic diversity in the BS and WS zones (Figure V. 4). Moreover, combining cumulative regional richness with mean station-level richness (Mean ± SD) revealed intra-zonal variability across the sampling sites. The most pronounced intra-zonal heterogeneity occurred in the NC zone, where local richness averaged 17.1 ± 11.4 taxa for morphology, 19.4 ± 5.6 for *cox1*, and 20.4 ± 8.3 for 18S, reflecting strong micro-habitat patchiness despite high cumulative diversity. In contrast, spatial variance was noticeably lower in the AW zone (morphology: 15 ± 1.4; *cox1*: 11.1 ± 2.9; 18S: 10.0 ± 2.8) and the WS zone (morphology: 8.2 ± 2.5; *cox1*: 8.9 ± 2.5; 18S: 7.2 ± 2.8), indicating a more homogenous meroplankton community structure across stations within these regions (Figure V. 4).

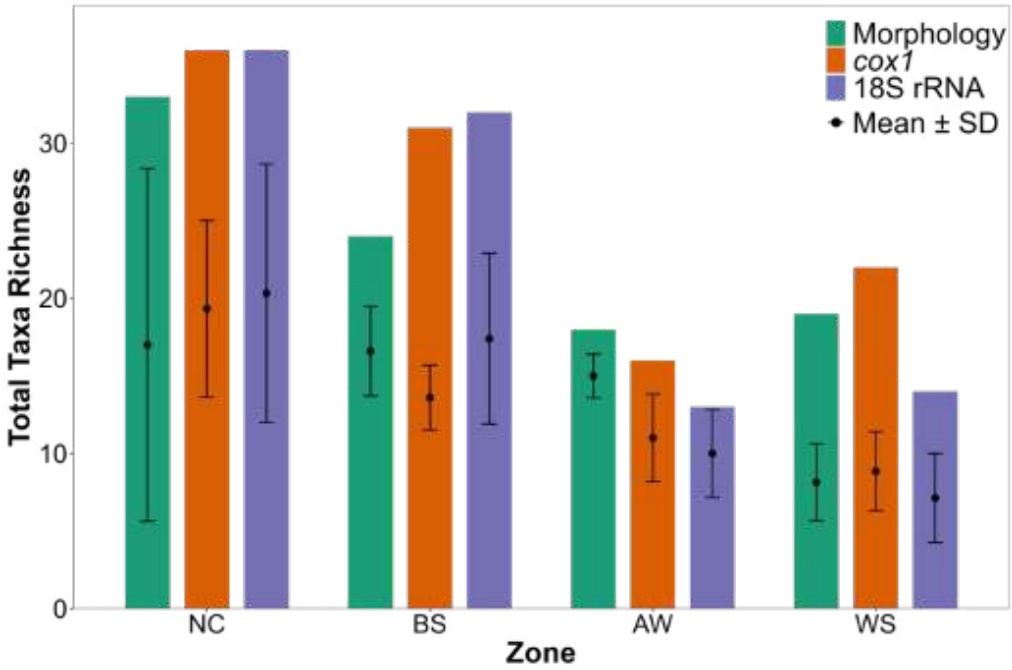

Figure V. 4 Regional and local meroplankton taxonomic richness across four study zones evaluated by morphological identification and metabarcoding (*cox1* and V1-V2 region of the 18S rRNA markers). Bars represent cumulative regional taxa richness per zone (Total), while overlaid black points with error bars indicate mean station-level richness ± standard deviation (Mean ± SD). Zone abbreviations (NC – Norwegian Coast; BS – Barents Sea; AW – Atlantic Water; WS – West Spitsbergen shelf).

5.3.3 Taxonomic composition and inter-methodological match

A comparison of the meroplankton community revealed methodological and spatial patterns, differing in resolution from species-genus level in molecular approach to broader taxonomic levels (phyla, class, family) in morphology (Figure V. 5). Morphological classification of organisms to higher ranks showed 10 groups in total (Echinodermata, Bivalvia, Polychaeta, Cirripedia, Bryozoa, Gastropoda, Decapoda, Anthozoa, Enteropneusta & Phoronidae). In contrast, based on molecular datasets, they revealed fewer taxa: 8 for *cox1* (detecting Nemertea, but not Phoronidae, Enteropneusta & Anthozoa) and 9 for the V1-V2 region of 18S (detecting Nemertea, but not Bryozoa & Anthozoa) (Figure V. 5). Each method presents a unique taxonomic perspective based on its specific resolution and identification markers.

The morphological dataset showed some shifts in dominance, particularly in the AW zone relative to the NC zone, reflecting its focus on easily distinguishable larval groups. In contrast, the *cox1* dataset revealed higher compositional dynamics between zones, indicating that this marker better captures community responses to the specific environmental conditions

of different zones. The 18S rRNA dataset showed a relatively stable community structure across zones, suggesting a similar core community (Figure V. 5).

Morphological data demonstrated a clear dominance pattern (relative abundance [%] based on ind m^{-3}) in which Echinodermata (>75% in AW), Polychaeta (~45% in NC), Cirripedia (>65% in BS), and Bivalvia (~90% in WS) encompassed the majority of the identified individuals in certain zones, providing a clear view of the dominant larval groups that may characterize the benthic recruitment pool (Figure V. 5). Both molecular based datasets (relative abundance [%] based on sequence reads after CSS normalization) showed completely different meroplankton community structure. The *cox1* data, by providing higher taxonomic resolution, showed a more complex community structure, where Bivalvia and Cirripedia (~10-30% and ~30-50%, respectively) showed significant variability in their relative abundance depending on the zone, indicating the ability of this marker to capture more differences in community composition that morphological examination and V1-V2 18S rRNA may overlook. The 18S rRNA dataset highlighted the considerable presence of Polychaeta and Echinodermata, which maintain high relative abundances across all zones (up to 50% and ~20%, respectively). The broad taxonomic categorization provided by 18S effectively highlighted the ubiquity of these groups across the zones (Figure V. 5). Each method highlights different dominant groups based on its identification threshold: 18S marked broader phyla with consistent dominance of soft-bodied groups like Polychaeta and Echinodermata, *cox1* revealed detailed taxonomic shifts in shelled larvae such as Bivalvia and Cirripedia, and morphology emphasized easily distinguishable meroplankton groups during their mass occurrences (Figure V. 5).

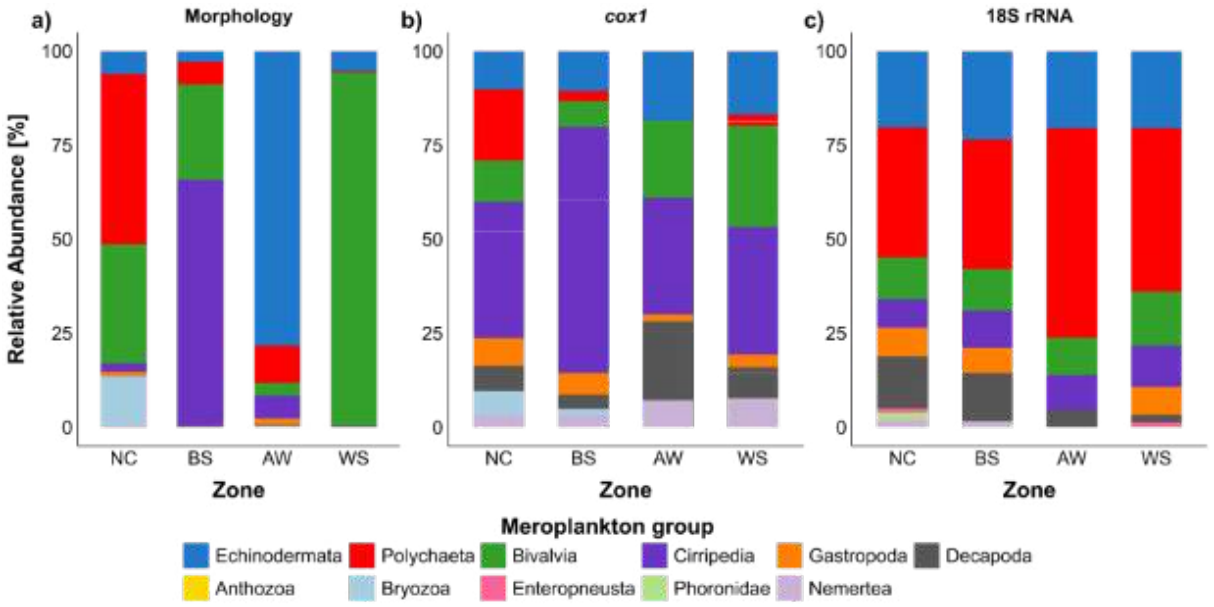

Figure V. 5 Relative abundance of major meroplankton groups across four study zones (NC – Norwegian Coast; BS – Barents Sea; AW – Atlantic Water; WS – West Spitsbergen shelf). The panels compare the taxonomic composition derived from morphological identification (a), *cox1* (b), and V1-V2 region of the 18S rRNA (c), highlighting the differences in resolution and dominant taxa captured by each method.

The effectiveness of the chosen identification methods appears to be group-specific. Morphological identification remains better for groups like Cirripedia and Decapoda (Figure V. 8 and Figure V. 9, respectively), where distinct larval stages appear (such as nauplii/cypris or zoea/megalopa). On the other hand, *cox1* was effective for Gastropoda (Figure V. 11) and 18S for Polychaeta (Figure V. 7), providing a detailed description that more accurately captured community differences between zones than morphological identification alone.

The morphological assessment revealed clear spatial differentiation based on larval development stages. Echinodermata showed high developmental diversity, up to 15 distinct larval morphotypes along the study area (Figure V. 6). The NC zone was characterized by three groups: Ophiuroidea, Echinoidea, and Asteroidea (mainly Ophio1, Echinopl1, Echinopl2, Echinopl3, EchiJuv1; Brach1), while the zones AW and WS were dominated by the Ophio1 morphotype up to nearly 90% in the WS zone. In the BS zone, however, the ~30% of contribution was noticed with Holothuroidea larvae (Figure V. 6). Also, Polychaeta showed a strong morphotype diversity, in which Poly_cf._Amphinomidae dominated NC zone, although the remaining zones includes more diverse community, i.e.: Poly_troch, Poly_metatroch, Poly_cf._Pollynoidae, or Poly_cf._*Prionospio* spp., among others (Figure V. 7). For Cirripedia,

morphological identification showed developmental stages, revealing a transition from naupliar to cyprid stages across the study area. Early nauplius stages (Cirr_nau_1 and Cirr_nau_2) dominated the NC zone (also with a high share of Cirr_cyp_1) and AW zones, whereas the BS and WS zones were characterized by an increased relative abundance of the cypris stage (Cirr_cyp_1 and Cirr_cyp_3) (Figure V. 8). This visual approach effectively highlighted the demographic shift in barnacle larval development that molecular markers masked through genus-level collapsing. In Decapoda, the morphological approach identified shifts in developmental stages. The NC and BS zones were diversified by early zoea stages of 3 taxa and a small percentage of megalopa (NC), whereas AW and WS were dominated by *Hyas* zoea specifically (Figure V. 9). In contrast, Bivalvia and Gastropoda did not have more detailed morphotype identification, therefore the information about possible zonation is lacking (Figure V. 10, 11).

The *cox1* marker provided a highly detailed view of local community variation, highlighting major differences between the study zones. In Echinodermata, *cox1* revealed a less diverse structure compared to morphological counts, dominated by *Ophiura*, *Ophiopholis,* and *Cucumaria* in NC and BS zones, with more pronounced *Ophiacten* appearing in AW and WS zones, and *Strongylocentrotus* contributing to the BS and WS zone (Figure V. 6). For Polychaeta, *cox1* showed clear spatial differences with *Paramphinome* dominating the NC zone and *Polydora* appearing in NC and BS zones. On the other hand, in the BS zone, diversity was the highest among all zones. However, sequence amplification completely failed for the AW zone (Figure V. 7). In Cirripedia, *cox1* represented the dominance of the genera *Balanus* and *Semibalanus* across all zones, with a minor presence of *Verruca* in NC, BS, and AW zones (Figure V. 8). In Decapoda, *cox1* revealed near-total dominance of the genus *Hyas* across all zones, contrasting with the distinct stage-based zonation identified morphologically (Figure V. 9). Bivalvia community exhibited spatial structuring, with *cox1* highlighting the ubiquity of *Panomya*, but detecting specific genera such as *Abra* and *Mya* exclusively in the NC and BS zones, respectively (Figure V. 10). Similarly, Gastropoda revealed distinct shifts in genus composition in which NC zone was characterized by high relative abundance of *Caronella* and *Euspira*, BS zone by *Lacuna* and *Euspira*, while WS zone had more even community (Figure V. 11). This indicates that the *cox1* dataset captures localized taxonomic signatures that distinguish the ecological profile of each zone.

The 18S dataset demonstrated significant taxonomic differences across the study area, with genus-level composition varying considerably between zones. In Echinodermata, the 18S marker uncovered 6 genera across zones, characterized by the presence of *Pentacta, Asterias,*

Lapidoplax, Ophiotrix, Canolampas and *Ophiotrix* (NC zone), while *Pentacta* and *Ophiotrix* dominating the WS zone (Figure V. 6). Moreover, the community structure of Polychaeta showed a clear gradient in taxa richness with specific genera consistently associated with the NC zone, which captured ~12 genera (e.g., *Eteone, Myriochele, Pectinaria, Protodrilus, Pisione, Owenia* and *Eumida*), while WS zone was represented by only 6 genera (*Eteone*, *Myriochele*, *Pectinaria*, *Protodrilus*, *Asetocalamyzas*, and *Nothria*), indicating strong zone-specific taxonomic associations (Figure V. 7). Conversely, for Cirripedia, 18S reflected a highly uniform taxonomic composition, where nearly 100% of contribution across all four zones were assigned to *Balanus*, with only a minor contribution of *Peltogaster* detected in BS zone (Figure V. 8). Furthermore, 18S effectively captured Decapoda diversity beyond *Hyas*, detecting additional genera from shrimp and langoustine apart from crabs genera found by *cox1* such as *Eualus*, *Nephrops* in the NC and BS zones, but with domination of one taxa in AW and WS zones (Figure V. 9). In the NC and BS zones, Bivalvia assemblages were highly diverse, showing genera such *Macoma, Hiatella, Dosinia*, *Fulvia, Panopea*, and *Parvicardium*. However, in AW and WS zones, the community was fully dominated by *Macoma* (Figure V. 10). In Gastropoda across all zones, 18S revealed noticeable shifts in community composition from highly diverse in the NC zone (dominated by *Scaphander*, *Calliopaea*, *Flabellina,* and *Onchidoris*), to reduced diversity in the WS zone shared by *Abyssochrysos* and *Doto* (Figure V. 11). This spatial transition highlights 18S as an effective marker for capturing broad-scale geographic shifts in larval assemblages.

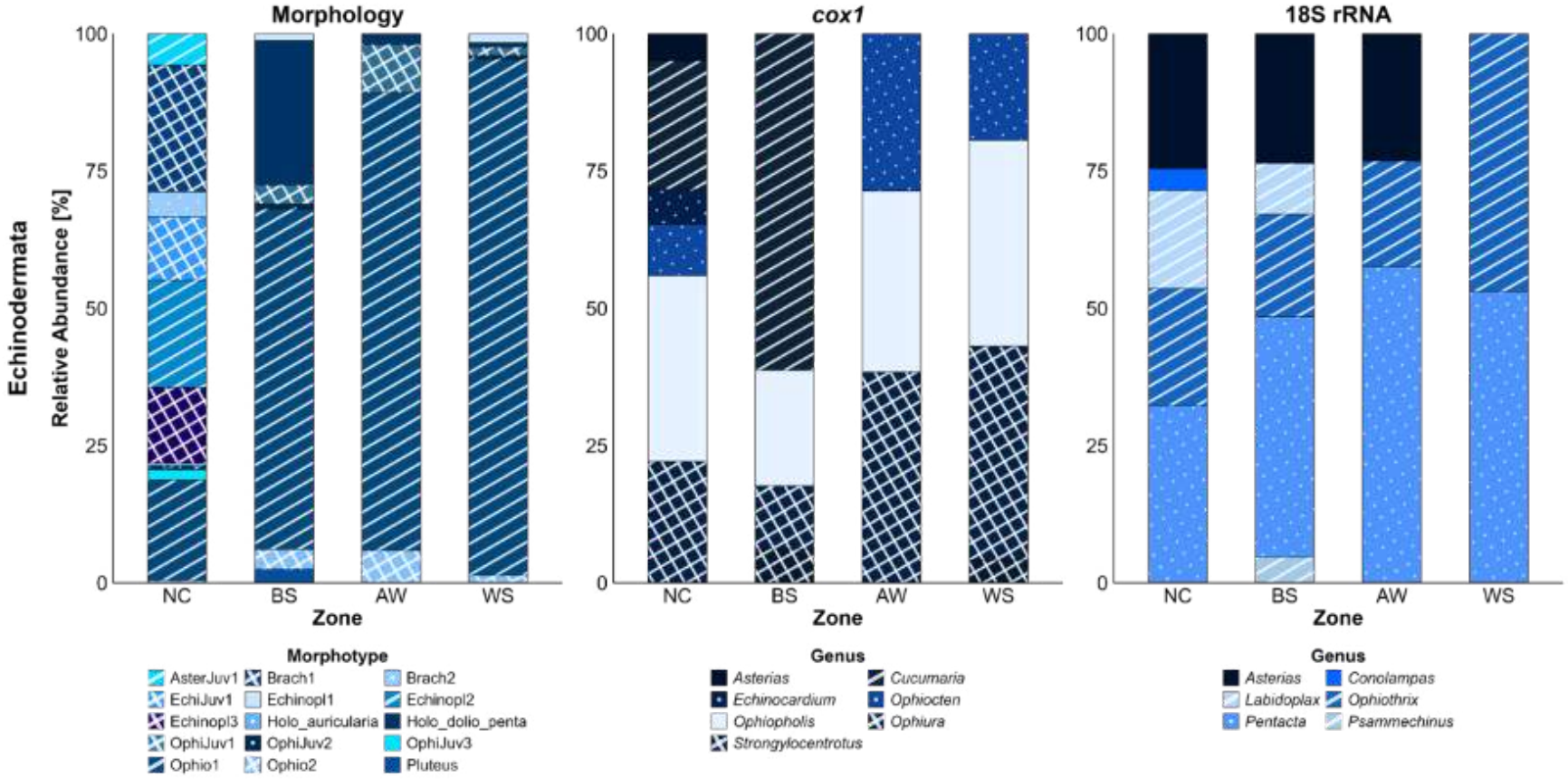

Figure V. 6 Comparison of taxonomic resolution and relative abundance [%] of Echinodermata larvae across three methodological approaches within four study zones (NC – Norwegian Coast; BS – Barents Sea; AW – Atlantic Water; and WS – West Spitsbergen shelf).

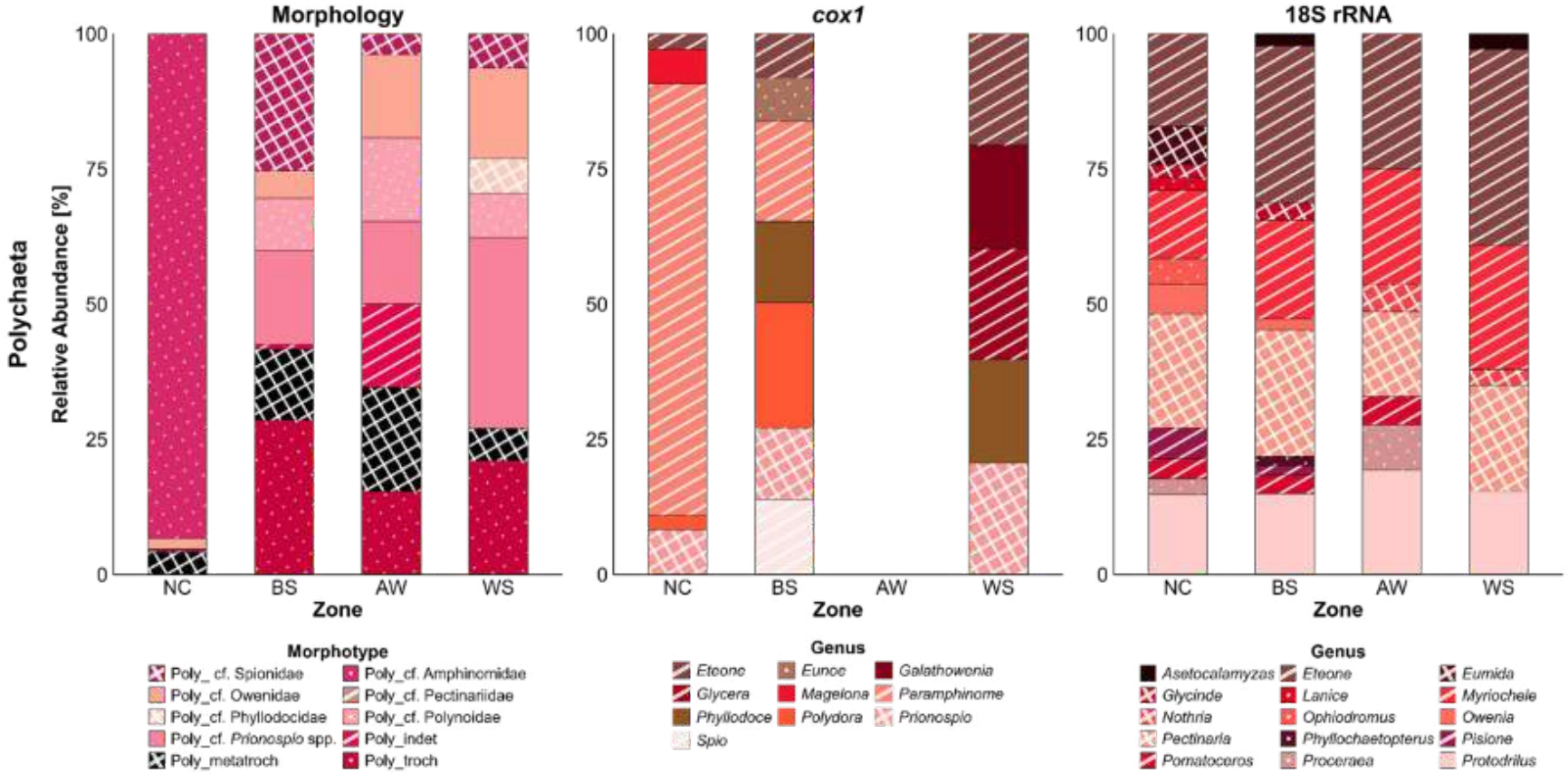

Figure V. 7 Comparison of taxonomic resolution and relative abundance [%] of Polychaeta larvae across three methodological approaches within four study zones (NC – Norwegian Coast; BS – Barents Sea; AW – Atlantic Water; and WS – West Spitsbergen shelf).

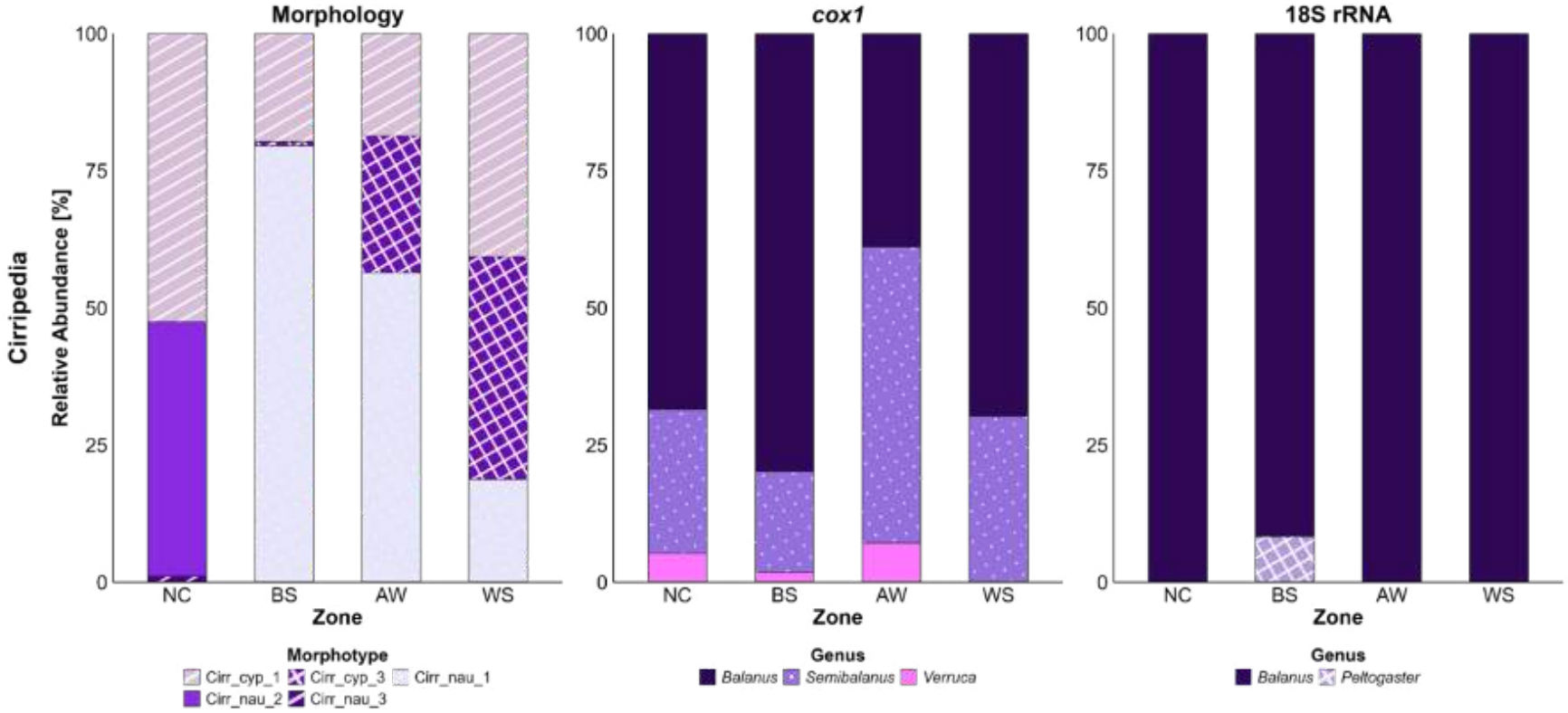

Figure V. 8 Comparison of taxonomic resolution and relative abundance [%] of Cirripedia larvae across three methodological approaches within four study zones (NC – Norwegian Coast; BS – Barents Sea; AW – Atlantic Water; and WS – West Spitsbergen shelf).

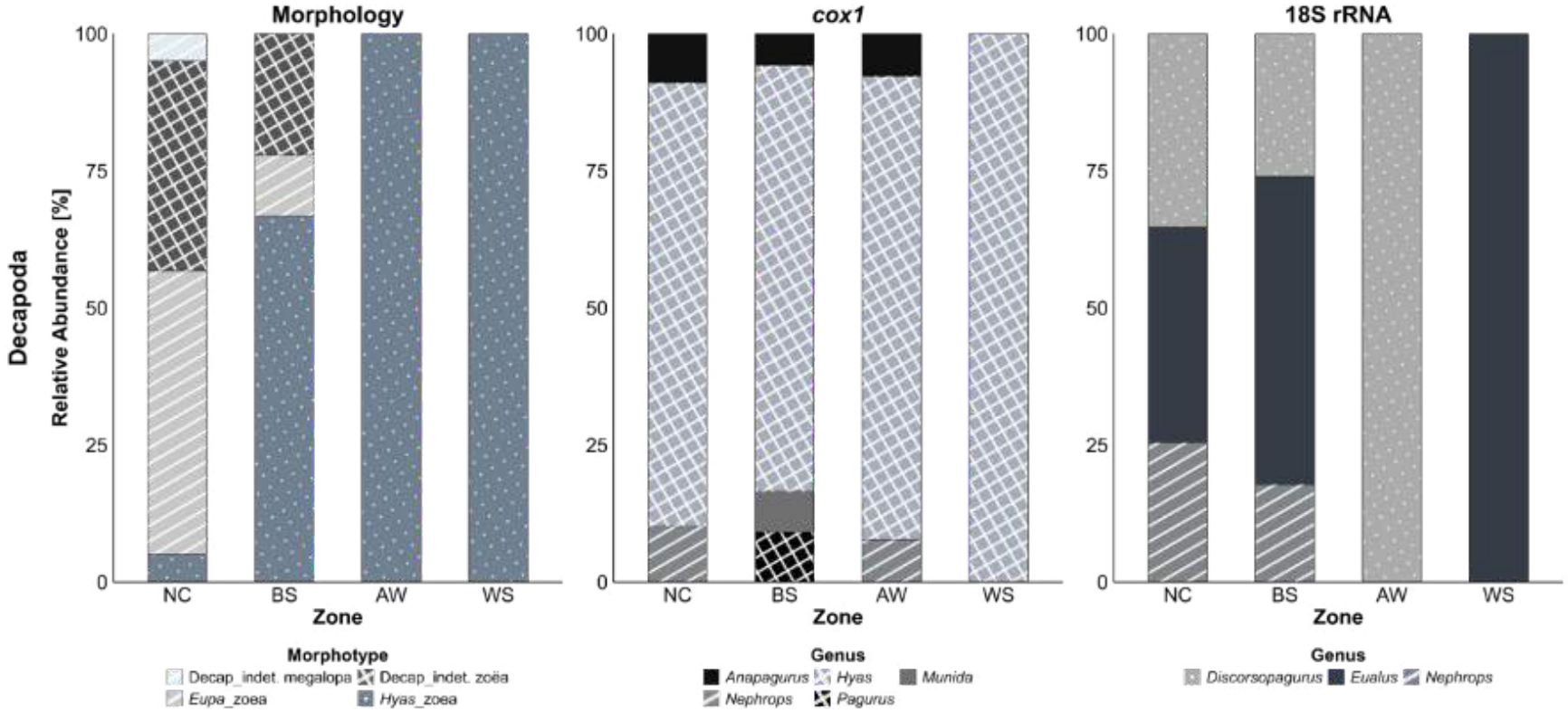

Figure V. 9 Comparison of taxonomic resolution and relative abundance [%] of Decapoda larvae across three methodological approaches within four study zones (NC – Norwegian Coast; BS – Barents Sea; AW – Atlantic Water; and WS – West Spitsbergen shelf).

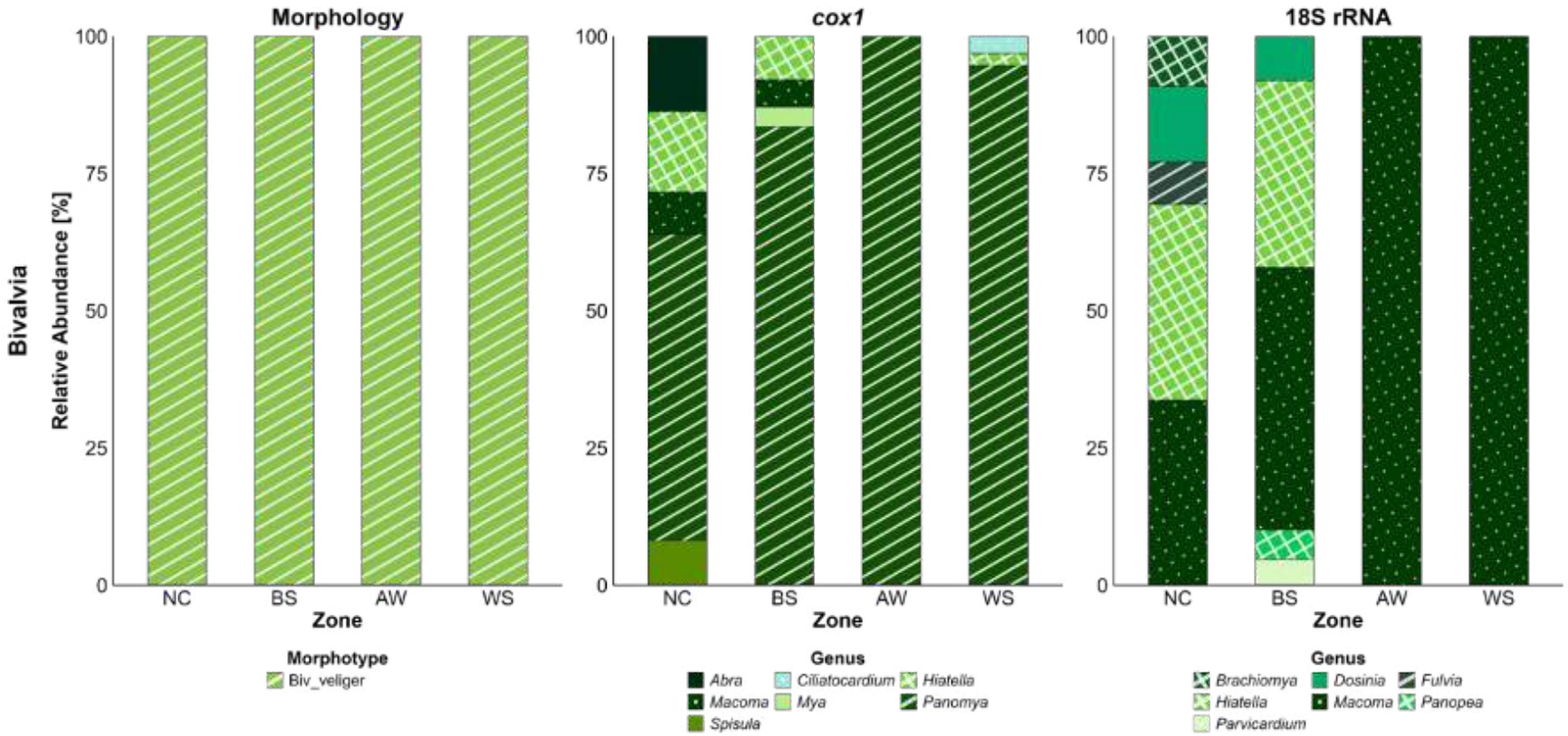

Figure V. 10 Comparison of taxonomic resolution and relative abundance [%] of Bivalvia larvae across three methodological approaches within four study zones (NC – Norwegian Coast; BS – Barents Sea; AW – Atlantic Water; and WS – West Spitsbergen shelf).

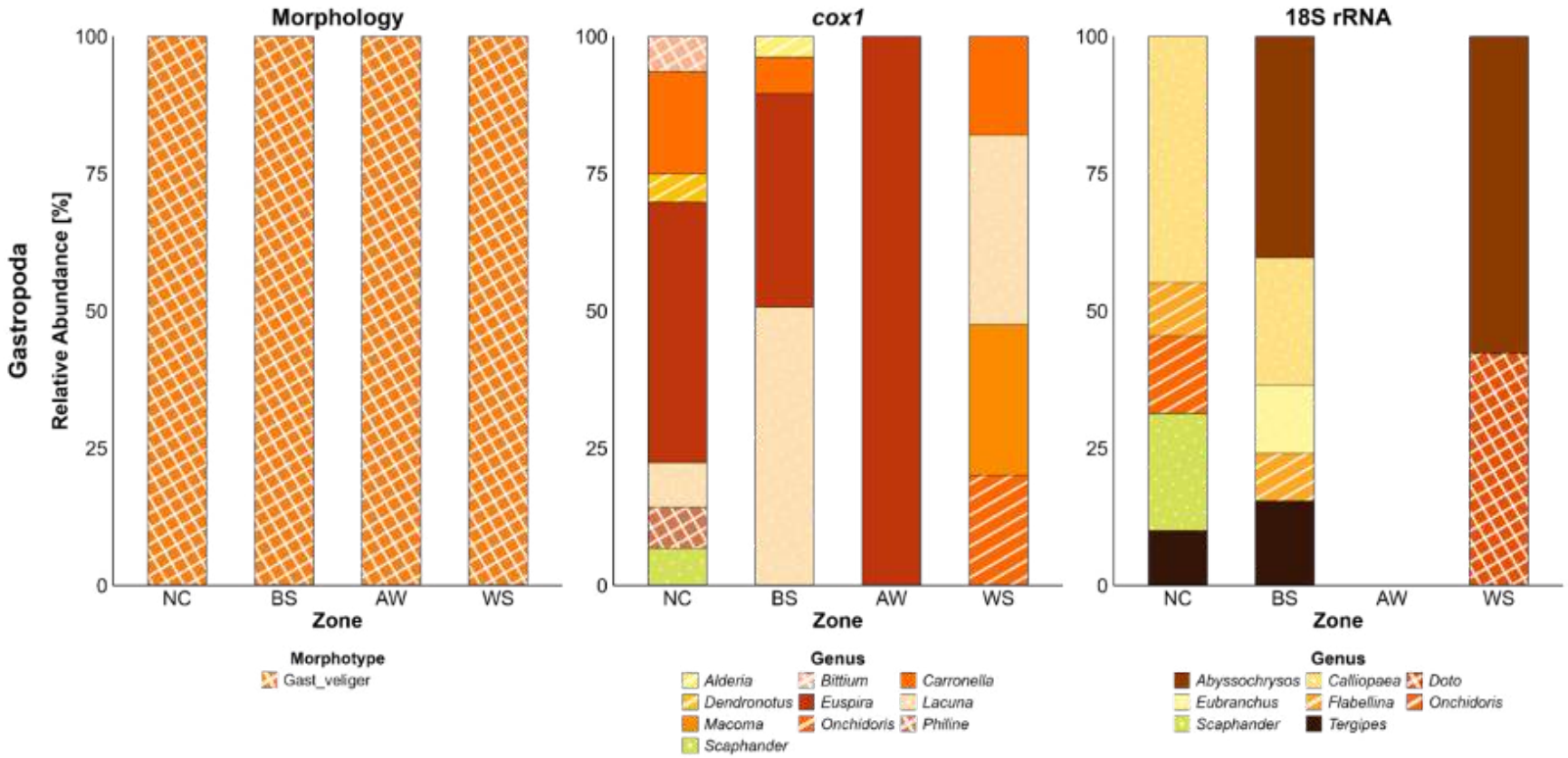

Figure V. 11 Comparison of taxonomic resolution and relative abundance [%] of Gastropoda larvae across three methodological approaches within four study zones (NC – Norwegian Coast; BS – Barents Sea; AW – Atlantic Water; and WS – West Spitsbergen shelf).

5.3.4 Meroplankton community structure and spatial patterns

The nMDS analyses revealed distinct community patterns across the 17 sampling stations, with varying degrees of spatial separation and dispersion depending on the method used. The morphological nMDS exhibited the highest degree of overlap between zones, with samples from BS, AW, and NC zones concentrating in the central region of the plot (Figure V. 12a). The tight clustering of the samples within distinct zones suggests that morphological identification results in a clear ecological separation between regions compared to the molecular-based datasets. In contrast, the *cox1*-based nMDS showed high intra-zonal dispersion and no specific spatial clustering among zones. While the NC zone cluster remained distinguishable in the lower part of the plot, the separation between BS, AW, and WS zones was less defined than in the 18S rRNA-based method (Figure V. 12b). This higher dispersion showed high sequence variability of the *cox1* marker across individual sampling stations. The 18S rRNA-based nMDS showed the clear differentiation between the NC zone cluster and the remaining zones (BS, AW, WS) (Figure V. 12c). However, although group separation is visible, the individual samples within these groups exhibit higher dispersion across the ordination space compared to the tighter clustering observed in the morphological dataset.

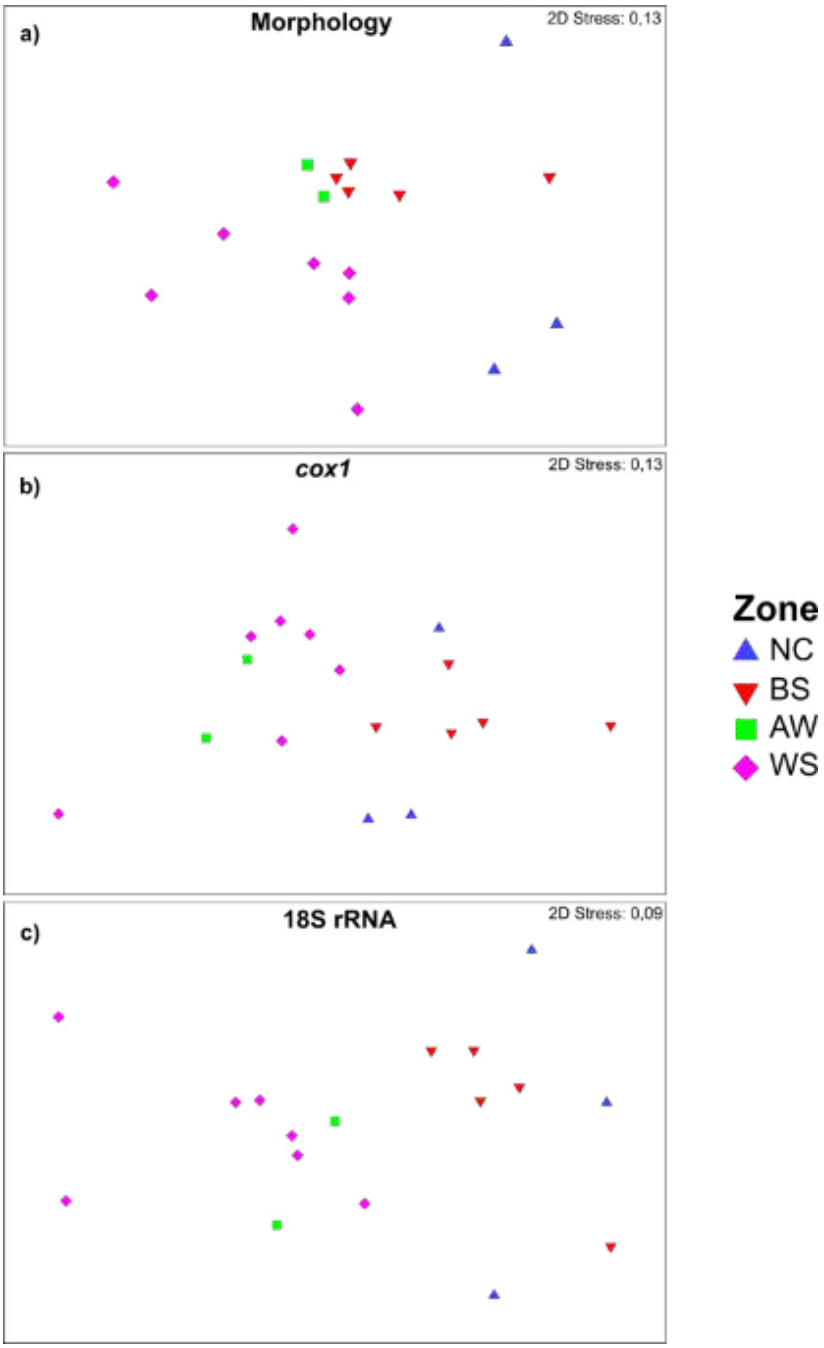

Figure V. 12 Non-metric Multidimensional Scaling (NMDS) analysis visualizing the similarity between four study zones (NC – Norwegian Coast; BS – Barents Sea; AW – Atlantic Water; WS – West Spitsbergen shelf) based on morphological data (a), *cox1* genetic marker (b), and V1-V2 region of the 18S rRNA genetic marker (c).

PERMANOVA analyses confirmed significant variations between zones across all methods (Table V. 3). The morphological dataset showed that the factor Zone explained 35.8% of the total community variation ($p<0.001$) (Table V. 3), with pair-wise tests revealing significant differences between 3 pairs of zones (NC/BS; NC/WS & BS/WS) with the strongest on between the BS & WS zones ($t=1.96$, $p=0.0038$, $P(MC)=0.0125$) (Table V. 3). The *cox1*

dataset, although explaining 18.21% of the variance by factor Zone ($p<0.001$), highlighted sensitivity in capturing community variations, showing significant differentiation only between BS/WS zones ($t=1.76$, $p=0.0014$, $P(MC)=0.0089$) highlighting the sensitivity of this marker in capturing community variations that may be less visible in other datasets. Regarding the 18S marker dataset, the factor Zone accounted for 41.65% of the total variance ($p<0.001$), identifying significant differentiation between NC/WS zones ($t=2.36$, $p=0.0087$, $P(MC)=0.0067$), BS/WS zones ($t=2.68$, $p=0.0018$, $P(MC)=0.0009$), and BS/AW zones ($t=1.83$, $p=0.0458$, $P(MC)=0.0395$), indicating this marker effectively captures distinct ecological signatures (Table V. 3; Table V. 4). The variance components analysis highlights that though all markers confirm significant community shifts, the 18S marker provides the highest explanatory power (41.65%) for the observed zoning, whereas morphological identification (35.8%) and *cox1* (18.21%) offer complementary perspectives on community structure, potentially reflecting different aspects of hidden diversity (Table V. 3; Table V. 4).

Analysis of average similarity within and between zones further characterized the community structure (Table V. 4). Across all three methods, the AW and BS zones generally showed higher within-zone similarity (e.g., 69.2% for AW and 60.7% for BS zones in morphology) compared to the NC zone, suggesting a more homogenous community structure in these regions. Furthermore, molecular methods presented distinct similarity profiles compared to morphology. Specifically, the lower similarity values in the *cox1* dataset (ranging from 30.50% to 36.24% within zones) reflected the higher resolution of this marker, which captures a wider spectrum of rare taxa and reduced the average similarity value compared to the more conservative morphological counts (Table V. 4). In 18S dataset, the similarity values ranged from 43.89% (NC zone) to 60.69% (BS and AW zones), reflecting the conserved character of the marker and possibility to obtain more stable taxonomic patterns in the entire studied area (Table V. 4). Moreover, pair-wise comparisons revealed differences between specific zone pairs, where molecular datasets, especially 18S showed stronger inter-zonal separation, compared to morphological analysis. (Table V. 4) .

Table V. 3 Results of the Global tests for Permutational Multivariate Analysis of Variance (PERMANOVA) for meroplankton community structure between four study zones (NC – Norwegian Coast; BS – Barents Sea; AW – Atlantic Water; WS – West Spitsbergen shelf) across the 18S rRNA, *cox1*, and morphological identification datasets.

Factor	df	SS	√ECV	ECV%	MS	Pseudo-F	P(perm)	Unique perms	P(MC)
Meroplankton community composition - Morphology									
Zone	3	12336	26.734	**35.8102**	4111.9	3.2096	0.0001	9893	0.0006
Residuals	13	16655	35.793	64.1898	1098.3				
Total	16	28991			1281.1				
Meroplankton community composition – cox1									
Zone	3	12573	22.271	**18.21855**	4191.1	1.8823	0.0007	9860	0.0133
Residuals	13	28945	47.186	81.78145	2226.5				
Total	16	41518							
Meroplankton community composition – 18S rRNA									
Zone	3	13238	28.689	**41.65519**	4412.7	3.8278	0.0002	9919	0.0011
Residuals	13	14986	33.953	58.34481	1152.8				
Total	16	28225							

Significant level was p=0.05,
Statistically significant results are marked in red values p<0.05,
Meroplankton morphology data = similarity resemblance matrix on fourth root transformed data,
Meroplankton *cox1*/18S data = similarity resemblance matrix on CSS analysis data,
df – degrees of freedom,
SS – sum of squares
√ECV – the square root of the estimated components of variation (ECV), indicating the relative magnitude of the effect for each factor,
ECV% - Percentage of the Estimated Components of Variation (ECV) to the total variation; represents the relative contribution of each term to the overall multivariate variance,
MS – means of squares,
Type I sequential sums of squares were applied to account for the hierarchical and unbalanced structure of the data. Unrestricted permutation of raw data and Monte Carlo tests (P(MC)) were performed for a small number of samples in the designated zone groups.

Table V. 4 Results of pair-wise PERMANOVA tests and average similarity analysis for meroplankton community structure between four study zones (NC – Norwegian Coast; BS – Barents Sea; AW – Atlantic Water; WS – West Spitsbergen shelf) across morphology, *cox1*, and 18S rRNA datasets. Pair-wise comparisons indicate significant differences between specific zone combinations ($p<0.05$), while the similarity matrix provides the average Bray-Curtis similarity [%] within and between zones.

Pair-wise tests												
	Morphology				*cox1*				*18S rRNA*			
Groups	**t**	**P(perm)**	**perms**	**P(MC)**	**t**	**P(perm)**	**perms**	**P(MC)**	**t**	**P(perm)**	**perms**	**P(MC)**
NC, BS	2.0261	0.0161	56	0.0198	1.1135	0.1604	56	0.3107	1.1589	0.1996	56	0.2677
NC, AW	1.7546	0.1041	10	0.092	1.2337	0.1026	10	0.2653	1.5224	0.2002	10	0.1523
NC, WS	2.0031	0.0187	120	0.01	1.3996	0.0067	120	0.0756	2.3574	0.0087	120	0.0067
BS, AW	1.1667	0.2844	21	0.283	1.5379	0.0528	21	0.0761	1.8341	0.0458	21	0.0395
BS, WS	1.9606	0.0038	791	0.0125	1.7585	0.0014	791	0.0089	2.6753	0.0018	791	0.0009
AW, WS	1.2739	0.2184	36	0.1967	0.79685	0.9196	36	0.6886	0.93582	0.5023	36	0.4659
	Average Similarity between/within Zones											
	Morphology				*Cox1*				*18S*			
	NC	BS	AW	WS	NC	BS	AW	WS	NC	BS	AW	WS
NC	39.621				30.484				43.886			
BS	31.8	60.707			31.586	36.239			48.715	58.129		
AW	28.251	61.15	69.154		24.863	21.443	34.216		36.322	43.401	60.695	
WS	26.443	41.8	47.807	48.501	24.787	23.66	37.997	33.683	26.885	34.805	56.59	54.405

5.3.5 Environmental drivers of meroplankton community

The dbRDA showed the relationship between meroplankton community composition and key environmental variables: mean temperature, mean salinity, and weighted mean of chlorophyll *a* concentration (Figure V. 13). For the morphological dataset, these variables explained 19.7% of the total variation in meroplankton community structure along the first axis (dbRDA1), where the influence of mean temperature and mean salinity confirms that shifts in these communities are closely related to the physical properties of the water masses (Figure V. 13a). Specifically, warmer and highly influenced by Atlantic waters (NC zone) were associated with a higher presence of specific larval forms, such as Bryozoa larvae (Bryo_cypho1, Bryo_cypho2), and Polychaeta larvae (Poly_cf. Amphinomidae), as well as Cirripedia nauplii (Cirr_nau_2). On the other hand, high-salinity and probably more influenced by Arctic-origin waters zones (WS, BS) clustered with juvenile Ophiuroidea (OphiJuv1) and Polychaeta larvae (Poly_cf. Spionidae), highlighting a clear segregation of larval types along the thermo-haline gradient. In the *cox1*-based analysis, the abiotic predictors accounted for 9.6% of the variation (dbRDA1), with mean temperature and chlorophyll *a* showing as influential factors for specific species assemblages (Figure V. 13b). Higher primary productivity strongly aligned with the presence of taxa such as *Strongylocentrotus* (Ophiuroidea), *Verruca* (Cirripedia), and *Prionospio* (Polychaeta). Bivalvia and Gastropoda veligers (*Mya*, *Lacuna*, *Euspira*) as well as Ophiuroidea larvae (*Ophiopholis*, *Ophiura*) were mainly positively correlated with temperature and salinity gradients toward the negative dbRDA1 values. In contrast, taxa like *Panomya* (Bivalvia), *Membranipora* (Bryozoa), and *Cucumaria* (Holothuroidea) were associated with specific coastal and transitional conditions (e.g., NC and BS zones). For the 18S-based community structure, environmental factors explained 16.8% of the total variation (dbRDA1). The vectors for mean temperature and mean salinity showed a strong influence on community composition, indicating that thermal and haline gradients define the structure of the broader taxonomic groups (Figure V. 13c). Taxa such as *Tergipes*, *Calliopaea* (Gastropoda), and *Pectinaria* (Polychaeta), showed a clear positive association with higher chlorophyll *a* concentrations, while *Eumida* (Polychaeta) aligned more strongly with the positive temperature vector. In contrast, taxa such as *Macoma* (Bivalvia) showed a broader distribution along the salinity gradient, reflecting varying environmental preferences among molecular ASVs.

The dbRDA plots demonstrated consistent patterns across datasets from two methodologies: morphology-based and metabarcoding-based (*cox1* and 18S rRNA). The

orientation of the temperature vector was correlated with a shift in community structure. Salinity and chlorophyll *a* concentration provided context for sample dispersion, with salinity variations indicating the influence of water mass origin on larval distribution and chlorophyll *a* representing a factor for specific larval populations, particularly in the *cox1* dataset. These environmental variables explain 32.3% of the total variation for the morphological dataset, 17.3% for *cox1,* and 22.8% for V1-V2 18S rRNA (both dbRDA axes), confirming that the observed biodiversity patterns are correlated with the physicochemical characteristics of the Northeast Atlantic shelf (Figure V. 13).

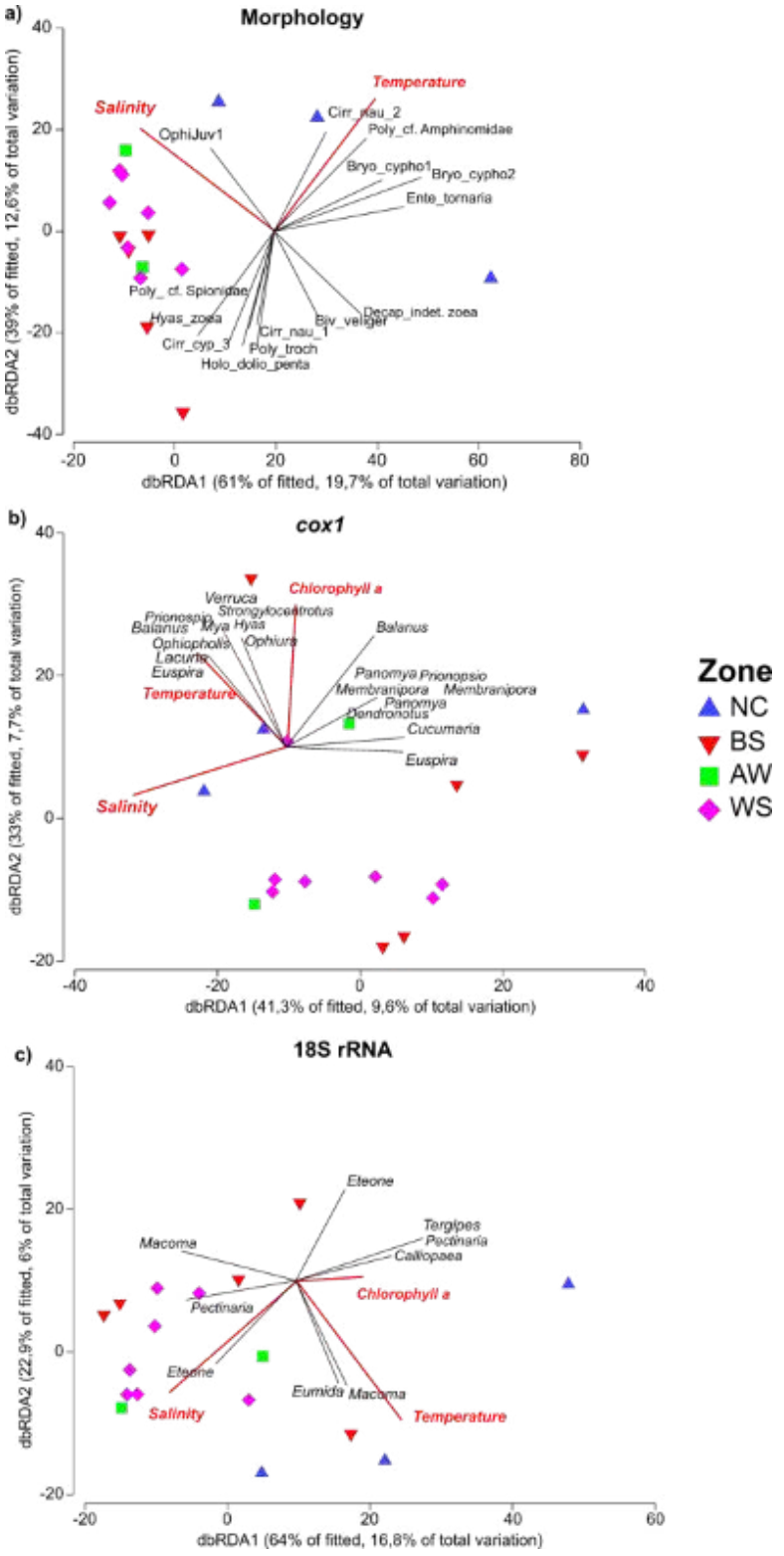

Figure V. 13 Distance-based Redundancy Analysis (dbRDA) plots illustrating the relationship between meroplankton community structure and environmental predictors between four study zones (NC – Norwegian Coast; BS – Barents Sea; AW – Atlantic Water; WS – West Spitsbergen shelf) for the morphological (a), *cox1* (b), and V1-V2 region of the 18S rRNA (c). Taxa vectors are displayed based on a Pearson correlation threshold = 0.55.

The DistLM analysis showed the relationships between the meroplankton community structure and environmental conditions (Table V. 5). Regarding the morphological dataset, mean temperature (p=0.0073), mean salinity (p=0.0014), and chlorophyll *a* concentration (p=0.0422) were all significantly related to community structure and together explained 46.66% of the variation. For the *cox1* dataset, no environmental variable was detected as a statistically significant predictor. Finally, for the 18S dataset, mean salinity was identified as the only significant individual predictor (Pseudo-F=2.4495, p=0.0492), accounting for a substantial proportion of the total variation (Table V. 5)

Table V. 5 Results of the distance-based linear model (DistLM) analysis testing the influence of environmental predictors on the meroplankton community structure between four study zones (NC – Norwegian Coast; BS – Barents Sea; AW – Atlantic Water; WS – West Spitsbergen shelf) across the 18S rRNA, *cox1*, and morphological identification datasets.

Marginal Test - Morphology				
Variable	SS(trace)	Pseudo-F	P	Prop.
Temperature	4765.1	2.9505	0.0054	0.16437
Salinity	5276.7	3.3377	0.0016	0.18202
Chlorophyll a	3485.2	2.0497	0.0453	0.12022
Marginal Test – *cox1*				
Variable	SS(trace)	Pseudo-F	P	Prop.
Temperature	2666.2	1.0294	0.3996	0.064218
Salinity	3456.6	1.3622	0.1296	0.083254
Chlorophyll a	2879.2	1.1177	0.2902	0.069349
Marginal Test – 18S rRNA				
Variable	SS(trace)	Pseudo-F	P	Prop.
Temperature	2352.1	1.3637	0.2176	0.083337
Salinity	3905	2.4086	0.0429	0.13835
Chlorophyll a	1233.5	0.68548	0.6426	0.043702

5.4 Discussion

This research confirmed the hypothesis that integrating the traditional approach to meroplankton analysis, specifically taxonomic identification under a stereomicroscope, with new molecular methods (in our case, DNA metabarcoding) significantly improves taxonomic resolution compared to morphological analysis alone. Such an integrative approach leads to more accurate conclusions regarding the meroplankton community's response to ecosystem changes and conditions on the Northeast Atlantic shelf, an area influenced by various currents and water masses. This combined analytical approach highlighted the specific strengths of each method. Molecular techniques provided much higher resolution, e.g., for groups such as

Bivalvia and Gastropoda, whereas morphological analysis showed greater insight into developmental stages, particularly in groups like Decapoda, Echinodermata, Cirripedia, and Bryozoa, which allowed us to identify specific larval cohorts (e.g., zoea, megalopa, or cyprid stages) that molecular methods alone cannot distinguish. Furthermore, the use of multiple methods revealed how meroplankton community structure interacts with environmental conditions, how the community is distributed, and which environmental factors drive these patterns. We found that the NC (Norwegian Coast zone) and BS (Barents Sea zone) assemblages exhibited the highest taxonomic diversity, effectively identifying these coastal and shelf regions as primary hotspots of meroplankton diversity along the NE Atlantic margin. In contrast, the AW (Atlantic Water zone) and WS (Western Spitsbergen shelf zone) show reduced diversity, probably due to the influence of the Arctic-origin waters.

5.4.1 From morphology to metabarcoding

Until recently, classical morphology-based approaches to zooplankton and meroplankton analysis relied on standard microscopic equipment. However, their application is increasingly constrained by the time-intensive nature of visual sorting and the growing scarcity of specialized taxonomic expertise (UNESCO, 1968). However, rapidly advancing technology may now push scientists to transition to new analytical methods, or at least integrate them into their research, across both marine (pelagic and benthic relationships) and terrestrial ecosystems (Ershova et al., 2019; Thorson, 1950; Wassmann et al., 2003). Knowing that the world is rapidly warming and that extreme changes are observed in polar regions, including the Arctic, which is the focus of our study, there is growing pressure to adopt new tools that enable higher temporal and spatial resolution in ecological and taxonomic monitoring of the effects of global warming within marine ecosystems (Hop et al., 2019; Screen & Simmonds, 2010; Shu et al., 2022; Timmermans & Marshall, 2020; Wassmann et al., 2015; Weydmann-Zwolicka et al., 2021b; Yadav et al., 2020). With this in mind, combining traditional approaches with new analytical methods can increase our ability to monitor these sensitive Arctic ecosystems, thereby revealing hidden biological and functional diversity and allowing for more accurate hypothesis testing (Ershova et al., 2019, 2021; Hop et al., 2019; Schrage et al., 2025; Walczyńska et al., 2019; Weydmann-Zwolicka et al., 2021a).

5.4.2 Traditional morphology-based meroplankton taxonomy: challenges and limitations

The traditional taxonomic-morphological approach for studying zooplankton diversity, including meroplankton assemblages, has a long history of research based on the microscopic

identification of morphological characteristics. These features enable researchers to assign a given taxon to a specific developmental stage or, in many cases, to a specific taxonomic level. This approach constitutes the foundation of ecological research on biological communities worldwide, including polar regions, providing solid knowledge regarding the structure and long-term dynamics of zooplankton and meroplankton (Głuchowska et al., 2016; Kwaśniewski et al., 2012; Scheltema, 1986; Thorson, 1950). In this study, morphological identification enabled data collection on the developmental stages of easily recognizable meroplankton groups, providing insight into community dynamics by considering not only taxonomic assignment but also population structure. This approach enabled the observation of stage-structured population data and cohort dynamics that cannot be obtained through molecular methods alone.

However, given current improvements in technology and analytical methods, including the metabarcoding approach used in this study, morphology-based research of meroplankton is increasingly limited by low taxonomic resolution. Larvae of marine benthic organisms show high morphological plasticity and closely resemble one another, making it easy to overlook cryptic or closely related species. Consequently, microscopic analysis is highly challenging when classifying larvae at the genus or species level (Ershova et al., 2019; Metaxas, 2001; Weydmann et al., 2018). That is particularly true for Bivalvia and Gastropoda veligers, the subjects of our study, where, without genetic methods, it is impossible to determine the taxonomic structure of these groups. Furthermore, the rapid development of analytical methods, which are undoubtedly faster, relatively cheaper, and provide more comprehensive data, has placed the traditional approach at a disadvantage. Challenges include a declining number of taxonomic experts, difficulties securing grants and funding for research that relies only on traditional analysis, and problems publishing such work in leading international journals (Dupérré, 2020; Kotov & Gololobova, 2016). Finally, it must be noted that this type of ecological monitoring is time-consuming, costly, and susceptible to subjective interpretation (Głuchowska et al., 2017; Hop et al., 2019; Walczyńska et al., 2019).

5.4.3 Integrating two markers to capture larval diversity

The marked differences in taxonomic diversity observed between the selected fragments of *cox1* and 18S rRNA molecular markers highlight the significant bias that can arise when analyses rely on a single genetic marker (Leray et al., 2013; Wangensteen et al., 2018). However, the taxonomic profiles obtained from these two markers differ due to a combination of biological and methodological factors, as well as the difficulties of the bioinformatics

pipeline. First, the DNA isolation process and its efficiency must be considered. The presence of diverse larval types in a sample, ranging from soft-bodied organisms to those with hard shells, influences isolation success and the suitability of the chosen protocol. Furthermore, metabarcoding is highly susceptible to biomass and copy-number biases. Unlike morphological counts, where a single small larva and a massive specimen are each recorded as individual organisms, high-throughput sequencing generates read counts that are roughly proportional to the overall DNA amount. Consequently, samples can easily be dominated by a single highly abundant or high-biomass taxon, such as microalgal blooms (e.g., *Phaeocystis* sp.), which can take over the sequencing pool and hide the detection of small, low-abundance, or hard-to-extract meroplanktonic larvae. Moreover, the subsequent PCR step can introduce amplification bias, specifically, variations in the copy number of the genetic material depending on whether the marker is mitochondrial (*cox1*) or nuclear (18S rRNA). That can skew read counts during sequencing, complicating reliable quantitative comparisons between the two markers. Access to the well-curated reference databases is also crucial, as sequencing would be meaningless without them (Wangensteen et al., 2018). These databases allow matching of the obtained genetic sequences to specific taxa, often down to the genus or species level. While *cox1* enables precise species-level identification, provided a matching record exists in the reference database (which is frequently not the case for Arctic marine invertebrates), amplification failures and database gaps often leave many sequences unassigned, particularly for less studied or harder-to-access high-latitude organisms. On the other hand, the V1-V2 region of the 18S rRNA marker offers greater universality and broader taxonomic coverage across divergent lineages due to its highly conserved nature. However, its lower sequence variation implies that even when comparing obtained sequences against well-curated reference databases, taxonomic resolution is often limited to higher levels, such as order, class, or family, with genus-level matches occurring only occasionally.

Furthermore, it must be noted that interpreting data obtained *via* metabarcoding is significantly more complex than interpreting data from traditional morphological methods. Molecular data require multiple stages of cleaning, filtering, and cross-validation, often involving the manual verification of unmatched sequences, to confidently assign a sequence to a specific taxon. This pipeline complexity is reflected in our dataset, where non-target unassigned sequences (mostly microeukaryotes such as *Phaeocystis* sp.) accounted for the vast majority of raw reads: 95.41% (15 138 501 reads) in 18S and 82.25% (9 303 583 reads) in *cox1*. After decontamination and spatial subsetting across the 17 study stations, the final retained

meroplankton dataset provided 19 388 reads for 18S and 54 694 reads for *cox1* before CSS normalization (Table SV. 1).

5.4.4 Integration of the two approaches, morphological and molecular

To overcome the difficulties and limitations associated with both morphological and molecular analyses of living organisms, not just meroplankton, an increasing number of scientists are moving towards combining these two approaches. This integration may involve DNA barcoding of individual specimens (Descôteaux et al., 2021) and DNA metabarcoding of environmental samples (Mazurkiewicz et al., 2024). Various genetic markers can be used to target different groups of organisms, depending on the study objectives and the specific information we aim to obtain. The two most widely used markers are the mitochondrial *cox1* gene for invertebrates (Leray et al., 2013) and the nuclear 18S (Leduc et al., 2019; Qihang et al., 2022; Wangensteen et al., 2018). Both markers facilitate the monitoring of complex eukaryotic communities across broad spatial and temporal scales (Ríos-Castro et al., 2021). This approach enables the detection of rare or difficult-to-identify taxa, as well as those susceptible to damage during sample collection or preservation.

The approach presented in this study combines both morphological and molecular methods. Regarding the morphological approach, the objective was to extend beyond standard taxonomic analysis, which typically covers higher-level groups such as Echinodermata or Polychaeta, and instead focus on specific larval forms or developmental stages whenever possible. That resulted in the creation of a larval atlas for the study area that could serve future researchers in their studies and in comparing results (Patuła, 2025). Meanwhile, the use of two genetic markers enabled the high-resolution taxonomic identification of the material, down to the genus level. Thereby confirming and revealing the hidden diversity of the meroplankton, particularly within groups such as Bivalvia and Gastropoda (Figure V. 6; Ershova et al., 2019; Weydmann et al., 2018).

The morphological identification approach provided insights into specific larval stages (e.g., zoea, megalopa, veliger) and other morphological groups, which are often overlooked by molecular markers (e.g., Anthozoa). In contrast, both *cox1* and 18S rRNA datasets demonstrated significantly higher taxonomic resolution at the genus level, revealing hidden diversity and confirming the presence of taxa that were morphologically identified only to the family or order level, particularly within Bivalvia, Gastropoda, and Polychaeta, among others (Figure V. 7, 10, 11; Ershova et al., 2021; Wangensteen et al., 2018). The *cox1* marker provided a detailed view, demonstrating high sensitivity in distinguishing among specific environmental

zones, despite identifying fewer taxa in groups such as Echinodermata (7 genera) than the morphological approach (15 morphotypes) (Figure V. 6; Leray & Knowlton, 2015; Ríos-Castro et al., 2021). The 18S rRNA marker showed a broader representation of diverse genera, suggesting its effectiveness in capturing the overall taxonomic structure of the meroplankton community. This spatial variation was strongly reflected in our taxonomic richness patterns across zones (Figure V.4). In the coastal and shelf zones (NC and BS), metabarcoding revealed peak richness, with V1-V2 region of 18S rRNA identifying 37 taxa in NC and *cox1* reaching 32 taxa in BS, compared to 33 and 24 taxa identified morphologically, respectively. This consistent peak in diversity confirms that coastal and shelf hydrographic regimes act as key biological hotspots for larval recruitment (Sowa et al., 2023; Søreide et al., 2022; Walkusz et al., 2009). In contrast, overall richness declined across all methods in the Atlantic Water zone (AW) and West Spitsbergen shelf zone (WS), to 14-23 taxa, respectively, highlighting how environmental conditions shape community diversity regardless of the detection method (Schauer et al., 2004; Tverberg et al., 2019). The observed differences between methods, especially the diversity between morphological and molecular datasets for Bivalvia and Gastropoda, highlight the complementarity of these approaches. Thus, the optimal methodological choice depends on the needs, e.g., meroplankton life-stage structure identification (morphology) versus deep meroplankton taxonomic resolution (molecular markers). This methodological complementarity is further shown in the spatial structuring of the communities in our multivariate ordination analyses. The nMDS analysis highlighted the complementary nature of the three approaches. Traditional morphology gave us a simple, low-dispersion, stable baseline based on general developmental stages and major morphotypes, but may be unable to resolve more variable water masses. On the other hand, metabarcoding (especially with *cox1*) can capture an extreme of micro-scale, station-specific sequence variation that leads to high intra-zonal dispersion, while the V1-V2 region of the 18S rRNA offers the best overall compromise, providing between-zonal resolution with high taxonomic diversity. Additionally, these multivariate patterns were further confirmed by PERMANOVA and similarity analyses, which revealed significant spatial variation across all methods while highlighting their distinct explanatory capacities. The V1-V2 region of the 18S rRNA marker provided the strongest ecological signal, explaining the highest proportion of community variance and revealing distinct inter-zonal separations alongside stable within-zone profiles.

In contrast, the lower intra-zonal similarity observed in the *cox1* dataset directly reflects its high resolution and sensitivity in capturing station-specific, rare, or cryptic taxa that remain undetected in other datasets. Ultimately, while morphology and V1-V2 region of the 18S rRNA

offer robust, stable baselines for regional zonation, *cox1* provides crucial complementary insights into fine-scale microecological community variation. The driving factors identified by dbRDA and DistLM further prove the distinct abiotic signals tracked by each approach. Abiotic variables explained a large share of the total variation in the morphology (32.3%) and 18S rRNA (23%) datasets, with DistLM identifying salinity as a significant individual driver of 18S rRNA community structure, in line with established evidence on larval salinity tolerance and response (Sameoto & Metaxas, 2008; Saranchova & Flyachinskaya, 2001; Vázquez & Young, 1996). These results are consistent with the expectation that 18S should largely reflect macroscale shifts in meroplankton composition aligned with water-mass zonation in the NE Atlantic (Rudels et al., 2005; Saloranta & Svendsen, 2001; Skagseth et al., 2004; Walczowski et al., 2012). Conversely, abiotic factors were less significant in the *cox1* dataset, accounting for only 16.7% of the variance, with no environmental variables identified as statistically significant by DistLM. Taken together, these findings indicate that morphology-based data, and to some extent 18S data, effectively reflect community shifts aligned with physical water-mass characteristics and environmental gradients across the NE Atlantic water masses. In contrast, variations in *cox1* community composition appear to be driven primarily by biological and ecological processes, such as dispersal limitation, spatial patchiness, and micro-habitat selection (Rumrill, 1990; Shanks, 2009; Thiébaut et al., 1992; Tremblay & Sinclair, 1990, 1992).

In summary, traditional morphological taxonomy combined with multi-marker metabarcoding of selected fragments of 18S rRNA and *cox1* genes provided significant improvements in taxonomic resolution and added ecological insights into meroplankton communities of the NE Atlantic Shelf. Morphologically based identification of larval developmental stages and cohort composition is consistent with innovative metabarcoding results that revealed hidden diversity in Bivalvia and Gastropoda. The combined multi-analytical approach successfully revealed high-resolution composition and regional zonation of the meroplankton community. Specifically, the Norwegian Coast and Barents Sea hydrographic regimes were identified as hotspots of meroplankton diversity, strongly shaped by temperature and salinity gradients. In addition, the differential signals captured by the nuclear hypervariable region V1-V2 of the 18S rRNA (macro-scale water-mass zonation) and the mitochondrial *cox1* (micro-scale station-specific community biodiversity) highlighted the need for a multi-marker usage in metabarcoding studies. The implementation of multiple, complementary analytical tools will be vital in establishing a comprehensive framework for long-term ecological monitoring/projections to assess the impacts of global warming on high-latitude marine

ecosystems (Szeligowska et al., 2020; Wassmann et al., 2015; Weydmann et al., 2014; Weydmann-Zwolicka et al., 2021a, b).

5.5 Conclusion

- A multi-marker approach that integrates metabarcoding of *cox1* and V1-V2 18S rRNA fragments with traditional morphology-based taxonomy not only greatly improves taxonomic resolution over morphology but is also a powerful way to characterize community composition and dynamics.
- Morphological identification of successive larval stages in species demonstrating complex larval development (e.g., zoea, veliger, or cypris) is essential for evaluating population cohort structure and maternal spawning timing, while molecular markers reveal hidden diversity at the genus and species level.
- The integrated multi-analytical approach successfully captured fine-scale spatial variations, conclusively identifying the Norwegian Coast (NC) and Barents Sea (BS) hydrographic regimes as primary hotspots of meroplankton diversity within the North-East Atlantic shelf ecosystem.
- The nuclear V1-V2 18S rRNA marker efficiently described meroplankton community shifts across water mass transition zones with broad taxonomic coverage, whereas the mitochondrial *cox1* marker discriminated micro-scale station-specific and uncovered hidden species richness within morphologically unresolved meroplankton groups.
- Meroplankton community patterns were primarily driven by the water temperature and salinity gradients across the study area. Combining larval stage analysis with multi-marker metabarcoding provides a strong foundation for tracking climate change in Arctic and sub-Arctic marine ecosystems.

The results presented in this chapter are being prepared for publication:
***Patuła, W**., Lubośny, M., Mazurkiewicz, M., Weydmann-Zwolicka, A., & Ronowicz, M. Integrating morphological and multi-marker metabarcoding (18S rRNA & cox1) to map meroplankton diversity along the NE Atlantic shelf (manuscript in preparation)*

Chapter VI Summary and Conclusions

6.1 Summary

This doctoral dissertation presents the results a series of analyses examining spatial, hydrographic, and interannual variability in meroplankton assemblages and assessing the influence of various environmental factors on their structure in Arctic and sub-Arctic waters of the Atlantic sector of the European Arctic.

To establish a standardized methodological framework for accurate taxonomic identification across newly collected sample sets, a comprehensive photographic atlas of meroplankton morphotypes was first developed (**Chapter II**; fulfilling **Obj. II. 1**), providing the essential taxonomic foundation for consistent morphological analyses throughout the thesis. Based on this foundation, the study combines long-term and fine-scale traditional morphology-based community approach (**Chapters III** & **IV**) with an integrative approach in its final **Chapter V**, where traditional microscopy is combined with DNA metabarcoding using two genetic markers, 18S rRNA gene (18S) and cytochrome c oxidase subunit I gene (*cox1*). This approach aims to significantly enhance taxonomic resolution, providing a baseline for climate monitoring and for assessing the current state of high-latitude marine ecosystems, such as the Arctic polar ecosystem.

Chapter III investigated the spatial and interannual variability of meroplankton assemblages in relation to environmental drivers, using a comprehensive 16-year time-series (2001-2016) dataset collected along the West Spitsbergen Current and adjacent shelf areas, based on classical microscopic identification. The results showed that meroplankton variability was determined by the physical properties of Atlantic waters masses, where transition between shelf, core and offshore waters acted as a distinct ecological barrier, whereas the core zone facilitated larval dispersal (supporting **H.1** (partially), **H.2** & **H.III. 1;** fulfilling **Obj. III. 2, Obj. III. 3**). The observed variability in community composition was not explained by the distinction between warm, intermediate, and cold years; however, the meroplankton assemblages responded strongly to specific hydrographic anomalies throughout the 16-year study period. Higher meroplankton taxonomic diversity was observed during cold years, whereas warmer years were characterized by a decline in diversity of dominant meroplankton groups, specifically Bivalvia and Echinodermata (supporting **H.III. 2**; fulfilling **Obj. III. 1, Obj. III. 4**). Given that meroplankton responded rapidly to environmental changes and fluctuations in hydrological factors, it serves as a sensitive bioindicator for the early detection of environmental shifts, such as the borealization of the Arctic. It may provide information on

the potential influx of boreal or invasive species into higher latitudes and can reveal changes in pelagic-benthic coupling processes faster than studies of long-lived adult benthic populations (supporting **H.III. 3**; fulfilling **Obj. III. 4**).

In **Chapter IV**, using the Kongsfjorden Transect as a model system, meroplankton distribution and taxonomic composition were assessed in relation to an environmental barrier, such as the halocline. Additionally, potential larval survival strategies were presented, largely shaped by physical parameters such as salinity gradients, food availability, Atlantic water inflow, water mixing, and freshwater input from melting glaciers or river runoff. The results showed that the halocline acts as a strong physical barrier, explaining approximately 30% of the total meroplankton variation and significantly differentiating community structure in the water column (supporting **H.3**, **H.IV. 1**; fulfilling **Obj. IV. 1**). Pronounced vertical stratification led to distinct taxonomic structure across water layers: Echinodermata larvae and Cirripedia cyprids were physically retained above the halocline, whereas Bivalvia veligers and Polychaeta larvae aggregated in deeper, more stable waters below the halocline. Hydrographic conditions and dynamic water mixing facilitated both the influx of larvae into the fjord and their export toward the shelf zone. In contrast, freshwater inflow and intensified stratification in the inner part of Kongsfjorden led to local larval retention. Distinct spatial patterns in taxonomic structure were observed: Echinodermata larvae, Cirripedia cyprids, and Bivalvia veligers (which were an order of magnitude more abundant above than below the halocline) were physically retained in the upper layer above the salinity gradient, whereas Polychaeta larvae aggregated primarily in deeper, more stable waters below this barrier. Overall, these findings provide key insights into the summer dynamics and vertical dynamics of meroplankton along the Kongsfjorden Transect (fulfilling **Obj. IV. 1**).

The methodological framework, integrating morphological and multi-marker genetic methods, presented in **Chapter V**, improved the detection of meroplankton diversity compared to classical morphological identification alone (supporting **H.2**, **H.4** & **H.V. 1**; fulfilling **Obj. V. 1**). The results demonstrated that while morphological identification remains essential for determining population structure, developmental stages (e.g., zoea, megalopa, nauplius, cypris), and abundance, there is a risk of misidentification due to high structural similarity among larvae. Consequently, integrating traditional morphology-based analysis with DNA metabarcoding, using the nuclear V1-V2 region of 18S rRNA and mitochondrial *cox1* genetic markers, significantly improved taxonomic resolution. The nuclear 18S rRNA marker provided highly accurate data on the taxonomic structure of soft-bodied larvae, while the mitochondrial *cox1* marker allowed for the differentiation of station-specific meroplankton taxonomic

structures at a small spatial scale. This multidisciplinary approach, combining various analytical techniques, achieved high spatial resolution, clearly identifying the Norwegian coast and the area around and north of Bear Island as key biodiversity hotspots for meroplankton on the Northeast Atlantic shelf (fulfilling **Obj. V. 2).** Given that both temperature and salinity significantly influenced changes in meroplankton structure, an integrated methodological approach forms the foundation for future monitoring of climate change and its impacts on Arctic and sub-Arctic marine ecosystems.

6.2 Conclusions and future perspectives

1) Meroplankton community structure in the West Spitsbergen Current (WSC) region is primarily shaped by Atlantic water inflow properties and bathymetry, with the shelf-offshore gradient acting as a stronger ecological barrier than latitudinal gradients;
2) Specific hydrographic extremes drive meroplankton community composition; colder years support higher taxonomic diversity, while warmer years exhibit very low overall taxonomic richness;
3) Progressive Arctic warming and Atlantification may lead to a reduction in meroplankton taxonomic richness, shifting communities toward low-diversity assemblages dominated by a few dominant taxa, such as Bivalvia and Echinodermata;
4) Due to the rapid interannual response, meroplankton community shifts may serve as sensitive early indicators of changes in marine ecosystems;
5) Continued warming alters pelagic-benthic coupling by decreasing the diversity of larval pools;
6) Halocline acts as a key structuring environmental barrier for meroplankton; salinity-driven stratification retains specific taxa within the inner fjord, whereas weaker stratification on the dynamic shelf promotes larval exchange with adjacent waters;
7) Dynamic shelf conditions facilitate larval recruitment into the fjord and export toward open waters. On the other hand, glacial runoff enhances stratification, driving local larval retention in the inner fjord (e.g., Polychaeta below the halocline, Bivalvia near glacial fronts, while Echinodermata and Cirripedia dominate the upper, dynamic layer, above the halocline);
8) Integrating traditional morphology-based taxonomic analysis with multi-marker metabarcoding provides higher taxonomic resolution: morphological data support the

identification of developmental stages, population structure, and abundance, while molecular approaches may reveal otherwise hidden diversity;

9) The V1-V2 region of the nuclear 18S rRNA gene was more effective in capturing broad-scale hydrographic boundaries. It was particularly informative for soft-bodied larvae, such as Polychaeta and Echinodermata. In contrast, the fragment of mitochondrial cytochrome c oxidase subunit I (*cox1*) revealed finer-scale, station-specific variations within shelled-bodied larvae, particularly Cirripedia and Bivalvia;

10) Integrating multi-marker metabarcoding with morphology-based taxonomic analysis may help identify areas of high meroplankton diversity (hotspots), such as the Norwegian coast and the waters surrounding Bear Island.

Based on the conclusions drawn and the methodological framework applied in this doctoral thesis, future research on meroplankton taxonomic structure and variability in the Arctic should aim to fill existing knowledge gaps. Addressing these gaps is essential to fully utilize this group of organisms as a key indicator of change in the rapidly warming Arctic. There is a need for long-term, year-round monitoring programs employing diverse techniques, such as plankton nets, sediment traps, and diver-based sampling, to capture both seasonal and interannual variability. Such programs would enable the identification of critical moments in pelagic-benthic coupling and larval spawning events, as well as the discovery of hidden diversity. Furthermore, combining and complementary use of molecular techniques (e.g., DNA metabarcoding or barcoding, utilizing the *cox1* and 18S rRNA genetic markers) with quantitative methods, such as the classical morphological approach, which reveals population structure in addition to abundance, would provide a more comprehensive picture of meroplankton community composition. Such an integrated framework would enable predictions of which benthic populations are likely to succeed in settling and colonizing new Arctic areas affected by climate change. Obtaining accurate information on meroplankton diversity in this way will enable far-reaching conclusions about the borealization of the Arctic and potential future scenarios, including larval dispersal, the influx of invasive species, shifts in distribution, and the location of meroplankton biodiversity hotspots.

References

1.Aagaard, K., Foldvik, A., Hillman, S.R. (1987). The West Spitsbergen Current: disposition and water mass transformation. Journal of Geophysical Research: Oceans, 92(C4), 3778-3784. https://doi.org/10.1029/ JC092iC04p03778

2.Abe, H., Sato-Okoshi, W., Nishitani, G., Endo, Y. (2014). Vertical distribution and migration of planktonic polychaete larvae in Onagawa. Memoirs of Museum Victoria, 71, 1-9.

3.Allen, J.D. (2008). Size-specific predation on marine invertebrate larvae. The Biological Bulletin, 214(1), 42-49.

4.Almeda, R., Møller, T., Henrik, H., Alcaraz, M., Calbet, A., Winding, B. (2009). Feeding and growth kinetics of the planktotrophic larvae of the spionid polychaete Polydora ciliata (Johnston). Journal of Experimental Marine Biology and Ecology, 382(1), 61-68. https://doi.org/10.1016/j.jembe.2009.09.017

5.Ambrose Jr, W.G., Renaud, P.E. (1995). Benthic response to water column productivity patterns: Evidence for benthic-pelagic coupling in the Northeast Water Polynya. Journal of Geophysical Research: Oceans, 100(C3), 4411-4421.

6.Ambrose, W.G., Renaud, P.E. (1997). Does a pulsed food supply to the benthos affect polychaete recruitment patterns in the Northeast Water Polynya?. Journal of Marine Systems, 10(1-4), 483-495.

7.Anderson, M.J. (2006). Distance-based tests for homogeneity of multivariate dispersions. Biometrics, 62(1), 245-253.

8.Anderson, M. (2008). PERMANOVA+ for PRIMER: guide to software and statistical methods. Primer-E Limited.

9.Anderson, M.J. (2014). Permutational multivariate analysis of variance (PERMANOVA). Wiley statsref: statistics reference online, 1-15.

10.Anderson, M.J., Gorley, R.N., Clarke, K.R. (2008). PERMANOVA+ for PRIMER user manual. Primer-E Limited., Plymouth, United Kingdom, 218.

11.Angelo, A.D., Giglio, F., Miserocchi, S., Sanchez-vidal, A., Aliani, S., Tesi, T., Viola, A., Mazzola, M., Langone, L. (2018). Multi-year particle fluxes in Kongsfjorden , Svalbard. Biogeosciences 15(17), 5343–5363.

12.Arar, E.J., Collins, G.B. (1997). Method 445.0: In vitro determination of chlorophyll *a* and pheophytin a in marine and freshwater algae by fluorescence (p. 22). Cincinnati: United States Environmental Protection Agency, Office of Research and Development, National Exposure Research Laboratory.

13.Arellano, S.M., Reitzel, A.M., Button, C.A. (2012). Variation in vertical distribution of sand dollar larvae relative to haloclines, food, and fish cues. Journal of Experimental Marine Biology and Ecology, 414, 28-37. https://doi.org/10.1016/j.jembe.2012.01.008

14.Årthun, M., Eldevik, T., Smedsrud, L.H., Skagseth, Ø., & Ingvaldsen, R.B. (2012). Quantifying the influence of Atlantic heat on Barents Sea ice variability and retreat. Journal of Climate, 25(13), 4736-4743.

15.Assmy, P., Cecilie Kvernvik, A., Hop, H., Hoppe, C.J.M., Chierici, M., David T., D., Duarte, P., Fransson, A., García, L.M., Patuła, W., Kwaśniewski, S., Maturilli, M., Pavlova, O., Tatarek, A., Wiktor, J.M., Wold, A., Wolf, K.K.E., Bailey, A. (2023). Seasonal plankton dynamics in Kongsfjorden during two years of contrasting environmental conditions. Progress in Oceanography, 213, 102996. https://doi.org/10.1016/j.pocean.2023.102996

16.Banse, K. (1986). Vertical distribution and horizontal transport of planktonic larvae of echinoderms and benthic polychaetes in an open coastal sea. Bulletin of Marine Science, 39(2), 162-175.

17.Bell, K.N.I., Brown, J.A. (1995). Active salinity choice and enhanced swimming endurance in 0 to 8-d-old larvae of diadromous gobies, including *Sicydium punctatum* (Pisces), in Dominica, West Indies. Marine Biology, 121(3), 409-417.

18.Berge, J., Daase, M., Renaud, P.E., Ambrose, W.G., Darnis, G., Last, K.S., ... & Callesen, T.A. (2015). Unexpected levels of biological activity during the polar night offer new perspectives on a warming Arctic. Current Biology, 25(19), 2555-2561.

19.Beszczyńska-Möller, A., Fahrbach, E., Schauer, U., Hansen, E. (2012). Variability in Atlantic water temperature and transport at the entrance to the Arctic Ocean, 1997 – 2010. ICES Journal of Marine Science, 69(5), 852-863. doi: 10.1093/icesjms/fss056

20.Bonicelli, J., Tyburczy, J., Tapia, F.J., Finke, G.R., Parragué, M., Dudas, S., Menge, B.A., Navarrete, S.A. (2016). Diel vertical migration and cross-shore distribution of barnacle and bivalve larvae in the central Chile inner-shelf. Journal of Experimental Marine Biology and Ecology, 485, 35-46. https://doi.org/10.1016/j.jembe.2016.08.013

21.Boyd, T.J., D'Asaro, E.A. (1994). Cooling of the west Spitsbergen current: wintertime observations west of Svalbard. Journal of Geophysical Research: Oceans, 99(C11), 22597-22618. https://doi.org/10.1029/ 94JC01824.

22.Brey, T. (1999). Growth performance and mortality in aquatic macrobenthic invertebrates. In Advances in Marine Biology (Vol. 35, pp. 153-223). Academic Press.

23.Broitman, B.R., Blanchette, C.A., Gaines, S.D. (2005). Recruitment of intertidal invertebrates and oceanographic variability at Santa Cruz Island, California. Limnology and oceanography, 50(5), 1473-1479. https://doi.org/10.4319/lo.2005.50.5.1473

24.Buchner D, Leese F. BOLDigger – a Python package to identify and organise sequences with the Barcode of Life Data systems. Metabarcoding and Metagenomics. (2020); 4:e53535. doi:10.3897/mbmg.4.53535

25.Bucklin, A., Lindeque, P.K., Rodriguez-Ezpeleta, N., Albaina, A., Lehtiniemi, M. (2016). Metabarcoding of marine zooplankton: prospects, progress and pitfalls. Journal of Plankton Research, 38(3), 393-400.

26.Callahan, B.J., McMurdie, P.J., Rosen, M.J., Han, A. W., Johnson, A.J., Holmes, S.P. (2016). DADA2: High-resolution sample inference from Illumina amplicon data. Nature Methods, 13(7), 581–583. https://doi.org/10.1038/nmeth.3869

27.Calleja, M.L., Kerhervé, P., Bourgeois, S., Kędra, M., Leynaert, A., Devred, E., Babin, M., Morata, N. (2017). Effects of increase glacier discharge on phytoplankton bloom dynamics and pelagic geochemistry in a high Arctic fjord. Progress in Oceanography, 159, 195-210. https://doi.org/10.1016/j.pocean.2017.07.005

28.Carroll, M.L., Ambrose, W.G. (2012). Benthic infaunal community variability on the northern Svalbard shelf. Polar biology, 35(8), 1259-1272. https://doi.org/10.1007/s00300-012-1171-x

29.Carstensen J., Weydmann A. (2012) Tipping points in the Arctic: Eyeballing or statistical significance? Ambio, 41(1), 34-43. doi: 10.1007/s13280-011-0223-8

30.Carstensen, J., Olszewska, A., Kwaśniewski, S. (2019). Summer mesozooplankton biomass distribution in the West Spitsbergen current (2001–2014). Frontiers in Marine Science, 6, 202.

31.Cheng, K., Shu, Q., Wang, Q., Song, Z., He, Y., Wang, S., .Pan, R., Bi, H., Qiao, F. (2025). Distinct impacts of increased Atlantic and Pacific ocean heat transport on Arctic ocean warming and sea ice decline. Journal of Geophysical Research: Oceans, 130(3), e2024JC021178.

32.Chia, F.S., Buckland, J., Young, C.M. (1984). Locomotion of marine invertebrate larvae: a review. Canadian Journal of Zoology, 62(7), 1205-1222.

33.Clarke, K.R., Gorley, R.N. (2015). PRIMER v7: user manual/tutorial. Primer-E Limited., Plymouth, UK, 296.

34.Clarke, K.R. Warwick, R.M. (2001) Change in Marine Communities: An Approach to Statistical Analyses and Interpretation. 2nd Edition, Primer-E Limited., Plymouth, 172 p.

35.Clarke, K.R., Gorley, R.N., Sommerfield, P.J., Warwick, R.M. (2014). Change in Marine Communities: An Approach to Statistical Analysis and Interpretation. 3rd Edition. Primer-E Limited., Plymouth, UK, 262.

36.Clough, L.M., Ambrose Jr, W.G., Ashjian, C.J., Piepenburg, D., Renaud, P.E., Smith, S.L. (1997). Meroplankton abundance in the Northeast Water Polynya: insights from oceanographic parameters and benthic abundance patterns. Journal of marine systems, 10(1-4), 343-357.

37.Coguiec, E., Ershova, E.A., Daase, M., Vonnahme, T.R., Wangensteen, O.S., Gradinger, R., Præbel, K., Berge, J. (2021). Seasonal variability in the zooplankton community structure in a sub-Arctic fjord as revealed by morphological and molecular approaches. Frontiers in Marine Science, 8, 705042.

38.Connor, N.J.O., Epifanio, C.E. (1985). The effect of salinity on the dispersal and recruitment of fiddler crab larvae. ournal of Crustacean Biology, 5(1), 137-145.

39.Cottier, F., Tverberg, V., Inall, M., Svendsen, H., Nilsen, F., Griffiths, C. (2005). Water mass modification in an Arctic fjord through cross-shelf exchange: The seasonal hydrography of Kongsfjorden, Svalbard. Journal of Geophysical Research: Oceans, 110(C12). https://doi.org/10.1029/2004JC002757

40.Cottier, F.R., Nilsen, F., Skogseth, R., Tverberg, V., Skardhamar, J., Svendsen, H. (2010). Arctic fjords: A review of the oceanographic environment and dominant physical processes. Geological Society, London, Special Publications, 344(1), 35-50. https://doi.org/10.1144/SP344.4

41.Cowen, R.K., Sponaugle, S. (2009). Larval dispersal and marine population connectivity. Annual review of marine science, 1, 443-466. https://doi.org/10.1146/annurev.marine.010908.163757

42.Crisp, D.J. (1974). Factors influencing the settlement of marine invertebrate larvae. Chemoreception in marine organisms, 177-265.

43.Cronin, T.W., Forward Jr., R.B. (1986). Vertical migration cycles of crab larvae and their role in larval dispersal. Bulletin of Marine Science, 39(2), 192-201.

44.Cushing, D.H. (1990). Plankton production and year-class strength in fish populations: an update of the match/mismatch hypothesis. In Advances in marine biology (Vol. 26, pp. 249-293). Academic Press.

45.Daase, M., Berge, J., Søreide, J.E., Falk-Petersen, S. (2021). Ecology of Arctic pelagic communities. Arctic ecology, 219-259.

46.Dąbrowska, A.M., Wiktor, J.M., Merchel, M., Wiktor, J.M. (2020). Planktonic Protists of the Eastern Nordic Seas and the Fram Strait: Spatial Changes Related to Hydrography During Early Summer. Frontiers in Marine Science, 7, 557. https://doi.org/10.3389/fmars.2020.00557

47.Daigle, R.M., Metaxas, A. (2011). Vertical distribution of marine invertebrate larvae in response to thermal stratification in the laboratory. Journal of experimental marine biology and ecology, 409(1-2), 89-98. https://doi.org/10.1016/j.jembe.2011.08.008

48.Dalpadado, P., Hop, H., Rønning, J., Pavlov, V., Sperfeld, E., Buchholz, F., Rey, A., Wold, A. (2016). Distribution and abundance of euphausiids and pelagic amphipods in Kongsfjorden, Isfjorden and Rijpfjorden (Svalbard) and changes in their relative importance as key prey in a warming marine ecosystem. Polar Biology, 39(10), 1765-1784. https://doi.org/10.1007/s00300-015-1874-x

49.Davis, N.M., Proctor, D.M., Holmes, S.P., Relman, D.A., Callahan, B.J. (2018). Simple statistical identification and removal of contaminant sequences in marker-gene and metagenomics data. Microbiome. 6(1):226. doi:10.1186/s40168-018-0605-2

50.Descamps, S., Aars, J., Fuglei, E., Kovacs, K.M., Lydersen, C., Pavlova, O., Pedersen, Å., Ravolainen, V., Strøm, H. (2017). Climate change impacts on wildlife in a High Arctic archipelago – Svalbard, Norway. Global Change Biology 23, 490–502. https://doi.org/ 10.1111/gcb.13381.

51.Descôteaux, R., Ershova, E., Wangensteen, O.S., Præbel, K., Renaud, P.E., Cottier, F., Bluhm, B.A. (2021). Meroplankton Diversity, Seasonality and Life-History Traits Across the Barents Sea Polar Front Revealed by High-Throughput DNA Barcoding. Frontiers in Marine Science, 8, 677732. https://doi.org/10.3389/fmars.2021.677732

52.Descôteaux, R., Huserbråten, M., Jørgensen, L.L., Renaud, P.E., Ingvaldsen, R.B., Ershova, E.A., Bluhm, B.A. (2022). Origin of marine invertebrate larvae on an Arctic inflow shelf. Marine Ecology Progress Series, 699, 1-17.

53.DeVries, M.C., Tankersley, R.A., Forward Jr., R.B., Kirby-Smith, W.W., Luettich Jr., R.A. (1994). Abundance of estuarine crab larvae is associated with tidal hydrologic variables. Marine Biology, 118(3), 403-413.

54.Dufresne, Y., Lejzerowicz, F., Perret-Gentil, L.A., Pawłowski, J., Cordier, T. (2019). SLIM: a flexible web application for the reproducible processing of environmental DNA metabarcoding data. BMC bioinformatics, 20(1), 88.

55.Dupérré, N. (2020). Old and new challenges in taxonomy: what are taxonomists up against?. Megataxa, 1(1), 59-62.

56.dos Santos, A., Miguel P Santos, A., Conway, D.V.P. (2007). Horizontal and vertical distribution of cirripede cyprid larvae in an upwelling system off the Portuguese coast. Marine Ecology Progress Series, 329, 145-155. https://doi.org/10.3354/meps329145

57.dos Santos, A., Santos, A.M.P., Conway, D.V.P., Bartilotti, C., Lourenço, P., Queiroga, H. (2008). Diel vertical migration of decapod larvae in the Portuguese coastal upwelling ecosystem : implications for offshore transport. Marine Ecology Progress Series, 359, 171-183. https://doi.org/10.3354/meps07341

58.Ebert, T.A., Russel, M.P. (1988). Latitudinal variation in size structure of the west coast purple sea urchin: A correlation with headlands 1. Limnology and Oceanography, 33(2), 286-294.

59.Edwards, M., Richardson, A.J. (2004). Impact of climate change on marine pelagic phenology and trophic mismatch. Nature, 430(7002), 881-884.

60.Eilertsen, H.C., Tande, K.S., Hegseth, E.N. (1989). Potential of herbivorous copepods for regulating the spring phytoplankton bloom in the Barents Sea. Rapports et Procès-Verbaux des Réunions du Conseil International pour l'Exploration de la Mer, 188, 154-163.

61.Epifanio, C.E., Garvine, R.W. (2001). Larval transport on the Atlantic continental shelf of North America: a review. Estuarine, coastal and shelf Science, 52(1), 51-77. https://doi.org/10.1006/ecss.2000.0727

62.Ershova, E., Descôteaux, R., Wangensteen, O., Iken, K., Hopcroft, R., Smoot, C., Grebmeier, J.M., Bluhm, B.A. (2019). Diversity and distribution of meroplanktonic larvae in the Pacific Arctic and connectivity with adult benthic invertebrate communities. Frontiers in Marine Science, 6, 490. https://doi.org/10.3389/fmars.2019.00490.

63.Ershova, E.A., Wangensteen, O.S., Descôteaux, R., Barth-Jensen, C., Præbel, K. (2021). Metabarcoding as a quantitative tool for estimating biodiversity and relative biomass of marine zooplankton. ICES Journal of Marine Science, 78(9), 3342-3355.

64.Esling, P., Lejzerowicz, F., Pawłowski, J. (2015). Accurate multiplexing and filtering for high-throughput amplicon-sequencing. Nucleic acids research, 43(5), 2513-2524. https://doi.org/10.1093/nar/gkv107

65.Esri. (2025). ArcGIS Pro (version: 3.4.0). Environmental Systems Research Institute, Redlands (CA).

66.Fabricius, K.E., Okaji, K., De'Ath, G. (2010). Three lines of evidence to link outbreaks of the crown-of-thorns seastar *Acanthaster planci* to the release of larval food limitation. Coral reefs 29, 593–605. https://doi.org/10.1007/s00338-010-0628-z

67.Fenaux, L., Strathmann, M.F., Strathmann, R.A. (1994). Five tests of food-limited growth of larvae in coastal waters by comparisons of rates of development and form of echinoplutei. Limnology and Oceanography, 39(1), 84-98. https://doi.org/10.4319/lo.1994.39.1.0084

68.Fernandes, L.D.A., Brandini, F.P., Gonçalves, R.D. (2012). Seasonal and interannual coupling between sea surface temperature, phytoplankton and meroplankton in the subtropical south-western Atlantic Ocean. Journal of Plankton Research, 34(3), 236–244.

69.Fonseca, V.G., Carvalho, G.R., Sung, W., Johnson, H.F., Power, D.M., Neill, S.P., ... & Creer, S. (2010). Second-generation environmental sequencing unmasks marine metazoan biodiversity. Nature Communications, 1(1), 98.

70.Głuchowska, M., Kwaśniewski, S., Promińska, A., Olszewska, A., Goszczko, I., Falk-Petersen, S., Hop, H., Węsławski, J.M. (2016). Zooplankton in Svalbard fjords on the Atlantic–Arctic boundary. Polar Biology 39, 1785–1802. https://doi.org/10.1007/s00300-016-1991-1

71.Głuchowska, M., Dalpadado, P., Beszczynska-Möller, A., Olszewska, A., Ingvaldsen, R.B., Kwaśniewski, S. (2017). Interannual zooplankton variability in the main pathways of the Atlantic water flow into the Arctic Ocean (Fram Strait and Barents Sea branches). ICES Journal of Marine Science, 74(7), 1921-1936.

72.Graf, G. (1989). Benthic-pelagic coupling in a deep-sea benthic community. Nature, 341(6241), 437-439.

73.Graf, G. (1992). Benthic-pelagic coupling: a benthic view, in: Barnes, M.; Ansell, A.D.; Gibson, R.N. (Ed.) (1992). Oceanography and Marine Biology: An Annual Review, 30. UCL Press: London. ISBN 1-85728-071-7. V, 627 pp.

74.Gray, J.S., Elliott, M. (2009). Ecology of marine sediments: from science to management. Oxford university press.

75.Grebmeier, J.M., Barry, J.P. (1991). The influence of oceanographic processes on pelagic-benthic coupling in polar regions: a benthic perspective. Journal of Marine Systems, 2(3-4), 495-518

76.Grebmeier, J.M., McRoy, C.P. (1989). Pelagic-benthic coupling on the shelf of the northern Bering and Chukchi Seas. Ill Benthic food supply and carbon cycling. Marine Ecology Progress Series, 53, 79-91.

77.Griffiths, J.R., Kadin, M., Nascimento, F.J., Tamelander, T., Törnroos, A., Bonaglia, S., ... & Winder, M. (2017). The importance of benthic - pelagic coupling for marine ecosystem functioning in a changing world. Global Change Biology, 23(6), 2179-2196.

78.Guillou, L., Bachar, D., Audic, S., Bass, D., Berney, C., Bittner, L., Boutte, C. (2013). The Protist Ribosomal Reference database (PR2): a catalog of unicellular eukaryote Small Sub-Unit rRNA sequences with curated taxonomy. Nucleic Acids Research. 41(D1), D597-D604.

79.Hansen, K.V. (1951). On the diurnal migration of zooplankton in relation to the discontinuity layer. ICES Journal of Marine Science, 17(3), 231-241.

80.Hargrave, B.T. (1973). Coupling carbon flow through some pelagic and benthic communities. Journal of the Fisheries Board of Canada, 30(9), 1317-1326.

81.Hart, M.W., Strathmann, R.R. (1994). Functional consequences of phenotypic plasticity in echinoid larvae. The Biological Bulletin, 186(3), 291-299.

82.Hays, G.C., Richardson, A.J., Robinson, C. (2005). Climate change and marine plankton. Trends in ecology & evolution, 20(6), 337-344.

83.Hellberg, M.E. (2009). Gene flow and isolation among populations of marine animals. Annual Review of Ecology, Evolution, and Systematics., 40(1), 291-310.

84.Heiskanen, A.S., Berg, T., Uusitalo, L., Teixeira, H., Bruhn, A., Krause-Jensen, D., ... & Borja, A. (2016). Biodiversity in marine ecosystems – European developments toward robust assessments. Frontiers in Marine Science, 3, 184.

85.Hidalgo, M., Reglero, P., Álvarez-Berastegui, D., Torres, A.P., Álvarez, I., Rodriguez, J.M., Carbonell, A., Zaragoza, N., Tor, A., Goñi, R., Mallol, S., Balbín, R., Alemany, F. (2014). Hydrographic and biological components of the seascape structure the meroplankton community in a frontal system. Marine Ecology Progress Series, 505, 65-80. https://doi.org/10.3354/meps10763

86.Hobson, K.A., Ambrose Jr, W.G., Renaud, P.E. (1995). Sources of primary production, benthic-pelagic coupling, and trophic relationships within the Northeast Water Polynya: insights from δ13C and δ15N analysis. Marine Ecology Progress Series, 128, 1-10.

87.Høeg, J.T., Deutsch, J., Chan, B.K., Semmler Le, H. (2015). "Crustacea": Cirripedia., in: Evolutionary Developmental Biology of Invertebrates 4: Ecdysozoa II: "Crustacea." pp. 153–181. https://doi.org/10.1007/978-3-7091-1853-5

88.Hop, H., Falk-Petersen, S., Svendsen, H., Kwaśniewski, S., Pavlov, V., Pavlova, O., Søreide, J.E. (2006). Physical and biological characteristics of the pelagic system across Fram Strait to Kongsfjorden. Progress in Oceanography, 71(2-4), 182-231. https://doi.org/10.1016/j.pocean.2006.09.007

89.Hop, H., Pearson, T., Hegseth, E.N., Kovacs, K.M., Wiencke, C., Kwaśniewski, S., Eiane, K., Mehlum, F., Gulliksen, B., Wlodarska-Kowalczuk, M., Lydersen, C., Weslawski, J.M., Cochrane, S., Gabrielsen, G.W., Leakey, R.J.G., Lønne, O.J., Zajaczkowski, M., Falk-Petersen, S., Kendall, M., Wängberg, S.Å., Bischof, K., Voronkov, A.Y., Kovaltchouk, N.A., Wiktor, J., Poltermann, M., Di Prisco, G., Papucci, C., Gerland, S. (2002). The marine ecosystem of Kongsfjorden, Svalbard. Polar Research. 21(1), 167–208. https://doi.org/10.1111/j.1751-8369.2002.tb00073.x

90.Hop, H., Wiencke, C. (2019). The Ecosystem of Kongsfjorden. Advances in Polar Ecology 2. https://doi.org/10.1007/978-3-319-46425-1_1 1

91.Hop, H., Wold, A., Vihtakari, M., Assmy, P., Kuklinski, P., Kwaśniewski, S., Griffith, G.P., Pavlova, O., Duarte, P., Steen, H. (2023). Tidewater glaciers as "climate refugia" for zooplankton-dependent food web in Kongsfjorden, Svalbard. Frontiers in Marine Science 10, 1161912. https://doi.org/10.3389/fmars.2023.1161912

92.Hop, H., Wold, A., Vihtakari, M., Daase, M., Kwaśniewski, S., Głuchowska, M., Lischka, S., Buchholz, F., Falk-Petersen, S. (2019). Zooplankton in Kongsfjorden (1996–2016) in Relation to Climate Change. The ecosystem of Kongsfjorden, Svalbard. https://doi.org/10.1007/978-3-319-46425-1_7

93.Ingvaldsen, R.B., Assmann, K.M., Primicerio, R., Fossheim, M., Polyakov, I.V., Dolgov, A.V. (2021). Physical manifestations and ecological implications of Arctic Atlantification. Nature Reviews Earth & Environment, 2(12), 874-889.

94.IPCC. (2021). Climate Change 2021: The Physical Science Basis. Contribution of Working Group I to the Sixth Assessment Report of the Intergovernmental Panel on Climate Change [Masson-Delmotte, V., P. Zhai, A. Pirani, S.L. Connors, C. Péan, S. Berger, N. Caud, Y. Chen, L. Goldfarb, M.I. Gomis, M. Huang, K. Leitzell, E. Lonnoy, J.B.R. Matthews, T.K. Maycock, T. Waterfield, O. Yelekçi, R. Yu, and B. Zhou (eds.)]. Cambridge University Press, Cambridge, United Kingdom and New York, NY, USA, 2391 pp. doi:10.1017/9781009157896

95.IPCC. (2022). Climate Change 2022: Impacts, Adaptation and Vulnerability. Contribution of Working Group II to the Sixth Assessment Report of the Intergovernmental Panel on Climate Change [H.-O. Pörtner, D.C. Roberts, M. Tignor, E.S. Poloczanska, K. Mintenbeck, A. Alegría, M. Craig, S. Langsdorf, S. Löschke, V. Möller, A. Okem, B. Rama (eds.)]. Cambridge University Press. Cambridge University Press, Cambridge, UK and New York, NY, USA, 3056 pp., doi:10.1017/9781009325844

96.James, M.K. (2021). Mechanisms of movement in meroplankton: A primer for dispersal. University of Plymouth.

97.Kelley, D.E., Richards, C., Layton, C. (2022). oce: an R package for Oceanographic Analysis. Journal of Open Source Software, 7(71), 3594. https://doi.org/10.21105/joss.03594

98.Kim, S., Cheon, S., Park, C., Soh, H. Y. (2025). Integrating DNA metabarcoding and morphological analysis improves marine zooplankton biodiversity assessment. Scientific Reports, 15, 12345.

99.Kinne, O. (1966). Physiological aspects of animal life in estuaries with special reference to salinity. Netherlands Journal of Sea Research, 3(2), 222-244.

100.Kirby, R.R., Beaugrand, G., Lindley, J.A. (2008). Climate-induced effects on the meroplankton and the benthic-pelagic ecology of the North Sea. Limnology and Oceanography, 53(5), 1805-1815.

101.Kotov, A.A., Gololobova, M.A. (2016). Traditional taxonomy: Quo vadis. Integrative Zoology, 11(6), 500-505.

102.Kukliński, P., Berge, J., McFadden, L., Dmoch, K., Zajączkowski, M., Nygård, H., Piwosz, K., Tatarek, A. (2013). Seasonality of occurrence and recruitment of Arctic marine benthic invertebrate larvae in relation to environmental variables. Polar Biology. 36, 549–560. https://doi.org/10.1007/s00300-012-1283-3

103.Kwaśniewski, S., Hop, H., Falk-Petersen, S., Pedersen, G. (2003). Distribution of *Calanus* species in Kongsfjorden, a glacial fjord in Svalbard. Journal of Plankton Research. 25(1), 1–20. https://doi.org/10.1093/plankt/25.1.1

104.Kwaśniewski, S., Głuchowska, M., Walkusz, W., Karnovsky, N.J., Jakubas, D., Wojczulanis-Jakubas, K., ... & Stempniewicz, L. (2012). Interannual changes in zooplankton on the West Spitsbergen Shelf in relation to hydrography and their consequences for the diet of planktivorous seabirds. ICES Journal of Marine Science, 69(5), 890-901.

105.Lalande, C., Moriceau, B., Leynaert, A., Morata, N. (2016). Spatial and temporal variability in export fluxes of biogenic matter in Kongsfjorden. Polar Biology. 39, 1725–1738. https://doi.org/10.1007/s00300-016-1903-4

106.Larink O., Westheide W. (Ed) (2011). Coastal Plankton: Photo Guide for European Seas. Second Edition; Verlag Dr. Friedrich Pfeil. ISBN: 9783899371277, 143 pp.

107.Leduc, N., Lacoursière-Roussel, A., Howland, K.L., Archambault, P., Sevellec, M., Normandeau, E., ... & Bernatchez, L. (2019). Comparing eDNA metabarcoding and species collection for documenting Arctic metazoan biodiversity. Environmental DNA, 1(4), 342-358.

108.Leray, M., Yang, J.Y., Meyer, C.P., Mills, S.C., Agudelo, N., Ranwez, V., ... & Machida, R.J. (2013). A new versatile primer set targeting a short fragment of the mitochondrial COI region for metabarcoding metazoan diversity: application for characterizing coral reef fish gut contents. Frontiers in zoology, 10(1), 34.

109.Leray, M., Knowlton, N. (2015). DNA barcoding and metabarcoding of standardized samples reveal patterns of marine benthic diversity. Proceedings of the National Academy of Sciences, 112(7), 2076-2081.

110.Lindeque, P.K., Parry, H.E., Harmer, R.A., Somerfield, P.J., Atkinson, A. (2013). Next generation sequencing reveals the hidden diversity of zooplankton assemblages. PloS one, 8(11), e81327.

111.Lindley, J.A., Williams, R. (1994). Relating plankton assemblages to environmental variables using instruments towed by ships-of- opportunity. Marine Ecology Progress Series, 107(3), 245–262.

112.Lindley, J. A., Kirby, R.R. (2007). Long-term changes in the meroplankton of the North Sea.

113.Lischka, S., Hagen, W. (2016). Seasonal dynamics of mesozooplankton in the Arctic Kongsfjord (Svalbard) during year-round observations from August 1998 to July 1999. Polar Biology. 39(10), 1859–1878. https://doi.org/10.1007/S00300-016-2005-Z

114.Luckenbach, M.W., Orth, J. (1992). Swimming velocities and behavior of blue crab (*Callinectes sapidus* Rathbun) megalopae in still and flowing water. Estuaries 15, 186–192.

115.Lydersen, C., Assmy, P., Falk-petersen, S., Kohler, J., Kovacs, K.M., Reigstad, M., Steen, H., Strøm, H., Sundfjord, A., Varpe, Ø., Walczowski, W., Marcin, J., Zajączkowski, M. (2014). The importance of tidewater glaciers for marine mammals and seabirds in Svalbard, Norway. Journal of Marine Systems, 129, 452-471. https://doi.org/10.1016/j.jmarsys.2013.09.006

116.Makatun, A., Weydmann-Zwolicka, A. (2025) Seasonal variability of meroplankton in the Gulf of Gdańsk, Southern Baltic Sea. Scientific Reports 15: 44612. https://doi.org/10.1038/s41598-025-28440-5

117.Maldonado, M., Young, C.M. (2009). Induction of settlement in merozooplankton. Marine Ecology. 339.

118.Mann, R., Campos, B.M., Luckenbach, M.W. (1991). Swimming rate and responses of larvae of three mactrid bivalves to salinity dicontinuities. Marine Ecology Progress Series, 68, 257–269. https://doi.org/10.3354/meps068257

119.Manuel, J.L., Gallager, S.M., Christopher, M., Manning, D.A., Dorl, R.K.O. (1996). Veligers from different populations of sea scallop *Placopecten magellanicus* have different vertical migration patterns. Marine Ecology Progress Series. 142, 147–163.

120.Mańko K.M., Głuchowska M., Weydmann-Zwolicka A. (2020) Footprints of Atlantification in the vertical distribution and diversity of gelatinous zooplankton in the Fram Strait (Arctic Ocean). Progress in Oceanography 189:102414. https://doi.org/10.1016/j.pocean.2020.102414.

121.Mańko M.K., Merchel M., Kwaśniewski S., Weydmann-Zwolicka A. (2022a) Atlantification alters the reproduction of jellyfish *Aglantha digitale* in the European Arctic. Limnology and Oceanography. doi: 10.1002/lno.12170.

122.Mańko M.K., Merchel M., Kwaśniewski S., Weydmann-Zwolicka A. (2022b) Oceanic fronts shape biodiversity of gelatinous zooplankton in the European Arctic. Frontiers in Marine Science, 9, 941025. doi: 10.3389/fmars.2022.941025.

123.Marshall, D.J., Keough, M.J. (2007). The evolutionary ecology of offspring size in marine invertebrates. Advances in marine biology, 53, 1-60.

124.Mazurkiewicz, M., Pawłowska, J., Angeles, I.B., Grzelak, K., Deja, K., Zaborska, A., ... & Włodarska-Kowalczuk, M. (2024). Sediment DNA metabarcoding and morphology provide complementary insight into macrofauna and meiobenthos response to environmental gradients in an Arctic glacial fjord. Marine Environmental Research, 198, 106552.

125.McMurdie, P.J., Holmes, S. (2013). phyloseq: An R package for reproducible interactive analysis and graphics of microbiome census data. PloS one, 8(4), e61217. doi:10.1371/journal.pone.0061217

126.McPherson, R., von Appen, W.-J., de Steur, L., Kanzow, T., Beszczynska-Möller, A., Renner, A.H.H. (2026). Decades of change: Warming trends and hydrographic variability of Atlantic Water as observed in the west Spitsbergen current (1997–2024). Deep Sea Research Part II: Topical Studies in Oceanography 227, 105637. https://doi.org/10.1016/j.dsr2.2026.105637

127.Metaxas, A. (2001). Behaviour in flow: Perspectives on the distribution and dispersion of meroplanktonic larvae in the water column. Canadian Journal of Fisheries and Aquatic Sciences, 58(1), 86-98. https://doi.org/10.1139/f00-159

128.Metaxas, A., Saunders, M. (2009). Quantifying the "Bio-" components in biophysical models of larval transport in marine benthic invertebrates: advances and pitfalls. The Biological Bulletin, 216(3), 257-272. https://doi.org/10.2307/25548159

129.Metaxas, A., Young, C.M. (1998a). Responses of echinoid larvae to food patches of different algal densities. Marine Biology, 130(3), 433-445. https://doi.org/10.1007/s002270050264

130.Metaxas, A., Young, C.M. (1998b). Behaviour of echinoid larvae around sharp haloclines: Effects of the salinity gradient and dietary conditioning. Marine Biology, 131(3), 443-459. https://doi.org/10.1007/s002270050337

131.Meyer, K.S., Sweetman, A.K., Kukliński, P., Leopold, P., Vogedes, D., Berge, J., Griffiths, C., Young, C.M., Renaud, P.E. (2017). Recruitment of benthic invertebrates in high Arctic fjords: Relation to temperature, depth, and season. Limnology and Oceanography, 62, 2732–2744. https://doi.org/10.1002/lno.10602

132.Michelsen, H.K., Svensen, C., Reigstad, M., Nilssen, E.M., Pedersen, T. (2017). Seasonal dynamics of meroplankton in a high-latitude fjord. Journal of Marine Systems, 168, 17-30.

133.Mileikovsky, S.A. (1971). Types of larval development in marine bottom invertebrates, their distribution and ecological significance: a re-evaluation. Marine Biology, 10(3), 193-213.

134.Morgan, C.A., Cordell, J.R., Simenstad, C.A. (1997). Sink or swim ? Copepod population maintenance in the Columbia River estuarine turbidity-maxima region. Marine Biology, 129(2), 309–317.

135.Nilsen, F., Skogseth, R., Vaardal-Lunde, J., Inall, M. (2016). A simple shelf circulation model: intrusion of Atlantic Water on the West Spitsbergen Shelf. Journal of Physical Oceanography, 46(4), 1209-1230.

136.Noda, T. (2004). Large-scale variability in recruitment of the barnacle *Semibalanus cariosus*: Its cause and effects on the population density and predator. Marine Ecology Progress Series, 278, 241-252. https://doi.org/10.3354/meps278241

137.Noufal, K.K., Najeem, S., Latha, G., Venkatesan, R. (2017). Seasonal and long term evolution of oceanographic conditions based on year-around observation in Kongsfjorden, Arctic Ocean. Polar Science, 11, 1-10. https://doi.org/10.1016/j.polar.2016.11.001

138.Oksanen, J., Simpson, G.L., Blanchet, F.G., Kindt, R., Legendre, P., Minchin, P.R., ... & Weedon, J. (2001). Vegan: community ecology package.

139.Ormańczyk, M.R., Głuchowska, M., Olszewska, A., Kwaśniewski, S. (2017). Zooplankton structure in high latitude fjords with contrasting oceanography (Hornsund and Kongsfjorden, Spitsbergen). Oceanologia, 59(1), 508–524. https://doi.org/10.1016/j.oceano.2017.06.003

140.Orvik, K. A., Niiler, P. (2002). Major pathways of Atlantic water in the northern North Atlantic and Nordic Seas toward Arctic. Geophysical Research Letters, 29: 1896, doi:10.1029/ 2002GL015002

141.Pawłowska, J., Włodarska-Kowalczuk, M., Zajączkowski, M., Nygård, H., Berge, J. (2011). Seasonal variability of meio- and macrobenthic standing stocks and diversity in an Arctic fjord (Adventfjorden , Spitsbergen). Polar Biology, 34, 833–845. https://doi.org/10.1007/s00300-010-0940-7

142.Pawłowski, J., Audic, S., Adl, S., Bass, D., Belbahri, L., Berney, C., ... & de Vargas, C. (2012). CBOL protist working group: barcoding eukaryotic richness beyond the animal, plant, and fungal kingdoms. PLoS biology, 10(11), e1001419.

143.Pearse, J.S., McClintock, J.B., Bosch, I. (1991). Reproduction of Antarctic benthic marine invertebrates: tempos, modes, and timing. American Zoologist, 65-80.

144.Pechenik, J. A., Wendt, D. E., Jarrett, J. N. (1998). Metamorphosis is not a new beginning: larval experience influences juvenile performance. Bioscience, 48(11), 901-910.

145.Peng, Y., How, C. M., Liu, D., Deconinck, D., Zhao, M. H. (2026). Zooplankton as indicators of coastal water quality: a comparative study of PlanktonScope imaging and DNA metabarcoding of seawater and mesh-screened samples. Marine Environmental Research, 215, 106000.

146.Piepenburg, D., Ambrose Jr, W.G., Brandt, A., Renaud, P.E., Ahrens, M.J., Jensen, P. (1997). Benthic community patterns reflect water column processes in the Northeast Water polynya (Greenland). Journal of Marine Systems, 10(1-4), 467-482.

147.Pineda, J., Hare, J.A., Sponaugle, S. (2007). Larval transport and dispersal in the coastal ocean and consequences for population connectivity. Oceanography 20, 22–39. https://doi.org/10.5670/oceanog.2007.27

148.Pires, A.C., Marinoni, L. (2010). DNA barcoding and traditional taxonomy unified through Integrative Taxonomy: a view that challenges the debate questioning both methodologies. Biota Neotropica, 10(2), 339-346.

149.Piwosz, K., Spich, K., Całkiewicz, J., Weydmann, A., Kubiszyn, A.M., Wiktor, J.M. (2015). Distribution of small phytoflagellates along an Arctic fjord transect. Environmental Microbiology, 17(7), 2393-2406. https://doi.org/10.1111/1462-2920.12705

150.Piwosz, K., Walkusz, W., Hapter, R., Wieczorek, P., Hop, H., Wiktor, J. (2009). Comparison of productivity and phytoplankton in a warm (Kongsfjorden) and a cold (Hornsund) Spitsbergen fjord in mid-summer 2002. Polar Biology, 32, 549–559. https://doi.org/10.1007/s00300-008-0549-2

151.Polyakov, I.V., Pnyushkov, A.V., Alkire, M.B., Ashik, I.M., Baumann, T.M., Carmack, E.C., ... & Yulin, A. (2017). Greater role for Atlantic inflows on sea-ice loss in the Eurasian Basin of the Arctic Ocean. Science, 356(6335), 285-291.

152.Polyakov, I.V., Alkire, M.B., Bluhm, B.A., Brown, K.A., Carmack, E.C., Chierici, M., ... & Wassmann, P. (2020). Borealization of the Arctic Ocean in response to anomalous advection from sub-Arctic seas. Frontiers in Marine Science, 7, 491.

153.Postel, L., Fock, H., Hagen, W. (2000). Biomass and abundance, in: ICES Zooplankton Methodology Manual. Academic Press, pp. 83–192. https://doi.org/10.13140/2.1.4985.3765

154.Patuła, W. (2025). Atlas of Meroplankton – European Arctic and West Norwegian Coast, https://www.iopan.pl/projects/HIMERO/index.php; https://doi.org/10.48457/himero

155.Patuła, W., Ronowicz, M., Kukliński, P., Weydmann-Zwolicka, A. (2026). Halocline as an environmental barrier for the larvae of Arctic marine benthic invertebrates. Progress in Oceanography, 242, 103649.

156.Paulson, J.N., Stine, O.C., Bravo, H.C., Pop, M. (2013). Differential abundance analysis for microbial marker-gene surveys. Nature Methods, 10(12), 1200–1202. doi.org

157.Qian, P.Y., Chia, F.S., (1991). Fecundity and egg size are mediated by food quality in the polychaete worm *Capitella* sp. Journal of Experimental Marine Biology and Ecology, 148(1), 11-25. https://doi.org/10.1016/0022-0981(91)90143-K

158.Qihang, L., Yuanming, C., Qianwen, S., Zaiming, W., Wei, X., Yadong, Z., ... & Dongsheng, Z. (2022). Metabarcoding survey of meroplankton communities in the South China Sea and Philippine Sea: Shedding light on inter-basin biogeography in the West Pacific. Frontiers in Marine Science, 9, 968666.

159.Queiroga, H., Blanton, J., (2005). Interactions Between Behaviour and Physical Forcing in the Control of Horizontal Transport of Decapod Crustacean Larvae. Advances in marine biology, pp. 107–214.

160.R Core Team (2025). R: A Language and Environment for Statistical Computing. R Foundation for Statistical Computing, Vienna, Austria. r-project.org.

161.Raby, D., Lagadeuc, Y., Dodson, J.J., Mingelbier, M. (1994). Relationship between feeding and vertical distribution of bivalve larvae in stratified and mixed waters. Marine Ecology Progress Series, 275-284.

162.Ramondenc, S., Eveillard, D., Metfies, K., Iversen, M. H., Nöthig, E. M., Piepenburg, D., ... & Soltwedel, T. (2025). Unveiling pelagic-benthic coupling associated with the biological carbon pump in the Fram Strait (Arctic Ocean). Nature Communications, 16(1), 840.

163.Ratnasingham, S., Hebert, P.D.N. (2007). BOLD: The Barcode of Life Data System (www.barcodinglife.org). Molecular Ecology Notes, 7(3), 355–364. doi.org

164.Renaud, P.E., Morata, N., Carroll, M.L., Denisenko, S.G., Reigstad, M. (2008). Pelagic–benthic coupling in the western Barents Sea: processes and time scales. Deep Sea Research Part II: Topical Studies in Oceanography, 55(20-21), 2372-2380.

165.Renaud, P.E., Sejr, M.K., Bluhm, B.A., Sirenko, B., Ellingsen, I.H. (2015). The future of Arctic benthos: expansion, invasion, and biodiversity. Progress in Oceanography, 139, 244-257.

166.Ríos-Castro, R., Romero, A., Aranguren, R., Pallavicini, A., Banchi, E., Novoa, B., Figueras, A. (2021). High-throughput sequencing of environmental DNA as a tool for monitoring eukaryotic communities and potential pathogens in a coastal upwelling ecosystem. Frontiers in Veterinary Science, 8, 765606.

167.Roberts Jr., M.H. (1971). Larval development of *Pagurus longicarpus* Say reared in the laboratory. III. Behavioral responses to salinity discontinuities. The Biological Bulletin, 140(3), 489-501. https://doi.org/10.2307/1540283

168.Ronowicz, M., Balazy, P., Chełchowski, M., Kukliński, P., Patuła, W., Sowa, A., Søreide, J.E., Weydmann-Zwolicka, A. (2024). Factors shaping pelagic-benthic coupling in the process of settlement in an Arctic fjord. Scientific Reports, 14(1), 23688. https://doi.org/10.1038/s41598-024-74062-8

169.Rowe, G.T., Clifford, C.H., Smith Jr, K.L., Hamilton, P.L. (1975). Benthic nutrient regeneration and its coupling to primary productivity in coastal waters. Nature, 255(5505), 215-217.

170.Różycki, O. (1992). Occurrence of Gastropoda and Bivalvia in Hornsund Fiord (West Spitsbergen , Svalbard). Polish Polar Research, 13(1), 41–51.

171.Rudels, B., Björk, G., Nilsson, J., Winsor, P., Lake, I., Nohr, C. (2005). The interaction between waters from the Arctic Ocean and the Nordic Seas north of Fram Strait and along the East Greenland Current: results from the Arctic Ocean-02 Oden expedition. Journal of Marine Systems, 55(1-2), 1-30.

172.Rumrill, S.S. (1990). Natural mortality of marine invertebrate larvae. Ophelia 32(1–2), 163–198. https://doi.org/10.1080/00785236.1990.10422030

173.Salis, R., Sunde, J., Gubonin, N., Franzén, M., Forsman, A. (2024). Performance of DNA metabarcoding, standard barcoding and morphological approaches in the identification of insect biodiversity. Molecular Ecology Resources, 24(8), e14018.

174.Saloranta, T.M., Svendsen. (2001). Across the Arctic front west of Spitsbergen: high resolution CTD sections from. Polar Research, 20, 177–184. https://doi.org/10.3402/ polar.v20i2.6515.

175.Sameoto, J.A., Metaxas, A. (2008). Can salinity-induced mortality explain larval vertical distribution with respect to a halocline? The Biological Bulletin, 214(3), 329-338. https://doi.org/10.2307/25470674

176.Saranchova, O.L., Flyachinskaya, L.P. (2001). The Influence of Salinity on Early Ontogeny of the Mussel *Mytilus edulis* and the Starfish *Asterias rubens* from the White Sea. Russian Journal of Marine Biology, 27(2), 87-93.

177.Schauer, U., Fahrbach, E., Osterhus, S., Rohardt, G. (2004). Arctic warming through the Fram Strait: oceanic heat transport from 3 years of measurements. Journal of Geophysical Research, 109(C06026), doi:10.1029/2003JC001823.

178.Scheltema, R. (1986). On dispersal and planktonic larvae of benthic invertebrates: an eclectic overview and summary of problems. Bulletin of marine science, 39(2), 290-322.

179.Schrage, K.R., Weston, J.N., Kraberg, A., McPherson, R., Von Appen, W.J., Lago, L., Meyer-Kaiser, K.S. (2025). Diversity, drivers, and dispersal of high Arctic meroplanktonic communities. Progress in Oceanography, 103656.

180.Screen, J.A., Simmonds, I. (2010). The central role of diminishing sea ice in recent Arctic temperature amplification. Nature, 464(7293), 1334-1337.

181.Shanks, A.L. (1995). Orientated swimming by megalopae of several eastern North Pacific crab species and its potential role in their onshore migration. Journal of Experimental Marine Biology and Ecology, 186(1), 1-16.

182.Shanks, A.L. (2009). Pelagic larval duration and dispersal distance revisited. The biological bulletin, 216(3), 373-385.

183.Short, J., Metaxas, A., Daigle, R. M. (2013). Predation of larval benthic invertebrates in St George's Bay, Nova Scotia. Journal of the Marine Biological Association of the United Kingdom, 93(3), 591-599.

184.Shu, Q., Wang, Q., Årthun, M., Wang, S., Song, Z., Zhang, M., Qiao, F. (2022). Arctic Ocean Amplification in a warming climate in CMIP6 models. Science advances, 8(30), eabn9755.

185.Sinniger, F., Pawłowski, J., Harii, S., Gooday, A. J., Yamamoto, H., Chevaldonné, P., ... & Creer, S. (2016). Worldwide analysis of sedimentary DNA reveals major gaps in taxonomic knowledge of deep-sea benthos. Frontiers in Marine Science, 3, 92.

186.Skagseth, Ø., Orvik, K.A., Furevik, T. (2004). Coherent variability of the Norwegian Atlantic Slope Current derived from TOPEX/ERS altimeter data. Geophysical Research Letters, 31: L14304, doi:10.1029/2004GL020057

187.Søreide, J.E., Dmoch, K., Błachowiak-Samolyk, K., Trudnowska, E., Daase, M. (2022). Seasonal mesozooplankton patterns and timing of life history events in high-arctic fjord environments. Frontiers in Marine Science, 9, 933461. https://doi.org/10.3389/fmars.2022.933461

188.Sowa, A., Kukliński, P., Weydmann-Zwolicka, A., Bałazy, P., Chełchowski, M., Søreide, J.E., Ronowicz, M. (2023). Factors shaping epibionts recruitment in the high Arctic (Isfjorden, Spitsbergen): A year-round investigation using experimental plates. Estuarine, Coastal and Shelf Science, 283, 108281. https://doi.org/10.1016/j.ecss.2023.108281

189.Stempniewicz, L., Weydmann-Zwolicka, A., Strzelewicz, A., Goc, M., Głuchowska, M., Kidawa, D., Walczowski, W., Węsławski, J.M., Zwolicki, A. (2021). Advection of Atlantic water masses influences seabird community foraging in a high-Arctic fjord. Progress in Oceanography 193, 102549. https://doi.org/10.1016/j.pocean.2021.102549.

190.Strathmann, M. F. (1987). Reproduction and Development of Marine Invertebrates of the Northern Pacific Coast: Data and Methods for the Study of Eggs, Embryos, and Larvae. University of Washington Press. http://www.jstor.org/stable/j.ctvcwnh8b

191.Strzelewicz, A., Przyborska, A., Walczowski, W. (2022). Increased presence of Atlantic Water on the shelf south-west of Spitsbergen with implications for the Arctic fjord Hornsund. Progress in Oceanography 200, 102714. https://doi.org/10.1016/j.pocean.2021.102714

192.Stübner, E.I., Søreide, J.E., Reigstad, M., Marquardt, M., Błachowiak-Samolyk, K. (2016). Year-round meroplankton dynamics in high-Arctic Svalbard. Journal of Plankton Research, 38(3), 522-536. https://doi.org/10.1093/planktfbv124

193.Svendsen, H., Beszczyńska-Möller, A., Hagen, J.O., Lefauconnier, B., Tverberg, V., Gerland, S., Børre Ørbæk, J., Bischof, K., Papucci, C., Zajączkowski, M., Azzolini, R., Bruland, O., Wiencke, C. (2002). The physical environment of Kongsfjorden–Krossfjorden, an Arctic fjord system in Svalbard. Polar research, 21(1), 133-166. https://doi.org/10.3402/polar.v21i1.6479

194.Szeligowska, M., Trudnowska, E., Boehnke, R., Błachowiak-Samołyk, K. (2022). Dark plumes of glacial meltwater affect vertical distribution of zooplankton in the Arctic. Scientific reports, 12(1), 17953. https://doi.org/10.1038/s41598-022-22475-8

195.Szeligowska, M., Trudnowska, E., Boehnke, R., Dąbrowska, A.M., Wiktor, J.M., Sagan, S., Błachowiak-Samołyk, K. (2020). Spatial Patterns of Particles and Plankton in the Warming Arctic Fjord (Isfjorden, West Spitsbergen) in Seven Consecutive Mid-Summers (2013–2019). Frontiers in Marine Science, 7, 584. https://doi.org/10.3389/fmars.2020.00584

196.Tagliabue, A., Furfaro, G., Pallavicini, A., Martino, F., Zane, L., Sattin, E., ... & Turon, X. (2026). Comparative Multi-Marker Environmental DNA Metabarcoding of Marine Metazoan Communities: Water vs. Sediment. Molecular Ecology Resources, 26(3), e70126.

197.Thiébaut, E., Dauvin, J., Lagadeuc, Y. (1992). Transport of *Owenia fusiformis* larvae (Annelida: Polychaeta) in the Bay of Seine. I. Vertical distribution in relation to water column stratification and ontogenic vertical migration. Marine Ecology Progress Series, 29-39.

198.Thompson, P.A., Harrison, P.J. (1992). Effects of monospecific algal diets of varying biochemical composition on the growth and survival of Pacific oyster (*Crassostrea gigas*) larvae. Marine Biology, 113(4), 645-654.

199.Thorson, G. (1950). Reproductive and larval ecology of marine bottom invertebrates. Biological reviews, 25(1), 1-45.

200.Timmermans, M.L., Marshall, J. (2020). Understanding Arctic Ocean circulation: A review of ocean dynamics in a changing climate. Journal of Geophysical Research: Oceans, 125(4), e2018JC014378.

201.Toonen, R.J., Grosberg, R.K. (2011). Causes of chaos: spatial and temporal genetic heterogeneity in the intertidal anomuran crab *Petrolisthes cinctipes*. Phylogeography and population genetics in Crustacea, 2011, 75-107.

202.Tremblay, M.J., Sinclair, M. (1992). Planktonic sea scallop larvae (*Placopecten magellanicus*) in the Georges Bank region: broadscale distribution in relation to physical oceanography. Canadian Journal of Fisheries and Aquatic Sciences, 49(8), 1597-1615.

203.Tremblay, M.J., Sinclair, M. (1990). Sea scallop larvae *Placopecten magellanicus* on Georges Bank: vertical distribution in relation to water column stratification and food. Marine Ecology Progress Series, 1-15.

204.Trudnowska, E., Szczucka, J., Hoppe, L., Boehnke, R., Hop, H., Blachowiak-Samolyk, K. (2012). Multidimensional zooplankton observations on the northern West Spitsbergen Shelf. Journal of Marine Systems, 98, 18-25.

205.Trudnowska, E., Stemmann, L., Błachowiak-Samołyk, K., Kwaśniewski, S. (2020). Taxonomic and size structures of zooplankton communities in the fjords along the Atlantic water passage to the Arctic. Journal of Marine Systems, 204, 103306. https://doi.org/10.1016/j.jmarsys.2020.103306

206.Tsubouchi, T., Våge, K., Hansen, B., Larsen, K.M.H., Østerhus, S., Johnson, C., ... & Valdimarsson, H. (2021). Increased ocean heat transport into the Nordic Seas and Arctic Ocean over the period 1993–2016. Nature Climate Change, 11(1), 21-26.

207.Tverberg, V., Skogseth, R., Cottier, F., Sundfjord, A., Walczowski, W., Inall, M.E., Falck, E., Pavlova, O., Nilsen, F. (2019). The Kongsfjorden Transect: Seasonal and Inter-annual Variability in Hydrography, in: The Ecosystem of Kongsfjorden, Svalbard. pp. 49–104. https://doi.org/10.1007/978-3-319-46425-1_3

208.UNESCO. (1968). Monographs on Oceanographic Methodology 2. Zooplankton Sampling. Geneve: UNESCO, Imprimeries Populaires, 174.

209.Vázquez, E., Young, C.M. (1996). Responses of compound ascidian larvae to haloclines. Marine Ecology Progress Series, 133, 179-190. https://doi.org/10.3354/meps133179

210.Walczowski, W., Piechura, J., Goszczko, I., Wieczorek, P. (2012). Changes in Atlantic water properties: an important factor in the European Arctic marine climate. ICES Journal of Marine Science, 69(5), 864-869.

211.Walczyńska, K.S., Søreide, J.E., Weydmann-Zwolicka, A., Ronowicz, M., Gabrielsen, T.M. (2019). DNA barcoding of Cirripedia larvae reveals new knowledge on their biology in Arctic coastal ecosystems. Hydrobiologia 837, 149–159. https://doi.org/10.1007/s10750-019-3967-y

212.Walkusz, W., Kwaśniewski, S., Falk-petersen, S., Hop, H., Tverberg, V., Wieczorek, P., Weslawski, J.M. (2009). Seasonal and spatial changes in the zooplankton community of Kongsfjorden, Svalbard. Polar Research, 28(2), 254-281. https://doi.org/10.1111/j.1751-8369.2009.00107.x

213.Wang, Z., Li, Z., Zeng, J., Liang, S., Zhang, P., Tang, F., ... & Ma, X. (2020). Spatial and temporal variations of Arctic sea ice from 2002 to 2017. Earth and Space Science, 7(9), e2020EA001278.

214.Wangensteen, O.S., Palacín, C., Guardiola, M., Turon, X. (2018). DNA metabarcoding of littoral hard-bottom communities: high diversity and database gaps revealed by two molecular markers. PeerJ, 6, e4705.

215.Wares, J.P., Cunningham, C. W. (2001). Phylogeography and historical ecology of the North Atlantic intertidal. Evolution, 55(12), 2455-2469.

216.Wassmann, P., Olli, K., Riser, C.W., Svensen, C. (2003). Ecosystem function, biodiversity and vertical flux regulation in the twilight zone. In Marine science frontiers for Europe (pp. 279-287). Berlin, Heidelberg: Springer Berlin Heidelberg.

217.Wassmann, P., Kosobokova, K.N., Slagstad, D., Drinkwater, K.F., Hopcroft, R.R., Moore, S.E., ... & Berge, J. (2015). The contiguous domains of Arctic Ocean advection: trails of life and death. Progress in Oceanography, 139, 42-65.

218.Weydmann, A., Carstensen, J., Goszczko, I., Dmoch, K., Olszewska, A., Kwaśniewski, S. (2014). Shift towards the dominance of boreal species in the Arctic: inter-annual and spatial zooplankton variability in the West Spitsbergen Current. Marine Ecology Progress Series, 501, 41-52.

219.Weydmann, A., Walczowski, W., Carstensen, J., Kwaśniewski, S. (2018). Warming of Subarctic waters accelerates development of a key marine zooplankton *Calanus finmarchicus*. Global Change Biology 24: 172-183. doi: 10.1111/gcb.13864.

220.Weydmann-Zwolicka, A., Bałazy, P., Kukliński, P., Søreide, J.E., Patuła, W., Ronowicz, M. (2021a). Meroplankton seasonal dynamics in the high Arctic fjord: Comparison of different sampling methods. Progress in Oceanography 190, 102484. https://doi.org/10.1016/j.pocean.2020.102484

221.Weydmann-Zwolicka, A., Prątnicka, P., Łącka, M., Majaneva, S., Cottier, F., Berge, J. (2021b). Zooplankton and sediment fluxes in two contrasting fjords reveal Atlantification of the Arctic. Science of the Total Environment, 773, 145599. https://doi.org/10.1016/j.scitotenv.2021.145599

222.Weydmann-Zwolicka A., Dąbrowska A.M., Mioduchowska M., Zwolicki A. (2024) Comparison of DNA metabarcoding and microscopy in analysing planktonic protists from the European Arctic. Marine Biodiversity 54: 44. https://doi.org/10.1007/s12526-024-01436-6

223.Węsławski, J.M., Wiktor Jr, J., Kotwicki, L. (2010). Increase in biodiversity in the arctic rocky littoral, Sorkappland, Svalbard, after 20 years of climate warming. Marine Biodiversity, 40(2), 123-130.

224.White, W.J., Carr, M.H., Caselle, J.E., Washburn, L., Woodson, C.B., Palumbi, S.R., Carlson, P.M., Warner, R.R., Menge, B.A., Barth, J.A., Blanchette, C.A., Raimondi, P.T., Milligan, K. (2019). Connectivity, Dispersal, and Recruitment. Oceanography 32(3), 50–59.

225.Wickham, H. (2016). ggplot2: Elegant Graphics for Data Analysis. Springer-Verlag New York. ISBN 978-3-319-24277-4.

226.Wickham, H., Bryan, J. (2023). readxl: Read Excel Files. R package version 1.4.3. r-project.org

227.Wickham, H., Averick, M., Bryan, J., Chang, W., McGowan, L. D. A., François, R., ... & Yutani, H. (2019). Welcome to the Tidyverse. Journal of open source software, 4(43), 1686.

228.Wickham, H., François, R., Henry, L., Müller, K., Vaughan, D. (2023). dplyr: A grammar of data manipulation.

229.Wickham, H., Vaughan, D., Girlich, M. (2024a). *tidyr: Tidy Messy Data.*

230.Wickham, H., Henry, L., Pedersen, T.L., Luciani, T., Decorde, M., Lise, V. (2024b). svglite: An 'SVG' Graphics Device. R package version 2.1.3. r-project.org

231.Wiencke, C., Hop, H. (2016). Ecosystem Kongsfjorden: new views after more than a decade of research. Polar Biol. 39, 1679–1687. https://doi.org/10.1007/s00300-016-2032-9

232.Williams, R. (1985). Vertical distribution of *Calanus finmarchicus* and *C. helgolandicus* in relation to the development of the seasonal thermocline in the Celtic Sea. Mar. Biol. 86(2), 145–149.

233.Willis, K., Cottier, F., Kwaśniewski, S., Wold, A., Falk-Petersen, S. (2006). The influence of advection on zooplankton community composition in an Arctic fjord (Kongsfjorden, Svalbard). Journal of marine systems, 61(1-2), 39-54. https://doi.org/10.1016/j.jmarsys.2005.11.013

234.Włodarska-Kowalczuk, M., Szymelfenig, M., Zajiczkowski, M. (2007). Dynamic sedimentary environments of an Arctic glacier-fed river estuary (Adventfjorden, Svalbard). II: Meio-and macrobenthic fauna. Estuarine, Coastal and Shelf Science, 74(1-2), 274-284.

235.Włodarska-Kowalczuk, M., Górska, B., Deja, K., Morata, N. (2016). Do benthic meiofaunal and macrofaunal communities respond to seasonality in pelagial processes in an Arctic fjord (Kongsfjorden, Spitsbergen)? Polar Biology, 39, 2115–2129. https://doi.org/10.1007/s00300-016-1982-2

236.Yadav, J., Kumar, A., Mohan, R. (2020). Dramatic decline of Arctic sea ice linked to global warming. Natural Hazards, 103(2), 2617-2621

237.Young, C.M. (1987). Abundance and distribution of pelagic larvae as influenced by predation, behaviour, and hydrographic factors. In Reproduction of marine Invertebrates, 385-463

238.Young, C.M. (1995). Behavior and locomotion during the dispersal phase of larval life. Ecology of marine invertebrate larvae, 249-277

239.Young, C.M., Sewell, M.A., Rice, M.E. (Ed.) (2002). Atlas of marine invertebrate larvae. Academic Press: San Diego. ISBN 0-12-773141-5. XIV, 626 pp.

List of Tables

Table II. 1 Photographic documentation of meroplankton morphotypes collected in the European Arctic and along the West Norwegian coast. Photo credit: W. Patuła. 48

Table III. 1 Classification of years (2001–2016) into thermal phase based on temperature anomalies, Hovmöller diagram analysis, and horizontal distributions of temperature (Figure III. 2a; Figure III. 3, Figure III. 4). 65

Table III. 2 Results of Distance-based linear model analysis (DistLM) for meroplankton taxonomic community and abundance with environmental factors; significant results are marked in red. 75

Table III. 3 Results of a four-factor multivariate PERMANOVA for meroplankton descriptor sets with 9999 permutations; significant results are marked in red. 78

Table IV. 1 Sampling details: water depths used for chlorophyll a concentration analysis and depth layers for meroplankton samples (AH – Above the halocline; BH – Below the halocline). 98

Table IV. 2 Classification of meroplankton: taxonomic assignment and larval morphotypes. Note that different morphotypes within a certain taxa may potentially correspond to different genera/species. 100

Table IV. 3 Results of Distance-based linear model analysis (DistLM) for meroplankton morphotype structure and abundance with environmental factors; Significant results are marked in red. 106

Table V. 1 Sampling details: water depths used for chlorophyll a concentration analysis and depth layers for meroplankton samples. 123

Table V. 2 Classification of meroplankton: Taxonomic assignment and morphotypes. Note that different morphotypes within a certain taxa may potentially correspond to different genera/species. 125

Table V. 3 Results of the Global tests for Permutational Multivariate Analysis of Variance (PERMANOVA) for meroplankton community structure between four study zones (NC – Norwegian Coast; BS – Barents Sea; AW – Atlantic Water; WS – West Spitsbergen shelf) across the 18S rRNA, cox1, and morphological identification datasets. 152

Table V. 4 Results of pair-wise PERMANOVA tests and average similarity analysis for meroplankton community structure between four study zones (NC – Norwegian Coast; BS – Barents Sea; AW – Atlantic Water; WS – West Spitsbergen shelf) across morphology, cox1, and 18S rRNA datasets. Pair-wise comparisons indicate significant differences between specific zone combinations ($p<0.05$), while the similarity matrix provides the average Bray-Curtis similarity [%] within and between zones. 153

Table V. 5 Results of the distance-based linear model (DistLM) analysis testing the influence of environmental predictors on the meroplankton community structure between four study zones (NC – Norwegian Coast; BS – Barents Sea; AW – Atlantic Water; WS – West Spitsbergen shelf) across the 18S rRNA, cox1, and morphological identification datasets. 157

List of Figures

Figure I. 1 Examples of marine benthic invertebrate larvae of major meroplankton groups. Photo credit: W. Patuła..... 31

Figure I. 2 Diagram of a generalized life cycle of a benthic invertebrates with a meroplanktonic larval stage (modified based on Maldonado & Young, 2009). 32

Figure III. 1 Study area and sampling locations (2001-2016) shown along the sections arranged from south to north. Stations are differentiated by spatial zones – shelf, core, offshore – represented by distinct colours, while marker shapes distinguish sections..... 62

Figure III. 2 Horizontal distributions of temperature averaged in the upper 200 m layer for the period 2001-2016 in the Atlantic water inflow region in the eastern Nordic Seas 68

Figure III. 3 Horizontal distributions of salinity averaged in the upper 200 m layer for the period 2001-2016 in the Atlantic water inflow region in the eastern Nordic Seas. 69

Figure III. 4 Normalized anomalies of temperature and salinity in the 200-0 m layer (y axis) at five sections (H; K; N; S; EB2) in 2001-2016. Anomalies are calculated relative to the long-term mean for each section (2001-2016)..... 71

Figure III. 5 Hovmöller diagrams of normalized temperature anomalies at five sections from the West Spitsbergen shelf towards the deep basin. Anomalies were calculated relative to the long-term mean (2001-2016) for each respective section (except S with the mean of 2004-2016 over the measurement period). Black dots indicate zooplankton sampling stations. The x-axis represents longitude, while the y-axis shows the temporal evolution from 2001 to 2016. Note the different zonal extent of each section. 73

Figure III. 6 The dbRDA ordination plot based on meroplankton community composition and abundance with environmental variables (red vectors). Colours indicate spatial zones, and symbols indicate sections. Data were fourth-root transformed, and resemblance was calculated using Bray-Curtis similarity. 76

Figure III. 7 Non-metric multidimensional scaling (nMDS) ordination plots based on bootstrap averages for meroplankton community composition. Plots were constructed from a Bray-Curtis similarity matrix of fourth-root transformed abundance data. Groupings are visualized across four main factors: (a) Spatial Zone, (b) Section, (c) Thermal phase, and (d) Year of sampling. Each point represents the group centroid, surrounded by 50% bootstrap probability regions

(based on n=25 bootstraps per group). 2D stress for each ordination is indicated within the individual panels. 79

Figure III. 8 Relative abundance and taxonomic composition of meroplankton community (2001-2016). Stacked bar charts show the annual relative abundance of individual taxa, illustrating long-term shifts in the meroplankton community structure across the study area. Years are marked with thermal phase (warm in red, intermediate in grey, cold in blue). 80

Figure III. 9 Interannual and spatial variability of meroplankton taxonomic composition across the West Spitsbergen shelf-to-basin gradient (Spatial Zones; 2001-2016). Panels show the relative abundance [%] of taxa within three distinct zones: shelf, core (Atlantic Water core), and offshore. The "All Years" panel provides a multi-year synthesis of the community structure for each spatial zone. Years are marked with thermal phase (warm in red, intermediate in grey, and cold in blue). 82

Figure III. 10 Interannual variability of meroplankton diversity indices (H′, J′) and taxonomic richness (S) across the West Spitsbergen shelf-to-basin gradient (Spatial Zones; 2001-2016). Boxplots represent the median and interquartile range; whiskers indicate the minimum and maximum values. Individual points represent all sampled data, providing a visualization of data distribution and sample size. Taxonomic richness (S) is displayed on the secondary y-axis. The "All Years" panel provides a multi-year synthesis for the entire study period. Years are marked with thermal phase (warm in red, intermediate in grey, cold in blue). 84

Figure III. 11 Interannual and spatial variability of meroplankton taxonomic composition across five sampling sections (2001-2016). Panels show the annual relative abundance [%] of individual taxa within five distinct sections: H, K, N, S, and EB2. The "All Years" panel provides a multi-year synthesis of the community structure for each section. Years are marked with thermal phase (warm in red, intermediate in grey, cold in blue). 86

Figure III. 12 Interannual variability of meroplankton diversity indices (H′, J′) and taxonomic richness (S) across five sampling sections (2001-2016). Boxplots represent the median and interquartile range; whiskers indicate the minimum and maximum values. Individual points represent all sampled data, providing a visualization of data distribution within each section. Taxonomic richness (S) is displayed on the secondary y-axis. The "All Years" panel provides a multi-year synthesis for each section over the entire study period. 88

Figure IV. 1 Study area: Svalbard Archipelago on a global map (a), with schematic ocean current circulation including their origin (based on Assmy et al. (2023)) (b), and sampling sites along the Kongsfjorden Transect, with stations divided into fjord and shelf regions based on Hop and Wiencke (2019) (c). 96

Figure IV. 2 Vertical profiles of temperature (red lines) and salinity (blue lines) with a marked halocline layer (green horizontal dashed lines) at each sampling station along the studied Kongsfjorden Transect. Note the station KB5, located in the innermost part of the fjord, has a different depth scale. 102

Figure IV. 3 The abundance of main meroplankton taxa at the sampling sites above (left) and below (right) the halocline along the Kongsfjorden Transect: from the shelf to the inner fjord. The right axis indicates the abundance of Bivalvia veligers (red dots). Note the different scales for abundance in both plots. 104

Figure IV. 4 A dendrogram based on CLUSTER analysis, on meroplankton morphotype structure and abundance at the sampling sites above and below the halocline along the studied transect. The solid lines represent significant splits according to the SIMPROF tests (type 1: analyse: samples – permute within: variables; no. of permutations: 9999; sig. level: 5%, resemblance measure: S17 Bray-Curtis similarity). 105

Figure IV. 5 The dbRDA ordination plot of all meroplankton morphotypes (blue arrows), environmental variables (red arrows), and samples. 107

Figure IV. 6 Meroplankton morphotype distribution at the sampling sites above and below the halocline for Echinodermata (A; B), Polychaeta (C; D), and the remaining taxa (E; F) along the Kongsfjorden Transect. Note that Figure IV. 6 (E; F) does not include Bivalvia veligers, which are presented in Figure IV. 3. Values above each bar represents the total abundance [ind m^{-3}] of larvae at the given station within the represented groups. 110

Figure V. 1 Study area: meroplankton sampling sites along the North-east Atlantic Shelf with stations divided into four study zones (NC – Norwegian Coast; BS – Barents Sea; AW – Atlantic Water, and WS – West Spitsbergen shelf), with schematic ocean current circulation including their origin (based on Assmy et al. (2023)). 122

Figure V. 2 Vertical hydrographic profiles of temperature and salinity across the 17 sampling stations. Red lines represent temperature ([°C], lower axis) and blue lines represent salinity (upper axis) plotted against depth [m] on the reversed y-axis. Note that the depth scale (y-axis) varies between stations to match local maximum sampling depths. 134

Figure V. 3 Vertical depth profiles of CTD fluorescence ([mg m^{-3}], dark green line] and discrete in situ chlorophyll a concentrations ([mg m^{-3}], red points) across 17 sampling stations plotted against depth [m] on the reversed y-axis. Note that the depth scale (y-axis) varies between stations to match local maximum sampling depths. 136

Figure V. 4 Regional and local meroplankton taxonomic richness across four study zones evaluated by morphological identification and metabarcoding (cox1 and V1-V2 region of the 18S rRNA markers). Bars represent cumulative regional taxa richness per zone (Total), while overlaid black points with error bars indicate mean station-level richness ± standard deviation (Mean ± SD). Zone abbreviations (NC – Norwegian Coast; BS – Barents Sea; AW – Atlantic Water; WS – West Spitsbergen shelf). 138

Figure V. 5 Relative abundance of major meroplankton groups across four study zones (NC – Norwegian Coast; BS – Barents Sea; AW – Atlantic Water; WS – West Spitsbergen shelf). The panels compare the taxonomic composition derived from morphological identification (a), cox1 (b), and V1-V2 region of the 18S rRNA (c), highlighting the differences in resolution and dominant taxa captured by each method. 140

Figure V. 6 Comparison of taxonomic resolution and relative abundance [%] of Echinodermata larvae across three methodological approaches within four study zones (NC – Norwegian Coast; BS – Barents Sea; AW – Atlantic Water; and WS – West Spitsbergen shelf). 143

Figure V. 7 Comparison of taxonomic resolution and relative abundance [%] of Polychaeta larvae across three methodological approaches within four study zones (NC – Norwegian Coast; BS – Barents Sea; AW – Atlantic Water; and WS – West Spitsbergen shelf). 144

Figure V. 8 Comparison of taxonomic resolution and relative abundance [%] of Cirripedia larvae across three methodological approaches within four study zones (NC – Norwegian Coast; BS – Barents Sea; AW – Atlantic Water; and WS – West Spitsbergen shelf). 145

Figure V. 9 Comparison of taxonomic resolution and relative abundance [%] of Decapoda larvae across three methodological approaches within four study zones (NC – Norwegian Coast; BS – Barents Sea; AW – Atlantic Water; and WS – West Spitsbergen shelf). 146

Figure V. 10 Comparison of taxonomic resolution and relative abundance [%] of Bivalvia larvae across three methodological approaches within four study zones (NC – Norwegian Coast; BS – Barents Sea; AW – Atlantic Water; and WS – West Spitsbergen shelf). 147

Figure V. 11 Comparison of taxonomic resolution and relative abundance [%] of Gastropoda larvae across three methodological approaches within four study zones (NC – Norwegian Coast; BS – Barents Sea; AW – Atlantic Water; and WS – West Spitsbergen shelf). 148

Figure V. 12 Non-metric Multidimensional Scaling (NMDS) analysis visualizing the similarity between four study zones (NC – Norwegian Coast; BS – Barents Sea; AW – Atlantic Water; WS – West Spitsbergen shelf) based on morphological data (a), cox1 genetic marker (b), and V1-V2 region of the 18S rRNA genetic marker (c). 150

Figure V. 13 Distance-based Redundancy Analysis (dbRDA) plots illustrating the relationship between meroplankton community structure and environmental predictors between four study zones (NC – Norwegian Coast; BS – Barents Sea; AW – Atlantic Water; WS – West Spitsbergen shelf) for the morphological (a), cox1 (b), and V1-V2 region of the 18S rRNA (c). Taxa vectors are displayed based on a Pearson correlation threshold = 0.55. 156

Supplementary materials

Chapter III

Supplementary Tables

Table SIII.1 Results of Kruskal-Wallis tests comparing Taxonomic Richness (S) across different zones within each sampling year (2001–2016). Yellow highlighting indicates years with statistically significant differences ($p < 0.05$), which were subsequently subjected to post-hoc pairwise comparisons.

	Year	Index	n	statistic	df	p	method
1	2001	S	14	7.8080062	2	0.0202	Kruskal-Wallis
2	2002	S	12	3.3470085	2	0.1880	Kruskal-Wallis
3	2003	S	9	5.9487179	2	0.0511	Kruskal-Wallis
4	2004	S	15	4.2949438	2	0.1170	Kruskal-Wallis
5	2005	S	17	7.2986440	2	0.0260	Kruskal-Wallis
6	2006	S	11	4.5338785	2	0.1040	Kruskal-Wallis
7	2007	S	9	4.2550725	2	0.1190	Kruskal-Wallis
8	2008	S	9	4.0792793	2	0.1300	Kruskal-Wallis
9	2009	S	15	6.6020221	2	0.0368	Kruskal-Wallis
10	2010	S	11	6.1111111	2	0.0471	Kruskal-Wallis
11	2011	S	6	1.7647059	2	0.4140	Kruskal-Wallis
12	2012	S	19	5.6241145	2	0.0601	Kruskal-Wallis
13	2013	S	14	6.0557760	2	0.0484	Kruskal-Wallis
14	2014	S	19	1.3648174	2	0.5050	Kruskal-Wallis
15	2015	S	13	4.4166667	2	0.1100	Kruskal-Wallis
16	2016	S	17	0.7474708	2	0.6880	Kruskal-Wallis

Table SIII.2 Results of Dunn's post-hoc pairwise comparisons for Taxonomic richness (S) between zones for 2001, 2005, 2009, 2010, and 2013. Yellow highlighting indicates nominal (unadjusted) p-values < 0.05. Statistically significant differences maintained after Bonferroni correction (p.adj < 0.05) are highlighted in red and marked with an asterisk (*).

	Year	Index	group1	group2	n1	n2	statistic	p	p.adj	p.adj.signif
1	2001	S	shelf	core	3	5	-0.2908007	0.77120375	1.00000000	ns
2	2001	S	shelf	offshore	3	6	-2.3102898	0.02087211	0.06261634	ns
3	2001	S	core	offshore	5	6	-2.3471184	0.01891924	0.05675772	ns
4	2005	S	shelf	core	4	6	-0.9302377	0.35224803	1.00000000	ns
5	2005	S	shelf	offshore	4	7	-2.5690365	0.01019817	0.03059452	*
6	2005	S	core	offshore	6	7	-1.8149824	0.06952662	0.20857985	ns
7	2009	S	shelf	core	4	4	-1.0427445	0.29706662	0.89119987	ns
8	2009	S	shelf	offshore	4	7	-2.5272661	0.01149544	0.03448631	*
9	2009	S	core	offshore	4	7	-1.3508916	0.17673016	0.53019049	ns
10	2010	S	shelf	core	3	2	-1.8333333	0.06675302	0.20025905	ns
11	2010	S	shelf	offshore	3	6	-2.3668232	0.01794150	0.05382451	ns
12	2010	S	core	offshore	2	6	0.0000000	1.00000000	1.00000000	ns
13	2013	S	shelf	core	3	4	0.6959507	0.48645967	1.00000000	ns
14	2013	S	shelf	offshore	3	7	-1.3881903	0.16507911	0.49523732	ns
15	2013	S	core	offshore	4	7	-2.3763935	0.01748281	0.05244842	ns

Table SIII.3 Results of Kruskal-Wallis tests comparing Taxonomic Richness (S) across all years (2001–2016) within different zones. Significant differences (p < 0.05) would be indicated in yellow; however, no such differences were observed (p > 0.05 in all cases).

	Zone	Index	n	statistic	df	p	method
1	shelf	S	46	16.88302	15	0.326	Kruskal-Wallis
2	core	S	70	17.73452	15	0.277	Kruskal-Wallis
3	offshore	S	94	15.04284	15	0.448	Kruskal-Wallis

Table SIII.4 Results of Kruskal-Wallis tests comparing the Shannon-Wiener diversity index (H') across different zones within each sampling year (2001–2016). Yellow highlighting indicates years with statistically significant differences ($p < 0.05$), which were subsequently subjected to post-hoc pairwise comparisons.

	Year	Index	n	statistic	df	p	method
1	2001	Shannon	14	6.9562408	2	0.0309	Kruskal-Wallis
2	2002	Shannon	12	0.1179487	2	0.9430	Kruskal-Wallis
3	2003	Shannon	9	3.3111111	2	0.1910	Kruskal-Wallis
4	2004	Shannon	15	4.4522727	2	0.1080	Kruskal-Wallis
5	2005	Shannon	17	6.1591970	2	0.0460	Kruskal-Wallis
6	2006	Shannon	11	2.2909091	2	0.3180	Kruskal-Wallis
7	2007	Shannon	9	6.1111111	2	0.0471	Kruskal-Wallis
8	2008	Shannon	9	1.8000000	2	0.4070	Kruskal-Wallis
9	2009	Shannon	15	3.0304114	2	0.2200	Kruskal-Wallis
10	2010	Shannon	11	1.3484848	2	0.5100	Kruskal-Wallis
11	2011	Shannon	6	2.3809524	2	0.3040	Kruskal-Wallis
12	2012	Shannon	19	3.4984962	2	0.1740	Kruskal-Wallis
13	2013	Shannon	14	0.8639456	2	0.6490	Kruskal-Wallis
14	2014	Shannon	19	0.6302632	2	0.7300	Kruskal-Wallis
15	2015	Shannon	13	0.1208791	2	0.9410	Kruskal-Wallis
16	2016	Shannon	17	1.5873016	2	0.4520	Kruskal-Wallis

Table SIII.5 Results of Dunn's post-hoc pairwise comparisons for Shannon diversity (H') between zones in 2001, 2005, and 2007. Yellow highlighting indicates nominal (unadjusted) p-values < 0.05. Statistically significant differences after Bonferroni correction ($p.adj < 0.05$) are highlighted in red and marked with an asterisk (*).

	Year	Index	group1	group2	n1	n2	statistic	p	p.adj	p.adj.signif
1	2001	Shannon	shelf	core	3	5	0.5242994	0.60007031	1.00000000	ns
2	2001	Shannon	shelf	offshore	3	6	-1.6357634	0.10188911	0.30566733	ns
3	2001	Shannon	core	offshore	5	6	-2.5424890	0.01100661	0.03301982	*
4	2005	Shannon	shelf	core	4	6	2.4798535	0.01314364	0.03943092	*
5	2005	Shannon	shelf	offshore	4	7	1.4556074	0.14550117	0.43650352	ns
6	2005	Shannon	core	offshore	6	7	-1.2373326	0.21596364	0.64789093	ns
7	2007	Shannon	shelf	core	2	3	-0.3333333	0.73888268	1.00000000	ns
8	2007	Shannon	shelf	offshore	2	4	-2.1081851	0.03501498	0.10504494	ns
9	2007	Shannon	core	offshore	3	4	-1.9920477	0.04636583	0.13909748	ns

Table SIII.6 Results of Kruskal-Wallis tests comparing Pielou's evenness (J′) for different zones within each sampling year (2001–2016). Yellow highlighting indicates years with statistically significant differences ($p < 0.05$), which were subsequently subjected to post-hoc pairwise comparisons.

	Year	Index	n	statistic	df	p	method
1	2001	Pielou	14	1.7179487	2	0.4240	Kruskal-Wallis
2	2002	Pielou	12	3.9576923	2	0.1380	Kruskal-Wallis
3	2003	Pielou	9	0.5000000	2	0.7790	Kruskal-Wallis
4	2004	Pielou	15	2.8484848	2	0.2410	Kruskal-Wallis
5	2005	Pielou	17	8.4852941	2	0.0144	Kruskal-Wallis
6	2006	Pielou	11	1.1454545	2	0.5640	Kruskal-Wallis
7	2007	Pielou	9	3.1000000	2	0.2120	Kruskal-Wallis
8	2008	Pielou	9	4.1250000	2	0.1270	Kruskal-Wallis
9	2009	Pielou	15	4.5527473	2	0.1030	Kruskal-Wallis
10	2010	Pielou	11	1.6145455	2	0.4460	Kruskal-Wallis
11	2011	Pielou	6	3.6000000	2	0.1650	Kruskal-Wallis
12	2012	Pielou	19	0.1716792	2	0.9180	Kruskal-Wallis
13	2013	Pielou	14	4.0495868	2	0.1320	Kruskal-Wallis
14	2014	Pielou	19	0.1388889	2	0.9330	Kruskal-Wallis
15	2015	Pielou	13	5.2197802	2	0.0735	Kruskal-Wallis
16	2016	Pielou	17	0.7783613	2	0.6780	Kruskal-Wallis

Table SIII.7 Results of Dunn's post-hoc pairwise comparisons for Pielou's evenness (J′) between zones for 2005. Yellow highlighting indicates nominal (unadjusted) p-values < 0.05. Statistically significant differences after Bonferroni correction (p.adj < 0.05) are highlighted in red and marked with an asterisk (*).

	Index	group1	group2	n1	n2	statistic	p	p.adj	p.adj.signif
1	Pielou	shelf	core	4	6	2.5489329	0.010805309	0.03241593	*
2	Pielou	shelf	offshore	4	6	2.6573981	0.007874639	0.02362392	*
3	Pielou	core	offshore	6	6	0.1212678	0.903478914	1.00000000	ns

Table SIII.8 Results of Kruskal-Wallis tests comparing the Shannon-Wiener diversity index (H′) across all years (2001-2016) within different zones. Yellow highlighting indicates zones with statistically significant differences ($p < 0.05$), which were subsequently subjected to post-hoc pairwise comparisons.

	Zone	Index	n	statistic	df	p	method
1	shelf	Shannon	46	20.70583	15	0.1460	Kruskal-Wallis
2	core	Shannon	70	16.35990	15	0.3590	Kruskal-Wallis
3	offshore	Shannon	94	27.67465	15	0.0237	Kruskal-Wallis

Table SIII.9 Results of Dunn's post-hoc pairwise comparisons for Shannon diversity (H′) between years (2001-2016) within the offshore zone. Yellow highlighting indicates nominal (unadjusted) p-values < 0.05. Statistically significant differences maintained after Bonferroni correction (p.adj < 0.05) are highlighted in red and marked with an asterisk (*).

	Index	group1	group2	n1	n2	statistic	p	p.adj	p.adj.signif
1	Shannon	2001	2002	6	5	2.409299	0.015983	1.0000000	ns
2	Shannon	2001	2003	6	3	0.268511	0.788306	1.0000000	ns
3	Shannon	2001	2004	6	7	0.212311	0.831864	1.0000000	ns
4	Shannon	2001	2005	6	7	2.429786	0.015108	1.0000000	ns
5	Shannon	2001	2006	6	5	1.426159	0.153822	1.0000000	ns
6	Shannon	2001	2007	6	4	2.092179	0.036422	1.0000000	ns
7	Shannon	2001	2008	6	5	1.049896	0.293766	1.0000000	ns
8	Shannon	2001	2009	6	7	1.387101	0.165411	1.0000000	ns
9	Shannon	2001	2010	6	6	2.530076	0.011404	1.0000000	ns
10	Shannon	2001	2011	6	3	0.822855	0.410591	1.0000000	ns
11	Shannon	2001	2012	6	8	0.990897	0.321736	1.0000000	ns
12	Shannon	2001	2013	6	7	3.06672	0.002164	0.259705	ns
13	Shannon	2001	2014	6	8	2.662238	0.007762	0.931476	ns
14	Shannon	2001	2015	6	6	2.78998	0.005271	0.632536	ns
15	Shannon	2001	2016	6	7	1.84475	0.065074	1.0000000	ns
16	Shannon	2002	2003	5	3	-1.7377	0.082264	1.0000000	ns
17	Shannon	2002	2004	5	7	-2.28982	0.022032	1.0000000	ns
18	Shannon	2002	2005	5	7	-0.1829	0.854877	1.0000000	ns
19	Shannon	2002	2006	5	5	-0.94128	0.346559	1.0000000	ns
20	Shannon	2002	2007	5	4	-0.1616	0.871618	1.0000000	ns
21	Shannon	2002	2008	5	5	-1.30153	0.193077	1.0000000	ns
22	Shannon	2002	2009	5	7	-1.1736	0.240554	1.0000000	ns
23	Shannon	2002	2010	5	6	0.003034	0.997579	1.0000000	ns
24	Shannon	2002	2011	5	3	-1.20096	0.229767	1.0000000	ns
25	Shannon	2002	2012	5	8	-1.62038	0.105151	1.0000000	ns
26	Shannon	2002	2013	5	7	0.422282	0.672819	1.0000000	ns
27	Shannon	2002	2014	5	8	-0.03706	0.970433	1.0000000	ns
28	Shannon	2002	2015	5	6	0.250842	0.801936	1.0000000	ns
29	Shannon	2002	2016	5	7	-0.73877	0.460047	1.0000000	ns
30	Shannon	2003	2004	3	7	-0.10397	0.917193	1.0000000	ns
31	Shannon	2003	2005	3	7	1.683815	0.092217	1.0000000	ns
32	Shannon	2003	2006	3	5	0.922525	0.356255	1.0000000	ns
33	Shannon	2003	2007	3	4	1.519622	0.128606	1.0000000	ns
34	Shannon	2003	2008	3	5	0.610544	0.541502	1.0000000	ns
35	Shannon	2003	2009	3	7	0.843175	0.39913	1.0000000	ns
36	Shannon	2003	2010	3	6	1.797288	0.07229	1.0000000	ns
37	Shannon	2003	2011	3	3	0.480076	0.631173	1.0000000	ns
38	Shannon	2003	2012	3	8	0.510012	0.610043	1.0000000	ns
39	Shannon	2003	2013	3	7	2.197328	0.027997	1.0000000	ns
40	Shannon	2003	2014	3	8	1.843281	0.065288	1.0000000	ns
41	Shannon	2003	2015	3	6	2.009498	0.044484	1.0000000	ns
42	Shannon	2003	2016	3	7	1.212144	0.225457	1.0000000	ns
43	Shannon	2004	2005	7	7	2.308021	0.020998	1.0000000	ns

44	Shannon	2004	2006	7	5	1.273121	0.202975	1.0000000	ns
45	Shannon	2004	2007	7	4	1.966193	0.049276	1.0000000	ns
46	Shannon	2004	2008	7	5	0.884012	0.37669	1.0000000	ns
47	Shannon	2004	2009	7	7	1.22276	0.22142	1.0000000	ns
48	Shannon	2004	2010	7	6	2.413273	0.01581	1.0000000	ns
49	Shannon	2004	2011	7	3	0.672004	0.501581	1.0000000	ns
50	Shannon	2004	2012	7	8	0.805771	0.420375	1.0000000	ns
51	Shannon	2004	2013	7	7	2.970963	0.002969	0.3562410	ns
52	Shannon	2004	2014	7	8	2.549813	0.010778	1.0000000	ns
53	Shannon	2004	2015	7	6	2.682987	0.007297	0.8756130	ns
54	Shannon	2004	2016	7	7	1.699096	0.089301	1.0000000	ns
55	Shannon	2005	2006	7	5	-0.8338	0.404391	1.0000000	ns
56	Shannon	2005	2007	7	4	-0.00209	0.998329	1.0000000	ns
57	Shannon	2005	2008	7	5	-1.22291	0.221362	1.0000000	ns
58	Shannon	2005	2009	7	7	-1.08526	0.277806	1.0000000	ns
59	Shannon	2005	2010	7	6	0.195798	0.844768	1.0000000	ns
60	Shannon	2005	2011	7	3	-1.11578	0.264516	1.0000000	ns
61	Shannon	2005	2012	7	8	-1.57794	0.114579	1.0000000	ns
62	Shannon	2005	2013	7	7	0.662942	0.507368	1.0000000	ns
63	Shannon	2005	2014	7	8	0.166099	0.868079	1.0000000	ns
64	Shannon	2005	2015	7	6	0.465512	0.641565	1.0000000	ns
65	Shannon	2005	2016	7	7	-0.60892	0.542574	1.0000000	ns
66	Shannon	2006	2007	5	4	0.725848	0.467932	1.0000000	ns
67	Shannon	2006	2008	5	5	-0.36024	0.718664	1.0000000	ns
68	Shannon	2006	2009	5	7	-0.1569	0.875325	1.0000000	ns
69	Shannon	2006	2010	5	6	0.986174	0.324048	1.0000000	ns
70	Shannon	2006	2011	5	3	-0.38578	0.699657	1.0000000	ns
71	Shannon	2006	2012	5	8	-0.57612	0.564536	1.0000000	ns
72	Shannon	2006	2013	5	7	1.438985	0.150155	1.0000000	ns
73	Shannon	2006	2014	5	8	1.007197	0.31384	1.0000000	ns
74	Shannon	2006	2015	5	6	1.233982	0.21721	1.0000000	ns
75	Shannon	2006	2016	5	7	0.277935	0.781062	1.0000000	ns
76	Shannon	2007	2008	4	5	-1.06549	0.286654	1.0000000	ns
77	Shannon	2007	2009	4	7	-0.92342	0.355789	1.0000000	ns
78	Shannon	2007	2010	4	6	0.17079	0.864389	1.0000000	ns
79	Shannon	2007	2011	4	3	-1.0064	0.314224	1.0000000	ns
80	Shannon	2007	2012	4	8	-1.33146	0.183037	1.0000000	ns
81	Shannon	2007	2013	4	7	0.567453	0.570407	1.0000000	ns
82	Shannon	2007	2014	4	8	0.142523	0.886667	1.0000000	ns
83	Shannon	2007	2015	4	6	0.403254	0.686761	1.0000000	ns
84	Shannon	2007	2016	4	7	-0.5172	0.605017	1.0000000	ns
85	Shannon	2008	2009	5	7	0.23221	0.816375	1.0000000	ns
86	Shannon	2008	2010	5	6	1.362437	0.17306	1.0000000	ns
87	Shannon	2008	2011	5	3	-0.0738	0.941168	1.0000000	ns
88	Shannon	2008	2012	5	8	-0.17646	0.859932	1.0000000	ns
89	Shannon	2008	2013	5	7	1.828094	0.067535	1.0000000	ns
90	Shannon	2008	2014	5	8	1.406852	0.159471	1.0000000	ns
91	Shannon	2008	2015	5	6	1.610245	0.107344	1.0000000	ns

92	Shannon	2008	2016	5	7	0.667044	0.504744	1.0000000	ns
93	Shannon	2009	2010	7	6	1.238483	0.215537	1.0000000	ns
94	Shannon	2009	2011	7	3	-0.27514	0.783208	1.0000000	ns
95	Shannon	2009	2012	7	8	-0.45709	0.647607	1.0000000	ns
96	Shannon	2009	2013	7	7	1.748203	0.080429	1.0000000	ns
97	Shannon	2009	2014	7	8	1.286952	0.198111	1.0000000	ns
98	Shannon	2009	2015	7	6	1.508197	0.131504	1.0000000	ns
99	Shannon	2009	2016	7	7	0.476336	0.633835	1.0000000	ns
100	Shannon	2010	2011	6	3	-1.24294	0.213888	1.0000000	ns
101	Shannon	2010	2012	6	8	-1.71387	0.086553	1.0000000	ns
102	Shannon	2010	2013	6	7	0.441136	0.659115	1.0000000	ns
103	Shannon	2010	2014	6	8	-0.04253	0.966078	1.0000000	ns
104	Shannon	2010	2015	6	6	0.259903	0.794939	1.0000000	ns
105	Shannon	2010	2016	6	7	-0.78083	0.4349	1.0000000	ns
106	Shannon	2011	2012	3	8	-0.06898	0.945004	1.0000000	ns
107	Shannon	2011	2013	3	7	1.629294	0.103251	1.0000000	ns
108	Shannon	2011	2014	3	8	1.264287	0.206127	1.0000000	ns
109	Shannon	2011	2015	3	6	1.455154	0.145627	1.0000000	ns
110	Shannon	2011	2016	3	7	0.64411	0.519504	1.0000000	ns
111	Shannon	2012	2013	8	7	2.262626	0.023659	1.0000000	ns
112	Shannon	2012	2014	8	8	1.805255	0.071035	1.0000000	ns
113	Shannon	2012	2015	8	6	1.991717	0.046402	1.0000000	ns
114	Shannon	2012	2016	8	7	0.949048	0.342596	1.0000000	ns
115	Shannon	2013	2014	7	8	-0.51858	0.60405	1.0000000	ns
116	Shannon	2013	2015	7	6	-0.17142	0.863892	1.0000000	ns
117	Shannon	2013	2016	7	7	-1.27187	0.20342	1.0000000	ns
118	Shannon	2014	2015	8	6	0.320376	0.748683	1.0000000	ns
119	Shannon	2014	2016	8	7	-0.79499	0.426617	1.0000000	ns
120	Shannon	2015	2016	6	7	-1.05055	0.293466	1.0000000	ns

Table SIII.10 Results of Kruskal-Wallis tests comparing Pielou's evenness (J′) across all years (2001-2016) within different zones. Yellow highlighting indicates zones with statistically significant differences ($p < 0.05$), which were subsequently subjected to post-hoc pairwise comparisons.

	Zone	Index	n	statistic	df	p	method
1	shelf	Pielou	46	16.23043	15	0.3670	Kruskal-Wallis
2	core	Pielou	70	21.57986	15	0.1190	Kruskal-Wallis
3	offshore	Pielou	94	25.20628	15	0.0472	Kruskal-Wallis

Table SIII.11 Results of Dunn's post-hoc pairwise comparisons for Pielou's evenness (J′) between all years (2001-2016) within the offshore zone. Yellow highlighting indicates nominal (unadjusted) p-values < 0.05. Statistically significant differences maintained after Bonferroni correction (p.adj < 0.05) are highlighted in red and marked with an asterisk (*).

	Index	group1	group2	n1	n2	statistic	p	p.adj	p.adj.signif
1	Pielou	2001	2002	4	5	1.888027	0.059022	1.0000000	ns
2	Pielou	2001	2003	4	2	0.993657	0.32039	1.0000000	ns
3	Pielou	2001	2004	4	4	0.733306	0.463372	1.0000000	ns
4	Pielou	2001	2005	4	6	1.663565	0.096199	1.0000000	ns
5	Pielou	2001	2006	4	4	1.123363	0.261283	1.0000000	ns
6	Pielou	2001	2007	4	4	2.293532	0.021817	1.0000000	ns
7	Pielou	2001	2008	4	4	0.499272	0.617588	1.0000000	ns
8	Pielou	2001	2009	4	5	1.381483	0.167130	1.0000000	ns
9	Pielou	2001	2010	4	5	2.407728	0.016052	1.0000000	ns
10	Pielou	2001	2011	4	2	0.9427	0.345834	1.0000000	ns
11	Pielou	2001	2012	4	7	0.573313	0.566433	1.0000000	ns
12	Pielou	2001	2013	4	6	3.218884	0.001287	0.1544290	ns
13	Pielou	2001	2014	4	8	1.333179	0.182473	1.0000000	ns
14	Pielou	2001	2015	4	6	2.700444	0.006925	0.8309630	ns
15	Pielou	2001	2016	4	6	0.900148	0.368041	1.0000000	ns
16	Pielou	2002	2003	5	2	-0.48526	0.627494	1.0000000	ns
17	Pielou	2002	2004	5	4	-1.11505	0.264827	1.0000000	ns
18	Pielou	2002	2005	5	6	-0.31823	0.750307	1.0000000	ns
19	Pielou	2002	2006	5	4	-0.7039	0.481496	1.0000000	ns
20	Pielou	2002	2007	5	4	0.529569	0.596411	1.0000000	ns
21	Pielou	2002	2008	5	4	-1.36175	0.173278	1.0000000	ns
22	Pielou	2002	2009	5	5	-0.53727	0.591081	1.0000000	ns
23	Pielou	2002	2010	5	5	0.551226	0.581479	1.0000000	ns
24	Pielou	2002	2011	5	2	-0.538	0.590576	1.0000000	ns
25	Pielou	2002	2012	5	7	-1.54931	0.121307	1.0000000	ns
26	Pielou	2002	2013	5	6	1.339742	0.180329	1.0000000	ns
27	Pielou	2002	2014	5	8	-0.78957	0.429779	1.0000000	ns
28	Pielou	2002	2015	5	6	0.787083	0.431233	1.0000000	ns
29	Pielou	2002	2016	5	6	-1.13204	0.257618	1.0000000	ns
30	Pielou	2003	2004	2	4	-0.39491	0.692906	1.0000000	ns
31	Pielou	2003	2005	2	6	0.261231	0.793914	1.0000000	ns
32	Pielou	2003	2006	2	4	-0.07644	0.939073	1.0000000	ns

33	Pielou	2003	2007	2	4	0.879004	0.379399	1.0000000	ns
34	Pielou	2003	2008	2	4	-0.586	0.557874	1.0000000	ns
35	Pielou	2003	2009	2	5	0.079118	0.936939	1.0000000	ns
36	Pielou	2003	2010	2	5	0.901944	0.367087	1.0000000	ns
37	Pielou	2003	2011	2	2	-0.04413	0.964801	1.0000000	ns
38	Pielou	2003	2012	2	7	-0.62509	0.531910	1.0000000	ns
39	Pielou	2003	2013	2	6	1.490819	0.136009	1.0000000	ns
40	Pielou	2003	2014	2	8	-0.05582	0.955485	1.0000000	ns
41	Pielou	2003	2015	2	6	1.080956	0.279717	1.0000000	ns
42	Pielou	2003	2016	2	6	-0.3423	0.732123	1.0000000	ns
43	Pielou	2004	2005	4	6	0.860268	0.389641	1.0000000	ns
44	Pielou	2004	2006	4	4	0.390057	0.696495	1.0000000	ns
45	Pielou	2004	2007	4	4	1.560226	0.118706	1.0000000	ns
46	Pielou	2004	2008	4	4	-0.23403	0.814959	1.0000000	ns
47	Pielou	2004	2009	4	5	0.60851	0.542849	1.0000000	ns
48	Pielou	2004	2010	4	5	1.634755	0.102100	1.0000000	ns
49	Pielou	2004	2011	4	2	0.343958	0.730878	1.0000000	ns
50	Pielou	2004	2012	4	7	-0.25397	0.799520	1.0000000	ns
51	Pielou	2004	2013	4	6	2.415587	0.015710	1.0000000	ns
52	Pielou	2004	2014	4	8	0.48643	0.626662	1.0000000	ns
53	Pielou	2004	2015	4	6	1.897148	0.057808	1.0000000	ns
54	Pielou	2004	2016	4	6	0.096851	0.922844	1.0000000	ns
55	Pielou	2005	2006	6	4	-0.43298	0.665027	1.0000000	ns
56	Pielou	2005	2007	6	4	0.848874	0.395951	1.0000000	ns
57	Pielou	2005	2008	6	4	-1.11664	0.264149	1.0000000	ns
58	Pielou	2005	2009	6	5	-0.24293	0.808062	1.0000000	ns
59	Pielou	2005	2010	6	5	0.893971	0.371337	1.0000000	ns
60	Pielou	2005	2011	6	2	-0.31528	0.75255	1.0000000	ns
61	Pielou	2005	2012	6	7	-1.28424	0.199059	1.0000000	ns
62	Pielou	2005	2013	6	6	1.7389	0.082052	1.0000000	ns
63	Pielou	2005	2014	6	8	-0.47666	0.633606	1.0000000	ns
64	Pielou	2005	2015	6	6	1.159267	0.246348	1.0000000	ns
65	Pielou	2005	2016	6	6	-0.85353	0.393368	1.0000000	ns
66	Pielou	2006	2007	4	4	1.17017	0.241933	1.0000000	ns
67	Pielou	2006	2008	4	4	-0.62409	0.532568	1.0000000	ns
68	Pielou	2006	2009	4	5	0.197355	0.84355	1.0000000	ns
69	Pielou	2006	2010	4	5	1.223599	0.221103	1.0000000	ns
70	Pielou	2006	2011	4	2	0.025478	0.979673	1.0000000	ns
71	Pielou	2006	2012	4	7	-0.69401	0.487675	1.0000000	ns
72	Pielou	2006	2013	4	6	1.988302	0.046778	1.0000000	ns
73	Pielou	2006	2014	4	8	0.036032	0.971257	1.0000000	ns
74	Pielou	2006	2015	4	6	1.469862	0.141599	1.0000000	ns
75	Pielou	2006	2016	4	6	-0.33043	0.741072	1.0000000	ns
76	Pielou	2007	2008	4	4	-1.79426	0.072772	1.0000000	ns
77	Pielou	2007	2009	4	5	-1.03611	0.30015	1.0000000	ns
78	Pielou	2007	2010	4	5	-0.00987	0.992127	1.0000000	ns
79	Pielou	2007	2011	4	2	-0.92996	0.352391	1.0000000	ns
80	Pielou	2007	2012	4	7	-2.01414	0.043995	1.0000000	ns
81	Pielou	2007	2013	4	6	0.706445	0.479911	1.0000000	ns

82	Pielou	2007	2014	4	8	-1.31516	0.188455	1.0000000	ns
83	Pielou	2007	2015	4	6	0.188006	0.850872	1.0000000	ns
84	Pielou	2007	2016	4	6	-1.61229	0.106899	1.0000000	ns
85	Pielou	2008	2009	4	5	0.855204	0.392438	1.0000000	ns
86	Pielou	2008	2010	4	5	1.881448	0.059911	1.0000000	ns
87	Pielou	2008	2011	4	2	0.535046	0.592618	1.0000000	ns
88	Pielou	2008	2012	4	7	0.010058	0.991975	1.0000000	ns
89	Pielou	2008	2013	4	6	2.671959	0.007541	0.9049190	ns
90	Pielou	2008	2014	4	8	0.756669	0.449248	1.0000000	ns
91	Pielou	2008	2015	4	6	2.153519	0.031278	1.0000000	ns
92	Pielou	2008	2016	4	6	0.353223	0.723922	1.0000000	ns
93	Pielou	2009	2010	5	5	1.088497	0.276376	1.0000000	ns
94	Pielou	2009	2011	5	2	-0.13186	0.895093	1.0000000	ns
95	Pielou	2009	2012	5	7	-0.96899	0.332549	1.0000000	ns
96	Pielou	2009	2013	5	6	1.900903	0.057315	1.0000000	ns
97	Pielou	2009	2014	5	8	-0.19352	0.84655	1.0000000	ns
98	Pielou	2009	2015	5	6	1.348244	0.17758	1.0000000	ns
99	Pielou	2009	2016	5	6	-0.57088	0.568082	1.0000000	ns
100	Pielou	2010	2011	5	2	-0.95469	0.339735	1.0000000	ns
101	Pielou	2010	2012	5	7	-2.1447	0.031977	1.0000000	ns
102	Pielou	2010	2013	5	6	0.764005	0.444864	1.0000000	ns
103	Pielou	2010	2014	5	8	-1.4011	0.161184	1.0000000	ns
104	Pielou	2010	2015	5	6	0.211346	0.832617	1.0000000	ns
105	Pielou	2010	2016	5	6	-1.70778	0.087678	1.0000000	ns
106	Pielou	2011	2012	2	7	-0.57005	0.568642	1.0000000	ns
107	Pielou	2011	2013	2	6	1.544867	0.122378	1.0000000	ns
108	Pielou	2011	2014	2	8	0	1.000000	1.0000000	ns
109	Pielou	2011	2015	2	6	1.135004	0.256374	1.0000000	ns
110	Pielou	2011	2016	2	6	-0.28826	0.773152	1.0000000	ns
111	Pielou	2012	2013	7	6	3.088778	0.00201	0.2411780	ns
112	Pielou	2012	2014	7	8	0.883122	0.37717	1.0000000	ns
113	Pielou	2012	2015	7	6	2.487265	0.012873	1.0000000	ns
114	Pielou	2012	2016	7	6	0.398491	0.690268	1.0000000	ns
115	Pielou	2013	2014	6	8	-2.33562	0.019511	1.0000000	ns
116	Pielou	2013	2015	6	6	-0.57963	0.562162	1.0000000	ns
117	Pielou	2013	2016	6	6	-2.59243	0.00953	1.0000000	ns
118	Pielou	2014	2015	8	6	1.715965	0.086168	1.0000000	ns
119	Pielou	2014	2016	8	6	-0.4358	0.662981	1.0000000	ns
120	Pielou	2015	2016	6	6	-2.01279	0.044136	1.0000000	ns

Table SIII.12 Results of Kruskal-Wallis tests comparing Taxonomic Richness (S) across different sections within each sampling year (2001–2016). Significant differences ($p < 0.05$) would be indicated in yellow; however, no such differences were observed ($p > 0.05$ in all cases).

	Year	Index	n	statistic	df	p	method
1	2001	S	14	4.6635874	4	0.3240	Kruskal-Wallis
2	2002	S	12	1.9273504	3	0.5880	Kruskal-Wallis
3	2003	S	9	6.9002849	3	0.0751	Kruskal-Wallis
4	2004	S	15	7.6624220	4	0.1050	Kruskal-Wallis
5	2005	S	17	7.8569536	4	0.0970	Kruskal-Wallis
6	2006	S	11	2.8232087	4	0.5880	Kruskal-Wallis
7	2007	S	9	3.1420290	4	0.5340	Kruskal-Wallis
8	2008	S	9	4.8588589	4	0.3020	Kruskal-Wallis
9	2009	S	15	4.4350490	4	0.3500	Kruskal-Wallis
10	2010	S	11	1.7206790	4	0.7870	Kruskal-Wallis
11	2011	S	6	0.8455882	3	0.8390	Kruskal-Wallis
12	2012	S	19	1.2796143	4	0.8650	Kruskal-Wallis
13	2013	S	14	0.5165895	4	0.9720	Kruskal-Wallis
14	2014	S	19	4.2132022	4	0.3780	Kruskal-Wallis
15	2015	S	13	3.5095238	3	0.3200	Kruskal-Wallis
16	2016	S	17	0.7415426	4	0.9460	Kruskal-Wallis

Table SIII.13 Results of Kruskal-Wallis tests comparing Taxonomic Richness (S) across all years (2001-2016) within different sections. Significant differences ($p < 0.05$) would be indicated in yellow; however, no such differences were observed ($p > 0.05$ in all cases).

	Section	Index	n	statistic	df	p	method
1	H	S	38	12.78429	14	0.544	Kruskal-Wallis
2	K	S	38	14.80882	15	0.465	Kruskal-Wallis
3	N	S	42	13.56579	15	0.712	Kruskal-Wallis
4	S	S	44	14.99274	14	0.379	Kruskal-Wallis
5	EB2	S	48	10.60496	13	0.644	Kruskal-Wallis

Table SIII.14 Results of Kruskal-Wallis tests comparing the Shannon-Wiener diversity index (H′) across different sections within each sampling year (2001–2016). Yellow highlighting indicates years with statistically significant differences ($p < 0.05$), which were subsequently subjected to post-hoc pairwise comparisons.

	Year	Index	n	statistic	df	p	method
1	2001	Shannon	14	3.1903451	4	0.5260	Kruskal-Wallis
2	2002	Shannon	12	0.6282051	3	0.8900	Kruskal-Wallis
3	2003	Shannon	9	5.7333333	3	0.1250	Kruskal-Wallis
4	2004	Shannon	15	4.6429091	4	0.3260	Kruskal-Wallis
5	2005	Shannon	17	4.4444444	4	0.3490	Kruskal-Wallis
6	2006	Shannon	11	6.3484848	4	0.1750	Kruskal-Wallis
7	2007	Shannon	9	3.3111111	4	0.5070	Kruskal-Wallis
8	2008	Shannon	9	6.1777778	4	0.1860	Kruskal-Wallis
9	2009	Shannon	15	8.0059630	4	0.0914	Kruskal-Wallis
10	2010	Shannon	11	4.3939394	4	0.3550	Kruskal-Wallis
11	2011	Shannon	6	0.8571429	3	0.8360	Kruskal-Wallis
12	2012	Shannon	19	6.5710526	4	0.1600	Kruskal-Wallis
13	2013	Shannon	14	1.1952381	4	0.8790	Kruskal-Wallis
14	2014	Shannon	19	5.1384211	4	0.2730	Kruskal-Wallis
15	2015	Shannon	13	9.1901099	3	0.0269	Kruskal-Wallis
16	2016	Shannon	17	5.2254902	4	0.2650	Kruskal-Wallis

Table SIII.15 Results of Dunn's post-hoc pairwise comparisons for Shannon diversity (H′) between sections for 2015. Yellow highlighting indicates nominal (unadjusted) p-values < 0.05. Statistically significant differences maintained after Bonferroni correction (p.adj < 0.05) are highlighted in red and marked with an asterisk (*).

	Index	group1	group2	n1	n2	statistic	p	p.adj	p.adj.signif
2	Shannon	K	S	3	4	-2.7176093	0.006575543	0.03945326	*
1	Shannon	K	N	3	1	0.1482499	0.882145581	1.00000000	ns
3	Shannon	K	EB2	3	5	-1.7345868	0.082814027	0.49688416	ns
4	Shannon	N	S	1	4	-2.0095924	0.044474348	0.26684609	ns
5	Shannon	N	EB2	1	5	-1.3126602	0.189297459	1.00000000	ns
6	Shannon	S	EB2	4	5	1.2057554	0.227911806	1.00000000	ns

Table SIII.16 Results of Kruskal-Wallis tests comparing Pielou's evenness (J′) for different sections within each sampling year (2001–2016). Yellow highlighting indicates years with statistically significant differences ($p < 0.05$), which were subsequently subjected to post-hoc pairwise comparisons.

	Year	Index	n	statistic	df	p	method
1	2001	Pielou	14	0.8589744	4	0.9300	Kruskal-Wallis
2	2002	Pielou	12	3.2179487	3	0.3590	Kruskal-Wallis
3	2003	Pielou	9	3.0000000	3	0.3920	Kruskal-Wallis
4	2004	Pielou	15	1.8212121	3	0.6100	Kruskal-Wallis
5	2005	Pielou	17	0.7867647	4	0.9400	Kruskal-Wallis
6	2006	Pielou	11	6.9818182	4	0.1370	Kruskal-Wallis
7	2007	Pielou	9	2.8666667	4	0.5800	Kruskal-Wallis
8	2008	Pielou	9	5.8888889	4	0.2080	Kruskal-Wallis
9	2009	Pielou	15	6.7912088	4	0.1470	Kruskal-Wallis
10	2010	Pielou	11	3.8181818	4	0.4310	Kruskal-Wallis
11	2011	Pielou	6	3.2000000	3	0.3620	Kruskal-Wallis
12	2012	Pielou	19	8.4707602	4	0.0758	Kruskal-Wallis
13	2013	Pielou	14	3.3112948	4	0.5070	Kruskal-Wallis
14	2014	Pielou	19	9.8859649	4	0.0424	Kruskal-Wallis
15	2015	Pielou	13	5.0637363	3	0.1670	Kruskal-Wallis
16	2016	Pielou	17	5.6102941	4	0.2300	Kruskal-Wallis

Table SIII.17 Results of Dunn's post-hoc pairwise comparisons for Pielou's evenness (J′) between sections for 2014. Yellow highlighting indicates nominal (unadjusted) p-values < 0.05. Statistically significant differences maintained after Bonferroni correction (p.adj < 0.05) are highlighted in red and marked with an asterisk (*).

	Index	group1	group2	n1	n2	statistic	p	p.adj	p.adj.signif
1	Pielou	H	K	3	3	-0.6882472	0.49129712	1.0000000	ns
2	Pielou	H	N	3	5	-2.1374549	0.03256101	0.3256101	ns
3	Pielou	H	S	3	4	-2.4729953	0.01339859	0.1339859	ns
4	Pielou	H	EB2	3	3	-2.4471012	0.01440104	0.1440104	ns
5	Pielou	K	N	3	5	-1.3679711	0.17132111	1.0000000	ns
6	Pielou	K	S	3	4	-1.7372281	0.08234691	0.8234691	ns
7	Pielou	K	EB2	3	3	-1.7588540	0.07860232	0.7860232	ns
8	Pielou	N	S	5	4	-0.4886629	0.62508038	1.0000000	ns
9	Pielou	N	EB2	5	3	-0.5984874	0.54951478	1.0000000	ns
10	Pielou	S	EB2	4	3	-0.1430658	0.88623818	1.0000000	ns

Table SIII.18 Results of Kruskal-Wallis tests comparing the Shannon-Wiener diversity index (H′) across all years (2001-2016) within different sections. Significant differences ($p < 0.05$) would be indicated in yellow; however, no such differences were observed ($p > 0.05$ in all cases).

	Section	Index	n	statistic	df	p	method
1	H	Shannon	38	18.47841	14	0.186	Kruskal-Wallis
2	K	Shannon	38	16.67614	15	0.339	Kruskal-Wallis
3	N	Shannon	42	21.76375	15	0.114	Kruskal-Wallis
4	S	Shannon	44	19.63141	14	0.142	Kruskal-Wallis
5	EB2	Shannon	48	18.13070	13	0.153	Kruskal-Wallis

Table SIII.19 Results of Kruskal-Wallis tests comparing Pielou's evenness (J′) across all years (2001-2016) within different sections. Significant differences ($p < 0.05$) would be indicated in yellow; however, no such differences were observed ($p > 0.05$ in all cases).

	Section	Index	n	statistic	df	p	method
1	H	Pielou	38	17.94523	14	0.209	Kruskal-Wallis
2	K	Pielou	38	12.24958	14	0.586	Kruskal-Wallis
3	N	Pielou	42	16.06893	15	0.388	Kruskal-Wallis
4	S	Pielou	44	19.14097	14	0.160	Kruskal-Wallis
5	EB2	Pielou	48	17.55585	13	0.175	Kruskal-Wallis

Chapter IV

Supplementary Figures

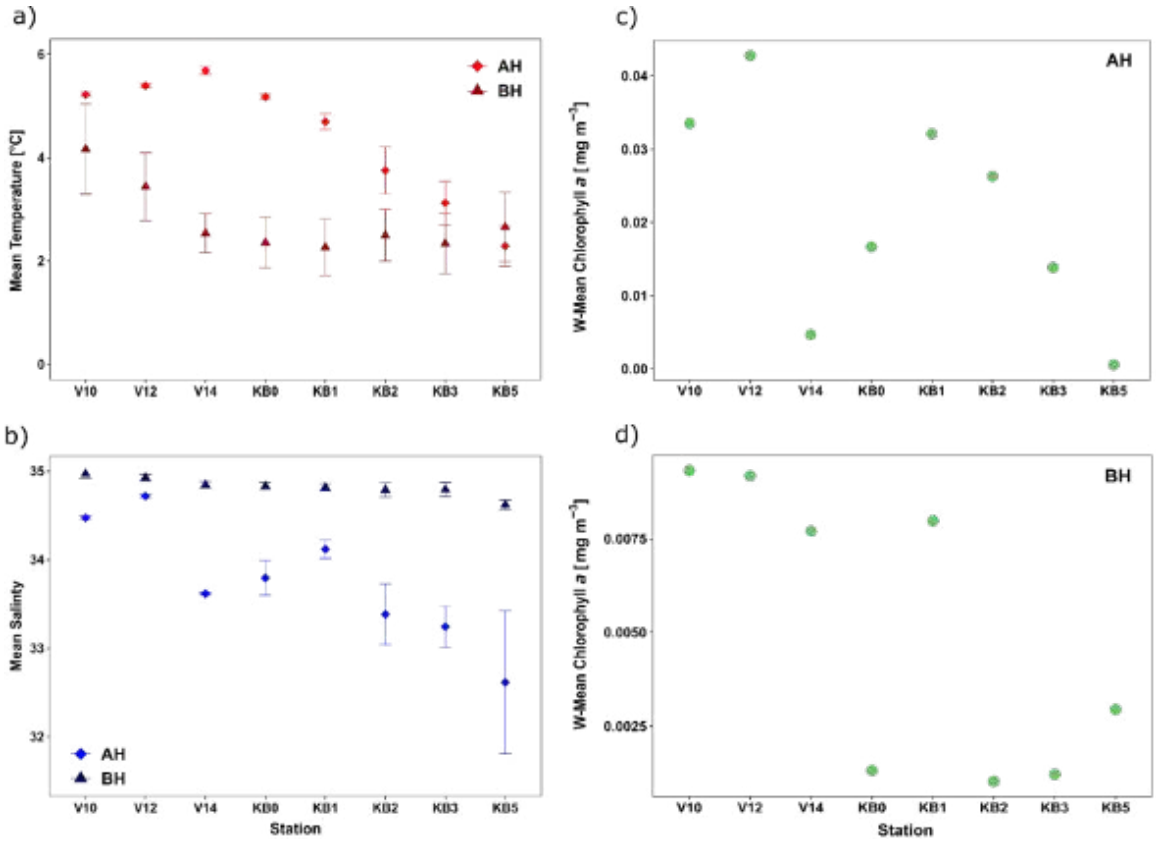

Figure SIV.1 Mean temperature (a) and salinity (b) with standard deviation (SD), and weighted mean chlorophyll a concentrations at the sampling sites above (c) and below (d) the halocline along the Kongsfjorden Transect in summer 2021. AH – above the halocline; BH – below the halocline

Chapter V

Supplementary Tables

Table SV.1 Summary of sequence processing and meroplankton filtering steps for 18S rRNA and *cox1* metabarcoding datasets.

	18S rRNA	***cox1***
ENTIRE SAMPLES POOL		
Initial total sequence reads	16 007 695	11 885 262
Raw samples reads (46 próbek)	15 943 268	11 609 074
Negative control sequence reads (% of initial reads)	64 427 (0.40%)	276 188 (2,38%)
Identified contaminants (% of initial reads)	76 161 (0,48%)	298 370 (2.57%)
Sum of reads in negative controls after decontamination	53 890	266 700
Contaminant reads in negative controls	10 537	9 488
Final reads after decontamination and negative control exclusion (raw 46 samples)	15 867 107	11 310 704
Unassigned reads (mostly *Phaeocystis* sp. for *cox1*; uncultured marine eukaryote, Calanoida, and *Phaeocystis* for 18S)	15 138 501 (95.41%)	9 303 583 (82.25%)
Non-meroplanktonic taxa filtered	728 606	1 776 386
Meroplankton ASVs retained	31 123	230 735
17 STUDY STATIONS SUBSET (without unassigned)		
Raw samples reads	392 715	337 513
Non meroplanktonic taxa	373 327	282 819
Final Meroplankton Dataset	19 388	54 694
CSS data normalization (on the full 17-study-station dataset), and after that, the meroplankton subset was filtered	Norm/log	Norm/log

Table SV.2 Station-level taxonomic richness of meroplankton across oceanographic zones assessed by morphological examination and metabarcoding targeting *cox1* and 18S rRNA markers. For molecular datasets, richness represents the total number of unique Amplicon Sequence Variants (ASVs) assigned to the lowest available taxonomic rank ((including multiple ASVs per genus)). The bottom row indicates the overall cumulative number of unique taxa identified by each methodology across all 17 sampling stations. Abbreviations for Zones: NC – Norwegian Coast; BS – Barents Sea; AW – Atlantic Water; WS – West Spitsbergen shelf.

Zone	Station	Morphology	*cox1*	18S rRNA
NC	PhM1	30	24	27
NC	PhM3	12	21	23
NC	PhM5	9	13	11
BS	V22	13	15	8
BS	V26	15	14	20
BS	V29	16	12	21
BS	V31	19	11	21
BS	V34	20	16	17
AW	H3	16	13	12
AW	K-3	14	9	8
WS	EB2-1	10	8	9
WS	EX3	9	13	9
WS	N4	10	9	3
WS	S3	11	6	7
WS	WB3	7	9	4
WS	Y5	5	6	7
WS	Z2	5	11	11
Total number of taxa noticed at all stations		41	52	46

Authors' contribution table

Since the research material presented in this dissertation has resulted in, or will contribute to, multi-author publications, the following table details the individual contributions of each co-author. This breakdown outlines each co-author's specific role in preparing the papers submitted (or intended for submission) to high-impact journals indexed by the Ministry of Science and Higher Education.

Task	**Chapter II**	**Chapter III**	**Chapter IV**	**Chapter V**
Conceptualization	**WP**	**WP**, PK; SK; MR; AWZ	**WP**; PK	**WP**; MM; AWZ; ML
Funding acquisition	**WP**	SK	**WP**	**WP**
Methodology	**WP**	**WP**; ABM	**WP**	**WP**; ML
Methodological guidance		AWZ	AWZ	MM
Investigation	**WP**	SK; AO	**WP**	**WP**; ML
Resources		SK; ABM	MR; PK	MR; AWZ; ML
Data curation	**WP**	**WP**; ABM; SK	**WP**	**WP**; MM
Formal analysis		**WP**; ABM;	**WP**	**WP**; MM
Visualisation		**WP**; ABM	**WP**	**WP**
Writing – Original draft		**WP**	**WP**	**WP**
Writing – review and editing		**WP**; ABM; SK; AO; MR; AWZ	**WP**; MR; PK; AWZ	**WP**; MR; AWZ; MM; ML
Project administration	**WP**	SK	**WP**	**WP**
Website design and technical support	**WP**; MW			

Weronika Patuła – WP; Sławomir Kwaśniewski – SK; Marta Ronowicz – MR; Agata Weydmann-Zwolicka – AWZ; Mikołaj Mazurkiewicz – MM; Marek Lubośny – ML; Agnieszka Beszczyńska-Möller – ABM; Anna Olszewska – AO; Piotr Kukliński – PK; Marcin Wichorowski - MW